online issn: 1307-6892

irc 2022
XVI. international research conference
proceedings

open science index 16 2022

july 19-20, 2022 copenhagen denmark
international scholarly and scientific research & innovation

Open Science

Open Science Philosophy

Open science encompasses unrestricted access to scientific research articles, access to data from public research, and collaborative research enabled by information and communication technology tools, models, and incentives. Broadening access to scientific research publications and data is at the heart of open science. The objective of open science is to make research outputs and its potential benefits available to the entire world and in the hands of as many as possible:

- Open science promotes a more accurate verification of scientific research results. Scientific inquiry and discovery can be sped up by combining the tools of science and information technologies. Open science will benefit society and researchers by providing faster, easier, and more efficient availability of research outputs.
- Open science reduces duplication in collecting, creating, transferring, and re-using scientific material.
- Open science increases productivity in an era of tight budgets.
- Open science results in great innovation potential and increased consumer choice from public research.
- Open science promotes public trust in science. Greater citizen engagement leads to active participation in scientific experiments and data collection.

Open Science Index

The Open Science Index (OSI) currently provides access to over thirty thousand full-text journal articles and is working with member and non-member organizations to review policies to promote and assess open science. As part of the open science philosophy, and by making open science a reality; OSI is conducting an assessment of the impact of open science principles and restructuring the guidelines for access to scientific research. As digitalization continues to accelerate science, Open science and big data hold enormous promise and present new challenges for policymakers, scientific institutions, and individual researchers.

OSI is helping the global scientific research community discover, evaluate, and access high-quality research output. Renowned for its editorially curated and refereed collection of the highest-quality publications, OSI has always been and will remain free-of-charge.

OSI provides an efficient and thorough discovery process to the open science research database and provides links and free access to full-text articles. There are 50 open access journal categories that are curated and refereed by international scientific committees, the in-house editorial team, and trusted partners. Since its inception in 2007, OSI has made more than thirty thousand peer-reviewed open access full-text journal articles (PDF versions) freely available online without cost, barriers, or restrictions.

Open Science Access

With the Open Science Index, researchers can discover and access trusted peer-reviewed open access full-text scientific research articles with confidence. OSI helps researchers find appropriate non-profit open access journals to publish their work.

OSI gives one-click access to online full-text PDFs and expands the reach to global society by giving users free access from anywhere around the globe. Through cutting-edge open science collaboration, in an innovative public partnership, the non-profit OSI is devoted to making science open and reusable.

To learn more, visit online at waset.org

Open Science

Open Society

An open society allows individuals to change their roles and to benefit from corresponding changes in status. Open science depends to a greater or lesser extent on digital technologies and innovations in structural processes by an open society. When realized, open science research and innovation can create investment opportunities for new and better products and services and therefore increase competitiveness and employment. Open science research and innovation is a key component of thematic open science priorities. Central to the open science digital infrastructure is enabling industry to benefit from digital technology and to underpin scientific advances through the development of an open society. Open science research and innovation can also contribute to society as a global actor because scientific relations can flourish even where global relations are strained. Open science has a critical role across many areas of decision making in providing evidence that helps understand the risks and benefits of different open science choices. Digital technology is making the conduct of open science and innovation more collaborative, more global, and more open to global citizens. Open society must embrace these changes and reinforce its position as the leading power for science, for new ideas, and for investing sustainably in the future.

It is apparent in open society that the way science works is fundamentally changing, and an equally significant transformation is taking place in how organizations and societies innovate. The advent of digital technology is making research and innovation more open, collaborative, and global. These exchanges are leading open society to develop open science and to set goals for research and innovation priority. Open science goals are materializing in the development of scientific research and innovation platforms and greater acceptance of scientific data generated by open science research. Open science research and innovation do not need help from open society to come up with great ideas, but the level of success ideas ultimately reach is undoubtedly influenced by regulation, financing, public support, and market access. Open society is playing a crucial role in improving all these success factors.

Open Science

Open science represents a new approach to the scientific process based on cooperative work and new ways of diffusing knowledge by using digital technologies and collaborative tools. These innovations capture a systemic change to the way science and research have been carried out for the last fifty years. Science is shifting from the standard practice of publishing research results in scientific publications after the research and reviews are completed. The shift is towards sharing and using all available knowledge at an earlier stage in the research process. Open science is to science what digital technology is to social and economic transactions: allowing end users to be producers of ideas, relations, and services and in doing so, enabling new working models, new social relationships and leading to a new modus operandi for science. Open science is as important and disruptive as e-commerce has been for the retail industry. Just like e-commerce, the open science research paradigm shift affects the whole business cycle of doing science and research. From the selection of research subjects to the carrying out of research, to its use and re-use, to the role of universities, and that of publishers are all dramatically changed. Just as the internet and globalization have profoundly changed the way we do business, interact socially, consume culture, and buy goods, these changes are now profoundly impacting how one does research and science.

The discussion on broadening the footprint of science and on novel ways to produce and spread knowledge gradually evolved from two global trends: Open Access and Open Source. The former refers to online, peer-reviewed scholarly outputs, which are free to read, with limited or no copyright and licensing restrictions, while open source refers to software created without any proprietary restriction and which can be accessed and freely used. Although open access became primarily associated with a particular publishing

or scientific dissemination practice, open access already sought to induce a broader practice that includes the general re-use of all kinds of research products, not just publications or data. It is only more recently that open science has coalesced into the concept of a transformed scientific practice, shifting the focus of researchers' activity from publishing as fast as possible to sharing knowledge as early as possible. Open science is defined as the idea that scientific knowledge of all kinds should be openly shared as early as is practical in the discovery process. As a result, the way science is done in the future will look significantly different from the way it is done now. Open science is the ongoing evolution in the modus operandi of doing research and organizing science. This evolution is enabled by digital technology and is driven by both the globalization of the scientific community and increasing public demand to address the societal challenges of our times. Open science entails the ongoing transitions in the way research is performed, researchers collaborate, knowledge is shared, and science is organized.

Open science impacts the entire research cycle, from the inception of research to its publication, and on how this cycle is organized. The outer circle reflects the new interconnected nature of open science, while the inner circle shows the entire scientific process, from the conceptualization of research ideas to publishing. Each step in the scientific process is linked to ongoing changes brought about by open science, including the emergence of alternative systems to establish a scientific reputation; changes in the way quality and impact of research are evaluated; the growing use of scientific blogs; open annotation; and open access to data and publications. All institutions involved in science are affected, including research organizations, research councils, and funding bodies. The trends are irreversible, and they have already grown well beyond individual projects. Theses changes predominantly result from a bottom-up process driven by a growing number of researchers who increasingly employ social media in their research and initiate globally coordinated research projects while sharing results at an early stage in the research process.

Open science is encompassed in five schools of thought:

- the infrastructure school, concerned with technological architecture
- the public school, concerned with the accessibility of knowledge creation
- the measurement school, concerned with alternative impact assessment
- the democratic school, concerned with access to knowledge
- the pragmatic school, concerned with collaborative research

According to the measurement school, the reputation and evaluation of individual researchers are still mainly based on citation-based metrics. The h-index is an author-level metric that attempts to measure both the productivity and citation impact of the publications of a scientist or scholar. The impact factor is a measure reflecting the average number of citations to articles published in an academic journal and is used as a proxy for the relative importance of a journal.

Numerous criticisms have been made of citation-based metrics, primarily when used, and often misused, to assess the performance of individual researchers. These metrics:

- are often not applicable at the individual level
- do not take into account the broader social and economic function of scientific research
- are not adapted to the increased scale of research
- cannot recognize new types of work that researchers are performing

Web-based metrics for measuring research output, popularized as altmetrics, have recently received much attention: some measure the impact at the article level, others make it possible to assess the many outcomes of research in addition to the number of scientific articles and references. The current reputation and evaluation system has to adapt to the new dynamics of open science and acknowledge and incentivize

engagement in open science. Researchers engaging in open science have growing expectations that their work, including intermediate products such as research data, will be better rewarded or taken into account in their career development. Vice-versa, the use, and reuse of open data will require appropriate codes of conduct requiring, for example, the proper acknowledgment of the original creator of the data.

These ongoing changes are progressively transforming scientific practices with innovative tools to facilitate communication, collaboration, and data analysis. Researchers that increasingly work together to create knowledge can employ online tools and create a shared space where creative conversation and collaboration can occur. As a result, the problem-solving process can be faster, and the range of problems that can be solved can be expanded. The ecosystem underpinning open science is evolving very rapidly. Social network platforms for researchers already attract millions of users and are being used to begin and validate more research projects.

Furthermore, the trends towards open access are redefining the framework conditions for science and thus have an impact on how open innovation is produced by encouraging a more dynamic circulation of knowledge. It can enable more science-based startups to emerge thanks to the exploitation of openly accessible research results. Open science, however, does not mean free science. It is essential to ensure that intellectual property is protected before making knowledge publicly available in order to subsequently attract investments that can help translate research results into innovation. If this is taken into account, fuller and broader access to scientific publications and research data can help to accelerate innovation. Investments that boost research and innovation in open science would benefit society with fewer barriers to knowledge transfer, open access to scientific research, and greater mobility of researchers. In this context, open access can help overcome the barriers that innovative organizations face in accessing the results of research funded by the public.

Open innovation

An open society is the largest producer of knowledge, but the phenomenon of open science is changing every aspect of the scientific method by becoming more open, inclusive, and interdisciplinary. Ensuring open society is at the forefront of open science means promoting open access to scientific data and publications alongside the highest standards of research integrity. There are few forces in this globe as engaging and unifying as science. The universal language of science maintains open channels of communication globally. Open society can maximize its gains through maintaining its presence at the highest level of scientific endeavor, and by promoting a competitive edge in the knowledge society of the information age. The ideas and initiatives described in this publication can stimulate anyone interested in open science research and innovation. It is designed to encourage debate and lead to new ideas on what and open society should do, should not do, or do differently.

An open society can lead to a research powerhouse; however, open society rarely succeeds in turning research into innovation and in getting research results to the global market. Open society must improve at making the most of its innovation talent, and that is where open innovation comes into play. The basic premise of open innovation is to open up the innovation process to all active players so that knowledge can circulate more freely and be transformed into products and services that create new markets while fostering a stronger culture of entrepreneurship. Open innovation is defined as the use of purposive inflows and outflows of knowledge to accelerate internal innovation. This original notion of open innovation was primarily based on transferring knowledge, expertise, and even resources from one company or research institution to another. This notion assumes that firms can and should use external ideas as well as internal ideas, and internal and external paths to market, as they seek to improve their performance. The concept of open innovation is continually evolving and is moving from linear, bilateral transactions and collaborations

towards dynamic, networked, multi-collaborative innovation ecosystems. This means that a specific innovation can no longer be seen as the result of predefined and isolated innovation activities but rather as the outcome of a complex co-creation process involving knowledge flows across the entire economic and social environment. This co-creation takes place in different parts of the innovation ecosystem and requires knowledge exchange and absorptive capacities from all the actors involved, whether businesses, academia, financial institutions, public authorities, or citizens.

Open innovation is a broad term, which encompasses several different nuances and approaches. Two main elements underpin the most recent conceptions of open innovation: the users are in the spotlight and invention becomes an innovation only if users become a part of the value creation process. Notions such as user innovation emphasize the role of citizens and users in the innovation processes as distributed' sources of knowledge. This kind of public engagement is one of the aims of open science research and innovation. The term 'open' in these contexts has also been used as a synonym for 'user-centric'; creating a well-functioning ecosystem that allows co-creation and becomes essential for open innovation. In this ecosystem, relevant stakeholders are collaborating along and across industry and sector-specific value chains to co-create solutions for socio-economic and business challenges. One important element to keep in mind when discussing open innovation is that it cannot be defined in absolutely precise terms. It may be better to think of it as a point on a continuum where there is a range of context-dependent innovation activities at different stages, from research to development through to commercialization, and where some activities are more open than others. Open innovation is gaining momentum thanks to new large-scale trends such as digitalization and the mass participation and collaboration in innovation that it enables. The speed and scale of digitalization are accelerating and transforming the way one designs, develops, and manufactures products, the way one delivers services, and the products and services themselves. It is enabling innovative processes and new ways of doing business, introducing new cross-sector value chains and infrastructures.

Open society must ensure that it capitalizes on the benefits that these developments promise for citizens in terms of tackling societal challenges and boosting business and industry. Drawing on these trends, and with the aim of helping build an open innovation ecosystem in open society, the open society's concept of open innovation is characterized by:

- combining the power of ideas and knowledge from different actors to co-create new products and find solutions to societal needs
- creating shared economic and social value, including a citizen and user-centric approach
- capitalizing on the implications of trends such as digitalization, mass participation, and collaboration

In order to encourage the transition from linear knowledge transfer towards more dynamic knowledge circulation, experts agree that it is essential to create and support an open innovation ecosystem that facilitates the translation of knowledge into socio-economic value. In addition to the formal supply-side elements such as research skills, excellent science, funding and intellectual property management, there is also a need to concentrate on the demand side aspects of knowledge circulation, making sure that scientific work corresponds to the needs of the users and that knowledge is findable, accessible, interpretable and reusable. Open access to research results aims to make science more reliable, efficient, and responsive and is the springboard for increased innovation opportunities, e.g. by enabling more science-based startups to emerge. Prioritizing open science does not, however, automatically ensure that research results and scientific knowledge are commercialized or transformed into socio-economic value. In order for this to happen, open innovation must help to connect and exploit the results of open science and facilitate the faster translation of discoveries into societal use and economic value.

Open Science

Collaborations with global partners represent important sources of knowledge circulation. The globalization of research and innovation is not a new phenomenon, but it has intensified in the last decade, particularly in terms of collaborative research, international technology production, and worldwide mobility of researchers and innovative entrepreneurs. Global collaboration plays a significant role both in improving the competitiveness of open innovation ecosystems and in fostering new knowledge production worldwide. It ensures access to a broader set of competencies, resources, and skills wherever they are located, and it yields positive impacts in terms of scientific quality and research results. Collaboration enables global standard-setting, allows global challenges to be tackled more effectively, and facilitates participation in global value chains and new and emerging markets.

To learn more, visit online at waset.org

Open Science

Scholarly Research Review

The scholarly research review is a multidimensional evaluation procedure in which standard peer review models can be adapted in line with the ethos of scientific research, including accessible identities between reviewer and author, publishing review reports and enabling greater participation in the peer review process. Scholarly research review methods are employed to maintain standards of quality, improve performance, provide credibility, and determine suitability for publication. *Responsible Peer Review Procedure:* Responsible peer review ensures that scholarly research meets accepted disciplinary standards and ensures the dissemination of only relevant findings, free from bias, unwarranted claims, and unacceptable interpretations. Principles of responsible peer review:

• Honesty in all aspects of research
• Accountability in the conduct of research
• Professional courtesy and fairness in working with others
• Good stewardship of research on behalf of others

The responsibilities of peer review apply to scholarly researchers at all stages of peer review: Fairness, Transparency, Independence, Appropriateness and Balance, Participation, Confidentiality, Impartiality, Timeliness, Quality and Excellence, Professionalism, and Duty to Report.

Scholarly Research Review Traits:
• Scholarly Research Review Identities: Authors and reviewers are aware of each other's identity

• Scholarly Research Review Reports: Review reports are published alongside the relevant article

• Scholarly Research Review Participation: The wider academic community is able to contribute to the review process

• Scholarly Research Review Interaction: Direct reciprocal discussion between author(s) and reviewers, and/or between reviewers, is allowed and encouraged

• Scholarly Research Pre-review Manuscripts: Manuscripts are made immediately available in advance of any formal peer review procedures

• Scholarly Research Review Final-version Reviewing: Editorial revision of the language and format is conducted on the final version of the manuscript for publication

• Scholarly Research Review Platforms: The scholarly research review process is independent of the final publication of the manuscript and it is facilitated by a different organizational entity than the venue of publication

All submitted manuscripts are subject to the scholarly research review process, in which there are three stages of evaluation for consideration: pre-review manuscripts, chair-review presentation, and final-review manuscripts. All submitted full text papers, that may still be withstand the editorial review process, are presented in the conference proceedings. Manuscripts are tracked and all actions are logged by internal and external reviewers according to publication policy. External reviewers' editorial analysis consists of the evaluation reports of the conference session chairs and participants in addition to online internal and external reviewers' reports. Based on completion of the scholarly research review process, those manuscripts meeting the publication standards are published 10 days after the event date.

To learn more, visit online at waset.org

TABLE OF CONTENTS

Principles and Practice of Therapeutic Architecture

Umedov Mekhroz, Griaznova Svetlana

***Abstract*—** The quality of life and well-being of patients, staff and visitors are central to the delivery of health care. Architecture and design are becoming an integral part of the healing and recovery approach.

The most significant point that can be implemented in hospital buildings is the therapeutic value of the artificial environment, the design and integration of plants to bring the natural world into the healthcare environment. The hospital environment should feel like home comfort. The techniques that therapeutic architecture uses are very cheap, but provide real benefit to patients, staff and visitors, demonstrating that the difference is not in cost but in design quality. The best environment is not necessarily more expensive - it is about special use of light and color, rational use of materials and flexibility of premises. All this forms innovative concepts in modern hospital architecture, in new construction, renovation or expansion projects.

The aim of the study is to identify the methods and principles of therapeutic architecture.

The research methodology consists in studying and summarizing international experience in scientific research, literature, standards, methodological manuals and project materials on the research topic.

The result of the research is the development of graphic-analytical tables based on the system analysis of the processed information; 3d visualization of hospital interiors based on processed information.

***Keywords*—** color scheme, environment, healthcare interiors, lighting, materials, sustainable design, therapeutic architecture.

U. M. Author is with the Architectural Department of the Design Institute LLC "M1 Project", Moscow, 123112, Russia (phone: +7 906-348-98-30; e-mail: 12mehroz@gmail.com).

G. S. Author is with the Architectural Department of the Design Institute LLC "M1 Project", Moscow, 123112, Russia (phone: +7 920-019-22-96; e-mail: svetlana.pub@gmail.com).

Principles and Practice of a Human-Centered Design Approach

Griaznova Svetlana, Umedov Mekhroz

***Abstract*—** The main task of human-centered design of medical facilities is a modern high-tech process of providing high-quality medical care that meets the requirements of modern standards of medical care. Architectural solutions are adjusted and continuously follow the development of scientific activity and modern trends, taking into account future needs. The principles of human-centered architecture apply to planning, design, construction and commissioning. In fact, none of the organizations have developed their own set of such health standards. However, organizations accredited by the Joint Commission and the JCI are expected to demonstrate processes and results that rely on an established environment for effective support.

In addition to focusing on patient-centered health care, environmentally sustainable health care is a growing concern. Buildings and the construction process must not harm patients or the environment. In other words, healthcare facilities should not, under the guise of patient care, pollute the air, flush chemicals into water, or overload landfills.

The purpose of the research is to identify the methods and principles of human-oriented architecture and their application in design solutions.

The research methodology consists in studying and summarizing international experience in scientific research, literature, standards, methodological manuals and project materials on the research topic.

The result of the research is the development of graphic-analytical tables based on the system analysis of the processed information; Revealing the principles and methodology of a human-centered design approach.

***Keywords*—** environment, healthcare, human-centered architecture, sustainable design.

S. G. Author is with the Architectural Department of the Design Institute LLC "M1 Project", Moscow, 123112, Russia (phone: +7 920-019-22-96; e-mail: svetlana.pub@gmail.com).

U. M. Author is with the Architectural Department of the Design Institute LLC "M1 Project", Moscow, 123112, Russia (phone: +7 906-348-98-30; e-mail: 12mehroz@gmail.com).

The Visualization of Plant-computer Interaction under the Sustainability Dialogue - Take Plant-smart Furniture as an Example

Hang Su, Yuan Liu

***Abstract*—**With the development of AI and electronic technique, scenarios of Human-Computer Interaction (HCI), represented by smart homes, have greatly integrated and improved people's quality of life, meanwhile, the space that coexists with plants is constantly being invaded. As an irreplaceable part of nature, plants are increasingly being presented in various artificial environments. Many interactive designs under the HCI framework have been discussed the hybrid of integrating plants and machines together. Inspired by Michael Pollan, we believe that the role of plants under the HCI environment needed to be reconsidered.

The research aims to explore the visualization of plants' emotions in aspects of HCI and electronic functionalities, and the methods of interaction between plants and human beings under the context of sustainable development. In other words, we determine to explore new possibilities for sustainability in future lifestyles by re-defining the plant-machine relationship. The major research methods include secondary research and case study, as an output, we both classify the typologies of plant-computer Interaction, along with the project-based discussion of interactive furniture, implementing to present and explain the role of plants.

This paper is divided into three main parts.

First, the paper discusses the value of survival strategies and emotional expression of plants in future lifestyles through the analysis of plants' needs and responses to the environment. Also, we argue plants as a secondary role within the modern domestic environment, theories and practices of Michael Pollan and Stefano Mancuso are considered fundamental for the state of art between plants and computer.

Secondly, by studying existing literature on relevant fields (Plant-computer Interaction, plants' expression), a typology of plant-computer interaction is re-defined, specifically: Communication medium, Passive ride, Physical symbiosis and Emotional personification. This part of study aims to offer guidance to the symbiotic relationship between plants, machines and human.

At last, we discuss a practice under the "Emotional personification" category through implementing called Plant-smart furniture. An explanation of how the non-human roles' emotions and appeal intervene between and influence HCI is made, then the reflective discussion of the symbiosis and integration of plants and machines is conducted. To conclude, the project presents a series of interactive furniture controlled by the "intelligence" of plants, including a Bamboo palm chair, a Vine coat stand and a Moss robot vacuum. As an experimental innovation, this project adopts computer technology, empowers plants the right to survival, and secures the rights of choice making and emotional expression under the interactive form of plants-computer symbiosis/plants driving machines.

The research is not only a response to the trend of biology-human-science integration, but also an exploration of the harmonious symbiosis of human and other forms of life under the framework of HCI and DFS. AI technology development may support better solutions for human-nature symbiosis both emotionally and commercially, which, the author believes, will be achieved in the family settings of the future.

***Keywords*—**Plant-computer, interaction, symbiosis, plants' emotion visualization, role of plants.

Hang Su is with the Central Saint Martins (University of the Arts London), London, UK (phone: +86 17801082519; e-mail: suhangdesign@163.com/ h.su0320201@arts.ac.uk).

Yuan Liu is with Beijing Institute of Fashion Technology, Beijing 100029, China. (e-mail: yuan.liu@polimi.it).

Augmented Reality Using Cuboid Tracking as a support for Early Stages of Architectural Design

Larissa Negris de Souza, Ana Regina Mizrahy Cuperschmid, Daniel de Carvalho Moreira

***Abstract*—** This paper's goal was to develop an Augmented Reality (AR) app using a three-dimensional marker inspired by the Rubik's Cube and evaluate its performance. This is an exploration of a new approach for early stages of architectural design coupling the acquired knowledge of traditional briefing methods and contemporary technology. We considered the concept of patterns to outline geometric forms and associations using visual programming. The Design Science Research was applied to develop the study. An SDK was used in a game engine to generate the AR app. The tool's functionality was assessed by verifying the readability and precision of the reconfigurable 3D marker. The results indicated an inconsistent response. To use AR in the early stages of architectural design the system must provide consistent information and appropriate feedback. Nevertheless, we conclude that our framework sets the ground for looking deep into AR tools for briefing design.

***Keywords*—**Augmented Reality; Cuboid Marker; patterns; early design stages.

I. Introduction

ARCHITECTURE, Engineering, and Construction (AEC) content is mostly communicated through visual representations. As the complexity of design increases, computational systems advance. Designers are called for action approaching more creative design methods [1–4], which focus on developing systems to enable better management of diverse types of data.

Each computer-aided design (CAD) tool requires a set of instructions, related to functions, to depict a specific type of information. Hence, the increasing application of digital technologies also broadened the possibilities of information exhibition. Each design process phase in architecture has a preconceived group of tools indicated based on their representational aspects, types of data accepted, or the amount of data supported.

However, the exploration of other applications for the same tools tends to bring a new perspective into the role that technology plays [5]. Augmented Reality (AR) is one of the technologies currently applied in architectural design. From its definition, AR projects virtual information onto real world environments. In other words, AR supplements the real world with computer-generated graphics that appear to coexist in the same space [6,7].

As a powerful visualization tool, AR can aid designers to communicate their ideas, improving dialog. It is possible to achieve this improvement from briefing to 3D modeling and construction, the latter ones being where it is normally applied. Nonetheless, inquiries on AR application in the early phases are an exciting opportunity to explore this technology and have the potential to promote interaction with other phases.

AR can alter the elaboration of architectural design, which relates to the cognition of representation, visualization, and perception. From the earliest stages of design, the study of relationships, zoning, and overall dimensions of the forms according to user needs is required. Such analysis is carried out using graphic representations where basic geometries are more important than structured ones.

With that in mind, our final purpose is to develop an AR app for briefing exploration. The AR app intends to support the early stages of architectural design to be used for internal design consultation specifically by architects. Basic features were considered to maintain early design requirements such as generic forms, and prompt design alterations. In this regard, the goal of our article is to develop this app and evaluate its performance. Using a three-dimensional marker inspired by the Rubik's Cube, we evaluated the app response to different configurations. The methodology allowed testing its building prerequisites and 3D model association.

Therefore, the novelty of this work is to propose a new approach to briefing design using AR, and attempted to address the following question: Inspired in the pattern language and the Rubik's Cube, is it possible to explore AR aiding in the early stages of the architectural design process? To answer this question an app is ideated, and its performance tested.

II. CONTEXT

The conception of a design starts in the architectural program, also known as briefing. The goal of this phase is to set the base for the latter building solution. The organization of ideas, the establishment of rules, the prioritization of functions, and the coordination of relations are some activities undertaken in this phase. At this moment, only general aspects of form are proposed [8,9].

As the ideas for the design are explored, they encompass basic forms that can be graphically represented. Bidimensional

Larissa Negris de Souza is with the School of Civil Engineering, Architecture and Urban Design, State University of Campinas (UNICAMP), Campinas, SP, Brazil (corresponding author, larissanegris@gmail.com

Ana Regina Mizrahy Cuperschmid is with the School of Civil Engineering, Architecture and Urban Design, State University of Campinas (UNICAMP), Campinas, SP, Brazil (cuper@unicamp.br)

Daniel de Carvalho Moreira is with the School of Civil Engineering, Architecture and Urban Design, State University of Campinas (UNICAMP), Campinas, SP, Brazil (damore@fec.unicamp.br)

The authors disclosed receipt of the following financial support for the research of this article: This work was supported by The São Paulo Research Foundation (FAPESP) [process number 2018/15863-8].

diagrams at this stage are frequently used to represent hierarchies, functions, distribution, and relations. In contrast, later phases of the design process focus on physical aspects and their final shapes.

Traditionally, hand-drawings of relation matrix and bubble diagrams are used to support the systematization and visualization of information at the early stages of the architectural design process [10,11]. Nonetheless, technology breaks into every step of the design process for better data management, and deeper connection of phases and information along the building design process. Advances in CAD systems have been leading AEC into a path in which the integration of information prevails, even in the beginning of architectural design.

Many studies analyze the use of 2D and 3D software for drafting, documenting, and modeling by AEC professionals [12–16]. The construction industry still has a large potential for improvement using innovative technologies such as Building Information Modelling (BIM), parametric design, AR, drones, 3D scanning, and printing, amongst others [17]. However, there is a lack of digital tools with appropriate functionalities to be used in the early stages of architectural design [11].

These early stages can be explored in the light of developing new strategies for technology applications developing new kinds of abstractions. The use of 3D virtual models in architecture to represent the object enhances object comprehension and demands less effort from the tool-user [18]. As one of the ways to work with 3D virtual models, AR still has more potential yet to be explored in AEC. This way, investigations in the architectural field are important to ensure AR implementation in the design process is up to date, and to discover new roles for these systems, as is the case of this study.

The use of AR at this stage requires the transformations of 2D diagrams and geometries into 3D ones. Thereby, it is essential to create digital models of cubes, and spheres, for example, and the study of other aspects to represent three-dimensional information such as hierarchies, zoning, connections, flow, etc. In this research, the reflection goes in this direction.

A. AR to support early stages of the design process

As AR technologies expand their application on gaming [19,20], heritage tourism [21,22], or military sectors [23,24], it is also possible to see their spread into the AEC industry. Particular aspects have to be considered in this area, though. To continually innovate and take advantage of all nuances of such technologies, the challenge is to explore their potentials beyond rendering and visualization, embedding them in other fields of the design and construction process [25,26].

A noticeable body of research exists presenting and validating the application of AR throughout the architectural design process [29–32,28,33,34,7,35–39,18,40,41]. The design process was explored on building redesign activity with students to enhance their skills in generating, visualizing, and assessing exterior walls by proposing a retrofit design to improve its sustainable performance [37]. In this case, AR was applied along with simulation game technologies to create different design scenarios.

AR employment is still rising, which means that there is room for AR tools research and performance evaluation [27]. In AEC, AR use includes visualizing buildings on-site and rendered interiors, integrating design and as-built environments, for example [25,28]. In heritage buildings, there is also an investigation aiming at developing guidelines for their enhancement and preservation [34].

As demonstrated, AR applications and studies cover design and visualization to production, maintenance, and assessment, also going through the interest in understanding the influence of different devices [42]. Yet, up to now, far too little attention has been paid to leveraging AR potentials during a briefing, or the early stages of the architectural process. Notwithstanding, a study in the field of mechanical engineering used AR for supporting abstract representations to aid design idea generation by novice students [43], which is inherently connected to the idea of working with architectural briefing information. This research was interested in conceptual design, seen as a process of exploring concepts. For this, the working principles, functions, or behavior were extracted from existing physical objects, which allowed understanding the spatial forces acting on such pieces as punching, pulling, leveling, cutting, and so on. With the AR-supporting tool, the students were able to archive existing artifacts, convert them into the mentioned abstract representations, map these abstract concepts into their generic physical elements in terms of AR markers, and observe animated 3D mechanical movements through AR function. This way, it was possible for the students to develop new designs starting from abstract solutions to concrete ones, a process that enables a higher level of idea generation for mechanisms.

Considering all this evidence, most research focuses on the late phases of the design process, according to the prevailing function of this technology. Concrete proposals are related to immersive environments, which include human-scale 3D models to be superimposed in built environments. We already know that AR allows architects to interact with virtual spatial data of the proposed designs in their final contexts [7]. However, it can also allow interaction with different types of data, for diverse purposes, relating to other phases of the design process. The AEC sector might leverage from these other outlooks, as shown and inspired by studies in other areas such as the one in mechanical engineering [43].

In other words, AR systems have many qualities besides enhancing the visual sense. Because of its inherent characteristics, AR can change the perception of space, without asking its users to lose complete contact with reality [44,45]. In general, as the AR application is developed, specific inputs are coordinated: types of interaction with devices, the user interface, the speed of data processing, sensors, among others [46].

Combining the positive evidence of working with 3D virtual models and associating this to the engagement induced by an immersive environment, the idea of using AR in the early stages can lead to a new perspective of this activity, and the whole design process. Thereby, the acquired knowledge using

traditional methods to collect briefing information can be taken to another level in architecture.

B. Design patterns and the early stages of architectural design

During the design work, architects have created many methods to deal with problem spaces (48–54,10). These methods might vary considerably among professionals' profiles, the nature of the problem, or even clients' needs (55). Nonetheless, it is possible, as has been done before, to indicate explicit and systematic manners for data collection, or highlight important pieces of thoughts one should bear in mind when designing.

For instance, White (52) proposed specific ways of working with architectural information during the early stages of design using diagrams for space adjacency analysis. Although not mandatory, such methods assist in a better assessment of possible solutions. The use of a visual language during architectural programming aids the abstraction of ideas and, as the author says, is also central to the process of recognizing, understanding, remembering, recalling, and synthesizing architectural concepts. He indicates the usage of the Matrix Relationship Diagram, Bubble Diagram, and Zoning Diagram, each one possessing guiding structures or rules, demanding specific inputs that direct decisions.

Rowe (53) is another important author that makes considerations in this field. In his discussion on design thinking, brings into light five classes of methods that can be distinguished, and used, during the design process. One of these, named "Environmental Relations", includes organizing information searching for appropriate connections among components of the building. This method has a strong relation to what White (52) indicates and, both are intended to be used during the early stages of design.

In this research, a particular approach is proposed based on well-defined and important architectural concepts. They were called primary generators by Lawson (8), or patterns by Alexander, Silverstein, and Ishikawa (54). The patterns are part of a repertoire for reasoning about early-stage information. They determine the point of departure, the direction the design will take (56), or the strategy from its early stages, and are related to the nature of the design problem (8).

According to Alexander et al. (54), every design begins with general and abstract solutions to guide the process of design and later construction, which are implemented numerous times without repeating the exact form of application. Therefore, thinking in terms of patterns while designing contributes to remembering recurring problems addressed by architecture and for which the project must provide a solution. Consequently, conducting this exploratory study based on the pattern language is an attempt to keeping in mind essential design relationships.

As we employ pattern-based thought or any considerations on the described methods for handling early-stage data, we have to consider their depiction. The graphic representation is essential, for this is the language architects mostly use to manipulate and transfer messages. At this phase of the design process, however, we avoid the exact physical morphology to keep the ideas fluid and open. Instead, simple geometric shapes should be used to represent general schemes of relationships, hierarchies, functions, connections, among other aspects.

III. SOFTWARE SETUP AND WORKFLOW

Applying Design Science Research (DSR), this study focuses on describing and exploring a research problem and designing and creating a system, which is an AR tool. Encompassing theory and AR artifact development sets the ground for the study. Under these premises, the research problem is raised based on the state of the art, followed by a solution proposition and functionality tests of the created tool (57,58).

In this study, we determined with which basic geometries to work (spheres and cubes) and which types of association (how they are put together), proposing possible manners to handle graphic information. We do not intend to cover an extensive list of variations since this research is the first attempt to explore using a configurable cuboid AR marker to visualize 3D models for briefing development. Notwithstanding, we take a step towards creating a repertoire to be accessed by architects, favoring previous acknowledgement and later application of requirements that otherwise might have been minimized or even forgotten.

In short, our research consists of five steps: (1) the investigation of current AR uses in architecture; (2) the comprehension of architectural design briefing development; (3) the establishment of a research problem to bridge the gap between program requirements and the possibility of creating an AR tool to aid this phase of design; (4) the proposition of an AR tool facing the problem; (5) the simulations and evaluation of app performance and related issues (development technology used, type of information, data processing characteristics, amongst others). The overall research process is represented in Figure 1.

A. App conception

Numerous methods and structures for the design process were previously discussed and applied in architecture (59,55,51–54,60). A critical aspect is to be aware of their nature: creative, rational, or of the design process control (55,60). The first one is a black box, and the line of thought runs according to the designer's reflections, being out of conscious control. The rational nature, however, is a glass box, and the designer knows why and when certain decisions were made. Nonetheless, both aspects create a great number of alternatives to be explored.

In their turn, methods based on controlling the design process create self-organized systems, which are valid recourses in face of the previous blind search for alternatives. Hence, this investigation seats within these last methods and traces the ideation of a new system. The research data in this work are drawn from one main source: the pattern language from Alexander et al. (54), to be considered and accessed during the early stages of the architectural design process. Currently, traditional methods for diagraming briefing information exist, but our endeavor is the conception of an AR app to explore new ways of briefing conduction. Indeed, inspired by the pattern

language (54), a particular approach to architectural design should be followed when using this app.

be freely adjusted as happens with the traditional Rubik's Cube. If so, controlled, and specific modification would be either

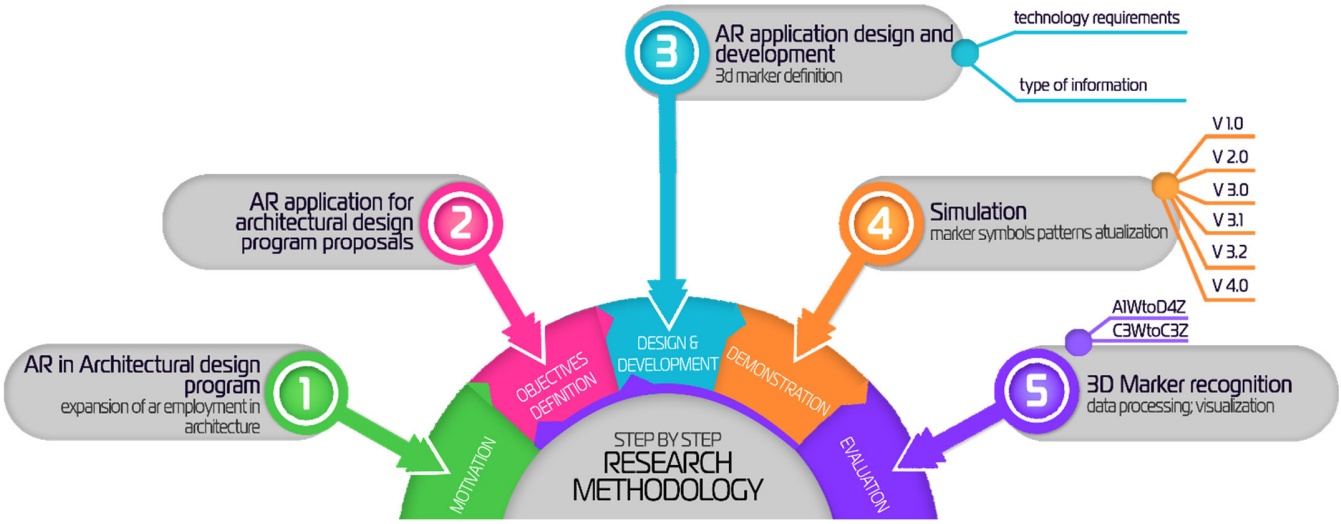

Fig. 1 Research Methodology Infographic
Font: authors.

For AR visualization, some aspects are considered based on equipment, element recognition, and computer-generated graphics associated. Different AR types exist influenced by how real environments are tracked and associated with digital models. Marker-based AR, markless AR, projections-based AR, and superimposition-based AR demand different construction approaches. In this research, a marker-based AR app was built using a tridimensional marker inspired by the Rubik's Cube.

Other AR technologies also use cubes to depict virtual 3D objects, as the MERGE Cube. Within this app, all cube faces are tracked simultaneously, and its rotation indicates the corresponding rotation of the associated digital model. The MERGE Cube app is based on a specific static cube recognition and objects displayed vary according to user theme selection in a pre-defined gallery.

Differently, the app created in this research intended to track configurable cube faces a proposal that seeks to guarantee tool-user interaction. In other words, we seek to enable app-users to modify the cube using different face combinations to evaluate architectural briefing alternatives. This way, digital models would be automatically generated and visualized from the cube faces modification making it possible for a single 3D marker to display diverse results

B. Characteristics of the physical 3D Marker Design

1. Physical 3D Marker Design

Although a Rubik's Cube has three degrees of freedom (3DoF), we proposed to use only one degree of freedom (1DoF), with three rows named "α", "β", and "γ" (Figure 2, original Rubik's Cube and axes, and Proposed Cube). The other two axes of the original cube were blocked, otherwise, it could over-complicated and unfriendly or impossible.

Such properties imposed upon the cube operation caused two faces to be blocked, while the other four could still vary by row spinning. Each row commanded a type of information, and three functions were established, two of them relating to geometric forms and one to the association of these forms. Row α refers to a cube, row β refers to a sphere, row γ refers to the association between the cube and the sphere.

In total, 64 results are possible, a number calculated according to the Fundamental Counting Principle (FCP), or counting rule, of combinatorial analysis (Figure 2, Number of Variations). FCP considers steps and moves association to determine possibilities. In this case, there are 3 steps, the rows "α", "β", and "γ", and 4 moves, the 4 cells of each row. An overview of the calculation is also shown in Figure 2, on the right side.

Each cell combination means a different cube configuration is created. Rows α and β promote scale variation, and row γ associate cube and sphere differently as face juxtaposition, face intersection, edge intersection, and edge juxtaposition. To better manage all variations, each cell of a row is named to make it easier to refer to them and associate the results. This way, cells of the α row (cuboid shape at different scales) are called "A"; "B", "C", and "D"; cells of the β row (spherical shape at different scales) are named "1", "2", "3", and "4"; and cells of the γ row (type of association) are "W", "X", "Y", and "Z". Figure 2, Cell Definition and Results, indicates these names and corresponding results.

Each cell of the physical marker received a different graphic representation to relate to the behavioral rules settled and to promote the visual association to digital results. For instance, in "row α - cell A" there is one square representing the 1st scale of the cube; in "cell B" there are two squares with different sizes; in cell C, three squares; and finally in cell D, four squares.

The same happens in row β regarding the sphere, and in row γ the type of association is depicted. A diverse combination of cells offers a set of cubes and spheres at different scales combined according to four variations, and at the bottom of Figure 2 that is an illustration of four of the possible combinations and one version of the design for the cells.

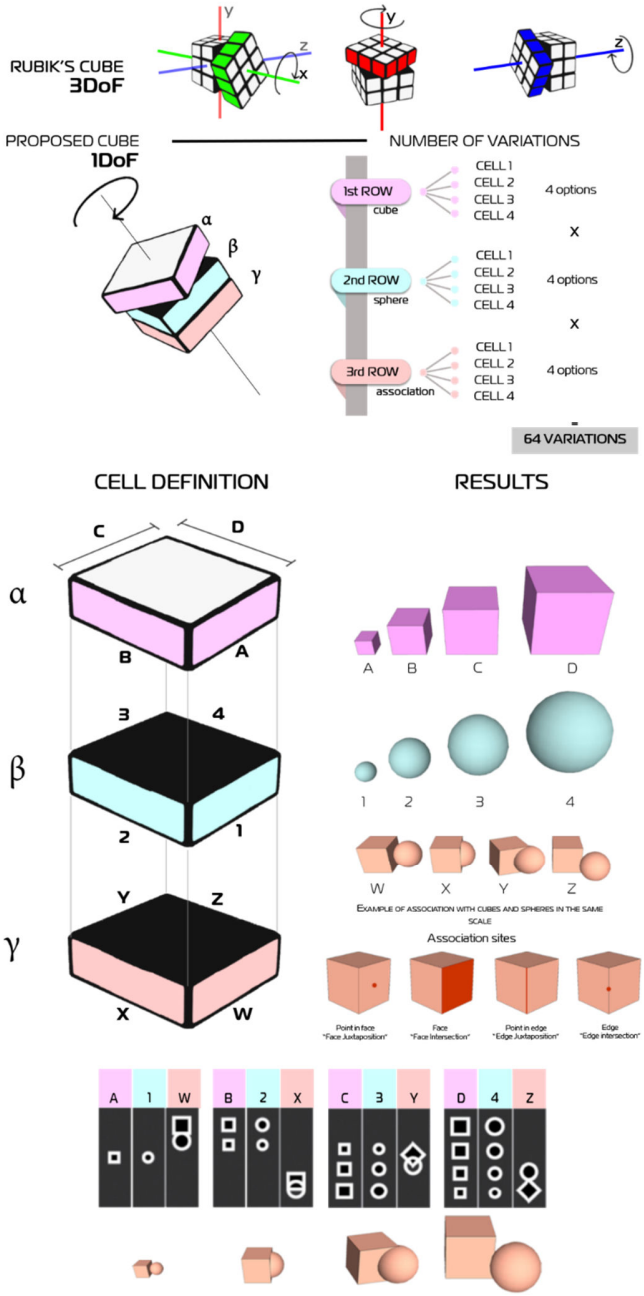

Fig. 2 Rubik's Cube, Proposed Cube mechanism and variations, Cells with corresponding results; and Example of graphic representation associated to markers
Font: authors.

C. App Development

Two steps were necessary to develop the app: (1) Definitions for 3D virtual model development - Rhino 5 associated with Grasshopper, an algorithmic modeling plugin; (2) Definitions for AR app development - Unity associated with Vuforia Software Development Kit (SDK), and tool visual design.

1. Rhinoceros & Grasshopper

Rhino with Grasshopper plugin was used for 3D digital models' construction, to the creation of the models to be superimposed with the physical marker. Within Grasshopper, one group of rules refers to the cube construction (Figure 3 - highlighted in pink rectangles) and the other four to the spheres in different associations to the cube (Figure 3 - highlighted in red, green, blue, and yellow rectangles).

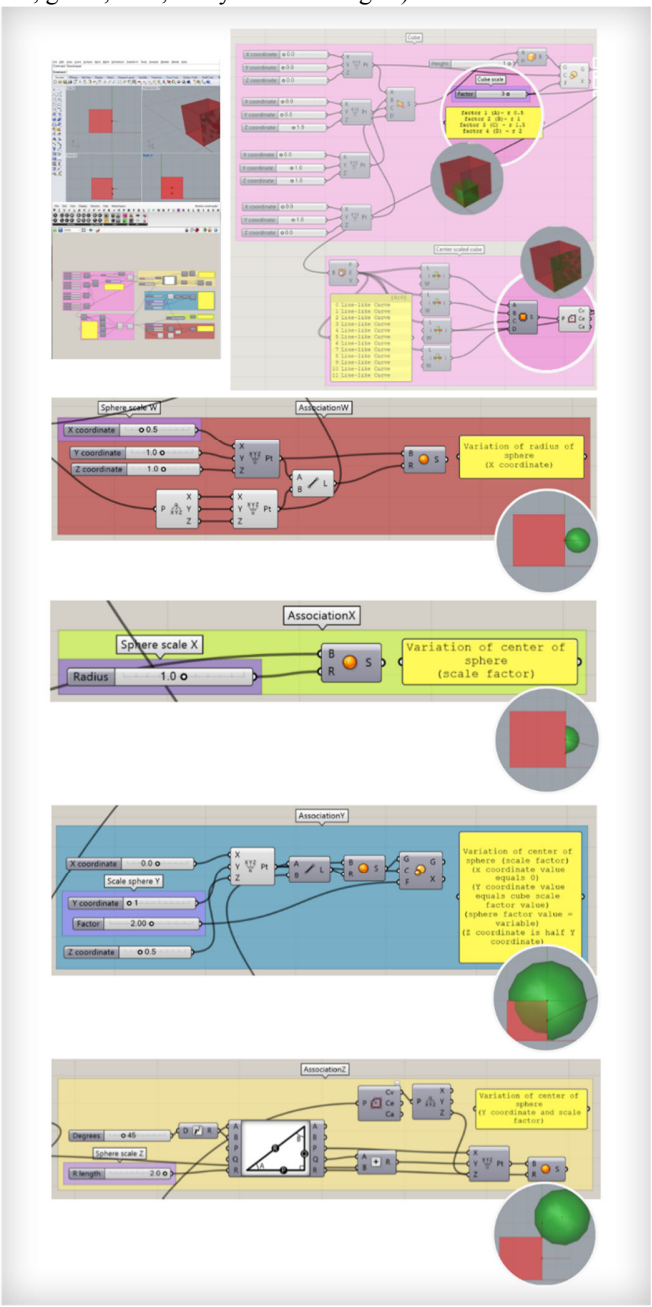

Fig. 3 Rhino Grasshopper interface
Font: Rhino/Grasshopper interface

For the cube design, four base points were determined

alongside a height value. Later, four scale factors (SF) were established varying from 1 to 4 in a proportion of growth indicating cubes A, B, C, and D (Figure 3). This scale variation is based on the size of the Rubik's Cube. Scale factor 1 (SF1) indicates the digital cube has the same size as the physical cube (size of 1 unit in Grasshopper), which represents a cube of 1x1x1u. SF2 has 1,5u, SF3 has 2u, and SF4, 2,5u. At last, one cube face was selected as a reference for sphere connection (Figure 3, in pink).

Sphere and cube were connected in four different ways. Therefore, we implemented four scripts whose parameters control sphere scale and positioning. Association "W" refers to the sphere juxtaposition to the cube (Figure 3, in red). To enable this connection, the center of the selected cube reference face was identified and used to guide sphere design. At this association, if we modify the cube SF, the values of the coordinates y and z of the sphere must be changed as well. The sphere SF is defined to be related to its radius, thus equal to the x coordinate value.

For the "X" association another script was written (Figure 3, in green). By connecting the sphere center to the center of the selected cube reference face we could establish the face intersection relation. This way, whenever the SF of the cube is modified, so is automatically the position of the sphere. The only variable manually modified in this case is the sphere SF which was named "radius".

A third script was created to design the "Y" association (Figure 3, in blue). Such geometry was described and controlled by four parameters responsible for connecting the sphere center to one edge's center of the cube, creating the edge intersection. To do so, the x coordinate value remains 0 in all cases, the y coordinate equals the cube's SF, and the z coordinate value is half of the y coordinate. The fourth parameter controls the sphere SF and is updated according to the cube SF.

The design of the "Z" association follows the code presented in Figure 3, in yellow. This association is called edge juxtaposition and the sphere location was calculated using a rectangle triangle trigonometry rule. The sphere SF is determined by changing "R length" values, which correspond to half of the cube's SF values.

2. Unity Project with Vuforia Engine

To develop the AR app, Vuforia SDK for Unity Engine was used. Initially, a multi target marker (cuboid) was selected inside the Vuforia target manager area. The cuboid marker requires six images to be constructed (Figure 4, top). Image attributes must be verified in the Vuforia online system of target star rating to enable the best detection and tracking. In this study, we used the ".png" file format for an RGB image with 60-100 KB, that received between 4 and 5-star ratings. Then, the cube dimensions were set according to a regular Rubik's Cube size.

After configuring markers and downloading the database from Vuforia, we imported both database and Rhino ".fbx" files inside Unity (Figure 4, bottom). Each model was associated with the corresponding marker. In addition, rotation and scale values of the models were updated within Unity to adapt them to the marker's size. In the experiment, the smaller model superimposes the exact size of the physical cube (6 x 6 cm). The largest model is 2.5 the size of the smallest - this value was settled aiming for the best fit in smartphone screens.

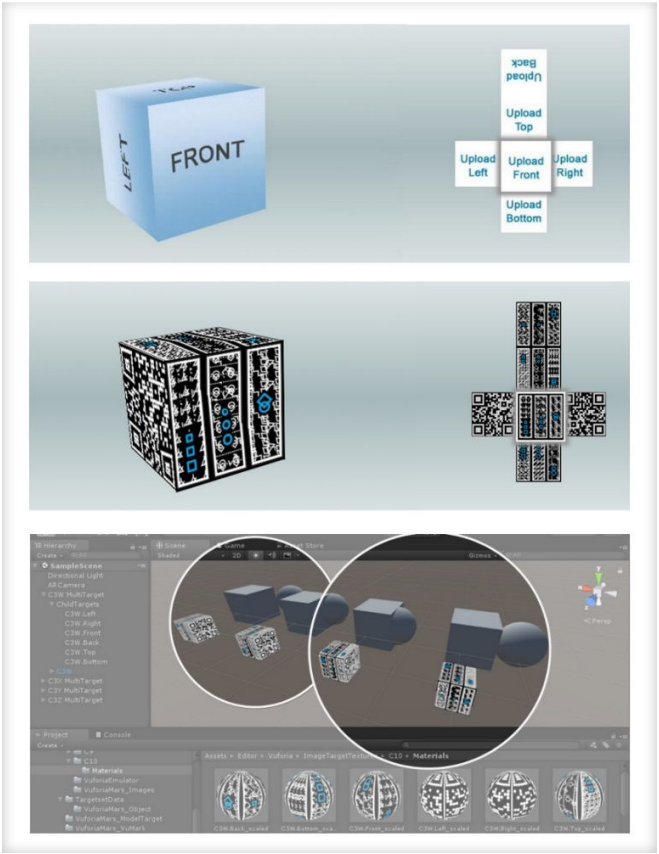

Fig. 4 Development interface of the cuboid marker in Vuforia and Marker-model association in Unity Engine
Font: Authors, from the Vuforia Engine and Unity Engine interfaces.
*For didactic reasons, the Cuboid markers being created are temporarily positioned in front of the digital 3D models to show their relation. Later, the digital models and the cuboid marker are superimposed.
Font: Authors, from the Unity Engine interface

IV. Results and Discussion

Tests were undertaken to analyze the performance of the targets created. To assess how the cube modification (rows rotation) regulates 3D model visualization, a series of studies was conducted. In this section, we describe the evaluation processes and the upgrades on tracking stability and target detection. Later, we discuss whether the research goals were achieved.

A. App development overview

To begin this process, as previously mentioned, Rhino/Grasshopper and Unity/Vuforia were defined to develop digital models, couple models, and targets, and create an AR visualization app. To test the app regarding detection, efforts in this study focused on working with a small sample of analysis. The design of the evaluation process was based on a specific

objective: to evaluate the capacity of the tracking system to correctly show the 3D models associated with the cuboid marker in each cell association.

To that end, we decided to set out the tests based on two groups of cell association. Criteria for selecting the groups were as follows:

1) First group:
a) Models/faces: A1W, B2X, C3Y, and D4Z.
b) Row rotation: No, all rows fixed.
2) Second group:
a) Models/faces: C3W, C3X, C3Y, and C3Z.
b) Row rotation: Yes, γ row. α and β rows fixed.

This way we were able to assess target detection, contrasting the results with and without row rotation.

B. App demonstration and evaluation

Several versions of apps were created due to the modification of cuboid markers assembly and image-pattern design. For each version, errors related to tracking stability and target detection were systematically registered and adjusted for the next version. From this in-depth investigation and arising adjustments, six variations for image patterns for cube faces were generated, Figure 5 (top). The first column represents the tests with QR codes as targets, which are simpler images due to their type of patterns. More complex drawing patterns were created in later versions (3.0, 3.1, 3.2, 4.0).

We noticed, as specified in Vuforia documentation, that the more detail and contrast on the one hand, and the less repetitive patterns on the other, the better target detection. For every modification in the targets' design, the new ones were uploaded to Vuforia and analyzed first by its Target Manager system. Amongst the versions, 4.0 was better rated due to a more complex target design.

The targets were printed and pasted in a Rubik's Cube. To ensure the detection of the entire cube as a 3D marker, QR codes were pasted on the fixed faces. Figure 5 (bottom) presents three physical cubes with different versions of targets on them.

During this process, other important aspects were considered. First, the patterns of each cell should be different from each other, which meant the creation of 12 variations. This was necessary because once it is possible to spin the three rows (α, β, γ), thus combining the rows freely, they need to be identified as unique elements that are put together to build one face. Second, the Vuforia camera focus influenced the tracking system, therefore requiring the inclusion of a C# script during app development to control this feature.

1. Testing Process

Following the creation of each version of the image patterns, a sequence of tests for cube detection in AR was conducted. In the first two versions we chose to only assess image recognition, and randomly observed the superimposition of the 3D models on the cube. A high level of tracking issues was observed in versions 1.0 and 2.0. This result may be explained by the lack of detail and contrast in such images.

From version 3.0 onward, we created a more systematic testing system for target assessment, as the Vuforia Target Manager system started to increase the image patterns' rating. The method adopted enabled us to evaluate the targets, evolving their design towards better trackable ones. The performance was assessed in four steps:

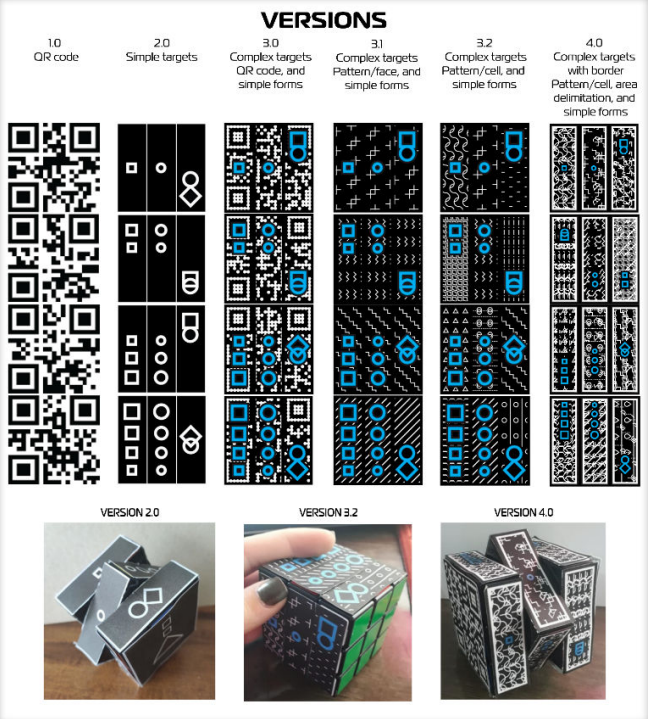

Fig. 5 Pattern variation of the four faces of the 6 versions of the cuboid markers (top), and Test for cuboid marker with tracking images (bottom)

1) Define the model to be visualized and set the cube cells accordingly.
2) Track the face corresponding to the model wanted for 5 seconds and then rotate the cube for 5 seconds without hiding the previously - 40 times in total, 10 times each face.
3) Register output to keep track of results.
4) Calculate hit level.

We considered one hit every time one face was tracked and the right model was shown. With that process hit level was 22,50%, representing that only 9 out of 40 tracking results were correct, Figure 6, first example. This means that while tracking one specific face, another model appeared instead of the right one. Tracking the same faces using version 3.1 we had a significant reduction in this number: 2,5% of hit level. From version 3.2 we returned to 22,50% of hit level, a number that decreased again when using version 4.0 of image patterns.

Surprisingly, there was no evidence that pattern variation influenced the tracking system, and consequently the results. These results are likely to be related to the cube remaining unchanged (with no row rotation): for tracking each of the four faces mentioned (A1W, B2X, C3Y, D4Z) it was only necessary to rotate the cube as a whole entity.

The second set of trials intended to evaluate the effectiveness of the row variation to form diverse combinations of cells. The steps followed were the same, but they can be found in Figure

6, second example, along with different models expected to be visualized (C3W, C3X, C3Y, and C3Z). On the bottom of Figure 6, one can see this second example visualized in AR.

Once all the faces change in every case due to row "γ" rotation, we had a significantly better result. With version 3.0, we scored 42,50%. Version 3.1 presented 45% of the hit level. A decrease in the hit level in version 3.2 was observed (27,5%), these cuboids are unlikely to be tracked as different ones. They will be detected as the same cuboid.

Generally, therefore, although we had an increase in the level of hits of up to 77,5%, this result should be interpreted with caution, once one of the issues it represents is still lack of tracking precision. Despite the efforts to follow all Vuforia SDK instructions when building image patterns, 100% of hits

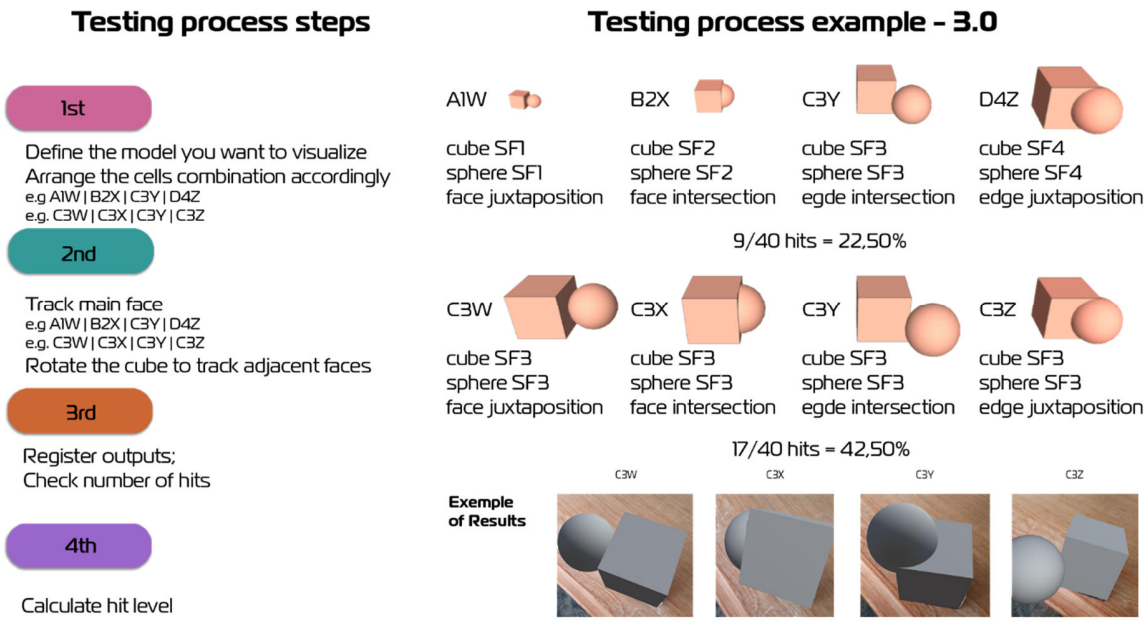

Fig. 6 Testing process steps and results (e.g.1 A1W-B2X-C3Y-D4Z, e.g.2 C3W-C3X-C3Y-C3Z), and AR examples

but a significant increase was detected with version 4.0: 77,5% of hits.

All the results were compiled in a single graph (Figure 7).

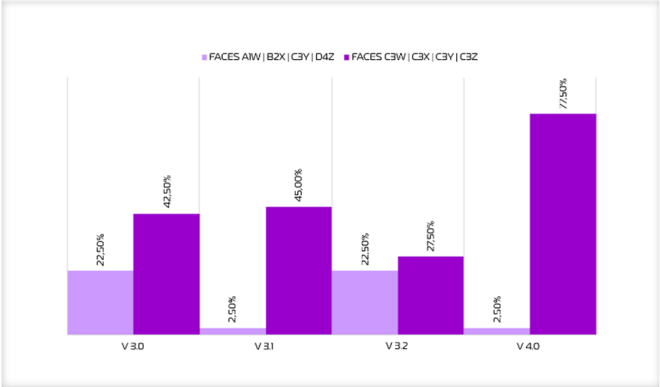

Fig. 7 Tracking results of versions

This experiment indicated that for tracking a cuboid format it is always necessary to first have a good rating of each face inside Vuforia Target Management. However, this only guarantees good tracking for a single cuboid. As we are inspired by Rubik's Cube, we must ensure that each cuboid is different from the other.

These findings suggest that in possession of six images, we can build several distinct cuboid markers by varying the position of the images according to the cuboid faces. However, were not yet achieved, which would frustrate potential users of the system. Hence, further investigation with more focus on other strategies to use a dynamic cube marker with face modification is suggested.

V.CONCLUSION

This study set out to develop an AR app with a configurable cuboid marker, inspired by the Rubik's Cube, to evaluate the app response with different proposals during the architectural program. The forms and associations proposed were based on the Design Patterns, an important source of information during the early stages of architectural design. The process of building such an AR system based on a configurable multi-target cube has been shown to be complex. An in-depth study of image patterns was conducted as an endeavor to increase the reliability levels of the AR system. In this case, this means the stability of displaying the right digital models related to the target associated.

Overall, the proposed system used a specific SDK that offered cuboid tracking, linking virtual models to the 3D object. In this research, we choose to work with cube and sphere models with different types of association as a concept proof for exploration regarding early phases of design. However, the strategy of developing an AR application using cuboid tracking provided a low-reliability level. The error rate presented by the system affected handling and visualizing briefing information.

Therefore, another strategy is needed to use the design patterns with AR in the early stages of the architectural design process. For that, it may be necessary to develop a specific system that would allow testing design alternatives.

Nevertheless, this research stands that AR can be employed in the early stages of architectural design, but first, the system must be consistent with the user input of information. Thereby, the main contribution of this work is to set the ground for looking deep into AR tools for briefing design, challenging the investigation of the AR potentials in the field of architectural design, specifically its early stages. This is the first attempt, in the literature, to address the design patterns in an AR system. This research provides such a change in perspective that can continue to be investigated to reach an adequate level of responsiveness.

Future studies on the current topic might turn, for instance, to analyze different strategies to incorporate more interaction options through a user interface. One way is creating a digital interface coupled with a cuboid marker, where a button-labeled menu would help changing the features of the geometric forms like size, color, shape, among others. Using this type of marker associated with other commands in the AR user interface could create a design environment that provides a variety of possibilities. This association might allow the connection of digital with the physical, one of the strengths of an AR tool, which supports multiple combinations towards changing the virtual object. Later, user tests should be developed regarding the context of the intended design.

ACKNOWLEDGMENT

The authors acknowledge the participation of Christina Figueiredo Prudencio during the course where we first had the idea and developed a first prototype and set of tests using the cuboid maker.

REFERENCES

[1] 1. Abdullah HK, Hassanpour B. Digital design implications: a comparative study of architecture education curriculum and practices in leading architecture firms. Int J Technol Des Educ [Internet]. 2020 Jan 2 [cited 2021 Mar 18]; Available from: https://doi.org/10.1007/s10798-019-09560-2

[2] 2. Roupé M, Johansson M, Maftei L, Lundstedt R, Viklund-Tallgren M. Virtual Collaborative Design Environment: Supporting Seamless Integration of Multitouch Table and Immersive VR. Journal of Construction Engineering and Management. 2020 Dec 1;146(12):04020132.

[3] 3. Zardo P, Mussi AQ, Silva JL da. The interfaces between technologies and the design process in AEC industry. In: Sousa, JP, Xavier, JP and Castro Henriques, G (eds), Architecture in the Age of the 4th Industrial Revolution - Proceedings of the 37th eCAADe and 23rd SIGraDi Conference - Volume 1, University of Porto, Porto, Portugal, 11-13 September 2019, pp 369-378 [Internet]. Porto: CUMINCAD; 2019 [cited 2018 Oct 23]. Available from: http://papers.cumincad.org/cgi-bin/works/paper/ecaadesigradi2019_144

[4] 4. Pantazis E, Gerber D. A framework for generating and evaluating façade designs using a multi-agent system approach. International Journal of Architectural Computing. 2018 Dec 1;16(4):248–70.

[5] 5. Kalay YE. Architecture's New Media: Principles, Theories, and Methods of Computer-Aided Design. Cambridge, London: The MIT Press; 2004.

[6] 6. van Krevelen R, Poelman R. A Survey of Augmented Reality Technologies, Applications and Limitations. The International Journal of Virtual Reality. 2010;9:1–20.

[7] 7. Fazel A, Izadi A. An interactive augmented reality tool for constructing free-form modular surfaces. Automation in Construction. 2018 Jan;85:135–45.

[8] 8. Lawson B. How Designers Think: The Design Process Demystified. Edição: 4. Routledge; 2006. 320 p.

[9] 9. Kowaltowski DCCK, Moreira D de C. O programa arquitetônico. In: Kowaltowski DCCK, Moreira D de C, Petreche JRD, Fabricio MM, editors. O processo de projeto em arquitetura: da teoria à tecnologia. São Paulo: Oficina de Textos; 2011. p. 101–8.

[10] 10. White ET. Introduction to Architectural Programming. Tucson: Architectural Media; 1972.

[11] 11. Bueno E, Turkienicz B. Supporting Tools for Early Stages of Architectural Design. International Journal of Architectural Computing. 2014 Dec;12(4):495–512.

[12] 12. Erdolu E. Lines, triangles, and nets: A framework for designing input technologies and interaction techniques for computer-aided design. International Journal of Architectural Computing. 2019 Dec 1;17(4):357–81.

[13] 13. Baldessin GQ, Vizioli SHT. A Aplicação De Softwares De Arquitetura E A Utilização Da Linguagem Visual Nos Trabalhos De Graduação Integrado. In: Anais GRAPHICA 2017 - XII International Conference on Graphics Engineering for Arts and Design [Internet]. Araçatuba; 2018 [cited 2019 Sep 27]. Available from: https://even3.com.br/anais/graphica201749633-A-APLICACAO-DE-SOFTWARES-DE-ARQUITETURA-E-A-UTILIZACAO-DA-LINGUAGEM-VISUAL-NOS-TRABALHOS-DE-GRADUACAO-INTEGRADO

[14] 14. Rocha APS, Moreira D de C. O Diagrama e o design da informação na arquitetura contemporânea. Arcos Design. 2014 Jun 1;8(1):49–61.

[15] 15. Xu X, Ma L, Ding L. A Framework for BIM-Enabled Life-Cycle Information Management of Construction Project. International Journal of Advanced Robotic Systems. 2014 Aug 22;11(8):126.

[16] 16. Tepavcevic B, Stojakovic V. Shape grammar in contemporary architectural theory and design. Facta universitatis - series: Architecture and Civil Engineering. 2012;10(2):169–78.

[17] 17. Celani G. Shortcut to the Fourth Industrial Revolution: The case of Latin America. International Journal of Architectural Computing. 2020 Jul 15;1478077120942193.

[18] 18. Cuperschmid ARM. Realidade Aumentada no processo de projeto participativo arquitetônico : desenvolvimento de sistema e diretrizes para utilização [Internet]. [Campinas]: Faculdade de Engenharia Civil, Arquitetura e Urbanismo/Universidade Estadual de Campinas; 2014 [cited 2020 Mar 27]. Available from: http://repositorio.unicamp.br/jspui/handle/REPOSIP/257945

[19] 19. Laato S, Rauti S, Islam AKMN, Sutinen E. Why playing augmented reality games feels meaningful to players? The roles of imagination and social experience. Computers in Human Behavior [Internet]. 2021;121. Available from: https://www.scopus.com/inward/record.uri?eid=2-s2.0-85104084803&doi=10.1016%2fj.chb.2021.106816&partnerID=40&md5=8b5f6c131217859445e62cf287a83416

[20] 20. Fazio S, Turner J. Bringing empty rooms to life for casual visitors using an AR adventure game: Skullduggery at Old Government House. Journal on Computing and Cultural Heritage [Internet]. 2020;13(4). Available from: https://www.scopus.com/inward/record.uri?eid=2-s2.0-85098144009&doi=10.1145%2f3418037&partnerID=40&md5=e3d1406cd91d09b706a84878c1c1353d

[21] 21. Fusté-Forné F. Mapping heritage digitally for tourism: an example of Vall de Boí, Catalonia, Spain. Journal of Heritage Tourism. 2020;15(5):580–90.

[22] 22. Koo S, Kim J, Kim C, Kim J, Cha HS. Development of an augmented reality tour guide for a cultural heritage site. Journal on Computing and Cultural Heritage [Internet]. 2019;12(4). Available from: https://www.scopus.com/inward/record.uri?eid=2-s2.0-85075639514&doi=10.1145%2f3317552&partnerID=40&md5=7f369fa00430c90020e421b8f66285f9

[23] 23. Pettijohn KA, Peltier C, Lukos JR, Norris JN, Biggs AT. Virtual and augmented reality in a simulated naval engagement: Preliminary comparisons of simulator sickness and human performance. Applied Ergonomics [Internet]. 2020;89. Available from: https://www.scopus.com/inward/record.uri?eid=2-s2.0-85087669370&doi=10.1016%2fj.apergo.2020.103200&partnerID=40&md5=68bce15eaf03cfb90403db4c3ad8ccf4

[24] 24. Tiwari A, Verma S, Chand T, Shravan Kumar RR, Karar V. A comparative study on display sources for augmented reality-based

technology in defense applications. Journal of Optics (India). 2019;48(3):302–7.
[25] 25. Wang X. Augmented Reality in Architecture and Design: Potentials and Challenges for Application. International Journal of Architectural Computing. 2009 Jun;7(2):309–26.
[26] 26. Schlickman E. GOING AFIELD: EXPERIMENTING WITH NOVEL TOOLS AND TECHNOLOGIES AT THE PERIPHERY OF LANDSCAPE ARCHITECTURE. Landsc Archit Front. 2019 Apr 15;7(2):84–91.
[27] 27. Endsley TC, Sprehn KA, Brill RM, Ryan KJ, Vincent EC, Martin JM. Augmented Reality Design Heuristics: Designing for Dynamic Interactions. Proceedings of the Human Factors and Ergonomics Society Annual Meeting. 2017 Sep;61(1):2100–4.
[28] 28. Kontovourkis O, Georgiou C, Stroumpoulis A, Kounnis C, Dionyses C, Bagdat S. Implementing Augmented Reality for the Holographic Assembly of a Modular Shading Device. In: Sousa, JP, Xavier, JP and Castro Henriques, G (eds), Architecture in the Age of the 4th Industrial Revolution - Proceedings of the 37th eCAADe and 23rd SIGraDi Conference - Volume 3, University of Porto, Porto, Portugal, 11-13 September 2019, pp 149-158 [Internet]. Porto: CUMINCAD; 2019 [cited 2018 Oct 23]. Available from: http://papers.cumincad.org/cgi-bin/works/paper/ecaadesigradi2019_506
[29] 29. Khan A, Sepasgozar S, Liu T, Yu R. Integration of BIM and Immersive Technologies for AEC: A Scientometric-SWOT Analysis and Critical Content Review. Buildings. 2021 Mar;11(3):126.
[30] 30. Casanova M, Greppi A. RESIDENTIAL BUILDINGS BY GIUSEPPE TERRAGNI IN COMO: PROPOSALS FOR INTEGRATION BETWEEN RESEARCH, COMMUNICATION AND VALORISATION OF HERITAGE. In: The International Archives of the Photogrammetry, Remote Sensing and Spatial Information Sciences [Internet]. Copernicus GmbH; 2019 [cited 2021 Jul 19]. p. 379–85. Available from: https://www.int-arch-photogramm-remote-sens-spatial-inf-sci.net/XLII-2-W11/379/2019/
[31] 31. Erzetic C. Enhancing User-Engagement in the Design Process through Augmented Reality Applications. In: Sousa, JP, Xavier, JP and Castro Henriques, G (eds), Architecture in the Age of the 4th Industrial Revolution - Proceedings of the 37th eCAADe and 23rd SIGraDi Conference - Volume 2, University of Porto, Porto, Portugal, 11-13 September 2019, pp 423-432 [Internet]. Porto: CUMINCAD; 2019 [cited 2018 Oct 23]. Available from: http://papers.cumincad.org/cgi-bin/works/paper/ecaadesigradi2019_027
[32] 32. Janusz J. Toward The New Mixed Reality Environment for Interior Design. IOP Conf Ser: Mater Sci Eng. 2019 Feb 1;471(10):102065.
[33] 33. Rahimian FP, Chavdarova V, Oliver S, Chamo F. OpenBIM-Tango integrated virtual showroom for offsite manufactured production of self-build housing. Automation in Construction. 2019 Jun 1;102:1–16.
[34] 34. Baratta AFL, Finucci F, Magarò A. Regenerating Regeneration: augmented reality and new models of minor architectural heritage reuse. VITRUVIO - International Journal of Architectural Technology and Sustainability. 2018 Dec 26;3(2):1–14.
[35] 35. Hernández JL, Martín Lerones P, Bonsma P, Van Delft A, Deighton R, Braun J-D. An IFC Interoperability Framework for Self-Inspection Process in Buildings. Buildings. 2018 Feb;8(2):32.
[36] 36. Rasmussen TA, Merritt T. ProjecTables: Augmented CNC tools for sustainable creative practices. International Journal of Architectural Computing. 2018 Sep 1;16(3):227–42.
[37] 37. Ayer SK, Messner JI, Anumba CJ. Augmented Reality Gaming in Sustainable Design Education. Journal of Architectural Engineering. 2016 Mar 1;22(1):04015012.
[38] 38. Gimenez-Mateu L, Navarro-Delgado I, Santana-Roma G, Redondo-Dominguez E. Application of ICT in the processes of design and construction of an Orthodox Church. Revista de la construcción. 2016 Aug;15(2):55–68.
[39] 39. Quattrini R, Pierdicca R, Frontoni E, Barcaglioni R. VIRTUAL RECONSTRUCTION OF LOST ARCHITECTURES: FROM THE TLS SURVEY TO AR VISUALIZATION. Int Arch Photogramm Remote Sens Spatial Inf Sci. 2016 Jun 15;XLI-B5:383–90.
[40] 40. Tonn C, Petzold F, Bimber O, Grundhöfer A, Donath D. Spatial Augmented Reality for Architecture — Designing and Planning with and within Existing Buildings. International Journal of Architectural Computing. 2008 Jan;6(1):41–58.
[41] 41. Seichter H. Augmented Reality Aided Design. International Journal of Architectural Computing. 2003 Dec;1(4):449–60.
[42] 42. Alsafouri S, Ayer SK. Leveraging Mobile Augmented Reality Devices for Enabling Specific Human Behaviors in Design and Constructability Review. Advances in Civil Engineering. 2019 Apr 1;2019:e3951986.
[43] 43. Liu Y-C, Kao C-Y, Chakrabarti A, Chen C-H. Innovation-supporting tools for novice designers: Converting existing artifacts and transforming new concepts. Advances in Mechanical Engineering. 2016 Jun 1;8(6):1687814016651370.
[44] 44. Kipper G, Rampolla J. Augmented Reality: An Emerging Technologies Guide to AR [Internet]. 1st ed. Waltham: Syngress; 2013 [cited 2020 Mar 13]. Available from: https://www.elsevier.com/books/augmented-reality/kipper/978-1-59749-733-6
[45] 45. Hofmann S, Mosemghvdlishvili L. Perceiving spaces through digital augmentation: An exploratory study of navigational augmented reality apps. Mobile Media & Communication. 2014 Sep 1;2(3):265–80.
[46] 46. Tsai C-H, Huang J-Y. Augmented reality display based on user behavior. Computer Standards & Interfaces. 2018 Jan 1;55:171–81.
[47] 47. Barba E. Toward a language of mixed reality in the continuity style. Convergence. 2014 Feb 1;20(1):41–54.
[48] 48. Souza LN de, Kowaltowski DCCK, Woolner P, Moreira D de C. School design patterns supporting learning through play. International Journal of Play. 2020 May 21;0(0):1–28.
[49] 49. Souza LN de. Arquitetura escolar, parâmetros de projeto e modalidades de aprendizagem [Internet] [Dissertação]. [Campinas]: Universidade Estadual de Campinas; 2018 [cited 2019 Nov 12]. Available from: http://repositorio.unicamp.br/jspui/handle/REPOSIP/331683
[50] 50. Nair P, Fielding R, Lackney J. The Language of School Design: Design Patterns for 21st Century Schools. Minneapolis: DesignShare; 2013.
[51] 51. Rittel H. Design methods: Theories, Research, Education and Practice. Impressions of Architecture 130: Notes and Observations on Professor Host W J Rittel's Classic Methods Course at Berkeley as Taught circa-1969-1974. 1995 Mar;29:2109–56.
[52] 52. White ET. Space Adjacency Analysis: Diagramming Information for Architectural Design. Tucson: Architectural Media; 1995.
[53] 53. Rowe PG. Design Thinking. Cambridge; London: The MIT Press; 1992.
[54] 54. Alexander C, Ishikawa S, Silverstein M. A pattern language: towns, buildings, construction. New York: Oxford University Press; 1977.
[55] 55. Andrade MLVX de, Ruschel RC, Daniel de C. Moreira. O processo e os métodos. In: Kowaltowski DCCK, Moreira D de C, Petreche JRD, Fabricio MM, editors. O Processo de Projeto em Arquitetura: da Teoria à Tecnologia. Edição: 1. São Paulo: Editora Oficina de Textos; 2011.
[56] 56. Bielefeld B, Khouli SE. Basics Design Ideas. Boston/Berlin, MA: Birkhauser Architecture; 2019. 80 p.
[57] 57. Peffers K, Tuunanen T, Rothenberger MA, Chatterjee S. A design science research methodology for information systems research. Journal of management information systems. 2007;24(3):45–77.
[58] 58. Dresche A, Lacerda DP, Antunes Jr. JAV. Design Science Research: A Method for Science and Technology Advancement. Porto Alegre: Springer; 2015.
[59] 59. Goldschmidt G. Linkography: Unfolding the Design Process. Cambridge: The MIT Press; 2014.
[60] 60. Jones C. Informe sobre la situación de la metodología del diseño. In: Broadbent G, editor. Metodología del diseño arquitectónico. Barcelona: Gustavo Gili; 1971. p. 385–95.

The Study of Thai Millennial Attitude toward End-Of-Life Planning

Rawissara Mawong

***Abstract*—** Millions of young people around the world have been affected by Covid-19 to their psychological and social effects. Millennials' stresses have been shaped by a few of the global issues, including climate change, political instability, and financial crisis. In particular, the spread of COVID-19 has become laying psychological and socioeconomic scars on them. When end-of-life planning turns into more widely discussed, the stigma and taboos around this issue are greatly lessened. End-of-life planning is defined as a future life plan, such as financial, legacy, funeral, and memorial planning. This plan would help millennials to discover the value and meaning of life.

This study explores the attitudes of Thai Millennials toward an end-of-life planning as a new normal awareness of life in order to initiate an innovative service solution to fit with their value and meaning. The study conducts an in-depth interview with 12 potential participants, who have awareness or action on the plan. The framework of customer journey map is used to analyze the responses to examine trigger points, barriers, believes, and their expectations.

The findings point to a service solution that improves knowledge of significant life worth, rather than death planning, encouraging people to reassess their lives in a positive way, resulting in higher self-esteem and intrinsic motivation, in this time of global crisis, to this generation.

***Keywords*—** End-of-life Planning, Millennial Generation, Service Design Solution, User Journey.

Rawissara Mawong is with the King Mongkut's University of Technology Thonburi, Thailand (e-mail: rawissara.m@mail.kmutt.ac.th).

Development of Non-Intrusive Speech Evaluation Measure using S-Transform and Light-GBM

A. Tusar Kanti Dash, B. Ganapati Panda

***Abstract*—** The evaluation of speech quality and intelligence is critical to the overall effectiveness of the Speech Enhancement Algorithms. Several intrusive and non-intrusive measures are employed to calculate these parameters. Non-Intrusive Evaluation is most challenging as very often, the reference clean speech data is not available. In this paper, a novel non-intrusive speech evaluation measure is proposed using audio features derived from the Stockwell transform. These features are used with the Light Gradient Boosting Machine for the effective prediction of speech quality and intelligibility. The proposed model is analyzed using noisy and reverberant speech from four databases and the results are compared with the standard Intrusive Evaluation Measures. It is observed from the comparative analysis that the proposed model is performing better than the standard Non-Intrusive models.

***Keywords*—** Non-Intrusive Speech Evaluation, S-Transform, Light GBM, Speech Quality, and Intelligibility

A. Dr. Tusar Kanti Dash is with the Electronics and Telecommunications Engineering, C V Raman Global University, Bhubaneswar, 752054, India (phone: 91-9337256321; e-mail: tusar@cvrce.edu.in).

B. Dr. Ganapati Panda is with the Electronics and Telecommunications Engineering, C V Raman Global University, Bhubaneswar, 752054, India (phone: 91-9437048906; e-mail: ganapati.panda@gmail.com)

An Alternative to Resolve Land Use Conflicts: the Rétköz Lake Project

Balázs Kulcsár PhD
associate professor
University of Debrecen Faculty of Engineering
Department of Basic Technical Studies
E-mail: kulcsarb@eng.unideb.hu

Abstract
Today, there is no part of the world that does not bear the mark of man in some way. This process seems unstoppable. So perhaps the best thing we can do is to touch that handprint gently and with the utmost care. There are multiple uses for the same piece of land, the coordination of which requires careful and sustainable spatial planning. The case study of the Rétköz lake in north-eastern Hungary illustrates a habitat rehabilitation project in which a number of human uses were coordinated with the conservation and restoration of the natural environment. Today, the good condition of the habitat can only be maintained artificially, but the project has paid particular attention to finding a sustainable solution. The rehabilitation of Lake Rétköz is considered a good practice in resolving land-use conflicts.

Keywords
sustainability, ecosystem service, land-use conflict, landscape utilization

Objectives
Present a project and its outcome, which is a good and sustainable practice for resolving land-use conflicts.

Methodologies
Case study.

Main Contributions
Human landscape use can be reconciled with the conservation and sustainable management of habitats.

Grey Wolf Optimization Technique for Predictive Analysis of Products in E-Commerce – An Adaptive Approach

Ms. Shital S. Borse
ME Student, Department of Information Technology
Terna Engineering College, Nerul, Navi Mumbai, India
shitalborse29@gmail.com

Mrs. Vijayalaxmi Kadrolli
Associate Professor, *Department of Information Technology*
Terna Engineering College, Nerul, Navi Mumbai, India
vijayalaxmikadroli@ternaengg.ac.in

Abstract. E-commerce industries nowadays implement the latest AI, ML Techniques to improve their own performance and prediction accuracy. This helps to gain a huge profit from the online market. Ant Colony Optimization, Genetic algorithm, Particle Swarm Optimization, Neural Network & GWO help many e-commerce industries for up-gradation of their predictive performance. These algorithms are providing optimum results in various applications, such as stock price prediction, prediction of drug-target interaction & user ratings of similar products in e-commerce sites, etc. In this study, customer reviews will play an important role in prediction analysis. People showing much interest in buying a lot of services& products suggested by other customers. This ultimately increases net profit. In this work, a convolution neural network (CNN) is proposed which further is useful to optimize the prediction accuracy of an e-commerce website. This method shows that CNN is used to optimize hyperparameters of GWO algorithm using an appropriate coding scheme. Accurate model results are verified by comparing them to PSO results whose hyperparameters have been optimized by CNN in Amazon's customer review dataset. Here, experimental outcome proves that this proposed system using the GWO algorithm achieves superior execution in terms of accuracy, precision, recovery, etc. in prediction analysis compared to the existing systems.

Keywords: Prediction Analysis; E-Commerce; Machine Learning; Grey Wolf Optimization; Particle Swarm Optimization &CNN.

1 Introduction

Prediction analysis as a part of a modern analytic approach, utilizes (ML) Machine Learning, Statistical algorithms, (AI) Artificial Intelligence, Data Mining to examine current data, perform thorough analysis & realize many different ideas for best assessments in the future. [1-2]. In this paper, the customer reviews over a particular product are considered as an input for Sentiment analysis, which will generate a product rating. A catalog consists of a distinctive sequence of products, which are abruptly recognized by their brand, model, and key features & differ following a category of product. [3]. The algorithms used for this analysis are Convolutional Neural Network (CNN), Particle Swarm Optimization (PSO) & Grey Wolf Optimization (GWO) [4]. These algorithms have been utilized for the resolution of optimization difficulties.

GWO algorithm imitates a grading of leadership & hunting structure of the gray wolf in the wild. categories of grey wolves are α, β, δ, ω used to simulate the hierarchy of leadership. In addition, 3 main phases like prey hunting, enclosing prey, and attacking it, are implemented for accurate outcomes. Similarly, PSO is one of the bio-inspired algorithms, use to search for an optimal solution & in combination with it, the CNN base model is used because CNN is having higher prediction rate & depicts good accuracy for classification.

Sequence of the Research is explained as: Section 2 describes different ideas implemented in previous research or other papers, Section 3 explains about the subject matter and project mechanism developed in E-Commerce filed, Section 4 is proposed methodology description, Section 5 is regarding Experimental Results in deep, Comparison of the succeeded GWO model with other available models for consideration of its Prediction accuracy, and at the end, Section 7 is conclusion of a project with future scope.

2 Related Works

Sentiment analysis comes under Natural Language Processing (NLP) which extracts emotions related to some raw text data & implements them to social media posts and customer reviews for quick understanding like if the reviews are positive, negative, neutral & why. various techniques like Hybrid Clustering, Segmentation, Feature Extraction, Pattern Recognition are utilized in E-commerce, & most of them face problems in creating a model which gives an accurate comparison of hybrid algorithms automatically [11]. So, a different approach has been shown which works on 2-3 algorithms, optimize their hyperparameters, and give more and more accurate values for a future prospectus.

"Rasmiranjan Mohakud, Rajshree Dash, (2021) [11]" proposed a method for the development of a GWO-based optimized hyperparameter by CNN classifier to detect skin cancer disease, an inexpensive, automated CNN with GWO technology is being developed which recognize a categorization of skin cancer from input data and a clear justification has been observed that there is an improvement in solving a problem of multi-class skin grouping. The image pre-processing with BI

to resize the image, followed by the conversion of colour images to grayscale, and the Gaussian filter approach is integrated into a model for CNN training.
Sonsare, Pravin. (2020) [12], proposed a Long Short Term Memory Network Using Grey Wolf Optimization for Stock Price Prediction.it would improve the exactness of prediction of stock cost and help the investors. traditional LSTM and LSTM with GWO are designed. The results of LSTM with GWO shows better result than LSTM.
Sasikala, P., Mary Immaculate Sheela, L. (2020) [13] investigated a DLMNN technique which is proposed aimed at SA of online products review and an IANFIS technique has put forward a point at online products future prediction & execution of all techniques have been examined also this execution output helps paper to prove that a CLB framework and IANFIS were conducted effectively for SA & online products future prediction. In future, a solution to keyword processing problem can be found by extending this system & hybridization algorithm will improve its performance in succeeding prediction procedures.
Vrbančič, Grega & Zorman, Milan & Podgorelec, Vili. (2019) [14] proposed a GWOTLT technique which became carried out the use of GWO algorithm & execute it for an issue in recognition of brain haemorrhage from a head CT scan figures & effects received display better classification overall performance for all the measured classification metrics. a GWO-CNN version has been initiated in [15] for systematic network anomaly detection in cloud setups, in which CNN has applied to a category of anomaly also GWO has been implemented in conveying the multi-goal characteristic removal issue. On average, the proposed version reveals the development like 8.25% detection rate, 4.08% fake positives, also 3.62% accuracy in phrases, comparing it with conventional GWO with CNN [14].
"Singla, Zeenia & Randhawa, Sukhchandan & Jain, Sushma. (2017) [16]." Proposed a technique for Sentiment evaluation of purchaser product evaluations by the usage of machine learning. Online evaluations have turned out to be a platform for constructing faith and influencing buyer-shopping patterns. With such dependency, there may be a necessity to address this sort of the massive extent of evaluations and gift credible evaluations earlier than the consumer. Our studies is aiming to attain this through accomplishing sentiment evaluation of smartphone evaluations and classifying the evaluations into positive and negative sentiments. After balancing the statistics with a nearly identical ratio of positive and negative evaluations, three classification models were used. Among all three i.e., Naïve Bayes, SVM, and Decision Tree, SVM shows best results in predictive accuracy & accuracy outcomes were cross-tested and the very best price of accuracy became 81.75% for SVM most of the three classification models.

3 Proposed Methodology

In this work, the proposed system is divided into Seven prime stages:

- Data gathering
- Data pre-processing

- keyword withdrawal
- keyword optimization
- Model creation
- Model training and
- Model Performance.

Inputs were gathered from Amazon customer evaluation data files and pre-processing was important for improving Amazon data quality. This pre-processing is for the filtration of customer reviews & its categorization includes three modes (disinfection, stemming, elimination of stop words). disinfection means cleaning a dataset as per requirement, removing unwanted columns, emoji's, hashtags, symbols and spaces, in short sanitization of a dataset. Stemming transform words in a sentence into dictionary form to bring out appropriate motto [6]. Stop words are commonly used words in customer reviews like 'i', 'the', 'is', 'are' etc. Natural Language Processing (NLP) is helping in removing stop words. Keyword withdrawl depends on part of speech presented by every token in review, then sentiment recognizer also called keyword optimizer analyses ratings as positive or negative or neutral supported their polarity. The rating generator offers ratings to reviews depending upon every week client sentiments concerning merchandise. Finally, Rating Predictor accumulates the previous rating for predicting benefits & failure of products [4]. data feeding to the model is possible using CNN Architecture, Particle Swarm Optimization (PSO) &Gray Wolf Optimizer (GWO) were implemented for training a model & Model Performance is nothing but the output values in the form of Accuracy, Precision & Recall. Metaheuristic Algorithms are having hyperparameters, so to optimize it CNN is used.
An algorithmic rule hybridization is then applied to the clean information set i.e., in these project CNN base models is used along with PSO & GWO for hyper parameter tuning. Proper tuning of hyperparameters can improvise the complete working & results of the CNN, PSO, and GWO models. Hence, this intention has forced many researchers to address the adjustment of the hyperparameters of CNN, PSO, and GWO as an optimization problem. because generally GWO algorithm is used for classification problems & for the first time in this paper it has been used for the optimization of the E-commerce Prediction System. Particle swarm optimization [17] univariate dynamic encoding [18] and multilevel evolutionary optimization [19] are a few optimization methodologies, applying for the optimization of hyper-parameters of CNN.

3.1 Convolutional Neural Network (CNN):

CNN consists of a standard algorithm for optimization & also has some default loss functions which is called Cross Entropy. CNN's multi-layered architecture comprises Conv1D, Bidirectional LSTM, Dropout, MaxPooling1D, and Dense layer. Every layer demonstrates a complex characteristic of straightforward characteristics [5].

Utilization of important layers of CNN are explained below:

(a) Bidirectional lstm - In this work, it is a method of constructing every neural network that has the sequence details in each direction backward (future to past) & forward (past to future) & is utilized for sequence prediction [7].

(b) Dropout Layer-this layer avoids overfitting of a model. Dropout is executed by randomly arranging the leading margins of unseen components to 0 every time a training phase is updated. [8].

(c) Dense Layer–a dense layer is powerfully connected with its preceding layer i.e., neurons that exist in a layer are attached with every neuron of its preceding layer. in artificial neural networks, this can be the foremost normally used layer [9].

(d) Time Distributed -The application of the same layer to several inputs. And its production of one output per input to get the result in time is nothing but time distributed layer.[10].

(e) Maxpooling Layer–Max pooling layer assists to scale back the spatial size of the convolved options & additionally also assists to minimize over-fitting by providing an abstracted illustration of them [11].

(f) Activation Layer–it is applicable for the transformation of the input values of neurons & introduces non-linearity into the neural networks so that the networks are capable of learning relationship between both the input and output values [9]. In short, the CNN algorithm is applied for model automation since it is efficient in taking out attributes from datasets along with training a model appropriately [10].

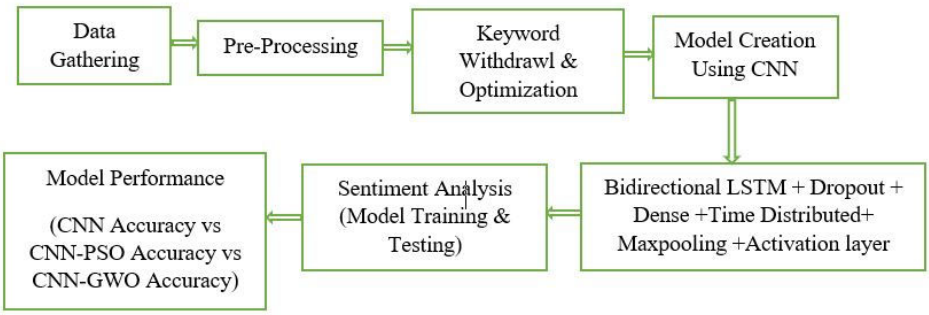

Fig 1: Block Diagram of the Proposed System

For smooth operation of prediction analysis, the whole project has been implemented on the Anaconda Platform in Jupyter Notebook. some libraries used are –

1) Tensorflow – CNN Architecture makes a machine learning model using Tensorflow & Keras library. It's an open-source software library for Machine Learning (ML) and Artificial Intelligence (AI) also has been utilized in a wide variety of activities but has a special focus on deep neural network training and

inference. Keras is an open-source software library which supplies a Python interface for artificial neural networks. Keras acts as an interface to the Tensorflow library. Tensorflow can use all Keras functions for model creation [21].

2) Pandas (pd) – It is used for copying the whole dataset from .csv file & putting it into its dataframe. Panda's functions convert rows & columns into vectorized form due to which the process becomes faster [22].

3) NumPy (np) – Computation is done in neural network & all calculations are in matrices (i.e., vector calculation) to make vector calculation faster NumPy is used. NumPy includes support for huge, multidimensional arrays and matrices, along with a large collection of high-level math functions that work with those arrays.

4) TextBlob - This library is useful for assigning polarity and subjectivity ratings for data. "All sentiment characteristics returns a named tuple of the form sentiment (polarity, subjectivity). The polarity score range is [-1.0, 1.0]. 1.0 is very subjective. Subjectivity is opinion-based, i. e. TexBlob subjectivity ratings are built upon keywords like "I", "my", "our", "mine" etc. while polarity is built upon sentiments, either positive or negative. [23].

3.2 Pre-Processing Results:

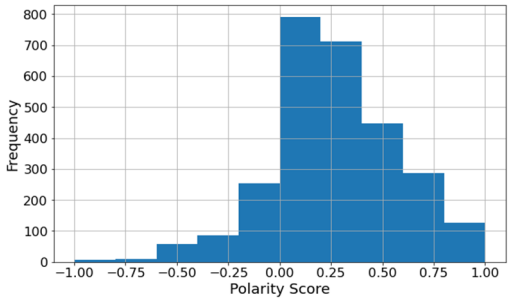

Fig 2 : Polarity Score

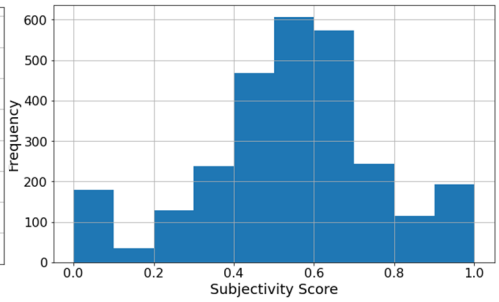

Fig 3: Subjectivity Score

Fig 2 depicts the polarity score which explains that the amazon reviews contain maximum no. of positive comments and very few negative comments in the dataset. Similarly, Fig 3 shows the maximum no. if reviews related to the subject are there. Very few are different from the product explanation. Sometimes model shows more positive scores or more negative scores, which is not feasible for model training because the model works only on one type of sentiment either positive or negative. i.e., a model is more optimistic, which is called biasing. If a database is showing any one type of value more, then model training will show results accordingly. So, to avoid it, the average value needs to calculate which will equalize the final result by reducing biasing.

The Project is divided into 4 parts –

1) Data Pre-processing - Sanitization & Cleaning

2) Model Creation – Data Feeding to the model
3) Model Training – Sentiment Analysis
4) Model Performance – Accuracy of CNN, PSO & GWO

Data Pre-processing more often concentrates on gathering and converting collected data into a usable format. The Pre-processor filters the reviews in such a way that the sentences have proper relations with each other & convert text from the dataset into a mathematical model which is called Tokenization. The tokenization process breaks the verification down into a token of words separated by spaces. Then, NLTK (Natural Language Toolkit) labelling activity does tagging of nouns, pronouns, verbs, adjectives, adverbs, and prepositions in every token in their check because these tokens are having a list of words, sentences, characters, numbers, etc. [20].

In the current past, GWO & PSO method has been regarded as a promising meta-heuristic method fixing distinct popular optimization problems, GWO mimicks a social hierarchy, focusing on grey wolf functions [24] though it's been applied for addressing the function extraction issue [15][25], weight initialization of CNN [26], training of CNN [27] however it has now no longer carried out for hyper-parameter optimization tasks [28-29]. therefore, in this research, for the primary time, it's far carried out for tuning the hyper-parameters of CNN in implementation to prediction evaluation of merchandise in E-commerce.

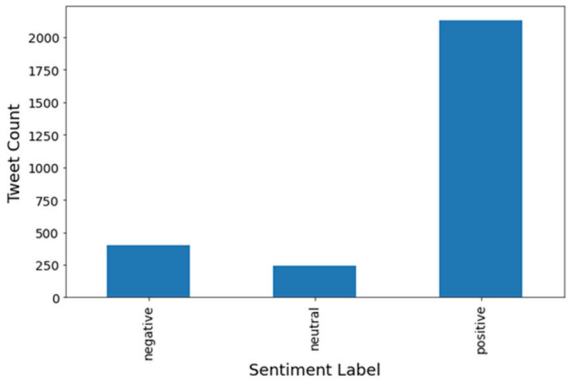

Fig 4: Graph showing the average value of Sentiment Analysis

After pre-processing, an efficient encoding technique was used to fit the hyperparameters into GWO. Having determined the architecture of the CNN, achieving the near-optimal values of the hyperparameters that are mainly involved in convolution, dropout and clustering layer is the aim of this document. The slowest part of hyperparameter tuning is CNN training, which is defined as the fitness function to be assessed in the GWO optimization process. CNN is used for its end-to-end training capabilities, automatic role selection, and classification accuracy. A profitable CNN model is created with the optimized hyperparameters from GWO and PSO. The proposed model is finally assessed based on some standard classification matrices such as Accuracy, Precision, Recovery, FScore

[30-33] along with the absolute cross-entropy loss value (loss) which is described as follows:

$$Loss = -\sum_{i=1}^{N} y_i \cdot \log \hat{y}_i \; Loss = -\sum_{i=1}^{N} y_i \cdot \log \hat{y}_i \quad (1)$$

where N - number of classes, Yi -predicted model value for ith class, it is a comparable target value.

$$\text{Accuracy} = \frac{T_P + T_n}{T_P + T_n + F_P + F_n} \quad (2)$$

$$Precisson = \frac{T_P}{T_P + F_P} \quad (3)$$

$$Recall = \frac{T_P}{T_P + F_n} \quad (4)$$

$$Fscore = \frac{2T_P}{2T_P + F_P + F_n} \quad (5)$$

where Tp – True Positive, Tn -True Negative, Fp -False Positive, Fn - False Negative.

4 Experimental results –

Finally, a model is confirmed by differentiating it with 2 alternative nature-inspired techniques like PSO and GWO. all experiments are supervised in python by exploiting the Keras, Scikit-learn, and OpenCV libraries. 80% of text information is chosen for training & 20% is utilized for testing. The accuracy and loss of various hyper-parameter optimized CNN Models obtained for the sample data set are shown in Fig 5,6 & 7. It proves that accuracy of the optimized CNN-GWO model is having more accuracy than PSO, initial values of the model were fluctuating but as the model has won extra training, the curve is smoothed. The loss function graph suggested that the GWO loss transition is smoother than others.

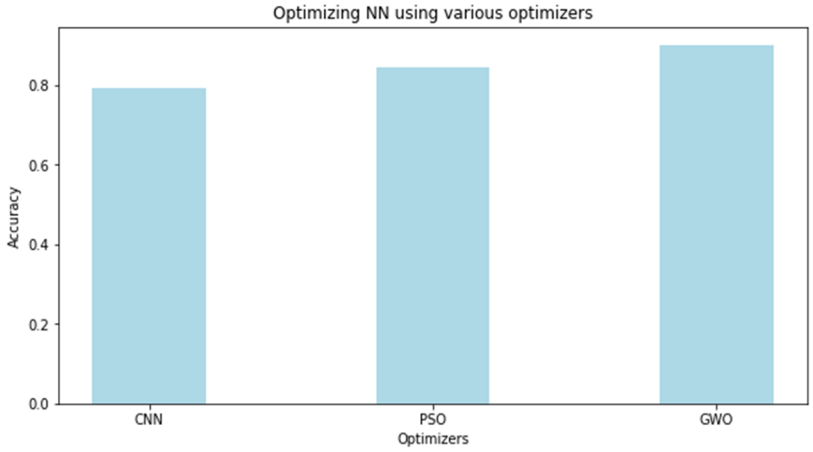

Fig 5: Performance Comparison of all three algorithms

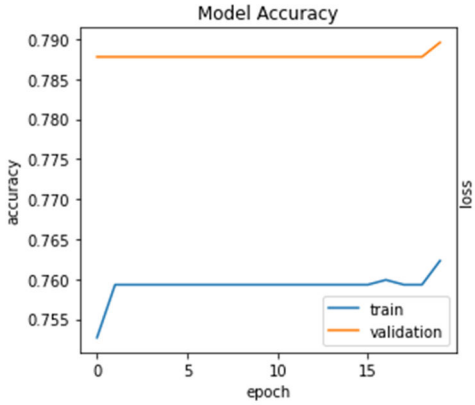

Fig 6: Model Accuracy

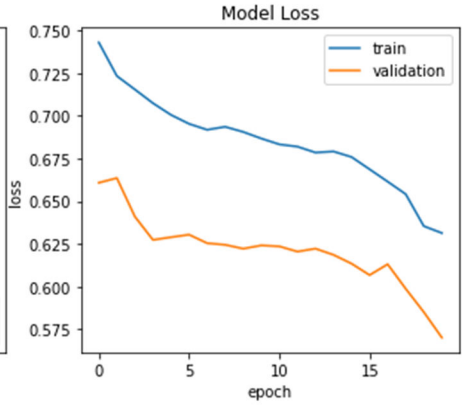

Fig 7: Model Loss

The model performance is compared to two other techniques developed using the CNN algorithm, as proven below:

Table 1. Performance analysis of all three models.

Model	Accuracy	Precision	Recall	F Score
CNN	Model attained an accuracy of 79.32%	85.38%	79.32%	82.53%

CNN-PSO	Model attained an accuracy of 84.42%	87.66%	82.81%	85.16%
CNN-GWO	Model attained an accuracy of 92.84%	94.07%	89.22%	91.57%

5 Conclusion

The CNN architecture with PSO & GWO algorithm gives an accuracy of 94.07%. &Sequential Model focuses on improvisation of predicting right products to customers & provides good performance. This model is trained up to 10 epochs. if no. of epochs were increased, accordingly accuracy will be improved. The performance of CNN-GWO model is superior to CNN-PSO &other CNN models. Taking into consideration all types of reviews from Amazon Dataset of 3000 entries to calculate the prediction accuracy of products helps E-commerce industries to take decisions properly & improve business accordingly by giving suggestions of relevant products to the customers. In the future hybridization of CNN with different metaheuristic algorithms except PSO & GWO will be a new scope towards technology advancement.

References

[1] Gaeth, Andrae. "Evaluating Predictive Analytics for Capacity Planning" (PDF). *www.hisa.org.au*. Retrieved 22 November 2018.

[2] Mohammad Salehan and Dan J. Kim, "Predicting the Performance of Online ConsumerReviews: A Sentiment Mining Approach", Elsevier Journal on Information Processing and Management, 2016.

[3] ShahriarAkter and Samuel FossoWamba, "Big data analytics in e-commerce: A systematic review and agenda for future research", Electronic Markets 26 173–194, 2016.

[4] Tuladhar J.G., Gupta A., Shrestha S., Bania U.M., Bhargavi K. (2018) Predictive Analysis of E-Commerce Products. In: Bhalla S., Bhateja V., Chandavale A., Hiwale A., Satapathy S. (eds) Intelligent Computing and Information and Communication. Advances in Intelligent Systems and Computing, vol 673. Springer, Singapore.

[5] Simonyan, K., &Zisserman, A. (2014). Very deep convolutional networks for large-scale image recognition. arXiv preprint arXiv:1409.1556.

[6] Kolhe, L., Jetawat, A.K. & Khairnar, V. Robust product recommendation system using modified grey wolf optimizer and quantum inspired possibilistic fuzzy C-means. *Cluster Comput* **24,** 953–968 (2021).

[7] https://machinelearningmastery.com/cnn-long-short-term-memory networks/

[8] https://towardsdatascience.com/machine-learning-part-20-dropout-keras-layers-explained-8c9f6dc4c9ab.

[9] https://analyticsindiamag.com/a-complete-understanding-of-dense-layers-in-neural-networks/

[10] https://medium.com/smileinnovation/how-to-work-with-time-distributed-data-in-a-neural-network-b8b39aa4ce00.

[11] Rasmiranjan Mohakud, Rajashree Dash, Designing a grey wolf optimization-based hyper-parameter optimized convolutional neural network classifier for skin cancer detection, Journal of King Saud University - Computer and Information Sciences,2021.

[12] Sonsare, Pravin. (2020). Long Short Term Memory Network Using Grey Wolf Optimization for Stock Price Prediction. Bioscience Biotechnology Research Communications. 13. 55-58. 10.21786/bbrc/13.14/13.

[13] Sasikala, P., Mary Immaculate Sheela, L. Sentiment analysis of online product reviews using DLMNN and future prediction of online product using IANFIS. *J Big Data* **7,** 33 (2020)

[14] Vrbančič, Grega & Zorman, Milan & Podgorelec, Vili. (2019). Transfer Learning Tuning Utilizing Grey Wolf Optimizer for Identification of Brain Hemorrhage from Head CT Images.

[15] Garg, S., Kaur, K., Kumar, N., Kaddoum, G., Zomaya, A.Y., Ranjan, R., 2019. A hybrid deep learning-based model for anomaly detection in cloud datacenter networks. IEEE Trans. Netw. Serv. Manage. 16 (3), 924–935.

[16] Singla, Zeenia & Randhawa, Sukhchandan & Jain, Sushma. (2017). Sentiment analysis of customer product reviews using machine learning. 1-5. 10.1109/I2C2.2017.8321910.

[17] Wang, Y., Zhang, H., Zhang, G., 2019. cPSO-CNN: An efficient PSO-based algorithm for fine-tuning hyperparameters of convolutional neural networks. Swarm Evol. Comput. 49, 114–123.

[18] Yoo, Y., 2019. Hyperparameter optimization of deep neural network using univariate dynamic encoding algorithm for searches. Knowl.-Based Syst. 178, 74–83.Best B, Nguyen HS, Doan NB et al (2019).

[19] Cui, H., Bai, J., 2019. A new hyperparameters optimization method for convolutional neural networks. Pattern Recogn. Lett. 125, 828–834.

[20] https://medium.com/predict/how-does-nlp-pre-processing-actually-work-8d097c179af1

[21] Dean, Jeff; Monga, Rajat; et al. (November 9, 2015). "TensorFlow: Large-scale machine learning on heterogeneous systems" (PDF). *TensorFlow.org*. Google Research. Retrieved November 10, 2015.

[22] "pandas.date_range – pandas 1.0.0 documentation". *pandas. 29 January 2020*. Retrieved 30 January 2020.

[23] Ahuja, S., & Dubey, G. (2017). Clustering and sentiment analysis on Twitter data. 2017 2nd International Conference on Telecommunication and Networks (TEL-NET). doi:10.1109/tel-net.2017.8343568

[24] Mirjalili, S., Mirjalili, S.M., Lewis, A., 2014. Grey wolf optimizer. Adv. Eng. Softw. 69, 46–61.

[25] Maddikunta, P.K.R., Parimala, M., Koppu, S., Reddy, T., Chowdhary, C.L., Alazab, M., 2020. An effective feature engineering for DNN using hybrid PCA-GWO for intrusion detection in IoMT architecture. Comput. Commun. 160, 139–149.

[26] Kumaran, N., Vadivel, A., Kumar, S.S., 2018. Recognition of human actions using CNN-GWO: a novel modelling of CNN for enhancement of classification performance Multimedia Tools Appl. 77 (18), 23115–23147.

[27] Chen, X., Kopsaftopoulos, F., Wu, Q., Ren, H., Chang, F.K., 2019. A self-adaptive 1D convolutional neural network for flight-state identification. Sensors 19 (2), 275.

[28] Xie, H., Zhang, L., Lim, C.P., 2020. Evolving CNN-LSTM models for time series prediction using enhanced grey wolf optimizer. IEEE Access 8, 161519–161541.

[29] Agarwal, R., Sharma, H., 2020. A New Enhanced recurrent extreme learning machine based on feature fusion with CNN Deep features for breast cancer detection. In:Advances in Computer, Communication and Computational Sciences, pp. 461–471.

[30] Siegel, R.L., Miller, K.D., Jemal, A., 2019. Cancer statistics, 2019. CA 69 (1), 7–34.

[31] Szegedy, C., Liu, W., Jia, Y., Sermanet, P., Reed, S., Anguelov, D., Erhan, D., Vanhoucke, V., Rabinovich, A., 2015. Going deeper with convolutions. In: Proceedings of the IEEE Conference On Computer Vision And Pattern Recognition, pp. 1–9.

[32] Badrinarayanan, V., Handa, A., &Cipolla, R. (2015). Segnet: A deep convolutional encoder-decoder architecture for robust semantic pixel-wise labelling. arXiv preprint arXiv:1505.07293.

[33] Li, Y., Xiao, J., Chen, Y., Jiao, L., 2019. Evolving deep convolutional neural networks by quantum behaved particle swarm optimization with binary encoding for image classification. Neurocomputing 362, 156–165.

Risk Assessment of Roof Structures in Concepcion, Tarlac in the Event of an Ash Fall

Jerome Michael J. Sadullo, Jamaica Lois A. Torres, Trisha Muriel T. Valino

***Abstract*—** In the Philippines, Central Luzon is one of the regions at high risk in terms of volcanic eruption. In fact, last June 15, 1991, which were the Mount Pinatubo has erupted, the most affected provinces were Zambales, Olangapo, Pampanga, Tarlac, Bataan, Bulacan and Nueva Ecija. During the Mount Pinatubo eruption, Castillejos, Zambales, has recorded the most significant damage to both commercial and residential structures. In this study, the researchers aim to determine and analyze the various impacts of ashfall on roof structures in Concepcion, Tarlac, during the event of a volcanic eruption. In able for the researcher to determine the sample size of the study, they have utilized Cochran's sample size formula. With the computed sample size, the researchers have gathered data through the distribution of survey forms, utilizing public records, and picture documentation of different roof structures in Concepcion, Tarlac. With the data collected, Chi-squared goodness of fit was done by the researcher in order to compare the data collected from the observed N (Concepcion, Tarlac) and expected N (Castillejos, Zambales). The results showed that when it comes to the roof constructions material used in Concepcion, Tarlac and Castillejos, Zambales. Structures in Concepcion, Tarlac were most likely to suffer worse when another eruption happens compared to the structures in Castillejos, Zambales. Yet, considering the current structural statuses of structure in Concepcion Tarlac and its location from Mount Pinatubo, they are less likely to experience ashfall.

***Keywords*—** risk assessment, Concepcion, Tarlac, Volcano Pinatubo, roof structures, ashfall.

Jerome Sadullo is with the Mapua University, Philippines (e-mail: jmjsadullo@mymail.mapua.edu.ph).

Design, Modelling, and Fabrication of Bioinspired Frog Robot for Synchronous and Asynchronous Swimming

Afaque Manzoor Soomro[1*], Faheem Ahmed[2], Fida Hussain Memon[1], Kyung Hyun Choi[2]

Abstract— **This paper proposes the bioinspired soft frog robot. All printing technology was used for the fabrication of the robot. Polyjet printing was used to print the front and back limbs, while ultrathin filament was used to print the body of the robot, which makes it a complete soft swimming robot. The dual thrust generation approach has been proposed by embedding the main muscle and antagonistic muscle in all the limbs, which enables it to attain high speed (18 mm/s), and significant control of swimming in dual modes (synchronous and asynchronous modes). To achieve the swimming motion of the frog, the design, motivated by the rigorous modelling and real frog dynamics analysis, enabled the as-developed frog robot (FROBOT) to swim at a significant level of consistency with the real frog. The FROBOT (weighing 65 g) can swim at different controllable frequencies (0.5–2Hz) and can turn in any direction by following custom-made LabVIEW software's commands which enables it to swim at speed up to 18 mm/s on the surface of deep water (100 cm) with excellent weight balance.**

I. INTRODUCTION

Soft robotics is incipient research area with wide range of new applications such as fully integrated soft octobot, octopus robot[1], worm robot[2] and soft multicomotion microbot[3]. For under water exploration, inspection, observation and rescue developing swimming robots with intrinsically soft materials and achieving flexibility with numerous degrees of freedom in their motion, have gradually attracted the attention of bionics[4]. In literature, numerous soft robots have been developed enabling proprioception based on shape memory alloy actuators[5], [6]. One of the SMA based soft robots is developed which uses micro meter range diameter SMA wire as an actuator, in concurrence with fully 3D printed hand for prosthesis application, it is light weight with flexible geometrical shape to attain silent movements [7][8][9][10][11]. Another interesting development is earthworm soft robot with fluid filled structure surrounded by muscular body which behaves more likely as real earthworm. This soft robot is mainly built with two viscoelastic silicon rubber elements which imitates a constant volume hydrostatical structure[4] causing peristaltic locomotion using radical twisting and bending of soft hydrostatical elements[12]. These hydrostatical elements are being energized through applying pressure to spring shaped SMA wires[2], [13].

[*]Research supported by SIBAU Internal Research Grant 2021

A.M. Soomro is with Jeju National University, Sukkur IBA University (0333 8864849; e-mail: afaquemanzoor@gmail.com).

The Frog-inspired robots have acquired an excellent value due to frog's amphibian nature. Currently, many experimental based studies on frog-inspired swimming and jumping robots based on modelling analysis and swimming mechanism have been reported [5], [14], [15]. These robots are relatively large in dimensions, complex in design aspects and a bit heavy, which makes robots relatively impossible to actually realize the swimming ang jumping mechanism[16].

Recent advancements in intelligent materials have made easy for their use as soft actuators due to their distinct and matchless soft characteristics[17]. For instant, shape-memory alloys materials have been at front end for last few years due to its characteristic of lacking in mechanical parts[18] or the capacity to upgrade the mechanical movables with the application of current with different rating relevant to dimensions of SMA used[19][20]. The intelligent material such as SMA [4], [17], [21], have made it possible for soft robots to become much capable of following animal movements. However, conventional stiff mechanical systems for robots are complex and it is more difficult to develop miniaturized mechanical systems to achieve desired animal motion in under water environments. SMAs are mostly available in wires, pipes, springs and ribbons types[15], [17].

Herein, we propose the design, fabrication and characterization of frog robot (FROBOT) that is capable of swimming underwater in synchronous and asynchronous modes. The robot was designed by printing its muscle wires embedded front and back limbs using PolyJet printing process. Dual thrust approach was implemented which enabled the FROBOT to swimm in both modes with the maximum speed of 18 mm/s at 1.5 Hz.

II. FABRICATION PROCESS

The fabrication of FROBOT was done using multi-step all-printed technology. For the functionally responsive front and back limbs, the polyJet printing was used. This process is taken from our previous studies [22]. As Shown in **Figure 1**, the first half part of all four limbs were printed which then were brought to custom-made multi-header printing system which inserted the muscle wires and necessary connections and sent back to PolyJet printing setup which printed the second half of the limbs. In parallel, the body of the frog robot

was printed using multi-header system. Herein, ultraflex filament (BLACKMAGIC3D, 1.75 mm) was used. the system was loaded with a CAD model of proposed robot design, which was fully optimized using simulation and mathematical work, as carried out in our previous work [22].

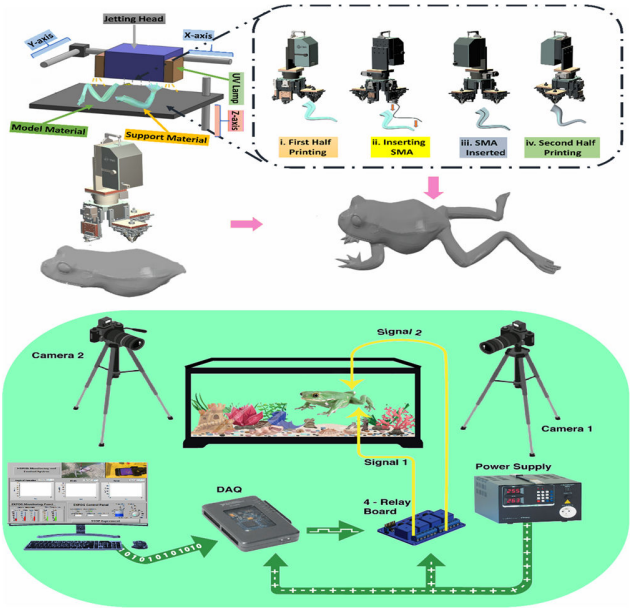

Fig.1 step by step FROBOT fabrication process, b) schematic of experimental setup; where the experiment is monitored using two high-definition imaging devices, thermal camera for monitoring real time temperature and myRIO for monitoring and control of the whole setup.

III. RESULTS AND DISCUSSION

The design of the FROBOT was inspired by the Anura, such as RANA Esculenta (semi aquatic frog). This infers that the proposed robot must be soft, bio-inspired and follows the swimming mechanism. Like the natural frog, which swims by its contraction and expansion of different muscles for effective and controllable swimming, the FROBOT follows the same by using dual-thrust approach. In the proposed design, two degrees of freedom were added; the knee joint and the flipper joint. In each limb, there are two muscles. Fig. 2 shows the actuation mechanism of FROBOT. The main muscles are responsible for the drag forces, while the antagonistic muscles create the lift force and enable the limbs and flippers to return their original positions. The sequential control of these muscles are time-bound and are activated when the other muscles are off. A deliberate delay of few hundred mili seconds has been added in the software to ensure the settling of each muscle wire.

In order to make sure, the muscle wires get the required heat level and the overall body of the frog is not damaged. The thermal characterization was carried out using IR thermal camera (FLIR ONE). Figure 2 shows the images taken from the video captured by high-definition imaging device. On the application of voltage to the FROBOT, the current starts flowing which causes the temperature to rise. A gradual increase in the heat can be seen in both, the front and back limbs. it seems like there is discontinuous temperature increase, however this is due to the fact, that the muscles wires were embedded inside the limbs which takes time to heat up the limbs completely. This also brings an advantage to the FROBOT as it does not provide any significant effect on the temperature of the environment where it swims.

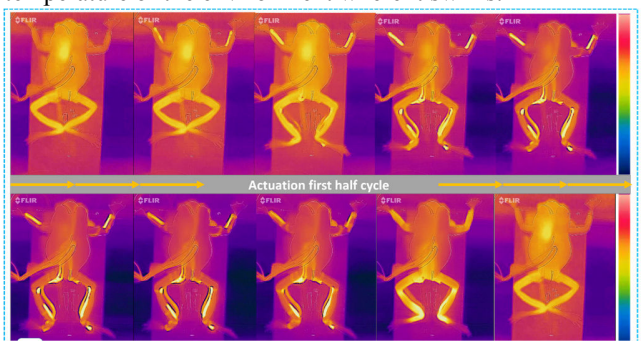

Fig. 2 Thermal characterization sequential images

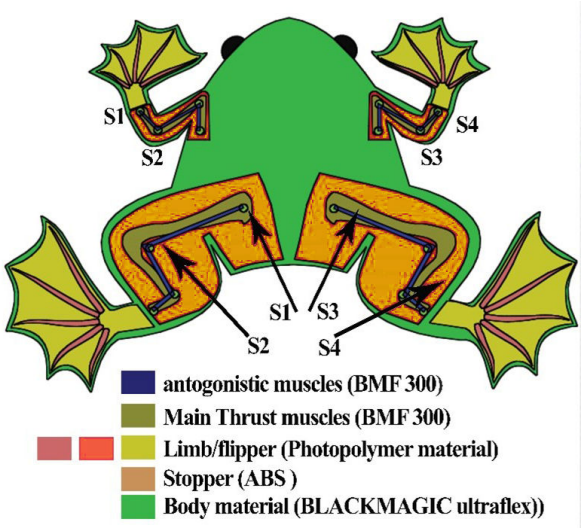

Fig. 3 working mechanism; with complete stroke operation, dual approach of thrust generation is shown in the top left figure (S1 and S3 are the main muscles for lift force generation, S2 and S4 are the antagonistic muscles responsible for drag force generation),

Furthermore, the concept of turning right or left was inspired from the two-wheel line following robots; in which, specific wheel is turned off, in order to move in the direction of blocked wheel. Following the same approach, in the case of turning right, the right limb was deactivated. However, from the practical observation, activating the right limb for the period of 20% duty cycle improved the stability of the robot significantly. Similarly, for turning left, S3 was activated, while S1 activated only for 20% duty cycle. During the whole experiment, the feedback from, IR gun for temperature measurement, thermal camera, resistance of the muscle wires and angle of actuation worked as the feedback for the controlled to enable robot swim efficiently. However, for the synchronous swimming, the control was quite simple; S1 and S3 were activated at the same time, while with some delay the

antagonistic muscle wires were activated to create the lift force. The bottom right picture in figure 4 shows the software that was developed using LabVIEW 2019 and interfaced with myRIO. The user has the liberty to intuitively select the swimming modes, frequency, real-time imaging (thermal and two high-definition cameras) and sensors data. Moreover, all the data was also logged to the computer. Fig. 4 shows the PWM waveforms used for controlling the FROBOT in the respective mode. In the asynchronous mode (turning right), S1was kept activated while S2 deactivated. However, after the deliberate delay of few mili seconds, the S3 was activated to control the direction.

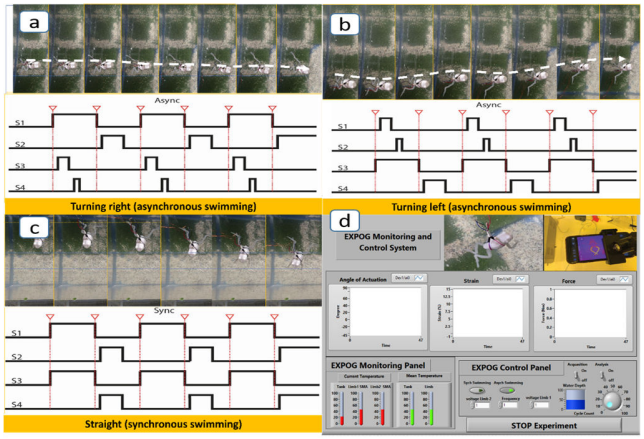

Fig. 4 a) continuous frames taken from videos of turning right, b) continuous frames taken from videos of turning left, c) PWM signals for each muscle wire, d) custom-made software with monitoring and control features (bottom right).

It is highly pertinent to determine the force each limb generates, which can help to predict the overall swimming performance of robot. For this, a setup was prepared where the each limb was attached to a shaft coupled with load cell. The sensor was interfaced with myRIO, which logged the real-time data after every pre-set sampling time. ~~The process~~ is given in Figure S1. The maximum force generated by each back limb was 0.135 N, moreover, the front limb could produce force of 0.8 N. The process of measurement was followed as in our previous work [22].

IV. Conclusion

We propose the design, fabrication and characterization of frog robot (FROBOT) that is capable of swimming underwater in synchronous and asynchronous modes. The robot was designed by printing its muscle wires embedded front and back limbs using PolyJet printing process. Whereas the body of the robot was printed using custom-made multi-header printing system which also placed the muscle wires during the printing phase. The proposed robot showed remarkable consistency in biomimicking the real frog locomotion with the power supply of 5V 1A. From the results, it is inferred that the FROBOT can be a strong candidate for the bioinspired environmental monitoring. Moreover, in future work, the attainment of higher efficiency, more delicate swimming styles is targeted.

References

[1] A. M. Soomro, M. A. U. Khalid, I. Shah, S. W. Kim, Y. S. Kim, and K. H. Choi, "Highly stable soft strain sensor based on Gly-KCl filled sinusoidal fluidic channel for wearable and water-proof robotic applications," *Smart Mater. Struct.*, vol. 29, no. 2, 2020, doi: 10.1088/1361-665X/ab540b.

[2] S. Chatterjee, R. Niiyama, and Y. Kawahara, "Design and Development of a Soft Robotic Earthworm with Hydrostatic Skeleton," *2017 IEEE Int. Conf. Robot. Biomimetics, ROBIO 2017*, vol. 2018-Janua, pp. 1–6, 2018, doi: 10.1109/ROBIO.2017.8324385.

[3] H. R. Choi *et al.*, "Micro robot actuated by soft actuators based on dielectric elastomer," *IEEE Int. Conf. Intell. Robot. Syst.*, vol. 2, no. October, pp. 1730–1735, 2002, doi: 10.1109/irds.2002.1044005.

[4] T. Du, J. Hughes, S. Wah, W. Matusik, and D. Rus, "Underwater Soft Robot Modeling and Control with Differentiable Simulation," *IEEE Robot. Autom. Lett.*, vol. 6, no. 3, pp. 4994–5001, 2021, doi: 10.1109/LRA.2021.3070305.

[5] H. Rodrigue, W. Wang, M. W. Han, T. J. Y. Kim, and S. H. Ahn, "An Overview of Shape Memory Alloy-Coupled Actuators and Robots," *Soft Robot.*, vol. 4, no. 1, pp. 3–15, 2017, doi: 10.1089/soro.2016.0008.

[6] Z. Zhakypov, J. L. Huang, and J. Paik, "A novel torsional shape memory alloy actuator: Modeling, characterization, and control," *IEEE Robot. Autom. Mag.*, vol. 23, no. 3, pp. 65–74, 2016, doi: 10.1109/MRA.2016.2582868.

[7] W. Zhao, Y. Zhang, and N. Wang, "Soft robotics: Research, challenges, and prospects," *J. Robot. Mechatronics*, vol. 33, no. 1, pp. 45–68, 2021, doi: 10.20965/jrm.2021.p0045.

[8] F. Simone, G. Rizzello, S. Seelecke, and P. Motzki, "A Soft Five-Fingered Hand Actuated by Shape Memory Alloy Wires: Design, Manufacturing, and Evaluation," *Frontiers in Robotics and AI*, vol. 7. 2020, doi: 10.3389/frobt.2020.608841.

[9] D. Copaci, J. Munõz, I. González, C. A. Monje, and L. Moreno, "SMA-Driven Soft Robotic Neck: Design, Control and Validation," *IEEE Access*, vol. 8, pp. 199492–199502, 2020, doi: 10.1109/ACCESS.2020.3035510.

[10] W. Wang, C. Y. Yu, P. A. Abrego Serrano, and S. H. Ahn, "Shape Memory Alloy-Based Soft Finger with Changeable Bending Length Using Targeted Variable Stiffness," *Soft Robot.*, vol. 7, no. 3, pp. 283–291, 2020, doi: 10.1089/soro.2018.0166.

[11] J. Shintake, B. Schubert, S. Rosset, H. Shea, and D. Floreano, "Variable stiffness actuator for soft robotics using dielectric elastomer and low-melting-point alloy," *IEEE Int. Conf. Intell. Robot. Syst.*, vol. 2015-Decem, pp. 1097–1102, 2015, doi: 10.1109/IROS.2015.7353507.

[12] D. S. Copaci, D. Blanco, A. Martin-Clemente, and L. Moreno, "Flexible shape memory alloy actuators for soft robotics: Modelling and control," *Int. J. Adv. Robot. Syst.*, vol. 17, no. 1, pp. 1–15, 2020, doi: 10.1177/1729881419886747.

[13] M. Liu, L. Hao, W. Zhang, and Z. Zhao, "A novel design of shape-memory alloy-based soft robotic gripper with variable stiffness," *Int. J. Adv. Robot. Syst.*, vol. 17, no. 1, pp. 1–12, 2020, doi: 10.1177/1729881420907813.

[14] A. Joshi, A. Kulkarni, and Y. Tadesse, "FludoJelly: Experimental study on jellyfish-like soft robot enabled by soft pneumatic composite (SPC)," *Robotics*, vol. 8, no. 3, 2019, doi: 10.3390/robotics8030056.

[15] J. Choi, S. H. Ahn, and K. J. Cho, "Design of fully soft actuator with double-helix tendon routing path for twisting motion," *IEEE Int. Conf. Intell. Robot. Syst.*, pp. 8661–8666, 2020, doi: 10.1109/IROS45743.2020.9341363.

[16] T. Ashuri, A. Armani, R. Jalilzadeh Hamidi, T. Reasnor, S. Ahmadi, and K. Iqbal, "Biomedical soft robots: current status and perspective," *Biomed. Eng. Lett.*, vol. 10, no. 3, pp. 369–385, 2020, doi: 10.1007/s13534-020-00157-6.

[17] C. C. Ulloa, S. Terrile, and A. Barrientos, "Soft underwater robot actuated by shape-memory alloys 'jellyrobcib' for path tracking through fuzzy visual control," *Appl. Sci.*, vol. 10, no. 20, pp. 1–22, 2020, doi: 10.3390/app10207160.

[18] R. Zhang, Z. Shen, and Z. Wang, "Ostraciiform Underwater Robot with Segmented Caudal Fin," *IEEE Robot. Autom. Lett.*, vol. 3, no.

4, pp. 2902–2909, 2018, doi: 10.1109/LRA.2018.2847198.

[19] D. Copaci, F. Martin, L. Moreno, and D. Blanco, "SMA Based Elbow Exoskeleton for Rehabilitation Therapy and Patient Evaluation," *IEEE Access*, vol. 7, no. c, pp. 31473–31484, 2019, doi: 10.1109/ACCESS.2019.2902939.

[20] C. D., C. E., M. L., and B. D., "New Design of a Soft Robotics Wearable Elbow Exoskeleton Based on Shape Memory Alloy Wire Actuators," *Appl. Bionics Biomech.*, vol. 2017, 2017.

[21] M. Cianchetti, C. Laschi, A. Menciassi, and P. Dario, "Biomedical applications of soft robotics," *Nat. Rev. Mater.*, vol. 3, no. 6, pp. 143–153, 2018, doi: 10.1038/s41578-018-0022-y.

[22] J. L. Software, F. Ahmed, and K. H. Kim, "Fully 3D printed Multi-Material Soft Bio-Inspired Frog for Underwater Synchronous Swimming," *Int. J. Mech. Sci.*, p. 106725, 2021, doi: 10.1016/j.ijmecsci.2021.106725.

Events as a Basis for Workflow Scheduling

David Marchant *Datalogisk Institut (DIKU), Copenhagen University*
Copenhagen, Denmark
d.marchant@ed-alumni.net, 0000-0003-4262-7138

Abstract—This paper evaluates using event-based scheduling as a basis for dynamic workflow management. To do this, the `WorkflowRunner` is introduced as a tool for conducting event driven scheduling in a robust manner. It is evaluated in comparison to Slurm and the `WorkflowRunner` is found to schedule analysis roughly 2.5x quicker than Slurm in most cases. An example workflow is also presented, demonstrating how this style of scheduling allows for complete modification of the workflow structure at runtime, something very difficult to achieve in traditional workflow management systems. These developments are expected to be of particular use in distributed analysis systems, and in heterogeneous systems such as those looking to accommodate human-in-the-loop interactions.

Keywords—Dynamic, Heterogeneous, MEOW, Workflows.

I. Introduction

Modern scientific research frequently involves the processing of large amounts of experiment data, in long running jobs, on dedicated hardware. This analysis often comprises of several different steps and is can be managed by Scientific Workflow Management Systems (SWMSs). These typically use Directed Acyclic Graphs (DAGs) as a basis for composing a workflow, with individual steps linked together in a linear progression. A DAG allows SWMSs to easily identify different jobs and their dependencies within a workflow, as well as making workflow composition straightforward for users. However, scientific workflows are exploratory in nature [10], and have an inherent need to be dynamic [24]. This need is not easily met through the use of a static DAG, and so alternatives are needed.

One alternative to the static DAG paradigm is the use of dynamic schedulers, where jobs are scheduled individually without a full workflow necessarily being understood at the start. Managing Event Oriented Workflows (MEOW) [23] is an example of this. It uses event monitors to respond to file events by scheduling individual jobs as part of a continuous, live system. This can potentially distributes control of the scheduling across multiple nodes, and enables dynamic processing that is not possible within a static, sequential system.

A. Existing SWMS Offerings

Unsurprisingly, a large number of tools for constructing and managing scientific workflows already exist. Many of these are dedicated tools such as Apache Airflow [18], Kepler [1], Pegasus [9], Taverna [29], Dask [34], DagOn* [26], Askalon [15], and DVega [36]. All of these systems use a data-flow model, where a pipeline of processing is constructed and data is passed from process to process. Each process will have defined inputs and outputs, and should always perform some modification on the input data. This model is maintained through the use of one or more DAGs. A DAG is a linked graph in which nodes are directionally connected such that a loop is never formed. Thus, a DAG is an easy analogue for a workflow, with a defined start and end, and with the dependencies between the different steps trivial to identify. The DAGs themselves are constructed by the user either through a web interface, or programatically. More than one DAG may be provided as individual steps within the workflow may be smaller workflows themselves.

Typically, the previously mentioned systems do not carry out processing themselves, but schedule jobs to be executed using tools such as Kubernetes [21], Slurm [42], Globus [17], corc [27], WLM [40], Torque [37], UNICORE [4], parsl [2], cwltool [7], MapReduce [8], or OGE [30]. These can each also be used on their own, though often have fewer usability aids such as a GUI. They also typically offer a lower-level control of job scheduling and frequently will have fewer extra features such as robust error handling. Several of these systems can be used in conjunction to create sub-workflows, though few have specific accommodation for sub-workflows not written in the same system as themselves. A note-able exception to this is the ambiguously named Hybrid Workflows system built on COMPS [3], presented in [41] and [33]. This presents two types of workflow, in-situ and task-based. In-situ workflows are run within a single resource. Task-based workflows however are large, task parallel batches of processing that may take place over all manner of remote resources, or be processed locally. Hybrid Workflows uses Decaf [12] to run in-situ workflows on performance systems. These in-situ workflows are managed by PyCOMPS [35], which runs each Decaf workflow as a step in a larger task-based workflow. This allows for a large chain of analysis, with individual steps tailored to their specific hardware needs, and allows users to exploit the benefits of both types of workflow.

One final workflow system that is worth considering is WED-flows [16]. WED-flows is interesting as it is an event-driven workflow system. In WED-flows, data is processed according to user defined trigger conditions. From one of these triggers a series of processing activities are started, in a control-flow fashion. The descriptions of WED-flows [16] are unclear on whether a DAG is specifically used or not in the creation and scheduling of processing tasks. It would certainly be a task appropriate for a DAG, and there is no more dynamic scheduling within those processing tasks than in any other SWMS. These sub-workflows themselves are not event-driven, and it is only the scheduling of the entire workflow itself that

This project has received funding from the European Union's Horizon 2020 research and innovation programme under the Marie Skłodowska-Curie grant agreement No 765604.

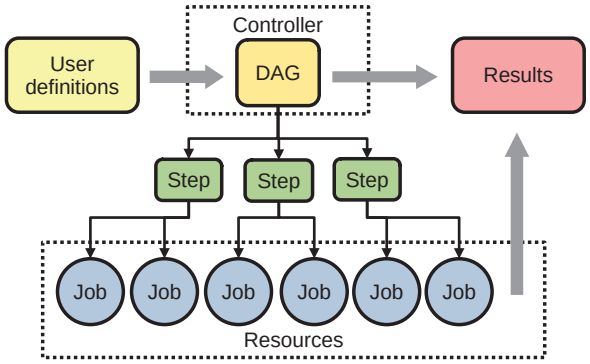

Fig. 1. A top-down workflow structure. Not shown is any data transfer or dependency between jobs.

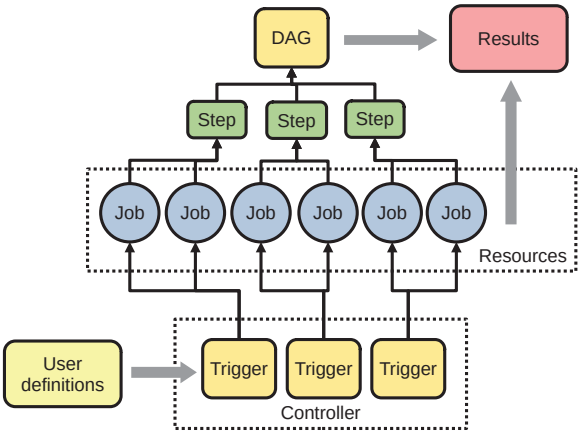

Fig. 2. A bottom-up workflow structure. Not shown is any data transfer or dependency between jobs.

is undertaken in response to an event.

Formally, all of these systems could be characterised as a top-down approach as a central workflow controller is determining the entire structure ahead of time and dictating it to individual jobs, as is shown in Figure 1. Here we can see that a user submits their workflow definitions to the system, either via a DAG, or something that from which a DAG can be derived. In either case the workflow controller will use this DAG to derive the steps. These steps in turn become the basis for identifying jobs, which are scheduled on resources. No data transfer or dependency between jobs has been shown in Figure 1, but at some point the final job will complete and any output will become part of the workflow results. The DAG will also form part of the results, independent of any job processing, as it is a very informative and crucial part of the workflow construction.

This top-down system of scheduling does not properly accommodate the need for scientific workflows to by dynamic [24]. This is as scientific workflows are inherently exploratory in nature, and so analysis should be capable of being changed at runtime [10]. Workflows should be capable of looping, branching, or otherwise being adapted at runtime in response to new knowledge or errors in execution. Many of the previously listed systems have some accommodation for some of these systems, but they are often imperfect patches onto an inherently static design.

B. Dynamic, Event-based Scheduling

An alternative design would be a bottom-up approach. Rather than a single controller identifying, scheduling and assigning all workflow jobs, individual jobs will be scheduled in isolation. By this it is meant that the system does not actively construct an entire workflow ahead of time, merely that it identifies individual jobs, as is shown in Figure 2. In this Figure we can see that as before, a user provides some definitions. These are not reduced to a DAG but are instead used as the basis for individual job scheduling. Once jobs have completed, they may be linked together into steps. These steps, along with any output from the jobs can then form the results of the *emergent* workflow. The word emergent has been highlighted as it is central to this new approach, and is fundamental to understanding it. To re-iterate, in a bottom-up workflow system, a user does not actually construct a workflow directly, they merely create the conditions such that individual jobs can be scheduled.

One system that adopts a bottom-up design is MEOW [23]. Within MEOW users schedule jobs by defining blocks of analysis code, referred to as a *Recipe*, along with the the conditions under which said processing is scheduled, referred to as a *Pattern*. Any combination of valid *Patterns* and *Recipes* are called *Rules.* The conditions that *Rules* respond to are events. For example, a *Recipe* might be some segmentation algorithm while a *Pattern* might identify raw image data being created at a particular file system location. If both the *Pattern* and *Recipe* are defined then a *Rule* will be created that any raw data created at that location will result in the automatic scheduling of the segmentation analysis on said data. If the raw data is ever updated then the analysis is also automatically re-run. The analysis should produce some output, which may trigger further *Rules*, and so form a chain of processing. This will form the design shown in Figure 4.

For an example of where this may be used consider the workflow structure shown in Figure 3. This shows a complete scientific analysis made up of six distinct systems, with the analysis within it scheduled in response to file events, such as a data file being written as some processing output. Currently, workflows like this exist at a variety of levels in scientific processing. For instance, this could represent many of the experiments carried out at large scientific experiment institutions such as EuXFEL [13] or MAX IV [25], In these typically researchers gather large amounts of data from instruments which must be initially cleaned up before being passed into some local storage. This local storage is limited and so data will need to be moved to longer term storage from where researchers will schedule varying forms of analysis using a variety of processing platforms, usually not local to the data storage. This style of workflow is not limited to large institutions, with smaller experiments using a similar structure of having to gather data then moving it between many specialised storage and compute systems throughout the lifetime of workflow [38].

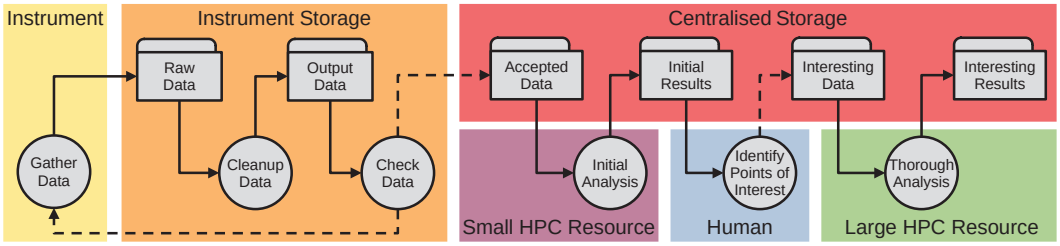

Fig. 3. A heterogeneous analysis. Data storage is shown as folders while processing, human interaction or the running of hardware shown as circles. In this example, scheduling would be any line leading to a circle. Note that solid lines show where all data inputs will produce output, while dotted lines show where only some inputs will produce outputs.

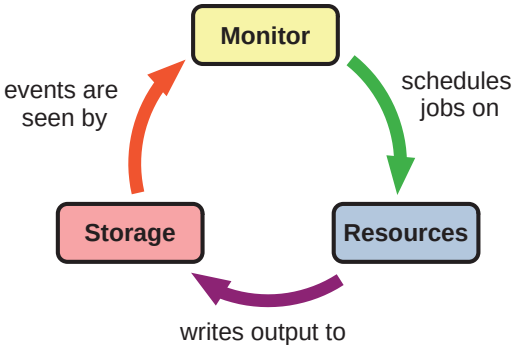

Fig. 4. MEOW's event-driven design structure.

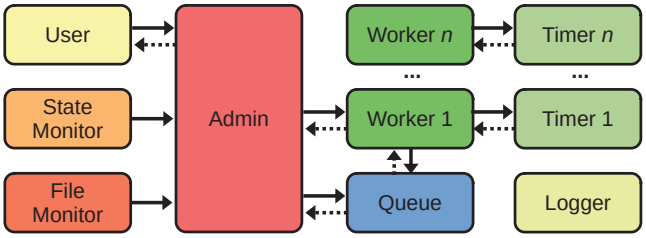

Fig. 5. Process structure of the `WorkflowRunner`, showing individual processes and their interactions. Connections to the logger have not been omitted for brevity. Secondary connections used only for replies are shown in dotted lines. Zero to n workers are created based on user input.

MEOW is well suited to this system for three core reasons. Firstly, in such a distributed system there is no obvious point of central control from which a more traditional SWMS can operate to accommodate the entire workflow from end to end. For example, while much analysis and storage can be managed remotely from a users personal workstation, the operation of scientific instruments often cannot be. Similarly, many dedicated analysis systems require access from on site, or from within specific networks.

Secondly, as there is more demand for heterogeneous systems or human-in-the-loop interactions, it will become more difficult to manage such a range of resources from a single script or tool. Whilst tools such as CUDA exist to hand off processing from a CPU to a GPU, such tools do not always exist for every piece of dedicated hardware or instrument. A lower level, generic approach such as reacting to data being produced simplifies what would otherwise be complex communication between different hardware systems.

Third and lastly, as the platforms for analysis become more disjointed, there is an expected to be an increased likelihood of errors throughout the workflow, especially in light of their exploratory nature. Moving data across networks is expensive in both time and data-usage and so repeated processing of already correct data should be avoided. By completing each job in isolation, MEOW can easily maintain completed analysis without one single error discarding an entire run of processing.

II. A Workflow Runner

MEOW was designed initially to function as part of a grid management solution, the Minimum intrusion Grid (MiG) [5]. The MiG is a large grid solution, and so obviously not suited to be deployed onto a wide variety of resources. Therefore, if we are to use the MEOW system outlined within it on varied hardware, then a new, smaller tool that only implements the event driven scheduling would be needed. To do this, a construct was created within the Python package `mig_meow` [22] for running MEOW systems locally on any machine capable of running Python 3. This tool was given the name `WorkflowRunner`. It is intended as a proof of concept of how event driven scheduling implementations can be used on individual resources, but also as a robust and performant implementation in its own right. Therefore it was designed with a parallel internal structure. To ensure freedom from deadlock and livelock a design utilising the principles of Communicating Sequential Processes (CSP) [19] was adopted as shown in Figure 5. As no circular loop of processing interactions exist we can conclude in accordance with CSP that it is impossible for this system to deadlock or livelock.

The USER process: The *User* process is the base process in which the constructor for the `WorkflowRunner` is called, and from which a `WorkflowRunner` object is returned. The `WorkflowRunner` object is then used as the entry point for any user interaction, with each sending an appropriate message to the `Admin` process. A response is always expected from the `Admin`. An exhaustive list of all provided functions will not be provided here, though they include all necessary functions for the creation, updating and deleting of *Patterns* and *Recipes*, and for monitoring the continued status of the `WorkflowRunner`

The STATE MONITOR process: Both the *State Monitor* and *File Monitor* inherit from the

`PatternMatchingEventHandler`, part of the `watchdog` API [39]. This catches file events. All defined *Patterns* and *Recipes* are saved to disk where they can be modified by a user. Any changes are picked up by the *State Monitor* and are reported to the `Admin` process. No response is ever expected from the `Admin`, so the *State Monitor* process should never be blocked, and is therefore always able to process new events.

The FILE MONITOR process: The *File Monitor* is identical to the *State Monitor* process, though rather than the internal directory for *Patterns* and *Recipes*, it monitors the wider file system, .

The ADMIN process: By far the most complex process is the *Admin*. It maintains the in-memory state of the runner, in which all currently registered *Patterns* and *Recipes* are stored and appropriate *Rules* are created. Updates to this state are provided by the *State Monitor* process.The *Admin* process will also receive input from the *File Monitor*. These events will be compared against the current *Rules*. If the event path matches a *Rule*, then the *Admin* will create a new job, and send its ID to the *Queue*.

As well as this core functionality, the *Admin* deals with requests from the *User* process, such as the previously mentioned adding or modifying *Patterns* and *Recipes*. Some requests, such as to query the current queue composition require further messages to be sent to the *Queue* before a response can be generated, but a response is inevitable and provided as soon as possible. The *Admin* process utilises a `wait` statement to hang until receiving input from either the *State monitor*, *User*, or *File Monitor* processes. These three inputs are prioritised in the order given, so that if multiple are available at the same time, only the first is read and processed.

Messages from the *State Monitor* are always of the highest priority as a fresh state will always be needed by the Admin. Changes in the state file system will also be finite in nature. Secondly, are messages from the *User* process, which can be replied to on a human time-frame. This means that they do not need to be responded to within nanoseconds and so can wait behind any *State Monitor* updates. Lastly, this leaves the *File Monitor*. This may produce a theoretically infinite number of messages as there is no limit on the number of files created or updated by jobs. Despite this being an unlikely use case, it is nevertheless a possibility and should be accounted for, therefore it must be the lowest priority as anything behind it could be eternally starved in this scenario.

The WORKER process: Jobs are executed within the *Worker* processes. The amount of these to be spawned is determined by the user, and at least one is needed if the workflow runner is to process jobs. A *Worker* will request a job from the *Queue* process. If a job is available, the ID will be sent to the *Worker*, and it will be executed. The job itself is processed by first parameterizing the input notebook using the python module `notebook_parameterizer` [28]. This is then run using `papermill` [31] in the same manner as is done on the MiG. Once execution has been completed, the job files are copied into a separate job output directory where they can be individually inspected. Jobs may produce output directly into the data directory, monitored by the *File Monitor*, in the same manner as can be done within the MiG. If no job was available in the *Queue*, the *Worker* sends a notification to its *Timer* process to start sleeping. If a job completes, or the *Worker* is notified by the *Timer*, it will poll the *Queue* for another job. This polling of the *Queue* will loop until manually stopped.

	Laptop	Threadripper
Cores	4	16
Hyperthreads	8	32
Processor	i7-8550U	Threadripper 1950X
Clockspeed	1.8 GHz	3.4 GHz
RAM	8GB	112GB
Disk	SSD	SSD

TABLE I
RESOURCES USED THROUGHOUT THIS PAPER.

The TIMER process: To prevent spamming the *Queue* process with requests for new jobs, each *Worker* has its own *Timer* process. This process will wait for a start signal from their *Worker* and then sleep. Once the sleep is over, it will send a signal to the *Worker*. By having the timer in a separate process rather than internal to the *Worker*, the *Worker* is still free to receive messages from the *Admin*, which would not be the case if it itself were sleeping.

The QUEUE process: The *Queue* process acts as a buffer for all jobs that have not yet been processed by a worker. It accepts messages either from the *Admin* or any of the *Worker* processes. From the *Admin*, the *Queue* will either receive the identity of a new job to be added to the queue, or a request for the current composition of the queue. Alternatively, any of the *Workers* may request the identity of a new job to execute. In any case, a response is always immediately generated and sent. It was necessary to separate the queue into its own process, rather than having it stored within the *Admin*, as otherwise there would be a risk of deadlock between *Workers* and the *Admin*.

The LOGGER process: The *Logger* process is just used to send debug messages to either the console or a log file.

III. INVESTIGATING FEASIBILITY

In order to recommend MEOW as a system for scheduling workflow jobs, we should demonstrate that event identification does not add significant overheads to the scheduling process, and that such a system is robust even at scale.

A. Testing `watchdog` Event Identification

As part of demonstrating the robustness of MEOW, we should test that all file events are caught by `watchdog`. Such a test was achieved by starting a monitor process using `watchdog` that would count every file event. Several writer threads would also be started that would concurrently create as many events as possible. Through testing it was determined that on the machine being used for the test, four writers each creating empty files was the fastest way of generating events. The test code is available at [14], with the results of four tests in Table II.

Events Made	Events Seen	Duration (s)	Events (per s)
1,000	1,000	0.35	2857.28
10,000	10,000	3.00	3328.19
100,000	100,000	31.69	3155.38
1,000,000	1,000,000	352.94	2833.31

TABLE II
RESULTS OF THE `watchdog` TEST. ALL RESULTS ARE A MEAN OF 20 RUNS AND ROUNDED TO 2 DECIMAL PLACES. RUN ON THE LAPTOP RESOURCE OUTLINED IN TABLE I.

These results demonstrate that event over long periods of time, `watchdog` does not get swamped and is capable of identifying all file system events. This shows that it is capable of scaling into large systems such as the MiG that may produce large numbers of data files in a short length of time.

B. Measuring MEOW Overheads

To investigate the overheads involved in a MEOW system, we first need a baseline to measure against. Here we will use Slurm. Although not a dedicated SWMS, it is a tool for the mass scheduling of jobs on distributed clusters of resources and so has a similar use case to MEOW. Each of the following tests were run in dedicated Docker [11] containers which can all be found at [14]. All tests were repeated 10 times to get a mean result, and each test was run from 10 to 500 jobs. These tests were not run evenly however, with the amount of jobs increasing at an accelerated rate as the jobs increase. This is as it was expected that the finer trends would be apparent with low amounts of jobs, while the overall relationship should be obvious with only a few larger tests.

Each test was run on both resources outlined in Table I. The laptop is a small machine, representative of the lower powered machines most researchers have as a personal workstation. Meanwhile the threadripper is a custom built machine designed for massive processing of scientific problems. As many of the tests are not explicitly parallelised, there will not be a massive performance difference between the two, but the threadripper will be less prone to being swamped by new threads or context switching, and as a desktop it will have much better cooling capabilities than a laptop. Due to space requirements, only the most pertinent results will be shown here, but full results can be seen at [14].

C. Overheads in Slurm

Slurm has two basic methods of scheduling jobs, `srun` and `sbatch`. Both will schedule one or more jobs, though `srun` is a blocking operation, where a user must wait for all jobs to schedule and execute before their script or terminal can progress. In contrast, `sbatch` schedules jobs in the background and so is a non-blocking operation. This is more akin to how the `WorkflowRunner` and most SWMS work and so `sbatch` will be used to measure against in most future tests.

To get a baseline for Slurm's performance, both `srun` and `sbatch` were used to schedule large numbers of jobs at once and how long it took the scheduling to complete was timed. Note that this does not include the execution time. As MEOW

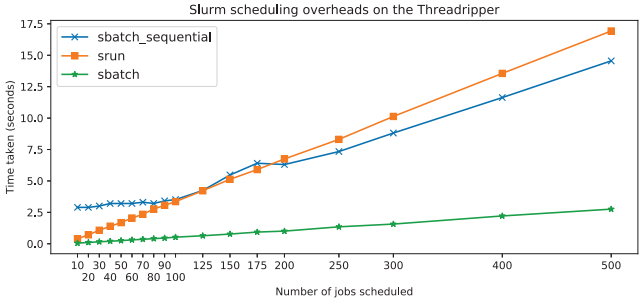

Fig. 6. Slurm scheduling durations on the Threadripper.

can also be used for continuous analysis we should also investigate the overhead of an ongoing system. Another test was therefore developed where jobs were scheduled individually, with each job scheduling a new job. This forms a chain of processing akin to how MEOW is expected to be used. Note that this second test includes execution times as each job needs to be executed to schedule the next. The results of all three tests on the Threadripper are shown in Figure 6. For each test the scheduling time, execution time, and a combination of both are shown. In the case of the `srun` and `sbatch` tests, the scheduling time is the pertinent part to look at and has been highlighted. In the case of the continuous scheduling test it is the combined time, which has also been highlighted. This is as the scheduling is in fact only the timing for scheduling the initial job and so shows an inaccurately fast time, while the combined time is the actual time for all jobs to be scheduled.

As Slurm is a relatively bare-bones system there is not much scope for overhead. This is reflected in the demonstrated very quick scheduling by `sbatch`. As the test was run with only a single Slurm worker, `srun` must wait for jobs to complete before scheduling the next, leading to the much larger overhead. Running `sbatch` sequentially runs is effectively doing the same thing, as each jobs needs to execute to schedule the next, but the use of `sbatch` means that a small amount of concurrency can happen between the scheduler and the processor, hence the slightly decreased overhead as the number of jobs increases. For low job numbers, the overhead in repeatedly starting new threads will slow down the sequential test compared to `srun`. Significantly, in all three tests the scheduling time per job is increasing linearly, meaning that Slurm will scale very well with larger job submissions.

D. Overheads in the `WorkflowRunner`

Within the `WorkflowRunner`, overheads will consist of the sum of the following components: Event identification in `watchdog`, *Rule* lookup, creating one or more new jobs, as well as any associated orchestration overhead. To help identify how much each of these components contribute to the total overhead, as well as to identify additional overheads, five different experiments were created. Unless otherwise noted the *Recipe* in each is some inconsequential execution. The five experiments would are as follows:

- **Single Pattern, Multiple Files (SPMF)**. In this experiment a single *Pattern* would be created that would

trigger on any file event within a directory. *N* files would then be created within the directory, causing the parallel scheduling of *N* jobs. This should allow us to identify the aggregate overheads of MEOW scheduling. This test can be directly compared against the Slurm `sbatch` test.

- **Single Pattern, Single Files, Parallel Scheduling (SPSFP)**. In this experiment a single *Pattern* would be created that would trigger on any file event within a directory. This *Pattern* would include an *N* wide parameter sweep over some variable. A single file would then be created within the directory, causing the parallel scheduling of *N* jobs. By comparing this to SPMF we should be able to identify the overhead caused by `watchdog` and event identification, by minimising it within this experiment. This test can be directly compared against the Slurm `sbatch` test.
- **Single Pattern, Single Files, Sequential Scheduling (SPSFS)**. In this experiment a single *Pattern* would be created that would trigger on any file event within a directory. The *Recipe* used by this *Pattern* would create another file in the same directory, so triggering the *Pattern* again. A variable will also be included so that a file is only created by the first *N*-1 jobs. This will result in sequential scheduling of *N* jobs. This test should illustrate the overhead in continuous, looping scheduling, the most anticipated use-case for a MEOW system. This test can be directly compared against the Slurm sequential `sbatch` test.
- **Multiple Patterns, Single File (MPSF)**. In this experiment *N Patterns* would be created that would trigger on any file event within a directory. A single file would then be created within the directory, causing the parallel scheduling of *N* jobs. When compared against the SPMF experiment, this can isolate the overhead in *Rule* lookup. This test can be directly compared against the Slurm `sbatch` test.
- **Multiple Patterns, Multiple Files (MPMF)**. In this experiment *N Patterns* would be created that would each trigger on a different specific file within a directory. *N* files would then be created within the directory, each matching to a single *Pattern* causing the parallel scheduling of *N* jobs. By comparing this to the other tests we should be able to identify the expected general overhead in a live system, where many differing events may happen at once, as well as the overhead for *Pattern* lookup in a larger memory construct compared to the SPMF test. This test can be directly compared against the Slurm `sbatch` test.

The results for the tests run on the Threadripper are shown in Figure 7 on a logarithmic scale. In the SPMF, MPSF and SPSFP tests the `WorkflowRunner` actually comes out ahead of the Slurm tests, with a speedup of roughly 2.5, though this varies by experiment and the amount of jobs. In each case the per-job scheduling time is reasonably constant demonstrating good scalability in these situations, as can be seen in Figure 8. The MPMF does not scale as well however, with it being slower than the Slurm past roughly 100 jobs

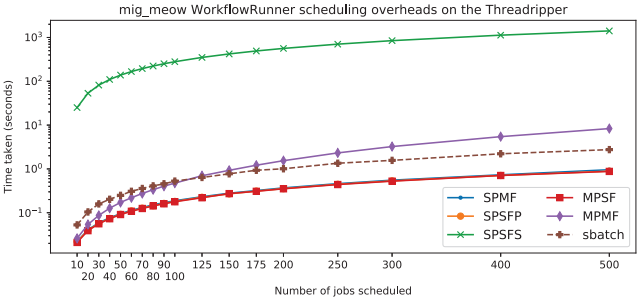

Fig. 7. Logarithmic WorkflowRunner scheduling durations on the Threadripper. The Slurm *sbatch* has also been shown as a dashed line for comparison.

at once. This is down to two parts. Firstly, each file event is identified and processed separately, and secondly it takes time for the `WorkflowRunner` to navigate the stored *Rules*. These overheads each occur in the SPMF or MPSF without adding any noticeable slowdown, and so at least for up to 500 jobs we can conclude that they are negligible in isolation, but have a quadratic effect on the per-job time when they both increase.

The performance of the SPSFS test was roughly 100 times slower than the sequential `sbatch` test. This is down to three key overheads, settling, querying, and executing. Firstly, each event has a 'settle time', where to prevent the `WorkflowRunner` getting swamped by multiple events from the same location any events that occur at the same location and very close in time are represented as a single event. This means after any single event the *File Monitor* process will wait for one second to catch any subsequent events at the same location. By definition, this will add at least one second of overhead to processing each event. This will occur in all tests, but in all others it will occur only once no matter how many jobs will be eventually scheduled, while in the SPSFS test it will occur for each sequential job. There is also the additional overhead of waiting for each job to be executed in turn. Aside from the raw time taken to execute the code, which is more complex in the `WorkflowRunner` jobs than in the Slurm testing, there will also be a delay inherent in the *Worker* process requesting a job from the *Queue* process. In these tests the *Worker* was set to query for new jobs every second. From all this we can conclude that in these tests at least the overhead from each of these was roughly a single second, and totalled 3 seconds. This is significantly slower that the approximately 0.035s achieved by the sequential `sbatch` test. However, it is worth highlighting that was in the case of the SPMF, MPSF and SPSFP tests, the SPSFS demonstrates very good scalability as it has a constant per-job overhead of approximately 3s. This overhead should remain constant even across a larger system of multiple users operating MEOW analysis at the same time.

E. Overheads on the MiG

Exactly the same tests were run on the MiG as on the `WorkflowRunner`. As with the other tests, the code and results are available at [14]. As can be seen in Figure 9,

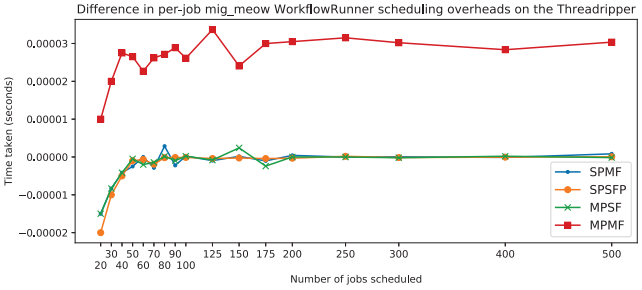

Fig. 8. Delta in per-job WorkflowRunner scheduling durations on the Threadripper. Note that the SPSFS result have been excluded as it has a much greater scale that crushes the rest of the results.

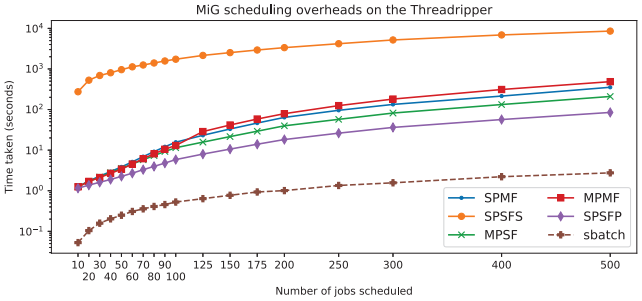

Fig. 9. Logarithmic MiG scheduling durations on the Threadripper. Each result is an average of 10 runs. The Slurm *sbatch* has also been shown as a dashed line for comparison.

performance from these tests is worse across the board, but this is to be expected. The MiG is a complete grid management system rather than a lightweight scheduler, so will always run much slower than either Slurm or the `WorkflowRunner`. With this in mind we shouldn't be too surprised that generally the MiG is roughly 25-50 time slower than `sbatch`. The sequential test is even slower at roughly 500 times slower than the sequential `sbatch` test. It is worth noting that whilst the SPSFS test demonstrates linear scalability, all others were quadratic in nature. This is demonstrated in Figure 10 where we can see that the difference in per-job timings is linear as the total number of scheduled jobs increases, which results in a quadratic increase in total scheduling time.

These broad increases are due to the nature of event processing on the MiG. As each event occurs the `watchdog` monitor will catch the event by performing some initial processing such as attaching a timestamp to it, and then matching it against the current list of *Rules*. This 'pre-processing' is kept to a minimum, and so any actions from a *Rule* match being carried out in a threaded function that must wait for processing resources to be available. This is done to keep the monitor process free to catch further events, but means that if many events happen at once then many different threads will be started. On the MiG this 'pre-processing' is quite extensive, with a number of authentication and robustness checks needed to be carried. Matching has been sped up through the use of regex, but the overheads are unavoidable. As many different matching events occur at the same time in these tests, more and more overheads are added by starting so many different

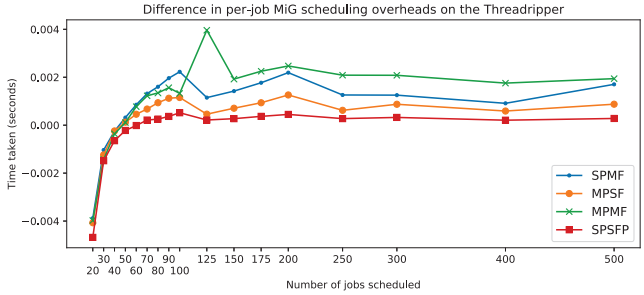

Fig. 10. Delta in per-job MiG scheduling durations on the Threadripper. Each result is an average of 10 runs. Note that the SPSFS result have been excluded as it has a much greater scale that crushes the rest of the results.

threads at the same time. Note that this does not occur on the `WorkflowRunner` as this uses the multiprocessing design does not require starting a new thread for each event.

Whilst it was expected that the MiG would run slowly, it was not expected that it would run quite as slowly as it has. Nevertheless, when we look at the results for the `WorkflowRunner` we can at least conclude that this is down to underlying issues within the MiG rather than with the MEOW system itself. as the same lack of scalability is not evident in the `WorkflowRunner`.

F. Evaluating the MEOW overheads

In light of all these tests we can conclude that MEOW does not add significant overhead to the scheduling process. It can be used to schedule large amounts of jobs at once, with a minimum of user definitions. This scheduling will demonstrate linear scaling when either a large amount of files or *Patterns* are in use at one moment. However, when both are in use at the same time the system can begin to experience greater and greater overheads. This is especially true in the MiG implementation. Even in the slowest non-sequential test (500 Laptop MPMF jobs) it must be remembered that only 0.97s was spent on scheduling each job and most tests ran considerably quicker than that. It does not seem unreasonable to expect that most scientific analysis would take considerably longer than this to complete, and so even this slow scheduling would quickly fade into the background compared to any execution time.

Although the scaling on sequential jobs is linear, a considerable amount of time can be spent before all required jobs are scheduled, as by definition all but one of them must be executed before they will all have been scheduled. We also see ever increasing overheads in the MPMF test. This is potentially concerning if MEOW were to be used as a central controller, such as in a large grid system like the MiG with many unique events occurring and being compared against many unique *Patterns*. If a sufficiently large enough number of users were using the system to schedule MEOW analysis, such that several hundred events were supposed to be triggering several jobs within the same few second then each user would begin to see increased overheads in line with the results presented in Figure 9. However, the proposed event driven systems is intended as a distributed one, with many schedulers on many

different resources each with only a few users at any one time. At the same time, the majority of scientific workflows do not produce masses of small files, but few large ones. Therefore, though this poor scalability from the MPMF test remains noteworthy, it should not be applicable the majority of MEOW use cases. Even with several users potentially creating many *Patterns and Recipes*, and producing numerous files at different locations, MEOW systems are capable of automatically scheduling analysis in trivial times at scale, especially compared to the hours or even days sometimes experienced in scientific processing. Regardless of the job processing time, MEOW can be expected to perform faster than Slurm with roughly a 2.5x speedup. As Slurm is already a widely adopted tool, this is an acceptable benchmark to pass and so we can conclude that MEOW has an acceptable level of performance in its scheduling.

IV. A Self-Modifying Workflow

A simple scientific example of a MEOW workflow has already been presented within [23] and so instead here we will examine a more interesting example of the new workflow structures made possible by the bottom-up design. Namely, the ability for a MEOW system to be self-modifying, and construct, modify or remove MEOW constructs at runtime. This is possible to do on both the MiG and within the new `WorkflowRunner` and so will be presented using both.

A. Problem Outline

In this example a user wishes to apply a filter to image data. However, the required filter regularly changes, even though the fundamental process does not. The users needs can be met with MEOW, by designing a system that will take configuration inputs to create new *Patterns*. Each of these *Patterns* will apply different filters to different data, according to their configuration. In this system the user only needs to manually write a single *Pattern*, and any subsequent requirements will be met by the MEOW system itself. This problem will therefore demonstrate how we can construct new MEOW *Patterns* from within a MEOW system to fundamentally alter the structure of the workflow. While *Recipes* perform the actual analysis, assembling a Jupyter notebook programmatically has been demonstrated numerous times before [6], and so will be overlooked here but is of course just as possible.

What we will create is a single *Pattern* and *Recipe*, resulting in one *Rule*. This *Rule* will schedule jobs to construct new *Patterns*, based on user provided configurations. The structure for this system is shown in Figure 11. Here we can see that our single *Rule* will respond to any configuration files placed in the *confs/* directory. This *Rule* will trigger jobs that will construct new *Patterns*, which will monitor different locations for data. These subsequent *Pattern* will create further *Rules*, that then schedule jobs as would be expected in any other MEOW *Rule*.

B. Predefined Patterns and Recipes

Before we define a Jupyter notebook for assembling new *Patterns*, let us describe the *Recipe* which the assembled *Patterns* will use. This is the *filter_recipe.ipynb* Jupyter notebook

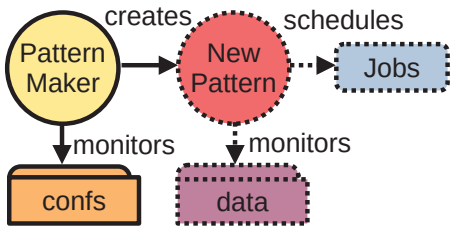

Fig. 11. The structure of the self-modifying example.

and in it image data is read in, a filter is applied to this image, and the filtered image is saved as a new file. The key part is that the filter command is created from the arguments provided to the Jupyter notebook. A valid filter command will be any of the filters available as part of the Python `ImageFilter` module [20], part of `Pillow` [32].

To construct new *Pattern* that will use the *filter_recipe.ipynb Recipe*, we will need a second Jupyter notebook. This is defined in *pattern_maker_recipe.ipynb*. This notebook reads in a configuration YAML file with then contents then parsed and used to construct a new `Pattern` programmatically. Once this new `Pattern` is complete, it is written to a specified directory. This is the directory where the `WorkflowRunner` will store the MEOW constructs, and is monitored by its *State Monitor* process. By writing a new `Pattern` directly to this location, we can insert it directly into the state of the `WorkflowRunner`.

At the start of the experiment, only a single `Pattern` is defined. This defines the directory path to be monitored, which in this case is just the *confs/* directory. All *Pattern* and notebook definitions, along with all input and output data files for both experiments can be seen in [14].

C. Using `WorkflowRunner`

A script was created to construct the necessary *Pattern* and *Recipes*, and then start a `WorkflowRunner` instance with them. Of note is that the internal state directory used by the `WorkflowRunner` is manually set to the same directory as the general file base directory, which in this example will be the *self-modifying/* directory. This means that both the State Monitor and File Monitor processes will be monitoring the same directory. Putting the state directory in the same place as the base file directory makes it easiest to access from within the jobs, which makes updating the `WorkflowRunner` state easier. This does mean there will be two monitors listening to the same file structure, so there may be some slowdown in responding to events due to each event being caught and processed twice. For a small proof-of-concept example like this on a local system, this will not create a significant overhead, though the problem will become more pronounced if used on something larger such as the MiG, and so is not generally advised.

When the `WorkflowRunner` is initially created, no data is present within the *confs/* directory, and so no *Pattern* creation jobs are scheduled. A user can also easily see the *Patterns* and *Recipes* that are registered in the system as they will each

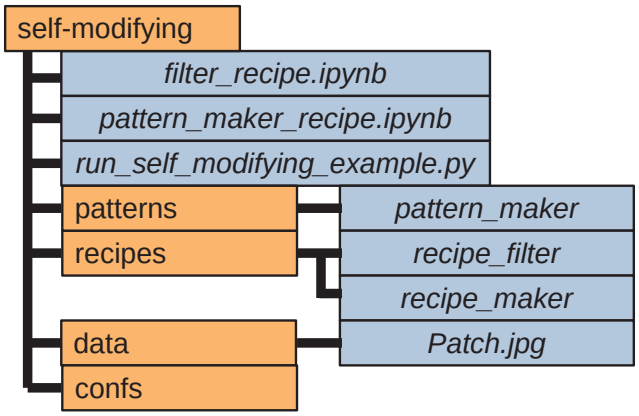

Fig. 12. The file structure of the self-modifying example before any configuration files are added to the `WorkflowRunner`. Directories are shown in orange and files in blue.

Fig. 13. Comparison of the input and output *Patch.jpg* data, used in the self-modifying example. Input data from *data/Patch.jpg* is shown on the left, with output data at *GaussianBlurred/Patch.jpg* on the right.

be in a *patterns/* and *recipes/* directory within *self-modifying/*. Before we start initiating jobs, we can add some image data in a *data/* directory. This will give us the overall structure shown in Figure 12. As no new *Patterns* have yet been created no processing can take place, even if the `WorkflowRunner` is running. To start scheduling some analysis we will need a configuration file to place in the *confs/* directory. Such a file is shown in Listing 1. This file is a YAML file containing a number of variable definitions, which match up to the expected inputs in the *pattern_maker.ipynb* Jupyter notebook. If this file is placed into the *confs/* directory, then the *Rule* created by *pattern_maker* will trigger, and a job will be scheduled.

```
input_path: data/*.jpg
output_path:
    '{VGRID}/GaussianBlurred/{FILENAME}'
filter: GaussianBlur
args:
    radius: 2
```

Listing 1. *input.yml* file contents.

This newly scheduled job will use the parameters specified in *input.yml* to create a new `Pattern`, which will be given the name *GaussianBlur_radius_2*, and will use the `GausianBlur` image filter in any resultant jobs. This *Pattern* will be saved into the *self-modifying/patterns/* directory, and so picked up by the `WorkflowRunner` for it to create a new *Rule*. As the *Rule* derived from this `pattern` will monitor the `data/` directory, and we have already placed an image file, *Patch.jpg* in said directory, a job will be immediately scheduled. In accordance with the already presented definitions, this will produce output which will be saved into the *GaussianBlur* directory. The sample input and output data used in this example are shown in Figure 13. As the `WorkflowRunner` is a continuous system, it will continue to monitor for additional events until the user stops it. Therefore we could add more data files, in which case more filter jobs will automatically be scheduled. Alternatively we can also add more configuration files to the *confs/* directory, which would create new *Patterns* and then lead to more filter jobs. If any of the configuration or data files were changed then the system would automatically reschedule the analysis without a user needing to restart anything. If any incorrect configuration were added, such as asking for a filter that did not exist, then naturally that job would fail. However that job would fail in isolation and all others could continue with no additional user input. This should demonstrate the utility of MEOW as a tool for scheduling jobs, in a robust, scalable and dynamic manner, where small parts or even the entire system can be changed at runtime.

D. Using the MiG

This same example was also carried out on the MiG, showing that although more difficult to achieve, the same results are possible even on a more restricted MEOW implementation. We cannot simply manipulate the MEOW state storage location on the MiG, as this part of the system is entirely hidden from the user. This is an intentional security feature, so that users do not manipulate data they do not have access to, or corrupt the state of a live system.

We can gain some limited access however by manipulating the mechanisms exposed in the inbuilt JSON messaging used in the `WorkflowWidget` [23]. To do so, we need to define some additional variables used within the MiG. Therefore we will update the old *pattern_maker.ipynb*, to a new *pattern_maker_mig.ipynb*. Mostly it is the same as before, but with the addition of the *WORKFLOWS_SESSION_ID*, *WORKFLOWS_URL* and *workgroup* variables. These will all be used in the modified *pattern_maker_recipe.ipynb* Jupyter notebook so that it can communicate directly with the MiG. As the *WORKFLOWS_SESSION_ID* is a security feature within the MiG, it has not been shown in the examples files in [14], but was of course used in the actual example run. The only other significant difference is that rather than writing directly to the state directory, we must instead communicate remotely with the MiG via JSON requests. In practice, this results in few code changes however, with locals writes being replaced with remote messages being sent.

As expected, once the `Pattern` and `Recipes` have been registered with the MiG, no jobs were scheduled until a file was added to the *confs/* directory. The same data file was added as before, and the *Pattern GaussianBlur_radius_2* was created on the MiG. This itself did not schedule any processing until the file *data/Patch.jpg* was added, at which point a second job was scheduled. This produced identical results to those shown in Figure 13, and so will not be repeated again here.

This is not an ideal solution however, as it depends on exposing security features of the MiG. This problem is limited in scope, as in order for a user to get to this stage they will need to have access to the MiG in order to spawn a Jupyter notebook with the necessary *WORKFLOWS_URL* and *WORKFLOWS_SESSION_ID* values. Therefore, as long as users are sensible with these credentials they will not be exposing data that would otherwise be secure. It is suspected that drawing attention to these variables which are otherwise hidden may encourage users to share them and so exacerbate the problem.

From a usability perspective though, the pressing problem is that *Patterns* and *Recipes* created in this manner will only be possible for as long as the *WORKFLOWS_SESSION_ID* remains valid. This is as only a *WORKFLOWS_SESSION_ID* will ever be registered for a user, and they will be regenerated throughout the lifetime of the MiG. However, creating a new *WORKFLOWS_SESSION_ID* will not update the variables passed in these *Patterns* and so when the resultant jobs try to send a message to the MiG they will be rejected. For this reason this solution is not suggested as a final implementation, but merely as a stop-gap demonstration of potential future functionality. A more robust implementation would be additional functionality within the MiG such as each job being assigned its own *WORKFLOWS_SESSION_ID*, thus allowing *Patterns* and *Recipes* interactions to be verified without having to share hard-coded credentials across jobs. A similar system is already in place on the MiG for SSH users within jobs, which allows individual job mount requests to be similarly authenticated, so it is not expected to be a significant challenge to do that same for MEOW interactions.

E. Concluding The Self-Modifying Example

Although this was somewhat of a toy example, with a simple configuration file taken as input, this is not the limit of the possibilities. Any input file could be taken in and parsed so as to produce new or modified MEOW constructs. Although only the dynamic creation of *Patterns* has been shown, it is perfectly possible for new *Recipes* to be constructed at runtime in the same manner, it would just take considerably more lines of code to create a new Jupyter notebook from scratch.

It is worth noting that we are not limited to merely adding new constructs, but can modify existing ones if we used some of the functions included in `mig_meow` for reading the current state of the workgroup. Here we could read in definitions, and write modified values back in the same manner as if we were altering them programatically within a Jupyter notebook. This means that a MEOW system can create, modify and delete itself, or its parts at runtime. It can also make decisions about when to do so within a suitably written *Recipe*, and so we can conclude that MEOW analysis is Turing complete at runtime. Whilst it would be bold claim to state that this is unique, none of the currently encountered SWMS have come close to this level of self modification.

V. Conclusions

This paper has explored event-based processing as a means for scheduling workflows in a dynamic and distributed manner. To better enable this a robust new tool has been introduced, the `WorkflowRunner` within `mig_meow`. Five benchmarks for event-based scheduling systems have also been described. These benchmarks demonstrate that event-based scheduling does not add significant overhead compared to traditional centrally controlled scheduling. Additionally, a short example is presented demonstrating how event-based systems can be so dynamic as to completely rewrite their own structure at runtime. This is something far more difficult to achieve in traditional top-down scheduling systems and so allows for new possibilities in workflow construction. This is expected to be of particular worth to distributed analysis systems, or in extremely heterogeneous systems accommodating human-in-the-loop interactions.

References

[1] Altintas, I., Berkley, C., Jaeger, E., Jones, M., Ludascher, B., Mock, S.: Kepler: An Extensible System for Design and Execution of Scientific Workflows. In: Proceedings. 16th International Conference on Scientific and Statistical Database Management, 2004. IEEE (2014)

[2] Babuji, Y., Woodard, A., Li, Z., Katz, D.S., Clifford, B., Kumar, R., Lacinski, L., Chard, R., Wozniak, J.M., Foster, I., Wilde, M., Chard, K.: Parsl: Pervasive Parallel Programming in Python. In: Proceedings of the 28th International Symposium on High-Performance Parallel and Distributed Computing. p. 25–36. HPDC '19, Association for Computing Machinery, New York, NY, USA (2019). https://doi.org/10.1145/3307681.3325400, https://doi.org/10.1145/3307681.3325400

[3] Badia, R.M., Conejero, J., Diaz, C., Ejarque, J., Lezzi, D., Lordan, F., Ramon-Cortes, C., Sirvent, R.: Comp superscalar, an interoperable programming framework. SoftwareX **3-4**, 32–36 (2015). https://doi.org/https://doi.org/10.1016/j.softx.2015.10.004, https://www.sciencedirect.com/science/article/pii/S2352711015000151

[4] Benedyczak, K., Schuller, B.T., Sayed, M., Rybicki, J., Grunzke, R.: Unicore 7 — middleware services for distributed and federated computing. pp. 613–620 (07 2016). https://doi.org/10.1109/HPCSim.2016.7568392

[5] Berthold, J., Bardino, J., Vinter, B.: A Principled Approach to Grid Middleware: Status Report on the Minimum Intrusion Grid. In: Xiang, Y., Cuzzocrea, A., Hobbs, M., Zhou, W. (eds.) Algorithms and Architectures for Parallel Processing, pp. 409–418. Springer (2011)

[6] Creating an IPython Notebook programatically. https://gist.github.com/fperez/9716279 (2016)

[7] cwltool. https://github.com/common-workflow-language/cwltool (2021)

[8] Dean, J., Ghemawat, S.: Mapreduce: Simplified data processing on large clusters. In: Proceedings of the 6th Conference on Symposium on Operating Systems Design & Implementation - Volume 6. p. 10. OSDI'04, USENIX Association, USA (2004)

[9] Deelman, E., Blythe, J., Gil, Y., Kesselman, C.: Pegasus: Planning for execution in grids. Tech. Rep. Technical Report 2002-20, GriPhyN (2002), http://pegasus.isi.edu/publications/ewa/pegasus_overview.pdf

[10] Dias, J., Guerra, G., Rochinha, F., Coutinho, A.L., Valduriez, P., Mattoso, M.: Data-centric iteration in dynamic workflows. Future Generation Computer Systems **46**, 114–126 (2015)

[11] Docker. https://www.docker.com/ (2021)

[12] Dreher, M., Peterka, T.: Decaf: Decoupled dataflows for in situ high-performance workflows. Tech. Rep. ANL/MCS-TM-371, Argonne National Laboratory, Lemont, IL (7 2017)

[13] EuXFEL. https://www.xfel.eu (2022)

[14] Experiment results. https://sid.erda.dk/sharelink/F0hrjh3aEN (2022)
[15] Fahringer, T., Jugravu, A., Pllana, S., Prodan, R., Junior, C., Truong, H.L.: Askalon: a tool set for cluster and grid computing. Concurrency and Computation: Practice and Experience **17** (02 2005). https://doi.org/10.1002/cpe.929
[16] Ferreira, J.E., Wu, Q., Malkowski, S., Pu, C.: Towards flexible event-handling in workflows through data states. In: 2010 6th World Congress on Services. pp. 344–351 (2010). https://doi.org/10.1109/SERVICES.2010.60
[17] Foster, I.: Globus Toolkit Version 4: Software for Service-Oriented Systems. In: IFIP International Conference on Network and Parallel Computing. pp. 2–13. Springer-Verlag (2006)
[18] Harenslak, B.P., de Ruiter, J.R.: Data Pipelines with Apache Airflow. Manning, 1 edn. (2021)
[19] Hoare, C.A.R.: Communicating sequential processes. Communications of the ACM **21**(8), 666–677 (1978)
[20] ImageFilter. https://pillow.readthedocs.io/en/5.1.x/reference/ImageFilter.html (2022)
[21] Kubernetes. https://kubernetes.io/ (2021)
[22] Marchant, D.: mig_meow on PyPi. https://pypi.org/project/mig-meow (2021)
[23] Marchant, D., Munk, R., Brenne, E.O., Vinter, B.: Managing event oriented workflows. In: 2020 IEEE/ACM 2nd Annual Workshop on Extreme-scale Experiment-in-the-Loop Computing (XLOOP). pp. 23–28 (2020). https://doi.org/10.1109/XLOOP51963.2020.00009
[24] Mattoso, M., Dias, J., A.C.S.Ocaña, K., Ogasawara, E., Costa, F., Horta, F., Silva, V., de Oliviera, D.: Dynamic steering of HPC scientific workflows: A survey. Future Generation Computer Systems **46**, 100–113 (2015)
[25] MAX IV. https://www.maxiv.lu.se (2022)
[26] Montella, R., Di Luccio, D., Kosta, S.: DagOn*: Executing Direct Acyclic Graphs as Parallel Jobs on Anything. In: Proceedings of WORKS 2018: 13th Workshop on Workflows in Support of Large-Scale Science, Held in conjunction with SC 2018: The International Conference for High Performance Computing, Networking, Storage and Analysis. pp. 64–73 (2019). https://doi.org/10.1109/WORKS.2018.00012
[27] Munk, R., Marchant, D., Vinter, B.: Cloud enabling educational platforms with corc. In: Proceedings of the 8th Workshop on Cloud Technologies in Education (CTE 2020) (2020)
[28] notebook-parameterizer. https://pypi.org/project/notebook-parameterizer/ (2021)
[29] Oinn, T., Addis, M., Ferris, J., Marvin, D., Senger, M., Greenwood, M., Carver, T., Glover, K., Pocock, M.R., Wipat, A., Li, P.: Taverna: a tool for the composition and enactment of bioinformatics workflows. Bioinformatics **20**(17), 3045–3054 (2004)
[30] Oracle Grid Engine. https://www.oracle.com/technetwork/oem/host-server-mgmt/twp-gridengine-overview-167117.pdf (2010)
[31] papermill. https://github.com/nteract/papermill (2021)
[32] Pillow. https://pillow.readthedocs.io/en/stable/ (2021)
[33] Ramon-Cortes, C., Lordan, F., Ejarque, J., Badia, R.M.: A programming model for hybrid workflows: Combining task-based workflows and dataflows all-in-one. Future Generation Computer Systems **113**, 281–297 (12 2020). https://doi.org/10.1016/j.future.2020.07.007, http://dx.doi.org/10.1016/j.future.2020.07.007
[34] Rocklin, M.: Dask: Parallel computation with blocked algorithms and task scheduling. In: Proceedings of the 14th python in science conference. pp. 126–132 (01 2015). https://doi.org/10.25080/Majora-7b98e3ed-013
[35] Tejedor, E., Becerra, Y., Alomar, G., Queralt, A., Badia, R.M., Torres, J., Cortes, T., Labarta, J.: PyCOMPSs: Parallel computational workflows in Python. International Journal of High Performance Computing Applications **31**(1), 66–82 (2017). https://doi.org/10.1177/1094342015594678
[36] Tolosana-Calasanz, R., Bañares, J., Álvarez, P., Ezpeleta, J.: On interlinking of grids: A proposal for improving the flexibility of grid service interactions. In: Proceedings of The Third International Conference on Internet and Web Applicaations and Services: ICIW 2008. pp. 714–720 (07 2008). https://doi.org/10.1109/ICIW.2008.39
[37] Torque Resource Manager. https://adaptivecomputing.com/cherry-services/torque-resource-manager/
[38] Voetmann, N.A.T.: Framework for Uploading Research data (FUR). Master's thesis, Niels Bohr Institute, University of Copenhagen (3 2021), https://sid.idmc.dk/sharelink/hZjJ5NSvlb
[39] watchdog. https://pypi.org/project/watchdog/ (2021)
[40] Workload Manager. https://www.ibm.com/docs/en/aix/7.2?topic=management-workload-manager (2021)
[41] Yildiz, O., Ejarque, J., Chan, H., Sankaranarayanan, S., Badia, R.M., Peterka, T.: Heterogeneous hierarchical workflow composition. Computing in Science Engineering **21**(4), 76–86 (2019). https://doi.org/10.1109/MCSE.2019.2918766
[42] Yoo, A., Jetter, M., Grondona, M.: Slurm: Simple linux utility for resource management. Lecture Notes in Computer Science **2862**, 44–60 (2015)

An Algebraic Approach to the Goldbach Conjecture

Jason South

Jason South is with the TTI, Inc, United States (e-mail: jrsouth@smu.edu).

Abstract. This paper will give both the necessary and sufficient conditions required to find a counter-example to the Goldbach Conjecture by using an algebraic approach where no knowledge of the gaps between prime numbers is needed. It will then be shown that it is impossible for such a counter-example to exist. To begin, let $2a$ be a counter-example to the Goldbach Conjecture where $a \in \mathbb{N}$, non-prime, and $a > 3$. It will be shown using the closure property of the integers, along with the Fundamental Theorem of Arithmetic, that finding a counter-example to the Goldbach Conjecture is equivalent to stating that for any prime $p_i < a$ there must exist some unique $q_i, \alpha_i \in \mathbb{N}$ where $2a = q_i + p_i$ and $\prod_{i=1}^{\pi(a)} q_i = \prod_{i=1}^{\pi(a)} p_i^{\alpha_i}$. The final step will be to prove that there are no integer solutions when $a > 3$ for the two equations above. A similar method will be employed to prove every even number is the difference of two primes. We start by assuming that there exists some $2a$, where $a \in \mathbb{N}$ and $a > 3$, which is not the difference of two primes where one prime is less than a. Again, using of the closure property of the integers, along with the Fundamental Theorem of Arithmetic, gives an equivalent relationship for a counter-example $2a$ to exist. This relationship states that for any prime $p_i \leq a$, there exists some unique $q_i, \alpha_i \in \mathbb{N}$ where $2a = q_i - p_i$ and $\prod_{i=1}^{\pi(a)} q_i = p_{\pi(a)+1}^{\beta(a+1)} \prod_{i=1}^{\pi(a)} p_i^{\alpha_i}$ with the condition that the function $\beta(a+1)$ is equal to one if $a+1$ is prime and zero otherwise. It will then be demonstrated that no integer solutions exist to the two equations above for $a > 3$. Once these theorems have been established Polignac's Conjecture will follow as a consequence.

1. Notation

$\mathbb{N}$	The set of Natural Numbers, including 0, unless stated otherwise.
$\mathbb{Z}$	The set of Integers.
$\mathbb{P}$	The set of Prime Numbers.
L.H.S.	Abbreviation for "left hand side" of an equation.
R.H.S.	Abbreviation for "right hand side" of an equation.
G.C.D.	Abbreviation for "Greatest Common Divisor."
F.T.A.	Abbreviation for "Fundamental Theorem of Arithmetic."
G.C.	Abbreviation for "Goldbach Conjecture."
$\pi(a)$	Prime counting function up to some number a.
p_i	A prime number with index $i \in \mathbb{N}$ where $1 \leq i \leq \pi(a)$ for a given $a \in \mathbb{N}$.
$x \in X$	The value x is an element of a particular set X.
$a\|b$	Given the non-zero integer a, then a is a divisor of b.
$a \nmid b$	Given the non-zero integer a, then a is not a divisor of b.
$\|\|a\|\|$	Absolute value or norm of a.
$a\#$	Primorial of some integer a.
$\exists x : P(x)$	There exists some x that satisfies the condition $P(x)$.
$\forall x : P(x)$	Every x satisfies the condition $P(x)$.
$\deg(F(x))$	Degree of the polynomial $F(x)$.

2. Introduction

The Goldbach Conjecture, page 117 in [7], appeared in a correspondence between Leonard Euler and Christian Goldbach in 1742 where it was suspected that every number greater than

two could be written as the sum of three primes. Since the number one was considered a prime, however, no longer is, this conjecture has been split up into a strong and a weak version. The strong version in some texts may be referred to as the "binary" Goldbach Conjecture. The weak version is sometimes named the "ternary" conjecture as it involves three prime numbers.

The strong version of the Goldbach Conjecture states that for every even integer greater than two there will exist two primes whose sum is that even number. Although this conjecture is simple to state all attempts to prove it, or find a counter-example, have failed. With that said, this conjecture has been verified to an astonishing degree. In July of 2000 Jörg Richstein published a paper [8] using computational techniques showing that the Goldbach Conjecture was valid up to 4×10^{14}. In November of 2013 a paper [3] was published by Thomás Oliveira e Silva, Siegfried Herzog, and Silvo Pardi which also used advances in computational computing proving that the binary form of the Goldbach Conjecture is true up to 4×10^{18}.

The weaker version of the Goldbach Conjecture, or Ternary Conjecture, states that every odd number greater than 7 can be written as the sum of three prime numbers. Much like the strong version, this conjecture has also been verified up to large orders of magnitude. As an example, in 1998 [10] Yannick Saouter proved this conjecture up to 10^{20}. In fact, it was shown that if the generalization of the Reimann Hypothesis were true, that the Ternary Conjecture would follow. This was proven by Hardy and Littlewood [4] in 1923. Since the Generalized Reimann Hypothesis is still an open question, this did not give a definitive answer as to the truth of the Ternary Conjecture, however, it did provide a possible path to follow.

Another breakthrough in the Ternary Conjecture came in 2013 when Herald Helfgott verified in a paper [6] that the Ternary Conjecture was valid up to 10^{30}. Later that year a preprint [5] by Helfgott was placed on the ARXIV claiming that the Ternary Conjecture is true. Although this paper has not been published as of yet, it has been accepted by many in the mathematics community as being true and provides a significant breakthrough in Number Theory.

With the Strong Goldbach Conjecture concerned about the relationship between even numbers and the sums of primes, an analogue to this conjecture may be given in the form of asking whether every even number may be written as the difference of two prime numbers. It will be shown that the answer to these questions can be used to prove a similar conjecture named after Alphonse de Polignac, 112 in [7], stating that for any even number there are an infinite number of prime pairs whose difference is that even number. This conjecture has also gone unproven for well over a century. In order for an answer to be given to these conjectures a new methodology will be introduced. This will be done in the next section.

3. Methodology and Summary of Results

All attempts to prove the aforementioned conjectures have failed. Many of these attempts rely on an analytic number theory approach such as analyzing the gaps between primes [13]. Another method is to assume a certain hypothesis is true, such as the Generalized Reimann Hypothesis, to show that hypothesis implies one of these conjectures [4]. If that hypothesis can then be proven, the conjecture would follow. There are also experimental [2] along with computational results from [8], [3], and [10], however, these methods will most likely require major breakthroughs in order to proceed. For this reason, a new approach is needed.

The method which will be explored in this paper is a novel technique that will be used to determine algebraically both the necessary and sufficient conditions for a counter-example to the Goldbach Conjecture to be discovered. It will also be shown that these same techniques, with slight modifications, can be used to determine both the necessary and sufficient conditions for an even number which can not be written as the difference of two prime numbers with one prime being less than that even number. The advantage of this method lies in the fact that it circumvents two main reasons why a proof of the Goldbach Conjecture, and whether every even number may be written as the differences of two prime numbers, have remained elusive.

The first of these difficulties in finding a proof lies in the fact that there is no known formula that allows one to determine precisely how many prime numbers there are in a given range.

The Prime Number Theorem[1] [11] does give an approximation to the number of primes up to a given value; however, this alone is not sufficient to give strong enough evidence that the conjectures hold for any value chosen. For this reason most probabilistic arguments about how many primes pairs there could be which sum up to a desired even number will fail.

The second issue is that there is no known parameterization of the prime numbers, or even a computationally efficient way to determine when a number is prime. Wilson's Theorem[2] [12] does provide both the necessary and sufficient conditions for determining if a number is prime; however, since it is a function of the factorial it is computationally inefficient to use in any practical manner. Because of these two facts, any question about additive properties of the primes has been destined to run into near insurmountable difficulties using current techniques.

To begin laying the foundation for this new method a thought experiment will be given. Suppose one wished to show that the number 20 satisfied the Goldbach Conjecture. A simple way to proceed is to take each prime up to 10, labeled by the sequence $p_1 < p_2 < p_3 < p_4$, and assign to it a unique q_i labeled by the sequence $q_1 > q_2 > q_3 > q_4$ where $20 = q_i + p_i$. This allows for the following set of arithmetic relationships.

$$20 = 18 + 2 = 17 + 3 = 15 + 5 = 13 + 7 \tag{3.1}$$

Assuming that 20 is not the sum of two prime numbers, it then follows from The Fundamental Theorem of Arithmetic [1] that there must exist a unique sequence of $\alpha_1, \alpha_2, \alpha_3, \alpha_4 \in \mathbb{N}$ where

$$q_1 q_2 q_3 q_4 = p_1^{\alpha_1} p_2^{\alpha_2} p_3^{\alpha_3} p_4^{\alpha_4}. \tag{3.2}$$

However,

$$18 \times 17 \times 15 \times 13 \neq 2^{\alpha_1} \times 3^{\alpha_2} \times 5^{\alpha_3} \times 7^{\alpha_4} \tag{3.3}$$

for any sequence of exponents restricted to the natural numbers. Since each q_i on the L.H.S. ranges between 10 and 20 it can be seen that equation 3.3 is true if and only if at least one number on the L.H.S. is not divisible by any prime on the R.H.S., thus proving at least one q_i is a new prime. Therefore, it may be concluded that 20 can be written as the sum of two primes without having any particular knowledge about the distribution of the prime numbers or which prime numbers sum up to 20. All that is needed is the closure property of the integers, page 1 in [7], along with the Fundamental Theorem of Arithmetic.

This method can be extended to a general case. Since the Goldbach Conjecture states that every even number greater than two is the sum of two primes, assuming a counter-example exists, given by $2a$, would provide two conditions that must be met. First, it can be seen trivially under the closure property of the integers that the following statement is true.

(3.4) For all prime $p_i \leq a$ where $a > 3$ there exists some unique q_i where $2a = q_i + p_i$.

As the statement above is true for any positive integer $a > 3$ independent of the truth of the Goldbach Conjecture, it will be shown in Propsition 4.1 that the 3.5 in conjunction with 3.4 will be met and produced directly from the Fundamental Theorem of Arithmetic if and only if there does exist a counter-example to the Goldbach Conjecture.

(3.5) For all prime $p_i \leq a$ there exists some unique $\alpha_i \in \mathbb{N}$ where $\prod_{i=1}^{\pi(a)} q_i = \prod_{i=1}^{\pi(a)} p_i^{\alpha_i}$.

Substituting $q_i = 2a - p_i$ into equation 3.5 for each q_i in equation 3.4 allows for the following.

$$\prod_{i=1}^{\pi(a)} (2a - p_i) = \prod_{i=1}^{\pi(a)} p_i^{\alpha_i} \tag{3.6}$$

It will be shown that the general solutions require a counter-example, $2a$, to be divisible by every prime less than a. Since Bertrand's Postulate, 108 in [7], states there is always a prime

[1] A good approximation for $\pi(n)$, where $n > 1$, is given by $\frac{n}{\ln(n)}$

[2] A number p is a prime only if there is some integer n where $(p-1)! + 1 = pn$.

between a and $2a$ for any $a \geq 1$, meaning $2a < a\#$ whenever $a > 4$, it is impossible for solutions to exist when $a > 3$. The following sections will show solutions to the equation 3.6 are only given trivially for $a = 2$ and for $a = 3$. The case of $2a = 6$ is given by the solutions below.

$$(6-2) \times (6-3) = (2)^2 \times (3)$$

This same method will be used to determine if every even number, again given by $2a$, is the difference of two primes where one prime is less than a. Slight modifications need to be made which will be made evident with a similar thought experiment used for the Goldbach Conjecture. To begin, assume that the number 20 was not the difference of two primes where one prime was less than 10. Taking the same approach as in the Goldbach Conjecture shows each prime up to 10, labeled by the sequence $p_1 < p_2 < p_3 < p_4$, may be assigned a unique q_i labeled by the sequence $q_1 < q_2 < q_3 < q_4$ where $20 = q_i - p_i$. This allows for the following

$$20 = 22 - 2 = 23 - 3 = 25 - 5 = 27 - 7. \tag{3.7}$$

At this point careful attention needs to be given to the fact that the $q_1 = 22$ term is divisible by a prime greater than 10, but composite. Defining $p_5 = 11$ will be useful as it is important to note that this is the only time this can occur since q_1 is the only even term. Hence, since any odd $20 < q_i \leq 30$, it can not be divisible by any primes greater than 10 unless it is itself prime. Assuming that 20 is not the difference of two prime numbers, then The Fundamental Theorem of Arithmetic states that there exists a unique sequence of $\alpha_1, \alpha_2, \alpha_3, \alpha_4 \in \mathbb{N}$ where

$$q_1 q_2 q_3 q_4 = p_1^{\alpha_1} p_2^{\alpha_2} p_3^{\alpha_3} p_4^{\alpha_4} p_5. \tag{3.8}$$

However,

$$27 \times 25 \times 23 \times 22 \neq 2^{\alpha_1} \times 3^{\alpha_2} \times 5^{\alpha_3} \times 7^{\alpha_4} \times 11 \tag{3.9}$$

for any sequence of exponents restricted to the natural numbers. Since each q_i on the L.H.S. ranges between 20 and 30 it can be seen that equation 3.9 is true if and only if at least one number on the L.H.S. is not divisible by any prime on the R.H.S., thus proving at least one q_i is a new prime. Therefore, 20 can be written as the difference of two prime numbers. As with the Goldbach Conjecture, formalizing this result to a general case and showing solutions cannot exist when $2a > 6$ is the intended goal. This is done with the following statements.

(3.10) For all prime $p_i \leq a$ there exists some unique q_i where $2a = q_i - p_i$.

As the statement above is true for any positive integer $a > 3$ independent of the truth of the analogue to the Goldbach Conjecture that every even number is the difference of two primes, the following condition will be met if and only if there is a counter-example. This condition will differ slightly from the Goldbach Conjecture because it must be taken into account whether $a+1$ is prime. Defining a function $\beta(a+1)$ where this function is equal to one if $a+1$ is prime and equal to zero otherwise makes it possible to use the Fundamental Theorem of Arithmetic to define a unique sequence of exponents given by $\alpha_1, \alpha_2, \alpha_3, \alpha_4 \in \mathbb{N}$ where the following must hold if and only if a number, $2a$, is not the difference of two primes with one prime less than a.

(3.11) For all prime $p_i \leq a$ there exists some unique $\alpha_i \in \mathbb{N}$ where $\prod_{i=1}^{\pi(a)} q_i = p_{\pi(a)+1}^{\beta(a+1)} \prod_{i=1}^{\pi(a)} p_i^{\alpha_i}$.

Again, via a substitution for each $q_i = 2a + p_i$ from equation 3.10 into equation 3.11 shows

$$\prod_{i=1}^{\pi(a)} (2a + p_i) = p_{\pi(a)+1}^{\beta(a+1)} \prod_{i=1}^{\pi(a)} p_i^{\alpha_i} \tag{3.12}$$

where it will be shown that largest integer solution is given by $a = 3$ below.

$$(6+3) \times (6+2) = 2^3 \times 3^2$$

Once these two theorems are established, it will be shown that the Ternary Conjecture, along with the Polignac Conjecture must follow as immediate consequences.

4. Producing a Counter-Example to the Goldbach Conjecture

This section will determine precisely when the Goldbach Conjecture fails. The following proposition will provide an algebraic approach deriving both the necessary and sufficient conditions needed for a counter-example, $2a$, to be given. It will be assumed moving forward that the primes are labeled in ascending order using the index i where

$$p_1 < p_2 < \cdots < p_{\pi(a)}.$$

Since any $2a$ may trivially be written as the sum of two primes when $a \in \mathbb{P}$, that condition will be left out and it will be assumed throughout that the integer a is not prime, unless stated.

Proposition 4.1. *The Goldbach Conjecture (G.C.) is false if and only if there exists some non-prime $a \in \mathbb{N}$ where $a > 3$ with the conditions that for each prime $p_i < a$ there exists a unique $q_i, \alpha_i \in \mathbb{N}$ where q_i is non-prime satisfying the following set of equations.*

$$2a = q_i + p_i \tag{4.1}$$

along with product relation

$$\prod_{i=1}^{\pi(a)} q_i = \prod_{i=1}^{\pi(a)} p_i^{\alpha_i}. \tag{4.2}$$

Proof. If the G.C. were false for some non-prime $a \in \mathbb{N}$ with $a > 3$, then the closure property of the integers ensures for any prime $p_i < a$ there exists some unique $q_i \in \mathbb{N}$ where equation 4.1 holds with no q_i being prime. With $a < \forall q_i < 2a$ and no $q_i \in \mathbb{P}$, the F.T.A. ensures a unique prime factorization follows where equation 4.2 is true for a unique set of $\alpha_i \in \mathbb{N}$.

To prove the converse of the above statement, begin by letting there exist some $a \in \mathbb{N}$ where $a < 3$ and for each prime $p_i < a$ there is some unique $q_i, \alpha_i \in \mathbb{N}$ where both equations 4.1 and 4.2 are satisfied. Solutions to these two equations would immediately provide a counter-example to the G.C. since each q_i must be comprised of only primes up to a under the F.T.A. □

From Proposition 4.1 it is possible to derive three corollaries that will be of future importance.

Corollary 4.2. *For any α_i it follows that $\alpha_i > 0$ if and only if $p_i | q_i$ or $p_i | q_j$ for some $j \neq i$.*

Proof. From equation 4.2 it can be seen upon inspection that if any $\alpha_i > 0$, then that p_i must be a divisor of the R.H.S. of the equation. Therefore, that p_i divides the L.H.S. of the equation and must divide its corresponding q_i or some other q_j.

Conversely, from equation 4.2 if any prime p_i is a divisor of its corresponding q_i or some other q_j, then that p_i divides the R.H.S. of equation 4.2 showing $p_i | p_i^{\alpha_i}$ where $\alpha_i > 0$. □

Corollary 4.3. *Under Proposition 4.1 for any prime $p_i < a$ it follows $p_i | 2a$ if and only if $p_i | q_i$.*

Proof. Under equation 4.1 in Proposition 4.1 it is seen upon inspection if $p_i | q_i$, then $p_i | 2a$. Conversely, from equation 4.1 it follows that if any $p_i | 2a$, then $p_i | q_i$, proving the corollary. □

Corollary 4.4. *For any prime $p_i < a$ in Proposition 4.1 if $p_i | q_i$, then $p_i \nmid q_j$ for any $j \neq i$.*

Proof. Under transitivity of equation 4.1 in Proposition 4.1 it follows for any primes $p_i, p_j < a$

$$q_i + p_i = q_j + p_j. \tag{4.3}$$

If some p_i existed where $p_i | q_i$ and $p_i | q_j$ for some $j \neq i$ in equation 4.3, then $p_i | p_j$. Since both p_i, p_j are primes, then $p_i \nmid p_j$ when $j \neq i$. Therefore, if any $p_i | q_i$, then $p_i \nmid q_j$ for any $j \neq i$. □

With Proposition 4.1 and its corollaries in place it is now possible to define a single polynomial that will aid in proving the G.C. This is done by a substitution using equations 4.1 and 4.2.

5. Production and Properties of the Goldbach Polynomial

From here it will be necessary to use the equations in Proposition 4.1 to derive a polynomial.

Definition 5.1. The Goldbach Polynomial is given by the equation

$$\prod_{i=1}^{\pi(a)}(2a-p_i)=\prod_{i=1}^{\pi(a)}p_i^{\alpha_i} \tag{5.1}$$

and is derived by substituting each $q_i = 2a - p_i$ from equation 4.1 into the equation 4.2.

Proposition 5.2. *$2a$ must be a divisor of the difference of products $\prod_{i=1}^{\pi(a)} p_i^{\alpha_i} - (-1)^{\pi(a)} \prod_{i=1}^{\pi(a)} p_i$.*

Proof. Expansion of the Goldbach Polynomial in equation 5.1 gives the polynomial in $2a$ below

$$(2a)^{\pi(a)}+c_{\pi(a)-1}(2a)^{\pi(a)-1}+c_{\pi(a)-2}(2a)^{\pi(a)-2}+\cdots+c_1(2a)+(-1)^{\pi(a)}\prod_{i=1}^{\pi(a)}p_i=\prod_{i=1}^{\pi(a)}p_i^{\alpha_i} \tag{5.2}$$

where it follows trivially

$$(2a)^{\pi(a)}+c_{\pi(a)-1}(2a)^{\pi(a)-1}+c_{\pi(a)-2}(2a)^{\pi(a)-2}+\cdots+c_1(2a)=\Big[\prod_{i=1}^{\pi(a)}p_i^{\alpha_i}-(-1)^{\pi(a)}\prod_{i=1}^{\pi(a)}p_i\Big]. \tag{5.3}$$

Since $2a$ is a factor of the L.H.S. of equation 5.3 it must also be a divisor of the R.H.S. □

To proceed it will be necessary to use Veita's Formulas [12] to analyze the coefficient c_1.

Proposition 5.3. *For any prime $p_i < a$ the $GCD(p_i, c_1) = 1$.*

Proof. The expansion of the L.H.S. of equation 5.1 returned the monic polynomial in $2a$ with non-zero, integer coefficients $c_{\pi(a)}, c_{\pi(a)-1}, \ldots, c_0$ given by 5.3. Vieta's Formulas show that

$$\begin{aligned}
c_{\pi(a)} &= 1\\
c_{\pi(a)-1} &= -(p_1+p_2+\cdots+p_{\pi(a)})\\
c_{\pi(a)-2} &= (p_1p_2+p_1p_3+\cdots+p_{\pi(a)-1}p_{\pi(a)})\\
&\vdots\\
c_1 &= (-1)^{\pi(a)-1}(p_1p_2\cdots p_{\pi(a)-2}p_{\pi(a)-1}+p_1p_2\cdots p_{\pi(a)-2}p_{\pi(a)}+\cdots+p_2p_3\cdots p_{\pi(a)-1}p_{\pi(a)})\\
c_0 &= \prod_{i=1}^{\pi(a)}p_i^{\alpha_i}-(-1)^{\pi(a)}\prod_{i=1}^{\pi(a)}p_i
\end{aligned}$$

where an inspection of the c_1 term shows it is the sum of products of $\pi(a) - 1$ primes. Since any prime $p_i < a$ is only absent from one product in the sum, no prime $p_i | c_1$ when $p_i < a$. □

Definition 5.4. Let the integer polynomial $P(2a)$ be equal to the L.H.S. of equation 5.3 where

$$P(2a)=(2a)^{\pi(a)}+c_{\pi(a)-1}(2a)^{\pi(a)-1}+c_{\pi(a)-2}(2a)^{\pi(a)-2}+\cdots+c_2(2a)^2+c_1(2a). \tag{5.4}$$

Since $2a|P(2a)$, and all coefficients are non-zero integers, a factoring out of $2a$ above shows

$$P(2a)=2a\big[(2a)^{\pi(a)-1}+c_{\pi(a)-1}(2a)^{\pi(a)-2}+c_{\pi(a)-2}(2a)^{\pi(a)-3}+\cdots+c_2(2a)+c_1\big]. \tag{5.5}$$

Defining a second integer polynomial, $Q(2a)$, where

$$Q(2a)=(2a)^{\pi(a)-1}+c_{\pi(a)-1}(2a)^{\pi(a)-2}+c_{\pi(a)-2}(2a)^{\pi(a)-3}+\cdots+c_2(2a) \tag{5.6}$$

allows for the simplified form of equation 5.4 below

$$P(2a)=2a[Q(2a)+c_1] \tag{5.7}$$

where $2a|Q(2a)$. Since it is assumed that $a > 3$ it follows that $\pi(a) \geq 2$. Under transitivity, and using Veita's Formula for c_0 in Proposition 5.3, equation 5.3 can be written in the form

$$2a[Q(2a)+c_1]=c_0. \tag{5.8}$$

Lemma 5.5. *From Definition 5.4, the* $\deg(P(2a)) = \pi(a)$ *and* $\deg(Q(2a)) = \pi(a) - 1$.

Proof. Upon inspection of equation 5.4 it can be seen that $\deg(P(2a)) = \pi(a)$. It can also be seen from equation 5.6 that $\deg(Q(2a)) = \deg(P(2a)) - 1 = \pi(a) - 1$, proving the lemma. □

An important corollary can be derived from Proposition 5.3 concerning the divisibility relationship between $2a$ and c_0. This will allow for an exploration of cases for solutions to exist.

Corollary 5.6. *Let* $c_0 = \prod_{i=1}^{\pi(a)} p_i^{\alpha_i} - (-1)^{\pi(a)} \prod_{i=1}^{\pi(a)} p_i$ *from Veita's Formulas in Proposition 5.3. Under Propositions 5.2, 5.3, along with Definition 5.4, it must follow that the* $GCD(2a, \frac{c_0}{2a}) = 1$.

Proof. From Proposition 5.3 it was shown for any prime $p_i < a$ the $GCD(p_i, c_1) = 1$. Therefore, it must be true that the $GCD(2a, c_1) = 1$ since a is assumed to be a non-prime, integer greater than 3. Therefore, with $2a|Q(2a)$ from equation 5.6, it can be seen that it trivially follows that $GCD(2a, \frac{c_0}{2a}) = 1$ as a consequence of Proposition 5.2 and equation 5.8 in Definition 5.4. □

Lemma 5.7. *The term* $c_0 = \prod_{i=1}^{\pi(a)} p_i^{\alpha_i} - (-1)^{\pi(a)} \prod_{i=1}^{\pi(a)} p_i$ *does not divide* $\big[Q(2a) + c_1\big]$.

Proof. From equation 5.8 in Definition 5.4, since $a \in \mathbb{N}$ and $2a > 6$, the lemma must hold. □

The final step of this section is to prove that the constant term, c_0, is non-zero.

Lemma 5.8. *Solutions to equation 5.8 show* $\big\|c_0\big\| = \big\| \prod_{i=1}^{\pi(a)} p_i^{\alpha_i} - (-1)^{\pi(a)} \prod_{i=1}^{\pi(a)} p_i\big\| > 0$.

Proof. If there are solutions to $2a$ where $c_0 = 0$, then it follows from equation 5.8 that

$$2a\big[Q(2a) + c_1\big] = 0. \tag{5.9}$$

Since it is assumed $2a > 6$ in Proposition 4.1, it must then follow from equation 5.9 that $Q(2a) = -c_1$. With the condition given for $Q(2a)$ in Definition 5.4 that $2a|Q(2a)$, it follows $2a|c_1$. However, this contradicts Corollary 5.6 since $GCD(2a, c_1) = 1$, proving that $\|c_0\| > 0$. □

6. Cases for Solutions to the Goldbach Polynomial

It will be proven that there exists only two cases for solutions to equation 5.8 in Definition 5.4 because of the constraints placed on $2a$ by the preceding propositions, corollaries, and lemmas.

Theorem 6.1. *There exist only two cases where equation 5.8 in Definition 5.4 is true.*

Proof. For solutions to exist to equation 5.8 in Definition 5.4, with careful attention given to Lemmas 5.7 and 5.8, it can be seen that the only two scenarios are given below.

Case 1. The first case will account for

$$2a = \left\| \prod_{i=1}^{\pi(a)} p_i^{\alpha_i} - (-1)^{\pi(a)} \prod_{i=1}^{\pi(a)} p_i \right\| \tag{6.1}$$

along with the condition that

$$\|Q(2a) + c_1\| = 1. \tag{6.2}$$

Case 2. The second case shows that

$$6 < 2a < \left\| \prod_{i=1}^{\pi(a)} p_i^{\alpha_i} - (-1)^{\pi(a)} \prod_{i=1}^{\pi(a)} p_i \right\| \tag{6.3}$$

along with the condition

$$1 < \big\|Q(2a) + c_1\big\| < \left\| \prod_{i=1}^{\pi(a)} p_i^{\alpha_i} - (-1)^{\pi(a)} \prod_{i=1}^{\pi(a)} p_i \right\|. \tag{6.4}$$

These two cases give the only possible counter-examples to the Goldbach Conjecture. □

7. An Analysis of Case 1 in Theorem 6.1.

In this section it will be shown that integer solutions do exist to Case 1 and follow trivially from the propositions, corollaries, and lemmas in the previous section. However, these solutions can not exist for any $a \in \mathbb{N}$ where $a > 3$. Thus, no counter-example will be given from Case 1.

To begin, additional criteria for any $\alpha_i > 0$ in the c_0 term will be determined. This will allow for solutions to Case 1 to be given since the divisibility properties of each q_i will be revealed.

Proposition 7.1. *Solutions to Case 1 show that $\alpha_i > 0$ if and only if $p_i|2a$.*

Proof. From equation 6.1 in Case 1 it can be seen upon inspection that if any $\alpha_i > 0$, then that corresponding p_i may be factored out of the R.H.S. of the equation and must be a factor of $2a$.

The converse must also be true since equation 6.1 shows for any prime p_i where $p_i|2a$, it must follow that that p_i is a factor of the R.H.S. showing its corresponding $\alpha_i > 0$. □

The next step is to determine the divisibility criteria for each q_i from equation 4.1 in Proposition 4.1. This will be achieved by proving there is no prime $p_i < a$ where $p_i|q_j$ when $j \neq i$.

Theorem 7.2. *There is no prime $p_i < a$ where $p_i|q_j$ for some $j \neq i$.*

Proof. Under the F.T.A., along with Proposition 4.1, it follows that each q_i in equations 4.1 and 4.2 must be the product of prime powers containing only primes less than a. Suppose that there exists some $p_i|q_j$ for some $j \neq i$. From Corollary 4.2 it then follows that $\alpha_i > 0$. With $\alpha_i > 0$, Proposition 7.1 and Corollary 4.3 can be used to determine that it is also true that $p_i|q_i$. Thus, $p_i|q_i$ and $p_i|q_j$ for some $j \neq i$. However, this contradicts Corollary 4.4 since no $p_i|q_i$ and $p_i|q_j$ for some $j \neq i$ proving there exists no prime $p_i < a$ dividing some q_j where $j \neq i$. □

With everything in place, it is now possible to find the solutions for Case 1.

Theorem 7.3. *There are no solutions to Case 1 in Proposition 6.1 when $a > 3$.*

Proof. From Theorem 7.2 it was shown that there is no scenario where any $p_i|q_j$ when $j \neq i$. Hence, the only solutions to Case 1 are given when each q_i is of the form $q_i = p_i^{\alpha_i}$. It can then be seen via a substitution into equation 4.1 of Proposition 4.1 that the following must hold.

$$2a = p_i^{\alpha_i} + p_i \text{ for all prime } p_i < a. \tag{7.1}$$

This forces all prime $p_i > a$ to be divisors of $2a$. However, since Bertrand's Postulate ensures $2a < a\#$ for $a > 4$, it is clear that solutions to Case 1 cannot exist when $a > 3$. □

Remark 7.4. Under the conditions of Case 1 it follows from Theorem 7.3 that solutions are given to Proposition 4.1 when $a = 3$ showing $2^2 + 2 = 6 = 3 + 3$ and $(6-3) \times (6-2) = 2^2 \times 3$. It should also be noted that $a = 2$ also satisfies the conditions above where $4 = 2+2$ and $2 = 2$.

8. An Analysis of Case 2 in Theorem 6.1 and a Proof for the G.C.

Under Case 1 it was shown that no solutions exist when $a > 3$. It will now be shown that even under Case 2 there are no solutions where $a \in \mathbb{N}$ and $\pi(a) > 2$. To begin, it is necessary to use Proposition 5.2 and Corollary 5.6 to prove the following proposition.

Proposition 8.1. *There exists $u, v \in \mathbb{Z}$ where $(2a)^2u + c_0v = 2a$.*

Proof. From Corollary 5.6 and Proposition 5.2, Bezout's Identity[3] shows that $\exists u, v \in \mathbb{Z}$ where

$$(2a)^2u + c_0v = 2a \tag{8.1}$$

and it can be seen that the conditions hold where $2a|c_0$ along with the $GCD(2a, \frac{c_0}{2a}) = 1$. □

With Proposition 8.1 in place, it will be shown that the $\deg(P(2a)) = 2$ in Definition 5.4. This will be sufficient to show that solutions can not exist to case 2 and is easily achieved showing that there are no solutions when $\deg(Q(2a)) > 1$ using the theorem below.

[3]Let $a, b \in \mathbb{Z}$ where $GCD(a, b) = d$. Then $\exists u, v \in \mathbb{Z}$ where $au + bv = d$.

Theorem 8.2. *There are no solutions of* $\deg(Q(2a)) > 1$ *to equation 5.8 in Definition 5.4.*

Proof. Substituting the c_0 term from equation 5.8 into equation 8.1 produces the following.

$$(2a)^2u + 2a[Q(2a) + c_1]v = 2a \tag{8.2}$$

dividing through by $2a$ gives the result

$$(2a)u + [Q(2a) + c_1]v = 1. \tag{8.3}$$

Since u, v, and c_1 are constants, it is possible to absorb the sign changes to isolate the polynomial

$$vQ(2a) = (2a)u + c_1v + 1. \tag{8.4}$$

It can be seen that the since v must be a non-zero constant, then the $\deg(vQ(2a)) = \deg(Q(2a))$. Thus, the general solutions are given when $\deg(Q(2a)) = 1$ from the equation above. □

Theorem 8.3. *The Goldbach Conjecture is true.*

Proof. From Definition 5.4 the $\deg(P(2a)) = \pi(a)$ and $\deg(Q(2a)) = \deg(P(2a)) - 1$. Thus, it follows from Theorem 8.2 that the general solutions are given by a polynomial $P(2a)$ where $deg(P(2a) = 2$. This shows that solutions are only given when $\pi(a) = 2$ and no solutions can exist to Case 2. Since no solutions to Case 1 or 2 exist when $\pi(a) > 2$, no counter-examples exist to the G.C. Therefore, Proposition 4.1 states the Goldbach Conjecture is true. □

Definition 1. A *prime reflective point (P.R.P.)* for $a \in \mathbb{N}$ is any $b \in \mathbb{N}$ where both $a \pm b \in \mathbb{P}$.

It should also be noted that this method allows for an even stronger condition can be proven.

Theorem 8.4. *Every* $a \in \mathbb{N}$ *where* $a > 3$ *has a non-zero, P.R.P.*

Proof. From Theorem 8.3 it follows that any non-prime $a \in \mathbb{N}$ where $a > 3$ must have a non-zero P.R.P. Since $2a = (a + b) + (a - b)$. Therefore, the only thing left to do is to show this is true for the case where $a \in \mathbb{P}$ and $a > 3$. Equations 4.1 and 4.2 in Proposition 4.1 show that when a is allowed to be prime and greater than 3 there is no change to the equations for the product relationship because $q_{\pi(a)} = a$ and will cancel out the product of a on the R.H.S. of equation 4.2. This leaves the Goldbach Polynomial in equation 5.1 unchanged, as well. Therefore, solutions will be no different than the ones already solved for, showing the theorem is true. □

Theorem 8.5. *Every odd number greater than seven is the sum of three odd, prime numbers.*

Proof. For any odd $n \in \mathbb{N}$ where $n > 7$, there exists some even $m \in \mathbb{N}$ where $n - 3 = m$ and $m \geq 6$. Given Theorem 8.3, it follows there exists odd $p_1, p_2, p_3 \in \mathbb{P}$ where $n = p_1 + p_2 + p_3$. □

9. On Whether Every Even Number is The Differences of Two Prime Numbers.

This section will prove that any even number, $2a$, may be written as the difference of two prime numbers where one prime is less than a. The methodology behind this proof will almost mirror exactly the G.C. proof as the constraints and equations for a counter-example are nearly identical. Where it will differ slightly is that the possibility of $a + 1$ being prime must be accounted for, which will be seen in the following propositions. It will also be assumed that $a \in \mathbb{N}$ and $a > 3$. The primes will labeled in ascending order in the index i where

$$p_1 < p_2 < p_3 < \cdots < p_{\pi(a)}.$$

Definition 9.1. Let the function $\beta(a + 1)$ be defined by characteristics

$$\beta(a+1) = \begin{cases} 1, & \text{if } a+1 \in \mathbb{P}, \\ 0, & \text{if } a+1 \notin \mathbb{P}. \end{cases} \tag{9.1}$$

To begin it is crucial to determine both the necessary and sufficient conditions which would produce an even number would not be the difference of two prime numbers.

Proposition 9.2. *An even integer, $2a > 6$, is not the difference of two primes, where one prime is less than a, if and only if for each prime $p_i \leq a$ there exists a unique $q_i, \alpha_i \in \mathbb{N}$ where*

$$2a = q_i - p_i \tag{9.2}$$

along with product relation

$$\prod_{i=1}^{\pi(a)} q_i = p_{\pi(a)+1}^{\beta(a+1)} \prod_{i=1}^{\pi(a)} p_i^{\alpha_i}. \tag{9.3}$$

Proof. If an even number, given by $2a$ where $a \in \mathbb{N}$ and $a > 3$ were not the difference of two primes, then the closure property of the integers ensures for any prime $p_i \leq a$ there exists some unique, non-prime $q_i \in \mathbb{N}$ where equation 9.2 holds true. With $2a < \forall q_i \leq 3a$, the only possible number which could be a composition of a prime greater than a and a prime less than a would be the term $q_1 = 2a + 2$, as $a + 1$ may be prime. Thus, the F.T.A., along with Definition 9.1, ensures there must exist a unique set of $\alpha_i \in \mathbb{N}$ producing equation 9.3.

Conversely, if for each prime $p_i \leq a$, there exists some unique $q_i, \alpha_i \in \mathbb{N}$ satisfying both equations 9.2 and 9.3, then no q_i is prime. This would immediately provide a counter-example by producing a number which was not the difference of two primes with one less than a. □

It is possible to derive three corollaries that will be used to find solutions to equations 9.2 and 9.3. From here $2a$ will be assumed to be a solution to those equations.

Corollary 9.3. *For any α_i it follows that $\alpha_i > 0$ if and only if $p_i | q_i$ or $p_i | q_j$ for some $j \neq i$.*

Proof. From equation 9.3 it can be seen that if any $\alpha_i > 0$, then that p_i must be a divisor of the R.H.S. of the equation. Therefore, that p_i divides the L.H.S. and must divide its corresponding q_i or some other q_j. Conversely, if any p_i is a divisor of its corresponding q_i from equation 9.3 or some other q_j, then p_i divides the R.H.S. showing $p_i | p_i^{\alpha_i}$ where it must follow that $\alpha_i > 0$. □

Corollary 9.4. *Under Proposition 9.2 any prime $p_i | 2a$ if and only if $p_i | q_i$.*

Proof. Under equation 9.2 in Proposition 9.2 it is seen upon inspection that for any prime $p_i \leq a$, if $p_i | q_i$, then $p_i | 2a$. Conversely, if $p_i | 2a$, then $p_i | q_i$, proving the corollary. □

Corollary 9.5. *Solutions for Proposition 9.2 require that if any $p_i | q_i$, then $p_i \nmid q_j$ for any $j \neq i$.*

Proof. Under Proposition 9.2, any primes $p_i, p_j \leq a$ require some non-prime q_i, q_j where

$$q_i - p_i = 2a = q_j - p_j. \tag{9.4}$$

If some p_i existed where $p_i | q_i$ and $p_i | q_j$ in equation 9.4, then $p_i | p_j$. Since both p_i, p_j are primes, it is impossible for $p_i | p_j$ when $j \neq i$. Therefore, if any $p_i | q_i$, then $p_i \nmid q_j$ when $j \neq i$. □

10. Properties of Solutions to Proposition 9.2

From here it will be necessary to use the equations in Proposition 9.2 to derive a polynomial. It will then be shown that, like the G.C., solutions do not exist where $a \in \mathbb{N}$ and $a > 3$.

Definition 10.1. The Prime Difference Polynomial (P.D.P.) is given by the equation

$$\prod_{i=1}^{\pi(a)} (2a + p_i) = p_{\pi(a)+1}^{\beta(a+1)} \prod_{i=1}^{\pi(a)} p_i^{\alpha_i} \tag{10.1}$$

and is derived by substituting each $q_i = 2a - p_i$ from equation 9.2 into the equation 9.3.

Proposition 10.2. *Under Proposition 9.2, solutions show* $2a$ *divides* $p_{\pi(a)+1}^{\beta(a+1)} \prod_{i=1}^{\pi(a)} p_i^{\alpha_i} - \prod_{i=1}^{\pi(a)} p_i$.

Proof. From Proposition 9.2 a substitution of $q_i = 2a + p_i$ for each q_i from equation 9.2 allows for the product relationship in equation 9.3 to be expressed as

$$\prod_{i=1}^{\pi(a)} (2a + p_i) = p_{\pi(a)+1}^{\beta(a+1)} \prod_{i=1}^{\pi(a)} p_i^{\alpha_i}. \tag{10.2}$$

An expansion of terms in 10.2 gives the following polynomial in $2a$ with integer coefficients.

$$(2a)^{\pi(a)} + c_{(\pi(a)-1}(2a)^{\pi(a)-1} + c_{\pi(a)-2}(2a)^{\pi(a)-2} + \cdots + c_1(2a) + \prod_{i=1}^{\pi(a)} p_i = p_{\pi(a)+1}^{\beta(a+1)} \prod_{i=1}^{\pi(a)} p_i^{\alpha_i}. \tag{10.3}$$

From the above equation it follows trivially that

$$(2a)^{\pi(a)} + c_{(\pi(a)-1}(2a)^{\pi(a)-1} + c_{\pi(a)-2}(2a)^{\pi(a)-2} + \cdots + c_1(2a) = p_{\pi(a)+1}^{\beta(a+1)} \prod_{i=1}^{\pi(a)} p_i^{\alpha_i} - \prod_{i=1}^{\pi(a)} p_i. \tag{10.4}$$

Since $2a$ is a factor of the L.H.S. in 10.4 it must be a factor of the R.H.S. □

Proposition 10.3. *For any prime* $p_i \leq a$ *the* $GCD(p_i, c_1) = 1$.

Proof. The expansion of the L.H.S. of equation 10.2 written out explicitly returns the monic polynomial in $2a$ with integer coefficients labeled by $c_{\pi(a)-1}, c_{\pi(a)-2}, \ldots, c_0$ and is given by equation 10.4. Using Vieta's Formulas it is possible to write the coefficients explicitly below.

$$\begin{aligned}
c_{\pi(a)} &= 1 \\
c_{\pi(a)-1} &= (p_1 + p_2 + \cdots + p_{\pi(a)}) \\
c_{\pi(a)-2} &= (p_1p_2 + p_1p_3 + \cdots + p_{\pi(a)-1}p_{\pi(a)}) \\
&\vdots \\
c_1 &= (p_1p_2 \cdots p_{\pi(a)-2}p_{\pi(a)-1} + p_1p_2 \cdots p_{\pi(a)-2}p_{\pi(a)} + \cdots + p_2p_3 \cdots p_{\pi(a)-1}p_{\pi(a)}) \\
c_0 &= p_{\pi(a)+1}^{\beta(a+1)} \prod_{i=1}^{\pi(a)} p_i^{\alpha_i} - \prod_{i=1}^{\pi(a)} p_i
\end{aligned}$$

From the equations above it can be seen that the c_1 term consists of the sum of products of $\pi(a) - 1$. Thus, it follows that any $p_i \leq a$ is only absent from one product in the sum for c_1, showing no prime $p_i \leq a$ divides c_1 which is sufficient to prove the proposition. □

As in the case of the G.C. analysis, the c_1 term will be of importance for future sections.

Definition 10.4. Let the polynomial $P(2a)$ be equal to the L.H.S. of equation 10.4 where

$$P(2a) = (2a)^{\pi(a)} + c_{\pi(a)-1}(2a)^{\pi(a)-1} + c_{\pi(a)-2}(2a)^{\pi(a)-2} + \cdots + c_2(2a)^2 + c_1(2a). \tag{10.5}$$

Since $2a|P(2a)$, and all coefficients are non-zero integers, a factoring out of $2a$ above shows

$$P(2a) = 2a\big[(2a)^{\pi(a)-1} + c_{\pi(a)-1}(2a)^{\pi(a)-2} + c_{\pi(a)-2}(2a)^{\pi(a)-3} + \cdots + c_2(2a) + c_1\big]. \tag{10.6}$$

Defining a second integer polynomial, $Q(2a)$, where

$$Q(2a) = (2a)^{\pi(a)-1} + c_{\pi(a)-1}(2a)^{\pi(a)-2} + c_{\pi(a)-2}(2a)^{\pi(a)-3} + \cdots + c_2(2a) \tag{10.7}$$

allows for the simplified form of equation 10.5 below

$$P(2a) = 2a[Q(2a) + c_1] \tag{10.8}$$

where $2a|Q(2a)$ since it is assumed that $a > 3$ requiring that $\pi(a) \geq 2$. Under transitivity, and using Veita's Formula for c_0 in Proposition 10.3, equation 10.4 may be written in the form

$$2a[Q(2a) + c_1] = c_0. \tag{10.9}$$

Lemma 10.5. *From Definition 10.4, the* $\deg(P(2a)) = \pi(a)$ *and* $\deg(Q(2a)) = \pi(a) - 1$.

Proof. Upon inspection of equation 10.5 it can be seen that $\deg(P(2a)) = \pi(a)$. It can also be seen from equation 10.7 that $\deg(Q(2a)) = \deg(P(2a)) - 1 = \pi(a) - 1$, proving the lemma. □

An important corollary can be derived from Proposition 10.3 concerning the divisibility relationship between $2a$ and c_0. This will allow for an exploration of cases for solutions to exist.

Corollary 10.6. *Let* $c_0 = p_{\pi(a)+1}^{\beta(a+1)} \prod_{i=1}^{\pi(a)} p_i^{\alpha_i} - \prod_{i=1}^{\pi(a)} p_i$ *from Veita's Formulas in Proposition 10.3. Under Propositions 10.2, 10.3, along with Definition 10.4, it must follow that* $GCD(2a, \frac{c_0}{2a}) = 1$.

Proof. From Proposition 10.3 it was shown for any prime $p_i \leq a$ the $GCD(p_i, c_1) = 1$. Therefore, it must be true that the $GCD(2a, c_1) = 1$ since a is assumed to be an integer greater than 3. Therefore, with $2a|Q(2a)$ from equation 10.7, it can be seen that it trivially follows the $GCD(2a, \frac{c_0}{2a}) = 1$ from Proposition 10.2 and equation 10.9 in Definition 10.4. □

Lemma 10.7. *The term* $c_0 = p_{\pi(a)+1}^{\beta(a+1)} \prod_{i=1}^{\pi(a)} p_i^{\alpha_i} - \prod_{i=1}^{\pi(a)} p_i$ *does not divide* $\big[Q(2a) + c_1\big]$.

Proof. From equation 10.9 in Definition 10.4, since $a \in \mathbb{N}$ and $2a > 6$, the lemma must hold. □

The final step of this section is to prove that the constant term, c_0, is non-zero.

Lemma 10.8. *Solutions to equation 10.9 show* $\big\|c_0\big\| = \big\|p_{\pi(a)+1}^{\beta(a+1)} \prod_{i=1}^{\pi(a)} p_i^{\alpha_i} - \prod_{i=1}^{\pi(a)} p_i\big\| > 0$.

Proof. If there are solutions to $2a$ where $c_0 = 0$, then it follows from equation 10.9 that

$$2a\big[Q(2a) + c_1\big] = 0. \tag{10.10}$$

Since it is assumed $2a > 6$ in Proposition 9.2, it must then follow from equation 10.10 that $Q(2a) = -c_1$. With the condition given for $Q(2a)$ in Definition 10.4 that $2a|Q(2a)$, it follows $2a|c_1$. However, this contradicts Proposition 10.3 since $GCD(2a, c_1) = 1$, proving $\|c_0\| > 0$. □

11. Cases for Solutions to the P.D.P. in Definition 10.4.

Theorem 11.1. *There exists only two cases where equation 10.2 in Proposition 10.2 is true.*

Proof. For solutions to exist to equation 10.9 in Definition 10.4, with careful attention given to Proposition 10.2 and Lemmas 10.7, 10.8, the only two scenarios are given below.

Case 3. The first case will account for the two conditions where

$$2a = \left\| p_{\pi(a)+1}^{\beta(a+1)} \prod_{i=1}^{\pi(a)} p_i^{\alpha_i} - \prod_{i=1}^{\pi(a)} p_i \right\| \tag{11.1}$$

along with the condition that

$$\|Q(2a) + c_1\| = 1. \tag{11.2}$$

Case 4. The second case shows that

$$6 < 2a < \left\| p_{\pi(a)+1}^{\beta(a+1)} \prod_{i=1}^{\pi(a)} p_i^{\alpha_i} - \prod_{i=1}^{\pi(a)} p_i \right\| \tag{11.3}$$

along with the condition

$$1 < \big\|2aQ(2a) + c_1\big\| < \left\| p_{\pi(a)+1}^{\beta(a+1)} \prod_{i=1}^{\pi(a)} p_i^{\alpha_i} - \prod_{i=1}^{\pi(a)} p_i \right\|. \tag{11.4}$$

These two cases give the only solutions where an even number greater than six is not the difference of two primes where one prime is less than that even number. □

With everything in place it will be possible to derive the solutions for Case 3 in the following section. This will be done with careful attention given to Corollaries 9.3 through 9.5.

12. An Analysis of Case 3 in Theorem 11.1.

In this section it will be shown that solutions do exist to Case 3 and follow trivially from the propositions, corollaries, and lemmas in the previous section. However, these solutions can not exist for any $a \in \mathbb{N}$ where $a > 3$. Thus, no counter-example will be given from Case 3.

To begin, it will be crucial to determine all criteria for any $\alpha_i > 0$. This will allow for solutions to Case 1 to be given since the divisibility properties of each q_i will be revealed.

Proposition 12.1. *Under Case 3 it follows that every $\alpha_i > 0$ if and only if $p_i|2a$.*

Proof. From equation 11.1 in Case 3, it can be seen that if any $\alpha_i > 0$, then that corresponding p_i may be factored out of the R.H.S. of the equation. Thus, it must be a factor of $2a$.

The converse must also be true since equation 11.1 shows for any prime p_i where $p_i|2a$, it must follow that that p_i is a factor of the R.H.S. showing its corresponding $\alpha_i > 0$. □

The next step is to show the divisibility criteria for each q_i in equation 9.2 in Proposition 9.2

Theorem 12.2. *There is no prime $p_i \leq a$ where $p_i|q_j$ for some $j \neq i$.*

Proof. Suppose there exists some $p_i|q_j$ for some $j \neq i$ in equations 9.2 and 9.3 of Proposition 9.2. From Corollary 9.3 it then follows that $\alpha_i > 0$. With $\alpha_i > 0$, Proposition 12.1 and Corollary 9.4 can be used to determine that it is also true that $p_i|q_i$. Thus, $p_i|q_i$ and $p_i|q_j$ for some $j \neq i$. However, this contradicts Corollary 9.5 since no $p_i|q_i$ and $p_i|q_j$ for some $j \neq i$. Hence, there can exist no prime $p_i \leq a$ dividing some q_j where $j \neq i$. □

Theorem 12.3. *There are no solutions to Case 3 in Theorem 11.1 when $a > 3$.*

Proof. The F.T.A. ensures that each q_i in equations 9.2 and 9.3 of Proposition 9.2 must have prime divisors since all $q_i > 1$. From Proposition 12.1 and Theorem 12.2 it follows directly that there is no scenario where any $p_i|q_j$ when $j \neq i$. Thus, the only solutions to Case 3 are given by each odd q_i of the form $q_i = p_i^{\alpha_i}$. Substituting into equation 9.2 of Proposition 9.2 gives

$$2a = p_i^{\alpha_i} - p_i \text{ for all odd prime } p_i \leq a. \tag{12.1}$$

This forces all prime $p_i \leq a$ to be divisors of $2a$. However, since Bertrand's Postulate ensures $2a < a\#$ for $a > 4$, it is clear that solutions to Case 3 cannot exist when $a > 3$. □

Remark 12.4. Under the conditions of Case 1 it follows from Theorem 7.3 that solutions are given to Proposition 9.2 when $a = 3$ showing $2^3 - 2 = 6 = 3^2 - 3$ and $(6+3) \times (6+2) = 2^3 \times 3^2$.

The final step is to show solutions can not exist to case 4.

13. An Analysis of Case 4 in Theorem 11.1

Under Case 3 it was shown that no solutions exist when $a > 3$. It will now be shown that even under Case 4 there are no solutions where $a \in \mathbb{N}$ and $\pi(a) > 2$. To begin, it is necessary to use Proposition 10.2 and Corollary 10.6 to prove the following proposition.

Proposition 13.1. *There exists $u, v \in \mathbb{Z}$ where $(2a)^2u + c_0v = 2a$.*

Proof. From Corollary 10.6 and Proposition 10.2, Bezout's Identity shows that $\exists u, v \in \mathbb{Z}$ where

$$(2a)^2u + c_0v = 2a \tag{13.1}$$

and it can be seen that the conditions hold where $2a|c_0$ along with the $GCD(2a, \frac{c_0}{2a}) = 1$. □

With the Proposition 13.1 in place, it will be shown that there can be no solutions to equation 10.4 when $\pi(a) > 2$. This will be sufficient to show that solutions can not exist to case 4.

Theorem 13.2. *The* $\deg(Q(2a)) = 1$ *in Case 4 of Theorem 11.1.*

Proof. Substituting the c_0 term from equation 10.9 into equation 13.1 produces the following.

$$(2a)^2u + 2a[Q(2a) + c_1]v = 2a \tag{13.2}$$

dividing through by $2a$ gives the result

$$(2a)u + [Q(2a) + c_1]v = 1. \tag{13.3}$$

Since u, v, and c_1 are constants, it is possible to absorb the sign changes to isolate the polynomial

$$vQ(2a) = (2a)u + c_1v + 1. \tag{13.4}$$

It can be seen that since v must be a non-zero constant, then the $\deg(vQ(2a)) = \deg(Q(2a))$. Thus, it follows that $\deg(Q(2a)) = 1$ from the equation above. □

Theorem 13.3. *Every even number is the difference of two prime numbers.*

Proof. From Definition 10.4 the $\deg(P(2a)) = \pi(a)$ and $\deg(Q(2a)) = \deg(P(2a)) - 1$. Thus, from Theorem 13.2 the general solutions are given by a polynomial $P(2a)$ where $deg(P(2a) = 2$. This shows that solutions are only given when $\pi(a) = 2$. Since no solutions to Case 3 or 4 exist when $\pi(a) > 2$, Proposition 9.2 shows every even number is the difference of two primes. □

14. An Analysis of the Polignac Conjecture

Theorem 14.1. *For any* $n \in \mathbb{N}$ *where* $2|n$*, there are infinitely many prime gaps of size* n*.*

Proof. Theorems 8.3 and 13.3 show for all even $m, n \in \mathbb{N}$, with $m \geq 6$, there exists odd $p_4, p_3, p_2, p_1 \in \mathbb{P}$, where it follows $p_4 - p_3 = m + n$, and $p_2 + p_1 = m$. Allowing n to be fixed for some even number, and m to cycle through all of the positive even numbers greater than 4 gives an infinite set of equations for n of the form $p_4 - (p_3 + p_2 + p_1) = n$. If the Polignac Conjecture were false for some n, there would be only finitely many primes that were the sum of three odd, prime numbers. Theorem 8.5, and Euclid's proof for the infinitude of the primes, shows this cannot be the case, proving the Polignac Conjecture must be true. □

References

[1] Apostol, Tom M. *"The Fundamental Theorem of Arithmetic."* Introduction to Analytic Number Theory. Springer, New York, NY, 1976. 13-23.

[2] Deshouillers, J-M., Herman JJ te Riele, and Yannick Saouter. *"New Experimental Results Concerning the Goldbach Conjecture."* International Algorithmic Number Theory Symposium. Springer, Berlin, Heidelberg, 1998.

[3] e Silva, Tomás Oliveira, Siegfried Herzog, and Silvio Pardi. *"Empirical Verification of the Even Goldbach Conjecture and Computation of Prime Gaps up to* $4 \cdot 10^{18}$*."* Mathematics of Computation (2014): 2033-2060.

[4] Hardy, Godfrey H., and John E. Littlewood. *"Some Problems of 'Partitio Numerorum'; III: On the Expression of a Number as a Sum of Primes."* Acta Mathematica 44.1 (1923): 1-70.

[5] Helfgott, Harald A. *"The Ternary Goldbach Conjecture is True."* arXiv preprint arXiv:1312.7748 (2013).

[6] Helfgott, Harald A., and David J. Platt. *"Numerical Verification of the Ternary Goldbach Conjecture up to* $8.875 \cdot 10^{30}$*."* Experimental Mathematics 22.4 (2013): 406-409.

[7] J. J. Tattersall *Elementary Number Theory in Nine Chapters.* Cambridge University Press, ISBN 978-0-521-58503-3, 1999.

[8] Jörg Richstein, *"Verifying the Goldbach Conjecture up to* $4 \cdot 10^{14}$*."* Mathematics of Computation 70.236 (2001): 1745-1749.

[9] Ruiz, Sebastián Martín. *"80.52 An Algebraic Identity Leading to Wilson's Theorem."* The Mathematical Gazette 80.489 (1996): 579-582.

[10] Saouter, Yannick. *"Checking the Odd Goldbach Conjecture up to* 10^{20}*."* Mathematics of Computation 67.222 (1998): 863-866.

[11] Selberg, Atle. *"An Elementary Proof of the Prime-Number Theorem."* Annals of Mathematics (1949): 305-313.

[12] Viéte, Francios. *"Opera Mathematica."* 1579. Reprinted Leiden, Netherlands, 1646.

[13] Zhang, Yitang. *"Bounded Gaps Between Primes."* Annals of Mathematics (2014): 1121-1174.

email: jrsouth@smu.edu

Dynamic Fast Tracing and Smoothing Technique for Geiger-Muller Dosimeter

M. Ebrahimi Shohani, S. M. Taheri, S. M. Golgoun

***Abstract*—**Environmental radiation dosimeter, is a kind of detector that measures the dose of the radiation area. Dosimeter registers the radiation and converts it to the dose according to the calibration parameters. The limit of a dose is different at each jobs and this limit should be notified and reported to the user and health physics department. The stochastic nature of radiation is the reason for the fluctuation of any gamma detector dosimetry. In this research we investigated Geiger-Muller type of dosimeter and tried to improve the dose measurement. Geiger-Muller dosimeter is a counter that converts registered radiation to the dose. Many techniques were applied to the registered counts to smooth statistical variations to set the alarm level and better data analysis. We proposed an innovative method to smooth these fluctuations much more and also proposed a dynamic way to trace rapid changes of radiations. Results show that our method is fast and reliable method in comparison the traditional method.

***Keywords*—**Geiger-Muller, radiation, detection, algorithms, dosimeter

I. Introduction

Various dosimeters are used to detect ionizing radiation in radiation environments. Radiation dosimeter is a kind of sensor that is used for many purposes. These useful devices are produced in different types, shapes with various sensitive materials to detect ionizing radiations like neutron, gamma, alpha, beta, and muon. Environmental dosimeters are a type of radiation detector and have different types, the two most common types of environmental dosimeters are gas and scintillation types [1]-[4]. Because of natural and artificial sources of radiation, using dosimeter is an obligation for radiation workers and is mandatory in any nuclear areas. Most dosimeters have simple dose measurement algorithms, but some also have more sophisticated algorithms, including artificial intelligence and neural network [5], [6]. One of the most common and cheapest dosimeters is Geiger-Muller (GM) dosimeter, which is a gas-sealed type detector, with or without an entrance window. Because of some specific parameters like dimension and high voltage of the GM, this gaseous dosimeter works by this principle that each incident radiation, could produce an avalanche of ion-pairs, then the dosimeter output signal is strong enough to detect that incident photon without a significant amplification when compared to the proportional counters [7]-[9].

Calibration of GM environmental dosimeter converts registered count per second (CPS) to the environmental dose. The stochastic nature of radiation is the reason for the CPS fluctuation of any gamma detection device. So many techniques are applied to smooth this fluctuation, and averaging is one of the simplest ones [10], [11]. The averaging method is necessary because some alarm levels and dose limitations should be determined according to each radiation area. The worst defect of averaging algorithms is that it's not sensitive to a rapid altering of doses. It means, if a radiation source, crosses fast around the detector, averaging algorithm, prevents fast radiation detection. For solving this problem, we proposed a new method of fast-tracing and smoothing solutions by applying statistical science, which is described below.

II. Materials and Method

Due to the random and statistical nature of the number of pulses counted (means CPS), different methods are usually used to average and smooth these changes. One of these methods is to create a buffer of the latest measured CPS values. For example, in a 10-item buffer by measuring the new CPS value, this value is stored in the last buffer cell and replaced on the first buffer cell value (the oldest value). All values also find a shift cell to be refreshed during each sampling cycle.

The smaller the buffer size, the higher the average dependence on the last instantaneous value, and the larger the buffer size, the lower the average dependence on the last instantaneous value (fluctuations also decrease).

Disadvantages of this method are occupying space from the microcontroller memory (depends on the size of a buffer) and performing buffer shifts per second (in addition to averaging all buffer cells), so this method is slow.

Another way is to use the EWMA (Exponentially Weighted Moving Average) formula. In this method, there is no need to use buffers and apply more calculations. The average value is calculated every 1 second using the same formula. Larger R_f values mean less dependence on the last instantaneous value (equivalent to a buffer with more cells), and smaller R_f values mean more dependence on the last instantaneous value and therefore more statistical fluctuation (equivalent to a small size buffer).

In routine GM dosimeters, pulse per second registers the CPS value, but in our research, 200 ms sampling was replaced instead of 1-second sampling. For averaging, EWMA operates as in:

$$Avg_{new} = \alpha Avg_{old} + (1 - R_f)c \qquad 0 < \alpha < 1 \qquad (1)$$

M. Ebrahimi Shohani and S. M. Taheri are with the Pars Isotope Company, P.O. Box 14376-63181, Tehran, Iran

S. M. Golgoun is with Department of Medical Radiation Engineering, Science and Research Branch, Islamic Azad University, Tehran, Iran, P.O. Box 14515-775 (corresponding author, +989124939602, e-mail: mohammad.golgoun@srbiau.ac.ir, sm_golgoun@yahoo.com).

which Avg_{new} is the average of current CPS, R_f is the smoothing factor, Avg_{old} is the average of passed CPS, and c is the raw instantaneous value of CPS.

The parameter that must be set correctly in this relation is the R_f value. For better understanding the effect of R_f on the detector output response, (1) for the various values of R_f is plotted in Fig. 1. In this figure, the horizontal axis is the sampling number, and the vertical axis is the read amount. As can be seen, in the 500th reading, the read amount has increased from 5 CPS to 10 CPS. This figure shows the relationship between smoothing factor and time needed for final detection results.

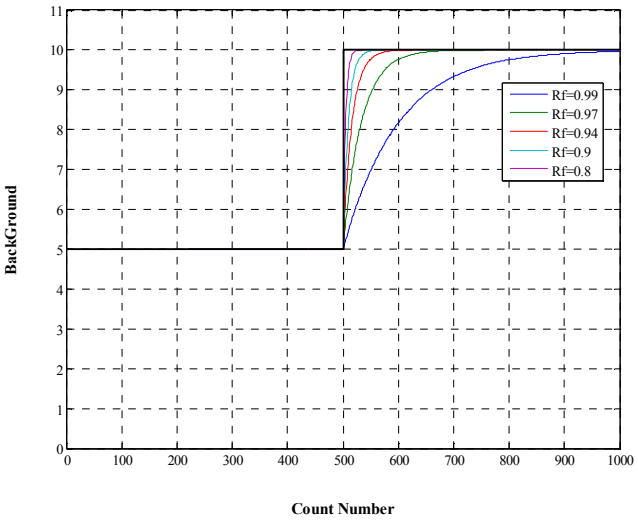

Fig. 1 Response variation related to the R_f parameter

From Fig. 1, for values close to 1 of R_f, more time must pass before U_i approaches its final value. In other words, this relationship reduces the fluctuations due to the statistical nature of the count. Equation (1) is a type of 1st-degree filter whose response to the step input is exponential. Therefore, the value of R_f should be adjusted according to the number of changes in the CPS and the required statistical dispersion of U_i. The closer value of the R_f parameter to one, the slower U_i's response to the CPS changes, and the smaller its statistical disperse. For each area and each detector system, measuring the background (BG) amount and subtracting it from the main amount is done as a pre-measurement process. In this research, selected GM is suitable for low dose areas and GM type is one model from LND company.

Fig. 2 shows the effect of pre-measurement from the BG of the environment. As shown in Fig. 1, some time must pass after the measurement starts to bring the measured counts closer to its final value due to the R_f parameter. In Fig. 2, pre-measurement is performed first by using (1), so the initial delay of BG measurement is no longer observed.

This measurement is performed in the presence of the background, so in measurements where the amount of radiation is low, due to the statistical nature of the counts, dose detection may be erroneous.

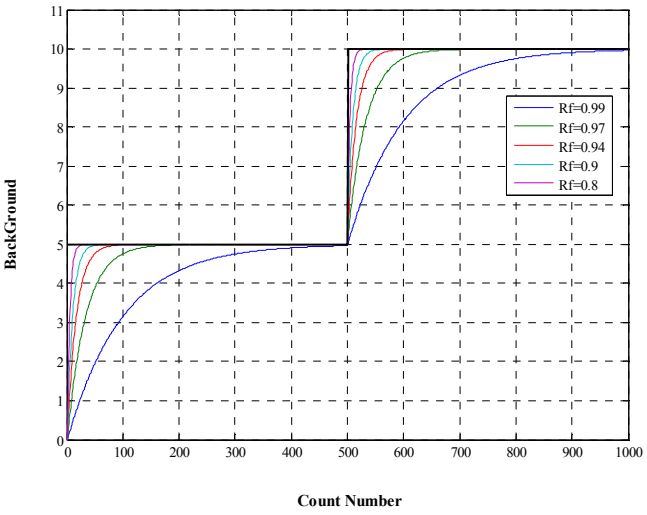

Fig. 2. The effect of pre-measurement

Despite a common method for averaging for calculation of smoothed CPS, the sample rate is about 200 ms and only considers the last-5 values. Then the algorithms find a median of the last-5 values and multiple it in 5. This value is now inserted in the EWMA formula for averaging, for c parameter. Fig. 3 shows the designed dosimeter program. The dosimeter information is sent and displayed online via a LAN connection to the computer. The TCP-Modbus protocol is used to communicate between the dosimeter and the computer.

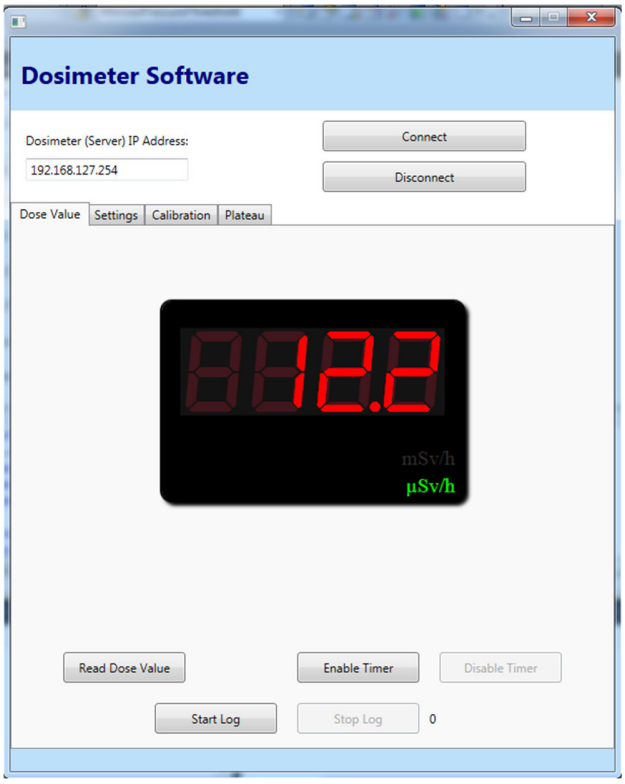

Fig. 3 Software of GM dosimeter

Also, according to Figure 4, through the same program, dosimeter parameters such as Alarm Levels, Dead Time, Calibration Factor, HV value of the working point, and etc. can be set. Furthermore, the plateau curve of the dosimeter can be obtained and the exact working point of the dosimeter can be determined from it.

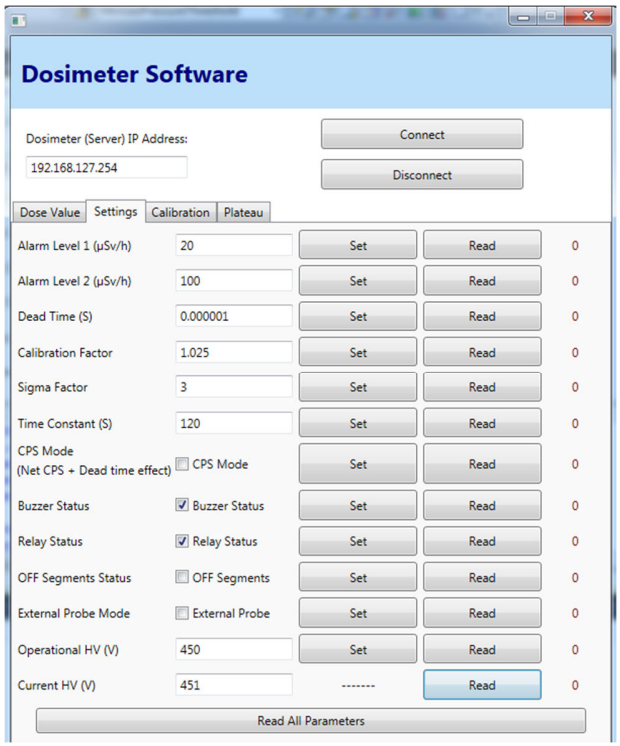

(a)

(b)

Fig. 4 Different parameters for adjustment of GM dosimeter

III. Results and Discussion

Due to the use of the median instead of direct averaging, outlier values are decreased in the dose calculations and therefore, the statistical fluctuations in the displayed dose amount are much less, consequently. So, CPS averaging will be much smoother than the common method at the end.

We continued our job to improve averaging much more by tracing technique. The R_f parameter in (1), is the value of smoothing in the EWMA formula. It means that, if this value is 1, the averaging does not relate to the instantaneous value, then the dosimeter will be smoothed and slow in measurement during rapid changes of radiation. Therefore, the dosimeter is stable but could not detect rapid changes of ionizing radiation. We implemented another method for our job, by tracing rapid changes. It means that our algorithms observe the last value of CPS continuously and calculate the average of CPS, then compare it to the instantaneous value at each 200 ms interval. If the instantaneous value is altered in ascending or descending manner 10 times consequently (means in 2 s), then by altering the factor to 0 value, the averaging will be related to the instantaneous value for fast tracing of dose changes. Then, the above procedure is repeated for smoothing dose calculation.

In this way, we have used the advantage of averaging without entering the outlier values into the averaging formula, and therefore the displayed doses in the dosimeter have less fluctuation than before. In addition to the above improvement, by considering current dosimeters that use statistical formulas, we have made it possible to trace rapid changes for environmental dose measurement without using traditional statistical formulas.

In our research, for better curve fitting, we divided outputs data into two sections with two curves of grade 2 and grade 4 (areas below 750 CPS and above it). Finally, according to the values provided by the calibration unit, we obtained the amount of environmental dose (with a maximum error of 3%) according to the following table:

TABLE I
ERRORS OF DOSE MEASUREMENT IN COMPARISON TO THE CALIBRATION UNIT RESULTS

Measured CPS	Calculated Dose	Calibration Dose	Error
140.88	11	11.1	1%
243.9	20.3	19.8	3%
488.96	44.7	44.36	1%
750.16	70.3	69.2	2%
1166.3	133.8	129.3	3%
1706.2	237.4	231.1	3%
2748	528.2	516.1	2%
3672	931.2	918.5	1%
4302	1317	1316	0%
5131	2010	2036	1%

Also, good agreement between calibration doses as a reference and our measurement doses is depicted in Fig. 4.

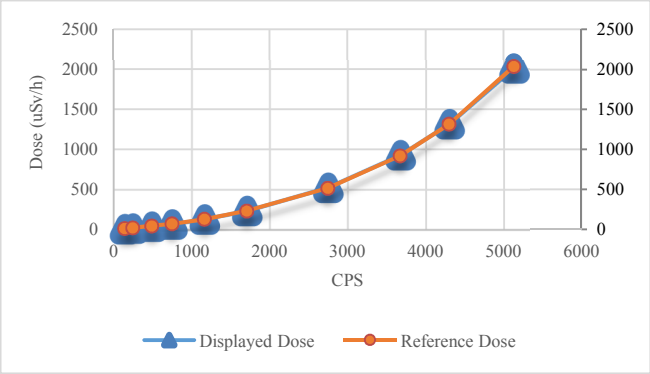

Fig. 4 Acceptable results between dynamic method and calibration results

IV. Conclusion

The dynamic method is compatible with calibration data. Also, this method succeeded to solve the problem of usual dosimeters, especially Geiger-Muller dosimeters. Even this method helps to measure environmental dose, much smoother than the common averaging algorithms.

References

[1] M. Ebrahimi Shohani, S.M. Golgoun, M. Aminipour, et al., "Study and full simulation of ten different gases on sealed Multi-Wire Proportional Counter (MWPC) by using Garfield and Maxwell codes," *Appl. Radiat. Isot.*, vol. 115, 2016

[2] M. Ebrahimi Shohani, S. M. Golgoun, M Aminipour, et al., "Geant4 comparative study of affecting different parameters on optical photons related to the plastic scintillation detector." *Journal of Physical Science and Application*, vol. 7,2017.

[3] J. Borbinha, Y. Romanets, P. Teles, et al., "Performance Analysis of Geiger–Müller and Cadmium Zinc Telluride sensors envisaging airborne radiological monitoring in NORM sites," *Sensors*, vol. 20, 2020.

[4] J. A. Posar, J. Davis, O. Brace, et al., "Characterization of a plastic dosimeter based on organic semiconductor photodiodes and scintillator," Phys. Imaging Radiat. Oncol., vol. 14, 2020.

[5] E. Nazemi, M. Aminipour, A. Olfateh, et al., "Proposing an intelligent approach for measuring the thickness of metal sheets independent of alloy type," *Appl. Radiat. Isot.*, vol. 149, 2019.

[6] S. Cheong, A. Cukierman, B. Nachman, et al., "Parametrizing the detector response with neural networks," *JINST*, vol. 15, 2020.

[7] P. Habrman, "Directional Geiger-Müller detector with improved response to gamma radiation" *JINST*, vol. 14, 2019.

[8] N. A. Graf, J. McCormick, "Physics and detector response simulations," *Phys. Procedia*, vol. 37, 2012.

[9] D. Barclay, "Improved Response of Geiger Muller Detectors," *IEEE Trans Nucl Sci*, vol. 33, 1986.

[10] S.M. Golgoun, D. Sardari, M. Sadeghi, et al., "Prediction of liquid density by gamma-ray measurement for materials with low atomic number," *MAPAN*, vol. 35, 2020.

[11] S.M. Golgoun, D. Sardari, M. Sadeghi, et al., "A novel method of combined detector model for gamma-ray densitometer: Theoretical calculation and MCNP4C simulation," *Appl. Radiat. Isot.*, vol. 118, 2016.

Between the House and the City: An Investigation of the Structure of the Family/Society and the Role of the Public Housing in Tokyo and Berlin

Abudjana H.W. Babiker

***Abstract*—**The middle of twenty century witnessed explosion in the public housing. After the great depression some of the capitalists and communist countries have launched policies and programs to produce public housing in the Urban areas. Concurrently, modernity was the leading architecture style at the time excessively supported the production, and principally was the instrument for the success of the public housing program due to the modernism manifesto for manufactured architecture as international style that serves the society and parallelly connect it to the other design industries which allowed for the production of the architecture elements.

After the second world war the public housing flourished especially in the communist's countries. The idea of the public housing was conceived as living spaces at the time, while the Workplaces preformed as place for production and labor. Michel Foucault - At the end of the twenty century- introduction of biopolitics has had highlighted the alteration in the production and labor inter-function. The house does not precisely preform as sanctuary, from the production, for the family, it opens the house to be -part of the city as- a space for production, not only to produce objects, but to reproduce the family as a total part of the production mechanism in the city. While the public housing kept altering from country to another after the failure of the modernist's public housing in the late 1970s the society continued changing parallelly with socio-economic condition in each political-economical system and the public housing thus followed.

The family structure in the major cities has been dramatically changing, single parenting and the long working hours for instance, have been escalating the loneliness in the major cities such as London, Berlin and

Tokyo, and the public housing for the families is no longer suits the single lifestyle for the individuals.

This Paper investigates the performance of both the single/individual lifestyle and the family/society structure in Tokyo and Berlin in a relation to utilization of the public housing under economical, policies and the socio-political environment that produced the individuals and the collective. The study is carried through the study of the undercurrent individual/society and case studies, to examine the performance of the utilization of the housing.

The major finding is that the individual/collective are revolving around the city, the city identified and acts as a system that magnetized and blurred the line between production and reproduction lifestyle. the mass public housing for families is shifting to be a combination between neo-liberalism and socialism housing.

***Keywords*—** Loneliness, production/reproduction, work/live, public housing.

A. B. Author, is with Department of Art and Architecture, Waseda University (phone: +81 090-9153-6193, email: abudjana@akane.waseda.jp).

Life Cycle Assessment of a Parabolic Solar Cooker

Bastien Sanglard, Lou Magnat, Ligia Barna, Julian Carrey, Sébastien Lachaize

***Abstract*—** Cooking is a primary need for humans, several techniques being used around the globe based on different sources of energy: electricity, solid fuel (wood, coal...), fuel or liquefied petroleum gas. However, all of them leads to direct or indirect greenhouse gas emissions and sometimes health damage in household. Therefore, the solar concentrated power represent a great option to lower the damages because of a cleaner using phase. Nevertheless, the construction phase of the solar cooker still requires primary energy and materials, which leads to environmental impacts. The aims of this work is to analyse the ecological impacts of a commercial aluminium parabola and to compare it with other means of cooking, taking the boiling of 2 litres of water three times a day during 40 years as the functional unit.

Life cycle assessment was performed using the software Umberto and the EcoInvent database. Calculations were realized over more than 13 criteria using two methods: the international panel on climate change method and the ReCiPe method. For the reflector itself, different aluminium provenances were compared, as well as the use of recycled aluminium. For the structure, aluminium was compared to iron (primary and recycled) and wood.

Results show that climate impacts of the studied parabola was 0.0353 $kgCO_2eq/kWh$ when built with Chinese aluminium and can be reduced by 4 using aluminium from Canada. Assessment also showed that using 32% of recycled aluminium would reduce the impact by 1.33 and 1.43 compared to the use of primary Canadian aluminium and primary Chinese aluminium, respectively. The exclusive use of recycled aluminium lower the impact by 17. Besides, the use of iron (recycled or primary) or wood for the structure supporting the reflector significantly lowers the impact. The impact categories of the ReCiPe method show that, the parabola made from Chinese aluminium has the heaviest impact - except for metal resource depletion - compared to aluminium from Canada, recycled aluminium or iron.

Impact of solar cooking was then compared to gas stove and induction. The gas stove model was a cast iron tripod that supports the cooking pot and the induction plate was as well a single spot plate. Results show the parabolic solar cooker has the lowest ecological impact over the 13 criteria of the ReCiPe method and over the global warming potential compared to the two other technologies. The climate impact of gas cooking is 0.628 $kgCO_2/kWh$ when used with natural gas and 0.723 $kgCO_2/kWh$ when used with a bottle of gas. In each case, the main part of emissions came from gas burning. Induction cooking has a global warming potential of 0.12 $kgCO_2eq/kWh$ with the electricity mix of France, 96.3% of the impact being due to electricity production. Therefore, the electricity mix is a key factor for this impact: for instance, with the electricity mix of Germany and Poland, impacts are 0.81$kgCO_2eq/kWh$ and 1.39 $kgCO_2eq/kWh$ respectively. Therefore, the parabolic solar cooker has a real ecological advantages compared to both gas stove and induction plate.

.

***Keywords*—** Life cycle assessement, solar concentration, cooking, sustainability.

B. Sanglard is with the Laboratoire de Physique Chimie des Nano-Objets, INSA, Toulouse, 31400 France (e-mail: sanglard@ insa-toulouse.fr).

L. Magnat was with the Laboratoire de Physique Chimie des Nano-Objets, INSA, Toulouse, 31400 France (e-mail: sanglard@ insa-toulouse.fr).

L. Barna is with Toulouse Biotechnology Institute, INSA, 31400 France (e-mail: lbarna@insa-toulouse.fr).

J. Carrey is with the Laboratoire de Physique Chimie des Nano-Objets, INSA, Toulouse, 31400 France (e-mail : jcarrey@insa-toulouse.fr).

S. Lachaize is with the Laboratoire de Physique Chimie des Nano-Objets, INSA, Toulouse, 31400 France (e-mail : slachaize@insa-toulouse.fr).

Iron Oxide Reduction Using Solar Concentration and Carbon-Free Reducers

Bastien Sanglard, Simon Cayez, Guillaume Viau, Thomas Blon, Julian Carrey, Sébastien Lachaize

***Abstract*—** The need to develop clean production processes is a key challenge of any industry. Steel and iron industries are particularly concerned since they emit 6.8% of global anthropogenic greenhouse gas emissions. One key step of the process is the high-temperature reduction of iron ore using coke, leading to large amounts of CO_2 emissions. One route to decrease impacts is to get rid of fossil fuels by changing both the heat source and the reducer. The present work aims at investigating experimentally the possibility to use concentrated solar energy and carbon-free reducing agents.

Two sets of experimentations were realized. First, *in situ* X-ray diffraction on pure and industrial powder of hematite was realized to study the phase evolution as a function of temperature during reduction under hydrogen and ammonia. Secondly, experiments were performed on industrial iron ore pellets, which were reduced by NH_3 or H_2 into a "solar furnace" composed of a controllable 1600W Xenon lamp to simulate and control the solar concentrated irradiation, of a glass reactor and of a diaphragm to control light flux. Temperature and pressure were recorded during each experiment via thermocouples and pressure sensors. The percentage of iron oxide converted to iron (called thereafter "reduction ratio") was found through Rietveld refinement. The power of the light source and the reduction time were varied.

Results obtained in the diffractometer reaction chamber show that iron begins to form at 300°C with pure Fe_2O_3 powder and 400°C with industrial iron ore when maintained at this temperature for 60 minutes and 80 minutes, respectively. Magnetite and wuestite are detected on both powders during the reduction under hydrogen; under ammonia iron nitride is also detected for temperatures between 400°C and 600°C. All the iron oxide was converted to iron for a reaction of 60 min at 500°C whereas a conversion ratio of 96% was reached with industrial powder for a reaction of 240 min at 600°C under hydrogen. Under ammonia, a full conversion was also reached after 240 min of reduction at 600 °C.

For experimentations into the solar furnace with iron ore pellets, the lamp power and the shutter opening were varied. An 83.2% conversion ratio was obtained with a light power of 67 W/cm^2 without turning over the pellets. Nevertheless, under the same conditions, turning over the pellets in the middle of the experiment permits to reach a conversion ratio of 86.4%. A reduction ratio of 95% was reached with an exposure of 16 min by turning over pellets at half time with a flux of 169 W/cm^2. Similar or slightly better results were obtained under an ammonia reducing atmosphere. Under the same flux, the highest reduction yield of 97.3% was obtained under ammonia after 28 minutes of exposure.

The chemical reaction itself, including the solar heat source, does not produce any greenhouse gases, so solar metallurgy represents a serious way to reduce greenhouse gas emission of metallurgy industry. Nevertheless, the ecological impact of the reducers must be investigated, which will be done in future work.

***Keywords*—**Solar concentration, Metallurgy, Ammonia, Hydrogen, Sustainability.

B. Sanglard is with the Laboratoire de Physique Chimie des Nano-Objets, INSA, Toulouse, 31400 France (e-mail: sanglard@ insa-toulouse.fr).

S. Cayez is with the Laboratoire de Physique Chimie des Nano-Objets, INSA, Toulouse, 31400 France (e-mail: cayez@insa-toulouse.fr).

G. Viau is with the Laboratoire de Physique Chimie des Nano-Objets, INSA, Toulouse, 31400 France (e-mail : viau@insa-toulouse.fr).

T. Blon is with the Laboratoire de Physique Chimie des Nano-Objets, INSA, Toulouse, 31400 France (e-mail : blon@insa-toulouse.fr).

J. Carrey is with the Laboratoire de Physique Chimie des Nano-Objets, INSA, Toulouse, 31400 France (e-mail : jcarrey@insa-toulouse.fr).

S. Lachaize is with the Laboratoire de Physique Chimie des Nano-Objets, INSA, Toulouse, 31400 France (e-mail : slachaize@insa-toulouse.fr).

Solar Technology: A Review of Government-Sponsored Green Energy

Christopher Battle

Christopher Battle is with the Cornell University, United States (e-mail: crb266@cornell.edu).

Abstract

The pursuit of a sustainable future is dependent on the ability of governments from the national to municipal level. The politics of energy and the development of state-sponsored photovoltaic cell expansion can nebulize in several ways based on a state or nation's physical and human geography. This study conducts a comparative analysis of the energy and solar program of Turkey, Pennsylvania, and Philadelphia. The study aims to assess the city of Philadelphia's solar policies in contrast with both its political history and the photovoltaic programs of Turkey, a world leader in solar system development, and Pennsylvania's history of energy regulation. This comparative study found that after hundreds of bills and regulations over decades, sustainable energy development in affordable housing and new construction is the next phase of State-Sponsored Green energy for the city of Philadelphia.

1. Introduction

Solar Power and Solar Power Research

Solar power and solar technology are the use of machines to convert the power emitting from the sun into a renewable source of energy. Sheets of metal, often silicon, and chemical layers are placed between glass as semi-conductors to create photovoltaic cells. These cells are grouped to form solar panels. Sunlight hits and refracts light from these panels and chemical reactions create energy which is then transferred into electricity [1]. Advancing technologies in solar focuses on increasing the effect of the current models as well as variation that take the technological framework of the solar cell and expand upon it. Over time, silicon sheets have been replaced by thinner sheets of copper and cadmium. Additions to the chemical layers within the structure and increased absorption layers have been developed to expand on existing solar cell efficiency. Multi-layer solar cells build on this same framework.

Organic solar cells developed after traditional solar cells were capped at their efficiency by current technology. Organic solar cells use natural chemical layers and organic semiconductors, expanding solar use and green space usage possibilities. As technology advanced, research on inner layer sheets or organic solar cells was replaced with the study of a dye-sensitized cell where an organic dye within the cells acts as semi-conductors, increasing solar efficiency and decreasing energy loss in the absorption process [1]. Current models and capacity for solar use span from residential use on rooftops to satellite dishes that focus heat from the sun to create energy. Advance solar technology and future models for solar cells efficiently utilize quantum dot technology. Quantum dots are nanoparticles, replacing inner layer sheets used as semiconductors and utilizing quantum properties. As a result, they have the potential to further the energy

harnessed from the sun and decrease the energy lost in the extraction process. Throughout the history of the research, the frame of advanced current technology takes precedence over new forms of photovoltaic technology [1].

As the role of technology grows, the research and academic exploration of the subject is a point of discussion. How this technology will be used in the future reflects the research and ideas explored today, so reviewing the literature on solar research and solar power is necessary to understand the role of solar technology as a distributive resource [2]. In reviewing the literature, much of the focus in solar power research has been related to physics, material science, chemistry, energy, and engineering, specifically, in the realm of polymer science and optic fields, where there has been an increase in the number of research articles related to solar power as a whole [3].

The United States currently leads the world in solar power research, with the developing nations of China, Japan, Germany, the United Kingdom, India, South Korea, France, Spain, and Italy. These nations make up the dominant field of solar power research around the world, focusing on solar cell efficiency and solar material science and optimizing the amount of energy being converted from solar cells into conventional commercial and residential electrical systems. In a league of their organic solar cells, dye-sensitized solar cells and organic materials for solar cell technology have been rapidly increasing over the past 20 years. As materials in technology changed throughout the years, the original and prototypical materials are likely to be the first for decentralized solar technology [2].

2. Methodology and Analysis

Centralized Solar Power: Turkey

Taking solar power and solar technology development from a global perspective, we see how solar power is captured and absorbed varies between counties based on technological and geological capacity. In the case of Middle Eastern countries, such as Turkey with a high level of government intervention when it comes to solar power and solar advancement, combining solar technology and state power to form concentrated solar technology [4]. Concentrated solar technology is the act of taking solar energy and the heat generated from solar energy extraction and using it to power steam engines, utilizing advanced technology with modern industrial systems. Concentrated solar technology can take three general forms with variations among each: the first would be the Parabola Trough System, where the direct solar radiation hits and heats an absorption pipe that contains water. The heated water is pumped into the steam generator which is used to power the steam turbine which is used to generate electricity.

The second method is the Dish/Stirling System, using a concentrated series of panels on a dish to focus the direct solar radiation into a thermal receiver and a heat engine generator to produce power and electricity. The final system is called the Power Tower System, which uses two access tracking mirrors on top of a tower called heliostats to reflect the direct solar radiation onto a receiver which is absorbed into a working fluid that's used to power a steam turbine. The Parabola Trial System and the Power Tower System have large economies of scale, meaning the larger you make them the more energy they will produce [4]. The Dish/Stirling System becomes less efficient the more you scale it up as a result the Dish/Stirling System of utilizing direct solar radiation will likely be the first decentralized solar power system when solar technology becomes priced for both residential in commercial use, crossing poverty lines and tax brackets.

When countries such as Turkey plan to use solar technology, there are serval factors that play into the capacity of a nation to offset its energy usage through direct solar radiation. Those factors are the solar resource which is the degree in the amount of solar radiation within a nation, the land use, and the ability to build solar structures, the land to build the structures on as well as land cover, and the ability to cover the land in solar materials, site topography, the topological and geographical ground levels that make up the country and the availability of water as the concentrated solar power systems are taking and utilizing the heat from the solar radiation and therefore must also have mechanisms and machinery cooled down the materials as well as the water being used in the turbines.

Turkey's ambitions to utilize its natural resources to absorb solar power, like the rest of the world, is still in its infancy, but the research shows possibilities the countries with the governmental capacity to utilize resources will be the first to maximize the use of solar radiation in their electrical systems [4].

Pseudo-Centralized Solar Power: The United States and Pennsylvania

The energy industry from the national state level shows how federal policy created energy monopolies in the mid-20th century. Energy companies controlled the three fundamental aspects of energy: generation, transmission, and distribution. This vertical domination over the marketplace gave utility companies regional monopolies wherever they were able to provide power. These monopolies lasted until the 1970s when an oil embargo froze the energy market economy causing an energy crisis. This prompted President Jimmy Carter to introduce the National Energy act of 1978 which contained the Public Utility Regulatory Policies Act (PURPA), which decentralized the extraction, transmission, and distribution process and required that all energy companies acquire portions of their energy from alternative sources, boosting the power of the Federal Energy Regulatory Commission who was in charge of the implementation of PURPA and this began what is known as the energy market decentralization of the 1990s [5].

The deregulation and decentralization of the energy market began with the Energy Policy act of 1992 which forced companies to unbundle their wholesale prices for generation transmission and distribution and provide all open access to their transmission lines, meaning all energy companies had to compete on the open energy market [5]. This prompted many states to individually deregulate their energy markets specific to their states, allowing for customers and consumers to have a choice in their energy supplier. Some states went a step further and uses deregulation to introduce renewable energy into their energy market. This came by the way of energy standards that regulated energy investors to purchase certain amounts of renewable energy.

In terms of Pennsylvania, the state took specific acts to deregulate its energy market. The first of which was the Electricity Generation Customer Service and Compensation Act, which allowed electric utility companies to own generation and transmission factories, but they were not allowed to factor in the cost of generation and the transmission of energy into the price of electricity. This along with the requirement that energy prices be approved by the state shifted the Pennsylvania energy market from a monopoly two more of a market economy as electric companies gain their revenue through the sale of electricity not the production of electricity. The Electricity Generation Customer Choice and Competition Act was the first step in reshaping Pennsylvania's energy policy toward more of a market economy and it only continued as the state moved into the 2000s.

Over a decade after the Electricity Generation Customer Choice and Competition Act, the state passed Act 129, which created the Energy Efficiency and Conservation Program, a set of electricity standards

aimed at reducing energy consumption and required electric public utility companies with over 100,000 customers to abide by it. Pennsylvania only continued with its energy deregulation and aims at renewable resources in 2004 with the passing of the Alternative Energy Portfolio Standards Act. This was aimed to increase the energy portfolio of the state and required Energy Generation Sources (EGS) and Energy Distribution Companies (EDC) to purchase a certain amount of solar power coming from alternative energy sources. The act enforced and incentivized these purchases through Alternative Energy Credits, which allow for companies to offset the cost of purchasing solar while adhering to state regulations. Companies can earn this credit by purchasing energy from solar technologies, or they can buy the alternative energy credits themselves and trade them for stocks or bonds [5].

Along with the Alternate Energy Portfolio Standards Act (AEPSA), the concept and idea of Net Metering were introduced. Net Metering allows residential consumers of EDCs to sell excess energy they get from solar technology back to the electric companies to offset the cost of their energy. Each one of these acts and initiatives came with an increased cost, so not only did the act allow energy companies to recoup the costs of the act, but the state also created the Alternate Energy Investment Act which provided funding the small business and residential consumers who are willing to solar panels through the Department of Environmental protection.

The ambitions and expansiveness of the AESPA have not met the state's intent goals. The provisions within the act focused on the legislative and policy obstacles but don't focus on the incurred and increasing costs of solar technology in the current day and age the lack of financial prospects in solar technology has decentralized investors into these solar programs. The idea of subsidizing the cost of solar panels only forces energy companies to regulate their rates which disproportionately affects low-income citizens [5].

Trying to address solar technology and obstacles to renewable energy natural inherent to resources within a given region is the prime concern within the United States. The two states with the most and most efficient solar programs are California and North Carolina. These states also happen to be the states that receive the most sunlight throughout the year. The cost of solar for states such as Wisconsin is drastically different than that of California so states like Arizona and North Carolina continue to lead the country in solar technology through their geological advantage. The rest of the nation must taper its solar aspirations to the geological factors that exist.

Striated energy models and the consequences of a lack thereof can be seen in the role solar technology plays in the overall framework of the utility industry. The utility industry's ability to profit from the distribution of electricity is regulated by the state, which considers the amount of money invested into the company, the operating cost the company incurs over time, and sets the market price at a flat price rate, limiting supply for the overarching demand. Utility companies' revenue is based on their ability to meet this demand within their given region, setting profits, but when customers can supply their electricity as well as sell it back to the energy distribution companies, the demand for electricity decreases, cutting profits. The utility companies then go back to the state to have the flat rate increased; this proportionately affects those at the lowest income [5].

Utility companies also charge a fee for residents and small business owners to connect their solar technology to the electrical grid to sell it back to the city. This fee is subject to change as the company sees fit because the state allows the utility company to recoup the loss that they gain from the exchange. Utility companies also cap the electricity residents can resale. The disproportionate effects of solar technology, the extended calls from utility companies to raise rates, the lack of expanded solar technologies, and the limits placed on those who can have them draw attention to a system failure, not towards the utility companies but at the state level where policy ambitions take precedence over economic and scientific evidence [5].

Despite the vast number of solar initiatives, incentives, and regulations. The infancy of solar technology is constantly overlooked at the policy level, and its influences the economic market. First, Pennsylvania as a state does not get is nearly as much sun as California or North Carolina and as solar panels used on the individual and commercial level have become popular over the years, there's no utility-scale solar system in Pennsylvania nor has there been a successful one since the rise in solar technology within the United States. This is because, at the current date in 2022, solar technology becomes decreasingly efficient when given economies of scale, regardless of residential commercial, or industrial settings. Research shows promise but on a purely economic level, the declines in solar technology prices show no ability to sustain entire communities nor cities or states within the next decade.

Research shows that striving for solar energy despite economic implications leads to disproportionate effects on low-income communities and low-income residents are affected from both ends of the solar technology spectrum. The cost of solar technology is high, therefore inaccessible for low-income residents, and those who do have access to solar technology drive up the rates of electricity for everybody leading to higher electric bills for low-income residents decreasing their capacity to afford solar technology.

Despite government programs such as loans and unguaranteed solar rebates, the steps to mitigating these issues begin with the state of Pennsylvania understanding its role in the greater solar economy as a city with the technology to increase the solar capacity but not the geological capacity to increase its solar use, the state is in a prime position to lead the nation in the material science and efficiency standards within the realm of solar, but the state needs to scale back its aspirations for its planned solar usage and distribution as both the consumer and the energy distribution companies cannot keep up with the pace of state policy.

Decentralized Solar Power: Philadelphia

Philadelphia's energy profile begins with the geographics and demographics of the city. Philadelphia is both a city and a county within Pennsylvania, giving it exclusive municipality rights. The city covers about 134 square miles and is the fifth-largest city in the country population of about 1.6 million people with an average income of $40,000 a year and has had numerous agencies and policies since the decentralization of its energy industry since the 20th century [6]. The city has become a service-based industry, departing from its industrial path, and leaving many of its industrial areas vacant, abandoned, or demolished to make way for the burgeoning development that the competitive areas of Philadelphia are expanding.

The political structure of this city is centralized within the office of the mayor, giving the mayor extensive executive powers for the rest of the city, cut between departmental boards, independent boards, and independent commissions with specific roles and perspectives on energy sustainability within Philadelphia. The primary of which would be the Philadelphia Gas Authority, the Gas Commission, the City Planning Commission, the Philadelphia airport, and the school district of Philadelphia all play fundamental roles in the city's office of the mayor, with the city council's central role within the city as far as finance and raising capital for expenditures. The city has a series of budgets that all have specific purposes and places within the Philadelphia economy [7]-[9]. The three most important are the operating budget, the budget for the school district of Philadelphia, and the capital budget for capital expenditures.

The uniqueness of Philadelphia's energy policy in urban sustainable energy development creates questions that arise regarding the nature of state and local governments and the relation between multi-level government relationships that factor into the structure of energy policy in the city's energy market [10]. The energy industry often limits the number of regional specific actors that play a role in the Philadelphia energy market. The Philadelphia energy company in the Philadelphia gas works supplies over 80% of the city's electricity and gas power making them the largest political utility entity in the area. The Philadelphia Gas

Works are the largest municipal gas utility in the country and the individualistic municipality of the city allows for non-government entities to have a major role in how sustainable development [5]. The Philadelphia gas works are the largest municipal gas utility in the country and the individualistic municipality of the city allows for non-government entities to have a major role in how sustainable development occurs.

Despite this, the city is already taken many measures to increase and incentivize the use of sustainable technology over the past 20 years. in 2008 the city released *GreenWorks Philadelphia*, a sustainability initiative that outlined the city's ambitions to become the country's greenest city. This framework outlined all the city's plans and goals for both climate change and urban sustainable energy development. This framework contains 15 target goals and 167 initiatives on how to build a more sustainable city the key five areas of interest are energy, environment, equity, economy, and engagement [5]. This framework was the first to begin the city cities interworking energy policy on a municipal and citywide level the framework focused on using financial powers, regulatory powers, pilot schemes, education, and community outreach to create a wide range of policy approaches to deal with the generation of renewable energy. The diaspora radical approach the city is taking to achieve energy policy has created a system where energy policy success is tantamount to the cooperation and incentive structures between departments city officials and non-governmental entities [10].

3. Discussion

The Philadelphia Electric Company (PECO) and the Philadelphia Gas Works (PGW) are the lead agencies and utility obstacles that the office of sustainability in the mayor's administration faces when trying to regulate energy policy. The city also must contend with the varying organizational structures around energy policy that have their interest in the Philadelphia alternative energy market. The overall market of energy within the area of sustainability planning is land use planning within the city and the rooted political economic cultural conditions that set up the Philadelphia market economy. The Philadelphia Solar Partnership, the Energy Benchmarking Ordinance, the Nonprofit Philadelphia Energy Coordinating Agency, the Neighborhood Energy Center, the Energy Efficient Buildings Hub, and the Consortium for Building Energy Innovation are all players in the market to increase the city's urban sustainable energy capacity.

Philadelphia's energy policy is also adherent to national energy initiatives The US Conference of Mayors Climate-protection Agreement in 2005 and the US involvement in the Kyoto Protocol treaty were used to lobby policies on a local, state, and federal level. Philadelphia constantly works in tandem with officials on the national level to recognize Philadelphia's progress in becoming a sustainably clean city. With all these actors and parties in play, there's no current mechanism for systemic energy policy within the city, leaving the city's energy future in the hands of whichever energy entity is dominating the area at the time. Currently, PECO and the PGW supply not just the city, but the greater Philadelphia area and most of southeastern Pennsylvania, holding energy and gas monopolies in the region.

The programs and incentives only continue at the international level. Philadelphia has joined the C40 cities climate leadership group, which is a coalition of cities across the world to share knowledge and development strategies and policies that increase alternative energy and decrease gas emissions. With this sharing of lessons and information and the ability to work in tandem with other nations for their energy policy in cohesion with the Obama administration, Philadelphia became a member of the Joint Initiative on Urban Sustainability, which is a public-private partnership between the US and Brazil to support investments on sustainable energy infrastructure in the city of Philadelphia also participates in the Carbon

Disclosure Cities Project, which implores cities to disclose their energy usage and their sustainable energy initiatives were taken within that year.

4. Conclusions

Philadelphia has taken numerous steps over the past decades to increase its presence essence and capacity for urban sustainable energy passing 100 laws, bills, ordinances, memorandums, initiatives, and organizations for the sole intent of the city's energy capacity and the research highlights the four key areas where Philadelphia's energy policy needs to focus on them before establishing itself as the international energy player. The role of the mayor, the ability of the city to increase its affordable energy development, provide energy capacity for the city's lowest-income residents, and the use of efficient building and development in the commercial sector on the local, state, and federal levels.

References

[1] Reddy, P. J. (2012). Solar power generation: technology, new concepts & policy. CRC Press.

[2] Dong, B., Xu, G., Luo, X., Cai, Y., & Gao, W. (2012). A bibliometric analysis of solar power research from 1991 to 2010. Scientometrics, 93(3), 1101-1117.

(3) Argyriou, I., Justice, J. B., Latham, W., & Warren, R. (2017). Urban sustainable energy development: A case study of the city of Philadelphia. Local Environment, 22(12), 1461-1478.

[4] Kaygusuz, K. (2011). Prospect of concentrating solar power in Turkey: the sustainable future. Renewable and Sustainable Energy Reviews, 15(1), 808-814.

[5] Alam, C. (2015). It's Not Always Sunny in Philadelphia: The Problem with the Pennsylvania Solar Initiatives. Pitt. J. Tech. L. & Pol'y, 16, 208.

[6] Anderson, E. (2000). The Emerging Philadelphia African American Class Structure. The Annals of the American Academy of Political and Social Science, 568(1), 54-77.

[7] Andersson, E., Borgström, S., Haase, D., Lanemeyer, J., Mascarenhas, A., McPhearson, T., ... & Herreros-Cantis, P. (2021). Context-sensitive systems approach for understanding and enabling ecosystem service realization in cities. Ecology and Society, 26(2).

[8] Blomley, N. (2008). Enclosure, common right, and the property of the poor. Social & Legal Studies, 17(3), 311-331.

[9] Beierschmitt, M., Klapper, L., Linderman, J., McIntyre, K., Tarullo, C., Williams, C., & Amberg-Blyskal, P. (2021). Gentrification and the Philadelphia Housing Authority: The Impact of PHA Property Sales from 2011-2019 on Local Communities.

[10) Crews-Williams, C., Scholar, M., Brownson, J. R., & Webster, N. (2018). "Perceptions and Impact of Solar Energy in the Context of Philadelphia" _. The Penn State McNair Journal, 97.

Daylight Performance of a Single Unit in Distinct Arrangements

Rifat Tabassoom

***Abstract*—**Recently multistoried housing projects are accelerating in the capital of Bangladesh- Dhaka, to house its massive population. Insufficient background research leads to a building design trend where a single unit is designed and then multiplied all through the buildings. Therefore, although having identical design, all the units cannot perform evenly considering daylight, which also alters their household activities. This paper aims to understand if a single unit can be an optimum solution regarding daylight for a selected housing project.

***Keywords*—**Daylight, Orientation, Performance, Simulations

Rifat Tabassoom is the faculty member of Architecture Department, Dhaka University of Engineering and Technology, Gazipur (phone: +880732804782; e-mail: rifattabassom@duet.ac.bd).

Quantum Entanglement and Thermalization in Superconducting Two- Qubit Systems

E. Karami, M. Bohloul, P. Najmadi

***Abstract*—** The superconducting system is a suitable system for quantum computers. Quantum entanglement is a fundamental phenomenon that is key to the power of quantum computers. Quantum entanglement has been studied in different superconducting systems. In this paper, we are investigating a superconducting two-qubit system as a macroscopic system. These systems include two coupled Quantronium circuits. We calculate quantum entanglement and thermalization for system evolution and compare them. We observe, thermalization and entanglement have different behavior and equilibrium thermal state has maximum entanglement.

***Keywords*—**macroscopic system, quantum entanglement, thermalization, **superconducting system.**

Mohammad Bohloul is with the Tabriz University, Iran (e-mail: m_bohlol@yahoo.com).

Model-Free Distributed Control of Dynamical Systems

Javad Khazaei and Rick S. Blum

***Abstract*—**Distributed control is an efficient and flexible approach for coordination of multi-agent systems. One of the main challenges in designing a distributed controller is identifying the governing dynamics of the dynamical systems. Data-driven system identification is currently undergoing a revolution. With the availability of high-fidelity measurements and historical data, model-free identification of dynamical systems can facilitate the control design without tedious modeling of high-dimensional and/or nonlinear systems. This paper develops a distributed control design using consensus theory for linear and nonlinear dynamical systems using sparse identification of system dynamics. Compared with existing consensus designs that heavily rely on knowing the detailed system dynamics, the proposed model-free design can accurately capture the dynamics of the system with available measurements and input data and provide guaranteed performance in consensus and tracking problems. Heterogeneous damped oscillators are chosen as examples of dynamical system for validation purposes.

***Keywords*—** Consensus tracking, distributed control, model-free control, sparse identification of dynamical systems.

I. Introduction

Data-driven modeling of dynamical systems has recently been revolutionized with the advances on machine learning approaches and unprecedented availability of high-resolution data from historical records. Several approaches have been introduced for capturing the dynamics of complex systems including: (i) dynamic mode decomposition [1], [2], dynamic mode decomposition with control [3], which heavily relies on a linear dynamics assumption but can handle high-dimensional data, (ii) Koopman operator with control [4], [5] that connects dynamic mode decomposition to nonlinear dynamics through the Koopman operator, (iii) genetic programming which constructs categories of candidate nonlinear functions for the rate of change of state variables in time [6]. A model is then selected as a Pareto optimal solution that provides a balanced between model complexity and predictive accuracy. (iv) Recently, a novel approach was developed to automatically select from several candidate terms those terms which are most suitable to describe the dynamics. This method is called sparse identification of system dynamics (SINDY), and uses a sparse regression technique from machine learning to identify dominant dynamics of candidate functions, and has shown promise in accurately modeling the unknown dynamics of complex systems [7], [8]. One of the main advantages of SINDY for control purposes is the sparsity technique that reduces the training time and heavy reliance of neural-network-based approaches for identification and control which can be hard to interpret. The proposed approach is fully interpretable based on classical control theories. The application of SINDY for capturing input-output models that are appropriate for control design purposes was reported in [8], [9]. It was shown in [8] that sparse identification can capture dynamics of feedback control systems in nonlinear dynamics and its application to model-predictive control of aircraft dynamics was reported in [9]. While these studies show the significant improvement in control design of unknown dynamics, the reported studies mainly focused on centralized control approaches that might not be practical for large-scale systems with distributed complex dynamics, i.e., transportation systems, power grids, buildings.

Distributed control in this case has a few advantages over conventional centralized approaches methods; first, system security, reliability, and scalability are improved [10], as no single point of failure (central unit) exists. Second, computational efforts are divided to many nodes instead of being performed all at the central unit as in centralized mechanisms [10]. However, the application of model-free data-driven approaches for distributed control of large-scale complex systems has not been reported yet.

The goal of this paper is to investigate the application of a sparse identification approach for distributed control design of complex dynamics. Using the sparse regression technique, input-output dynamics of the unknown heterogeneous dynamical systems will be predicted. The learned dynamics can then be used to design distributed cooperative controllers that minimize the error between the desired and actual states. The tracking control of dynamical systems using the sparse identification technique will also be investigated. Contributions of the paper are listed as:

- Designing a distributed controller with minimum communication requirements for damped oscillators using only measurements
- Providing guaranteed stability of the designed consensus tracking control problem
- Accurately identifying the dynamics of damped oscillators using sparse identification technique

The rest of the paper is organized as follows: Section II formulates the sparse identification problem and Section III includes the proposed distributed control design. Numerical results are included in Section IV and Section V concludes the paper.

Javad Khazaei is an assistant professor in the electrical and computer engineering (ECE) department at Lehigh University and Rick S. Blum is a professor in the ECE department at Lehigh University, Bethlehem, PA. (emails: khazaei@Lehigh.edu, & rblum@lehigh.edu).

II. Model-Free Identification of Dynamical Systems

A robust approach in identifying the governing equations of nonlinear/linear systems is to construct families of candidate functions for the rate of change of state variables in time. Among all candidate functions, since most dynamical systems have few nonlinear terms in the dynamics, sparsity promoting techniques can be used to identify the candidate functions with most impact in forming the system dynamics using available measurements. This method is called sparse identification of nonlinear dynamics (SINDY), which was originally proposed in [7]. SINDY combines symbolic regression and sparse representation to come up with the dynamics of the system. Symbolic regression is a machine learning approach for determining a function relating the input to output using available data. In this research, SINDY will be used to identify governing dynamics of a dynamical system for distributed control design purposes. In the following, an overview of sparse identification technique is included.

The sparse identification relies on the fact that many dynamical systems of the form $\dot{x} = f(x, u)$ have relatively few terms in the right hand side of their governing equations. Assume the actual dynamics of a system is represented by:

$$\frac{d}{dt}\mathbf{x}(t) = \dot{\mathbf{x}}(t) = f(\mathbf{x}(t), \mathbf{u}(t)) \tag{1}$$

where $\mathbf{x}(t) = [x_1(t)\ x_2(t)\ \dots\ x_n(t)] \in \mathbb{R}^n$ is a vector of states and $\mathbf{u}(t) \in \mathbb{R}^n$ is a vector of controllable inputs. In regression problems, only a few terms are important and sparse feature selection can be used to identify the most dominant terms representing the dynamics. To identify the governing equations of the system in (1), a time-history of the state vector $\mathbf{x}(t)$, input $\mathbf{u}(t)$, and $\dot{\mathbf{x}}(t)$ is required. In most practical systems, only $\mathbf{x}(t)$ and $\mathbf{u}(t)$ are available and $\dot{\mathbf{x}}(t)$ needs to be estimated from $\dot{\mathbf{x}}(t)$. If the measurement data is sampled at m intervals $t_1,\ t_2,\ \dots,\ t_m$ and measurements are arranged into a matrix $\mathbf{X}$,

$$\mathbf{X} = \begin{bmatrix} \mathbf{x}^T(t_1) \\ \mathbf{x}^T(t_2) \\ \vdots \\ \mathbf{x}^T(t_m) \end{bmatrix} = \begin{bmatrix} x_1(t_1) & x_2(t_1) & \dots & x_n(t_1) \\ x_1(t_2) & x_2(t_2) & \dots & x_n(t_2) \\ \vdots & \vdots & \ddots & \vdots \\ x_1(t_m) & x_2(t_m) & \dots & x_n(t_m) \end{bmatrix} \tag{2}$$

and inputs for t_m samples are written into a matrix $\mathbf{U}$,

$$\mathbf{U} = \begin{bmatrix} \mathbf{u}^T(t_1) \\ \mathbf{u}^T(t_2) \\ \vdots \\ \mathbf{u}^T(t_m) \end{bmatrix} = \begin{bmatrix} u_1(t_1) & u_2(t_1) & \dots & u_n(t_1) \\ u_1(t_2) & u_2(t_2) & \dots & u_n(t_2) \\ \vdots & \vdots & \ddots & \vdots \\ u_1(t_m) & u_2(t_m) & \dots & u_n(t_m) \end{bmatrix} \tag{3}$$

the measurements for derivatives can be approximated numerically from $\mathbf{X}$ following the procedure in the next section.

A. Savitzky-Golay Filtering

In [11], Savitzky-Golay developed a filter that is used to smooth out a noisy signal. This is necessary before estimating the derivatives of $\mathbf{X}$. Savitzky-Golay filters are also called digital smoothing polynomial filters or least-square smoothing filters. The main advantage of these filters compared to other filters (i.e., finite impulse response (FIR) filters) is their ability to minimize the least-squares errors in fitting a polynomial to frames of noisy data. The basic idea behind Savitzky-Golay filter is that having a group of $2M + 1$ samples of a signal $x[n]$, centered at $n = 0$, the coefficients of a polynomial $p(n)$ that minimizes the mean-squared approximation error for the group of samples are obtained [12]. The polynomial is defined as:

$$p(n) = \sum_{k=0}^{N} a_k n^k \tag{4}$$

and the coefficients a_k are obtained to minimize the mean-squared approximation error (MSE) expressed by [12]:

$$\text{MSE} = \sum_{n=-M}^{M} (p(n) - x[n])^2 \tag{5}$$

where M is denoted as the half-width of the approximation interval. Savitzky and Golay showed in [11] that during each interval, the output obtained by sampling the fitted polynomial is equivalent to a fixed linear combination of the local set of input samples. This observation simplified the smoothing process by the fact the the output samples can be computed by a discrete convolution sum of the form [12]:

$$y[n] = \sum_{m=-M}^{M} h[m]\ x[n-m] \tag{6}$$

instead of differentiating (5) with respect to each of $N + 1$ unknown coefficients of the polynomial and setting the corresponding derivative equal to zero. In this paper, the existing Savitzky-Golay filter function of MATLAB is used to smooth out the measurement samples $\mathbf{X}$ before estimating the derivatives.

B. Estimating the Derivatives, $\dot{\mathbf{X}}$

Difference approximations are used to numerically solve for the solution of ordinary and partial differential equations. Considering a smooth function in the neighborhood of point x, the derivatives can be approximated using Taylor series expansion at specified mesh points. Since the central difference approximation is more accurate for smooth functions, it is used in our paper. In this case, $\dot{\mathbf{X}}$ can be approximated by [13]:

$$\dot{\mathbf{X}} \approx \frac{\mathbf{X_f}(i+1) - \mathbf{X_f}(i-1)}{2h} \tag{7}$$

where $\mathbf{X_f}(i+1)$ is the filtered data at sample $i+1$ and h is the mesh spacing, which is considered the same as the sampling time of the simulation in this study, i.e., $5e^{-5}$ seconds.

$$\Theta(\mathbf{X},\mathbf{U}) = \begin{bmatrix} | & | & | & | & | & & | & | & | & \\ 1 & \mathbf{X} & \mathbf{U} & \mathbf{P_2}(\mathbf{X},\mathbf{U}) & \mathbf{P_3}(\mathbf{X},\mathbf{U}) & \dots & \sin(\mathbf{X},\mathbf{U}) & \cos(\mathbf{X},\mathbf{U}) & \sin(\mathbf{2}(\mathbf{X},\mathbf{U})) & \dots \\ | & | & | & | & | & & | & | & | & \end{bmatrix} \tag{8}$$

C. Sparse Identification of System Dynamics

Having calculated $\dot{\mathbf{X}}$, the library of candidate functions will be constructed as linear and nonlinear functions of the columns of $\mathbf{X}$ and $\mathbf{U}$. A typical choice of candidate functions include polynomials and trigonometric functions for nonlinear systems such as (8).

In (8), $\mathbf{P_2}(\mathbf{X},\mathbf{U})$ and $\mathbf{P_3}(\mathbf{X},\mathbf{U})$ denote nonlinear combination of second- and third-order polynomials of $\mathbf{X}$ and $\mathbf{U}$ columns, respectively. For example, for the second-order polynomial, the candidate function $\mathbf{P_2}(\mathbf{X},\mathbf{U})$ is expressed in (9) as:

$$\mathbf{P_2}(\mathbf{X},\mathbf{U}) = \begin{bmatrix} x_1^2(t_1) & x_1(t_1)x_2(t_1) & \dots & x_2^2(t_1) & x_1(t_1)u_1(t_1) & \dots & u_1^2(t_1) & \dots \\ x_1^2(t_2) & x_1(t_2)x_2(t_2) & \dots & x_2^2(t_2) & x_1(t_2)u_2(t_2) & \dots & u_2^2(t_2) & \dots \\ \vdots & \vdots & \ddots & \vdots & \ddots & \vdots & \dots & \\ x_1^2(t_m) & x_1(t_m)x_2(t_m) & \dots & x_2^2(t_m) & x_1(t_m)u_1(t_m) & \dots & u_1^2(t_m) & \dots \end{bmatrix} \tag{9}$$

The sparse coefficients of the matrix $\mathbf{\Gamma}$ can be solved using the following equation [8]:

$$\dot{\mathbf{X}} = \Theta(\mathbf{X},\mathbf{U})\mathbf{\Gamma}, \tag{10}$$

where each column of Γ represents a sparse vector of coefficients identifying which terms are active. The coefficients of Γ can be found using the sparse regression formulation presented in **Algorithm 1**. If the intent is to identify the signal $\mathbf{U}$ for feedback control, i.e., $\mathbf{U} = G(s)\mathbf{X}$, where $G(s)$ is the transfer function of the controller, the matrix of inputs can be identified using [8]:

$$\mathbf{U} = \Theta(\mathbf{X})\mathbf{\Gamma_u} \tag{11}$$

where $\Theta(\mathbf{X})$ is the matrix of candidate functions and the terms corresponding to $\mathbf{U}$ have been removed from $\Theta(\mathbf{X})$, i.e., as in (12). $\mathbf{\Gamma_u}$ can be found using the sparse regression algorithm similar to $\mathbf{\Gamma}$.

In summary, (10) predicts the dynamics of the system using available measurements and then the predicted dynamics can be used for control design purposes, which will be discussed in the next section. An example of a two-dimensional controlled damped harmonic oscillator with linear dynamics is considered to validate the effectiveness of the sparse regression algorithm in identifying the dynamics. The dynamic system is represented by:

$$\frac{d}{dt}\dot{\mathbf{x}} = A_i\mathbf{x} + B_i\mathbf{u} = \begin{bmatrix} -0.1 & 2 \\ -2 & -0.1 \end{bmatrix}\begin{bmatrix} x_1 \\ x_2 \end{bmatrix} + \begin{bmatrix} 1 \\ 0 \end{bmatrix}\mathbf{u} \tag{13}$$

After learning the dynamics, the system with these dynamics was first run for 25 seconds with a random input shown in the third subplot in Fig. 1 and the model was trained for this input. Dynamic response of x_1 and x_2 in response to this input is depicted in the first two subplots in Fig. 1 and compared to the actual model in (15), confirming a perfect prediction of the regression model. The input then was changed from 25 to 50 seconds to a completely different type (sinusoidal)

Algorithm 1 Sparse Regression Algorithm

Input: Measurements $\mathbf{X}, \mathbf{U}$
Input: Estimated derivatives$\dot{\mathbf{X}}$
procedure LEAST-SQUARE
$\Gamma = \Theta \backslash \dot{\mathbf{X}}$ (least-square solution)
  for k $= 1 : 10$ **do** (number of iterations)
    Set λ (sparcification knob)
    $|\Gamma| < \lambda \longrightarrow ind_{small}$
    $\Gamma(ind_{small}) \longrightarrow 0$
    for k $= 1 :$ n **do** (n dimension of state $\mathbf{X}$)
      $ind_{big} \neq ind_{small}(:,k)$
      $\Gamma(ind_{big},k) = \Theta(:,ind_{big}) \backslash \dot{\mathbf{X}}(:,k)$
    end for
  end for
Output: sparse matrix Γ

$$\Theta(\mathbf{X}) = \begin{bmatrix} | & | & | & | & | & | & | & \\ 1 & \mathbf{X} & \mathbf{P_2}(\mathbf{X}) & \mathbf{P_3}(\mathbf{X}) & \dots & \sin(\mathbf{X}) & \cos(\mathbf{X}) & \sin(\mathbf{2X}) & \dots \\ | & | & | & | & | & | & | & \end{bmatrix} \tag{12}$$

that the model was not trained for, as it can be observed, the sparse identification results give accurate prediction of system dynamics and inputs for this example.

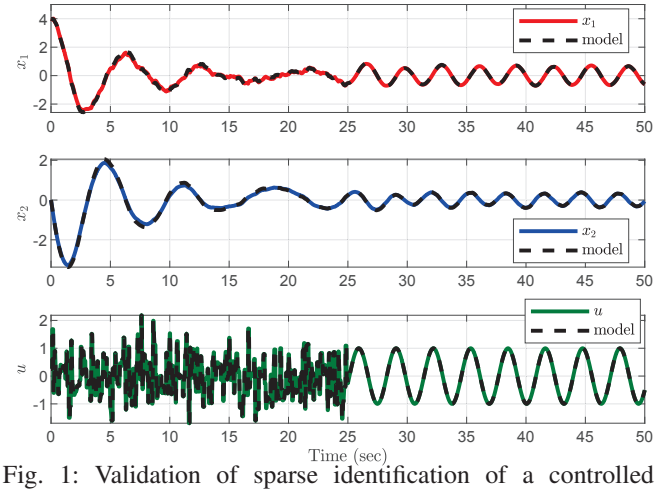

Fig. 1: Validation of sparse identification of a controlled damped oscillator.

III. Distributed Control Design

In this section, the distributed control design for multiple dynamical systems with unknown dynamics is explored. This is a practical problem in real-world applications and often the exact dynamics of the dynamical system of interest are not exactly known. Classical distributed control design requires the detailed dynamics of each distributed unit in order to guarantee the optimality and stability of the design. It is interesting to investigate whether the learned dynamics using sparse identification can directly be used to design distributed controllers with good performance. The predicted dynamics of the controlled undamped oscillator are used to design a distributed controller that can synchronize the response of controllable variables (i.e., x_1 in this example) using a consensus following protocol and track a global reference using a consensus tracking protocol. The structure of the proposed model-free distributed control design is depicted in Fig. 2. Assuming there exits n damped oscillators with different dynamics (heterogeneous), a sparse identification engine can be dedicated to each dynamical system to identify its dynamics using available measurements. Once the dynamics are identified, a control input can be designed for the predicted system using communications between the dynamical systems (information sharing following a communication graph) and the designed input is supplemented to the actual system with unknown dynamics.

A. Graph Theory

To design consensus algorithms for damped oscillators, multi-agent system (MAS) theory is implemented by considering each damped oscillator as an agent. Let us assume an undirected graph $\mathcal{G}$ with its vertex set $\mathcal{V}$ and edge set $\mathcal{E}$, for the communication system between dynamical systems. In this notation, a vertex represents an agent and an edge $(k,j) \in \mathcal{E}$ corresponds to the connection between agents k and j. The neighboring set of agent k is denoted by $\mathcal{N}_k \triangleq \{j \in \mathcal{V} : (k,j) \in \mathcal{E}\}$. Furthermore, let a_{kj} denote the kj^{th} element of the adjacency matrix $\mathcal{A}$ of $\mathcal{G}$, i.e. $a_{kj} = 1$ if $(k,j) \in \mathcal{E}$ and $a_{kj} = 0$ if $(k,j) \notin \mathcal{E}$. Then the degree matrix of $\mathcal{G}$ is denoted by $\mathcal{D} = \text{diag}\{d_k\}_{k=1,\dots,n}$, where $d_k \triangleq \sum_{j\in\mathcal{N}_k} a_{kj}$. Consequently, the Laplacian matrix $\mathcal{L}$ associated to $\mathcal{G}$ is defined by $\mathcal{L} = \mathcal{D} - \mathcal{A}$.

B. Control Design

Using the relative state information $x_i \in \mathbb{R}^n$, the control input $u_i \in \mathbb{R}^k$ for the average consensus protocol is defined as:

$$u_i = K \sum_{j\in\mathcal{N}_i} a_{ij}(x_j - x_i) \tag{14}$$

where $K \in \mathbb{R}^{k\times n}$ is a control gain that can be designed in the sense that all the states in the subsystem converge to the same value asymptotically when:

$$K = B^T P \tag{15}$$

where B is the input matrix and P is a positive definite matrix that satisfies:

$$A^T P + PA - 2\beta PBB^T P + \xi PP + \frac{\eta_0^2}{\xi} I_n < 0 \tag{16}$$

where $\eta = [\eta_1^T, \eta_2^T, \dots, \eta_N^T]$ and $\eta_i = x_i - \sum_{j=1}^{N} r_j x_j$ (r_j is the left eigenvector of graph laplacian matrix) is the state disagreement vector, ξ is any positive real number, and $\beta = \min\{\lambda_1, \dots, \lambda_{n_\lambda}, \alpha_1, \dots, \alpha_{n_\mu}\}$ (λ_i are n_λ real eigenvalues of laplacian matrix, and $\alpha_i \pm \beta_i$ are n_μ complex eigenvalues of laplacian matrix. In the above equation, η_0 is defined as:

$$\eta_0 = 2N\text{sing}(T)\text{sing}(T^{-1}) \left\|r\right\|_2 \tag{17}$$

where $N = 1 + n_\lambda + 2n_\mu$ and $\text{sing}(T)$ is the largest singular value of a nonsingular matrix T satisfying $T^{-1}LT = J$, where J includes a diagonal matrix with 0 as its first element and other diagonal terms include the eigenvalues of laplacian matrix as in (18):

$$J = \begin{bmatrix} 0 & \dots & \dots & \dots & \dots & \dots & 0 \\ 0 & \lambda_1 & \dots & \dots & \dots & \dots & 0 \\ 0 & \dots & \ddots & \dots & \dots & \dots & 0 \\ 0 & \dots & \dots & \lambda_{n_\lambda} & \dots & \dots & 0 \\ 0 & \dots & \dots & \dots & \lambda_1 & \dots & 0 \\ \vdots & \vdots & \vdots & \vdots & \vdots & \ddots & \vdots \\ 0 & \dots & \dots & \dots & \dots & \dots & \lambda_{n_\mu} \end{bmatrix} \tag{18}$$

The proof for the above conditions can be found in [14]. If the objective is to design a consensus tracking problem so that state x_i of the dynamical system tracks a reference x_0, the input can be designed as:

$$u_i = K \sum_{j\in\mathcal{N}_i} a_{aj}(x_j - x_i) - K_0 a_{0i}(x_0 - x_i) \tag{19}$$

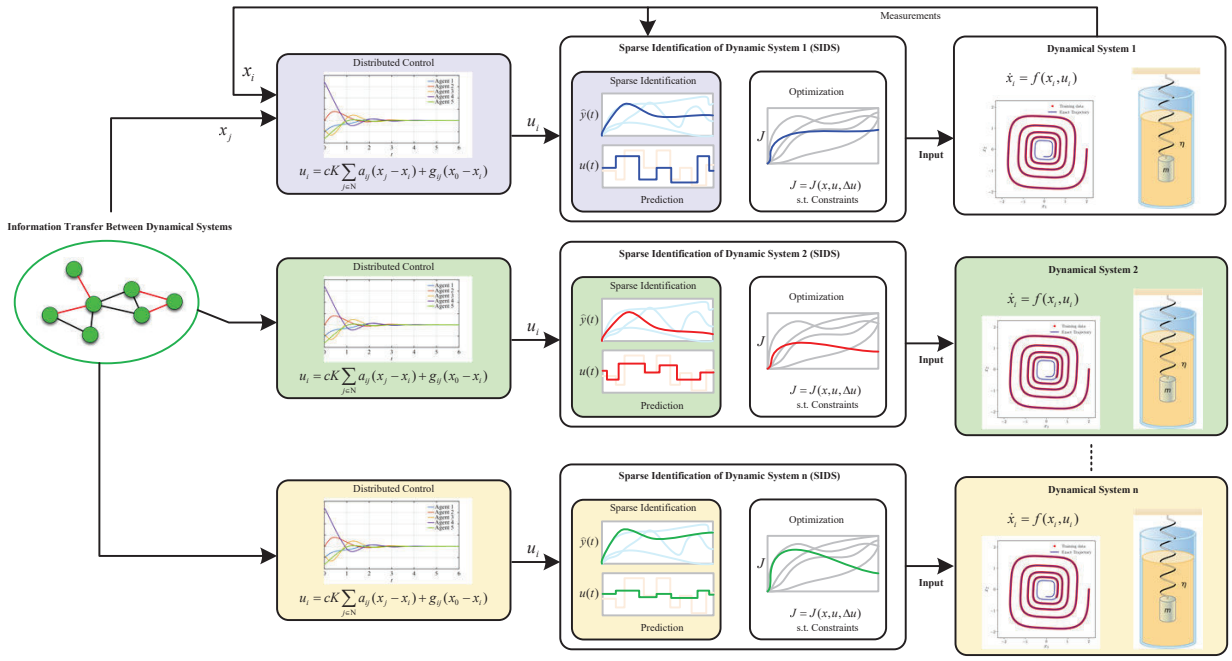

Fig. 2: Structure of the proposed model-free distributed control.

where a_{0i} denotes the adjacency element between the leader (one of the agents that receive reference information and shares with its neighbors) and other agents (followers), which is 1 if there is a connection between agent i and the leader (agent 0), and is 0 otherwise. The gain K_0 can be designed similar to gain K. The above input supplemented to the dynamical system guarantees the error between state x_i and reference x_0 will approach zero, i.e., $x_i \longrightarrow x_0$.

IV. Case Studies

To validate the effectiveness of the proposed model-free distributed control, three controlled damped oscillators have been considered. The actual but assumed unknown dynamics of the heterogeneous oscillators are governed by their state matrices in the following:

$$A_1 = \begin{bmatrix} -0.1 & 2 \\ -2 & -0.1 \end{bmatrix}, \; B_1 = \begin{bmatrix} 1 \\ 0 \end{bmatrix} \tag{20}$$

$$A_2 = \begin{bmatrix} -0.2 & 3 \\ -2 & -0.41 \end{bmatrix}, \; B_2 = \begin{bmatrix} 1 \\ 0 \end{bmatrix} \tag{21}$$

$$A_3 = \begin{bmatrix} -0.15 & 1 \\ -1 & -0.21 \end{bmatrix}, \; B_3 = \begin{bmatrix} 1 \\ 0 \end{bmatrix} \tag{22}$$

First, each heterogeneous oscillator is supplemented with a sparse identification model that received its measurements and identifies the governing dynamics. For $\Theta(\mathbf{X},\mathbf{U})$, polynomials up to degree 3 are considered as in (23). The resulting $\mathbf{\Gamma_i}$ matrices for these heterogeneous oscillators are listed in Table I. Once the dynamics of the oscillators are identified, the distributed controllers are designed in two case studies using the ideas in Section II.

TABLE I: Performance measures of the proposed optimization model.

Row	Γ_1	$\mathbf{\Gamma_2}$	$\mathbf{\Gamma_3}$
Row 1	[0 0]	[0 0]	[0 0]
Row 2	[-0.149 1.997]	[-0.32 2.99]	[-0.147 0.997]
Row 3	[-1.939 -0.11]	[-1.88 -0.412]	[-1.012 -0.176]
Row 4	[1.043 0]	[1.029 0]	[0.995 0]
Rows 5-13	[0 0]	[0 0]	[0 0]

Fig. 3 depicts the simulation results for distributed control of heterogeneous damped oscillators, where the left subplots depict the control design performance (convergence to desired values) on the actual systems (physical models) and the subplots on the right illustrate the control design on the predicted sparse identification dynamics. The first subplots on the top depict the dynamics of state 1 (x_1) for these three oscillators when no controller is supplemented to the system. Due to the heterogeneity of the dynamical systems, the responses of these systems show different settling time and overshoots (due to various initial conditions), but they all stabilize at their equilibrium point (0) eventually. It can also be confirmed

$$\Theta(\mathbf{X},\mathbf{U}) = \begin{bmatrix} 1 & \mathbf{x_1} & \mathbf{x_2} & \mathbf{u} & \mathbf{x_1}^2 & \mathbf{x_1x_2} & \mathbf{x_2}^2 & \mathbf{x_1}^3 & \mathbf{x_1}^2\mathbf{x_2} & \mathbf{x_1x_2}^2 & \mathbf{x_2}^3 & \mathbf{x_1u} & \mathbf{x_2u} \end{bmatrix} \tag{23}$$

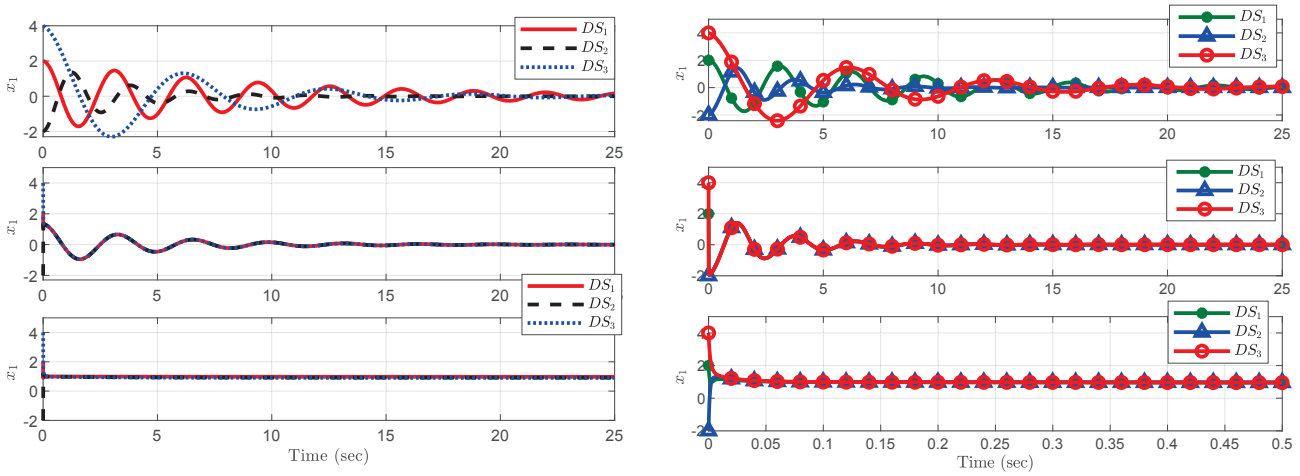

Fig. 3: Comparison between the distributed control design on the actual dynamics of damped oscillators (left) and predicted dynamics using sparse identification (right).

that the learned dynamics exactly match with the physical dynamics of the systems, denoting a successful identification of system dynamics. Subplots in the middle demonstrate the effectiveness of consensus following protocol in synchronizing these damped oscillators. Due to the implementation of the consensus protocol in (14), all damped oscillators reach to their equilibrium at the same settling time and frequencies. It can also be confirmed that the learned dynamics (left subplot) exactly matches the distributed control design on the physical dynamics. Finally, the consensus tracking protocol was supplemented to the system by enabling oscillator 1 to be leader with a setpoint of $x_0 = 1$. As a result of the consensus tracking protocol in (19), all the units will track the same reference and the equilibrium point of all damped oscillators changes to 1 (reference) confirming a successful tracking control design. It is noted that the consensus design on learned dynamics (right subplots) perfectly matches with the design on the physical system without knowing the dynamics of the physical system. The results suggest a potential for implementation of distributed controllers for more complex cyber-physical systems, i.e. robots, air crafts, and buildings, without complex modeling procedures.

V. Conclusion

In this paper, a model-free distributed control design of dynamical systems was studied. Using sparse identification of system dynamics with control along with available measurements, dynamics of the system were predicted with candidate polynomial functions. The learned dynamics were then used to design a distributed controller for consensus tracking and following problems. The proposed research demonstrates the effectiveness of the sparse identification technique for distributed control design of linear and nonlinear systems. Such formulation can significantly enhance the control design issue of complex dynamical systems. Future research will focus on the application of distributed consensus design using sparse identification technique in smart grid applications.

References

[1] M. Liu, L. Tan, and S. Cao, "Method of dynamic mode decomposition and reconstruction with application to a three-stage multiphase pump," *Energy*, vol. 208, p. 118343, 2020.

[2] H. Lu and D. M. Tartakovsky, "Prediction accuracy of dynamic mode decomposition," *SIAM Journal on Scientific Computing*, vol. 42, no. 3, pp. A1639–A1662, 2020.

[3] C. Folkestad, D. Pastor, I. Mezic, R. Mohr, M. Fonoberova, and J. Burdick, "Extended dynamic mode decomposition with learned koopman eigenfunctions for prediction and control," in *2020 american control conference (acc)*. IEEE, 2020, pp. 3906–3913.

[4] M. Al-Gabalawy, "Deep learning for koopman operator optimal control," *ISA transactions*, 2021.

[5] A. Mauroy, I. Mezić, and Y. Susuki, *The Koopman Operator in Systems and Control: Concepts, Methodologies, and Applications*. Springer Nature, 2020, vol. 484.

[6] M. Schmidt and H. Lipson, "Distilling free-form natural laws from experimental data," *science*, vol. 324, no. 5923, pp. 81–85, 2009.

[7] S. L. Brunton, J. L. Proctor, and J. N. Kutz, "Discovering governing equations from data by sparse identification of nonlinear dynamical systems," *Proceedings of the national academy of sciences*, vol. 113, no. 15, pp. 3932–3937, 2016.

[8] ——, "Sparse identification of nonlinear dynamics with control (sindyc)," *IFAC-PapersOnLine*, vol. 49, no. 18, pp. 710–715, 2016.

[9] E. Kaiser, J. N. Kutz, and S. L. Brunton, "Sparse identification of nonlinear dynamics for model predictive control in the low-data limit," *Proceedings of the Royal Society A*, vol. 474, no. 2219, p. 20180335, 2018.

[10] D. Ding, Q.-L. Han, Z. Wang, and X. Ge, "A survey on model-based distributed control and filtering for industrial cyber-physical systems," *IEEE Transactions on Industrial Informatics*, vol. 15, no. 5, pp. 2483–2499, 2019.

[11] A. Savitzky and M. J. Golay, "Smoothing and differentiation of data by simplified least squares procedures." *Analytical chemistry*, vol. 36, no. 8, pp. 1627–1639, 1964.

[12] R. W. Schafer, "What is a savitzky-golay filter? [lecture notes]," *IEEE Signal Processing Magazine*, vol. 28, no. 4, pp. 111–117, 2011.

[13] S. Larsson and V. Thomée, *Partial differential equations with numerical methods*. Springer, 2003, vol. 45.

[14] Z. Ding, "Consensus control of a class of nonlinear systems," in *2013 9th Asian Control Conference (ASCC)*. IEEE, 2013, pp. 1–6.

CSPG4 Molecular Target in Canine Melanoma, Osteosarcoma and Mammary Tumors for Novel Therapeutic Strategies

Paola Modesto, Floriana Fruscione, Isabella Martini, Simona Perga, Federica Riccardo, Mariateresa Camerino, Davide Giacobino, Cecilia Gola, Luca Licenziato, Elisabetta Razzuoli, Katia Varello, Lorella Maniscalco, Elena Bozzetta, Angelo Ferrari

***Abstract*—** Canine and human melanoma, osteosarcoma (OSA), and mammary carcinomas are aggressive tumors with common characteristics making dogs a good model for comparative oncology. Novel therapeutic strategies against these tumors could be useful to both species. In humans, chondroitin sulphate proteoglycan 4 (CSPG4) is a marker involved in tumor progression and could be a candidate target for immunotherapy. The anti-CSPG4 DNA electrovaccination has shown to be an effective approach for canine malignant melanoma (CMM) [1]. An immunohistochemistry evaluation of CSPG4 expression in tumour tissue is generally performed prior to electrovaccination. To assess the possibility to perform a rapid molecular evaluation and in order to validate these spontaneous canine tumors as the model for human studies, we investigate the CSPG4 gene expression by RT qPCR in CMM, OSA, and canine mammary tumors (CMT). The total RNA was extracted from RNAlater stored tissue samples (CMM n=16; OSA n=13; CMT n=6; five paired normal tissues for CMM, five paired normal tissues for OSA and one paired normal tissue for CMT), retro-transcribed and then analyzed by duplex RT-qPCR using two different TaqMan assays for the target gene CSPG4 and the internal reference gene (RG) Ribosomal Protein S19 (RPS19). RPS19 was selected from a panel of 9 candidate RGs, according to NormFinder analysis following the protocol already described [2]. Relative expression was analyzed by CFX Maestro™ Software. Student t-test and ANOVA were performed (significance set at $P<0.05$). Results showed that gene expression of CSPG4 in OSA tissues is significantly increased by 3-4 folds when compared to controls. In CMT, gene expression of the target was increased from 1.5 to 19.9 folds. In melanoma, although an increasing trend was observed, no significant differences between the two groups were highlighted. Immunohistochemistry analysis of the two cancer types showed that the expression of CSPG4 within CMM is concentrated in isles of cells compared to OSA, where the distribution of positive cells is homogeneous. This evidence could explain the differences in gene expression results.CSPG4 immunohistochemistry evaluation in mammary carcinoma is in progress. The evidence of CSPG4 expression in a different type of canine tumors opens the way to the possibility of extending the CSPG4 immunotherapy marker in CMM, OSA, and CMT and may have an impact to translate this strategy modality to human oncology.

***Keywords*—** canine melanoma, canine mammary carcinomas, canine osteosarcoma, CSPG4, gene expression, immunotherapy.

Paola Modesto is with the Veterinary Medical Research Institute for Piemonte, Liguria and the Valle D'Aosta, Italy (e-mail: paola.modesto@izsto.it).

Fucoidan: A Potent Seaweed-Derived Polysaccharide with Immunomodulatory and Anti-Inflammatory Properties

Tauseef Ahmad[1], Muhammad Ishaq[2], Mathew Eapen[1], Ahyoung Park[3], Sam Karpiniec[3], Vanni Caruso[2], Rajaraman Eri[1]

[1]School of Health Sciences, University of Tasmania, 7248 Launceston, Australia
[2]School of Pharmacy and Pharmacology, University of Tasmania, 7005 Hobart, Australia
[3]Marinova Pty Ltd, Cambridge, 7170 Hobart TAS, Australia

***Abstract*—** Fucoidans are complex, fucose-rich sulfated polymers discovered in brown seaweeds. Fucoidans are popular around the world, particularly in the nutraceutical and pharmaceutical industries, due to their promising medicinal properties. Fucoidans have been shown to have a variety of biological activities, including anti-inflammatory effects. They are known to inhibit inflammatory processes through a variety of mechanisms, including enzyme inhibition and selectin blockade. Inflammation is a part of the complicated biological response of living systems to damaging stimuli, and it plays a role in the pathogenesis of a variety of disorders, including arthritis, inflammatory bowel disease, cancer, and allergies.

In the current investigation, various fucoidan extracts from *Undaria pinnatifida, Fucus vesiculosus, Macrocystis pyrifera, Ascophyllum nodosum,* and *Laminaria japonica* were assessed for inhibition of pro-inflammatory cytokine production (TNF-α, IL-1β, and IL-6) in LPS induced human macrophage cell line (THP-1) and human peripheral blood mononuclear cells (PBMCs). Furthermore, we also sought to catalogue these extracts based on their anti-inflammatory effects in the current *in-vitro* cell model.

Materials and methods

To assess the cytotoxicity of fucoidan extracts, MTT (3-[4,5-dimethylthiazol-2-yl]-2,5, -diphenyltetrazolium bromide) cell viability assay was performed. Furthermore, a dose-response for fucoidan extracts was performed in LPS induced THP-1 cells and PBMCs after pre-treatment for 24 hours and levels of TNF-α, IL-1β, and IL-6 cytokines were measured using Enzyme-Linked Immunosorbent Assay (ELISA).

Results

The MTT cell viability assay demonstrated that fucoidan extracts exhibited no evidence of cytotoxicity in THP-1 cells or PBMCs after 48 hours of incubation. The results of the sandwich ELISA revealed that all fucoidan extracts suppressed cytokine production in LPS-stimulated PBMCs and human THP-1 cells in a dose-dependent manner. Notably, at lower concentrations, the lower molecular fucoidan (5-30 kDa) extract from *Macrocystis pyrifera* was a highly efficient inhibitor of pro-inflammatory cytokines. Fucoidan extracts from all species including *Undaria pinnatifida, Fucus vesiculosus, Macrocystis pyrifera, Ascophyllum nodosum*, and *Laminaria japonica* exhibited significant anti-inflammatory effects. These findings on several fucoidan extracts provide insight into strategies for improving their efficacy against inflammation-related diseases.

Conclusion

In the current research, we have successfully catalogued several fucoidan extracts based on their efficiency in LPS-induced macrophages and PBMCs in downregulating the key pro-inflammatory cytokines (TNF-, IL-1, and IL-6), which are prospective targets in human inflammatory illnesses. Further research would provide more information on the mechanism of action, allowing it to be tested for therapeutic purposes as an anti-inflammatory medication.

***Keywords*:** Fucoidan; PBMCs; THP-1; TNF-α, IL-1β, and IL-6; Inflammation

Selective Immobilization of Fructosyltransferase onto Glutaraldehyde Modified Support and Its Application in the Production of Fructo-oligosaccharides

Milica B. Veljković, Milica B. Simović, Marija M. Ćorović, Ana D. Milivojević, Anja I. Petrov, Katarina M. Banjanac, Dejan I. Bezbradica

Abstract**—**In recent decades, the scientific community has recognized the growing importance of prebiotics, and therefore, numerous studies are focused on their economical production due to their low presence in natural resources. It has been confirmed that prebiotics are a source of energy for probiotics in the gastrointestinal tract (GIT) and enable their proliferation, consequently leading to the normal functioning of the intestinal microbiota. Also, products of their fermentation are short-chain fatty acids (SCFA), which play a key role in maintaining and improving the health not only of the GIT but also of the whole organism. Among several confirmed prebiotics, fructo-oligosaccharides (FOS) are considered interesting candidates for use in a wide range of products in the food industry. They are characterized as low-calorie and non-cariogenic substances that represent an adequate sugar substitute and can be considered suitable for use in products intended for diabetics. The subject of this research will be the production of FOS by transforming sucrose using a fructosyltransferase (FTase) present in commercial preparation Pectinex® Ultra SP-L, with special emphasis on the development of adequate FTase immobilization method that would enable selective isolation of the enzyme responsible for the synthesis of FOS from the complex enzymatic mixture. This would lead to considerable enzyme purification and allow its direct incorporation into different sucrose-based products, without the fear that action of the other hydrolytic enzymes may adversely affect the products functional characteristics. Accordingly, the possibility of selective immobilization of the enzyme using support with primary amino groups, Purolite® A109, which was previously activated and modified using glutaraldehyde (GA), was investigated. In the initial phase of the research, the effects of individual immobilization parameters such as pH, enzyme concentration and immobilization time were investigated to optimize the process using support chemically activated with 15% and 0.5% GA to form dimers and monomers, respectively. It was determined that highly active immobilized preparations (371.8 IU/g of support - dimer and 213.8 IU/g of support – monomer) were achieved under acidic conditions (pH 4) provided that an enzyme concentration was 50 mg/g of support after 7 h and 3 h, respectively. Bearing in mind the obtained results of the expressed activity, it is noticeable that the formation of dimers showed higher reactivity compared to the form of monomers. Also, in the case of support modification using 15% GA, the value of the ratio of FTase and pectinase (as dominant enzyme mixture component) activity immobilization yields was 16.45, indicating the high feasibility of selective immobilization of FTase on modified polystyrene resin. After obtaining immobilized preparations of satisfactory features, they were tested in a reaction of FOS synthesis under determined optimal conditions. The maximum FOS yields of approximately 50% of total carbohydrates in the reaction mixture were recorded after 21 h. Finally, it can be concluded that the examined immobilization method yielded highly active, stable and more importantly refined enzyme preparation that can be further utilized on a larger scale for development of continual processes for FOS synthesis, as well as for modification of different sucrose-based mediums.

Keywords**—**Chemical modification, fructo-oligosaccharides, glutaraldehyde, immobilization of fructosyltransferase.

M. B. Veljković is with Innovation Center of Faculty of Technology and Metallurgy, University of Belgrade, Belgrade, Serbia (e-mail: mveljkovic@tmf.bg.ac.rs).

M. B. Simović is with Department of Biochemical Engineering and Biotechnology, Faculty of Technology and Metallurgy, University of Belgrade, Belgrade, Serbia.

M. M. Ćorović is with Department of Biochemical Engineering and Biotechnology, Faculty of Technology and Metallurgy, University of Belgrade, Belgrade, Serbia.

A. D. Milivojević is with Innovation Center of Faculty of Technology and Metallurgy, University of Belgrade, Belgrade, Serbia.

A. I. Petrov is with Innovation Center of Faculty of Technology and Metallurgy, University of Belgrade, Belgrade, Serbia.

K. M. Banjanac is with Innovation Center of Faculty of Technology and Metallurgy, University of Belgrade, Belgrade, Serbia.

D. I. Bezbradica is with Department of Biochemical Engineering and Biotechnology, Faculty of Technology and Metallurgy, University of Belgrade, Belgrade, Serbia.

Evaluation of Herbal Extracts for Their Potential Application as Skin Prebiotics

Anja I. Petrov, Milica B. Veljković, Marija M. Ćorović, Ana D. Milivojević, Milica B. Simović, Katarina M. Banjanac, Dejan I. Bezbradica

Abstract**—**One of the fundamental requirements for overall human well-being is a stable and balanced microbiome. Aside from the microorganisms that reside within the body, a large number of microorganisms, especially bacteria, swarming the human skin are in homeostasis with the host and represent a skin microbiota. Even though the immune system of the skin is capable of distinguishing between commensal and potentially harmful transient bacteria, the cutaneous microbial balance can be disrupted under certain circumstances. In that case, reduction in the skin microbiota diversity, as well as changes in metabolic activity, result in dermal infections and inflammation. Probiotics and prebiotics have the potential to play a significant role in the treatment of these skin disorders. The most common resident bacteria found on the skin, *Staphylococcus epidermidis*, can act as a potential skin probiotic, contributing to the protection of healthy skin from pathogen colonization, such as *Staphylococcus aureus*, which is related to atopic dermatitis exacerbation. However, as it is difficult to meet regulations in cosmetic products, another therapy approach could be topical prebiotic supplementation of the skin microbiota. In recent research, polyphenols are attracting scientists' interest as biomolecules with possible prebiotic effects on the skin microbiota. This research aimed to determine how herbal extracts rich in different polyphenolic compounds (lemon balm, St. John's wort, coltsfoot, pine needle and yarrow) affected the growth of *S. epidermidis* and *S. aureus*. The first part of the study involved screening of plants to determine if they could be regarded as probable candidates to be skin prebiotics. The effect of each plant on bacterial growth was examined by supplementing the nutrient medium with their extracts and comparing it with control samples (without extract). The results obtained after 24 h of incubation showed that all tested extracts influenced the growth of the examined bacteria to some extent. Since lemon balm and St. John's wort extracts displayed bactericidal activity against *S. epidermidis*, whereas coltsfoot inhibited both bacteria equally, they were not explored further. On the other hand, pine needle and yarrow extract led to an increase in *S. epidermidis*/*S. aureus* ratio, making them prospective candidates to be used as skin prebiotics. By examining the prebiotic effect of two extracts at different concentrations, it was revealed that, in the case of yarrow, 0.1% of extract dry matter in the fermentation medium was optimal, while for the pine needle extract, a concentration of 0.05% was preferred, since it selectively stimulated *S. epidermidis* growth and inhibited *S. aureus* proliferation. Additionally, total polyphenols and flavonoids content of two extracts were determined, revealing different concentrations and polyphenol profiles. Since yarrow and pine extracts affected the growth of skin bacteria in a dose-dependent manner, by carefully selecting the quantities of these extracts, and thus polyphenols content, it is possible to achieve desirable alterations of skin microbiota composition, which may be suitable for the treatment of atopic dermatitis.

Keywords**—**Herbal extracts, polyphenols, skin microbiota, skin prebiotics.

A. I. Petrov is with Innovation Center of Faculty of Technology and Metallurgy, University of Belgrade, Belgrade, Serbia.

M. B. Veljković is with Innovation Center of Faculty of Technology and Metallurgy, University of Belgrade, Belgrade, Serbia (e-mail: mveljkovic@tmf.bg.ac.rs).

A. D. Milivojević is with Innovation Center of Faculty of Technology and Metallurgy, University of Belgrade, Belgrade, Serbia.

K. M. Banjanac is with Innovation Center of Faculty of Technology and Metallurgy, University of Belgrade, Belgrade, Serbia.

M. M. Ćorović is with Department of Biochemical Engineering and Biotechnology, Faculty of Technology and Metallurgy, University of Belgrade, Belgrade, Serbia.

M. B. Simović is with Department of Biochemical Engineering and Biotechnology, Faculty of Technology and Metallurgy, University of Belgrade, Belgrade, Serbia.

D. I. Bezbradica is with Department of Biochemical Engineering and Biotechnology, Faculty of Technology and Metallurgy, University of Belgrade, Belgrade, Serbia.

Gender, Trauma, and Memory in Post-9/11 Literature: Cormac Mccarthy's the Road, Jonathan Safran Foer's Extremely Loud and Incredibly Close, and Khaled Hosseini's the Kite Runner

Margrét Ann Thors

***Abstract*—** On September 11, 2001, two hijacked planes crashed into the World Trade Center, tumbling the Twin Towers and shocking the world to a halt. Nearly two decades have passed since the attacks, yet the consequences of this acute trauma are chronic and extend well beyond Ground Zero. The surge in anti-Muslim sentiment, the subsequent terror attacks in several major European cities, the European migrant crisis of the mid-2010s, the current rise of nationalist, populist movements around the world, and even the opioid crisis and air of fear, anxiety, and xenophobia that pervades much of contemporary western society can be credibly linked to the events of 9/11.

The very nature of trauma is to shatter the existing order—and indeed, 9/11 was an order-shattering event for much of the world. It therefore stands to reason that literature, which captures in language and character truths about what it means to be human, must reckon with this trauma.

This paper investigates portrayals of gender, representations of trauma, and invocations of cultural memory in the post-9/11 works The Road by Cormac McCarthy, Extremely Loud and Incredibly Close by Jonathan Safran Foer, and The Kite Runner by Khaled Hosseini. Taking these novels as a case study, this paper asks: What senses has post-9/11 literature made of the attacks and their aftermath? More specifically, what is the relationship between shared trauma, gender, and cultural memory in literature after this event—particularly in books like these, which are not about the attacks, per se, but which nonetheless conjure their aftermath? Drawing on discourse analysis and pluralistic theories of trauma, I critically interrogate the rhetorical tools and techniques McCarthy, Foer, and Hosseini use to narrate trauma and its aftereffects. In so doing, I contribute to the vital conversation of what it means to read, write, and live in a post-9/11 world.

***Keywords*—** trauma, literature, gender, memory, McCarthy, foer, Hosseini, 9/11, September 11.

Margrét Ann Thors is with the University of Iceland, Iceland (e-mail: mat34@hi.is).

Assessment of Artists' Socioeconomic and Working Conditions: The Empirical Case of Lithuania

R. Kregzdaite, E.Godlevska, M. Vidunaite

***Abstract*—** The main aim of this research is to explore existing methodologies for artists' labour force and create artists' socio-economic and creative conditions an assessment model. Artists have a dual aims in their creative working process: 1) income, and 2) artistic self-expression. The valuation of their conditions takes into consideration both sides: the factors related to income and the satisfaction for creative process and its result. The problem addressed in the study: tangible and intangible artists' criteria used for assessments creativity conditions.

The proposed model includes objective factors (working time, income, etc.) and subjective factors (salary covering essential needs, self-satisfaction). Other intangible indicators taken into account : the impact on the common culture, social values, and the possibility to receive awards, to represent the country in the international market. The empirical model consists of 59 separate indicators, grouped into eight categories. The deviation of each indicator from the general evaluation allows identifying the strongest and the weakest components of artists' conditions.

***Keywords*—**artists condition, artistic labor force, cultural economy, cultural policy

R.Kregzdaite, PhD, is researcher at Vytautas Magnus University, Kaunas, Lithuania. (email: rusne.kregzdaite@gmail.com).

E.Godlevska , PhD, is founder and researcher at Future Society institute, Vilnius, Lithuania (email: erika@futuresoc.com)

M.Vidunaite is PhD student at Vytautas Magnus University, Kaunas, Lithuania (email: vidunaite@gmail.com)

Namibian Inhabitants' Appeals for Recognition at the United Nations, 1947-1962

Seane Mabitsela

Abstract**—**The Territory of Namibia was entrusted to South Africa as a Mandate under the League of Nations Covenant. After the dissolution of the League of Nations and the commencement of United Nations operations, South Africa's conception of its legal obligations under the mandate varied from those of other members of the United Nations. Because of that, the General Assembly requested the International Court of Justice for an Advisory Opinion on the international obligations of South Africa arising therefrom. The International Court of Justice declared that South West Africa was still a mandatory territory under the Covenant of the League of Nations. It also held that South Africa continued to transmit petitions from inhabitants of the territory, the supervisory functions to be exercised by the United Nations, to which the annual reports and the petitions were to be submitted. Subject to this judgement, the question of South West Africa remained a dispute relating to the mandate brought before the International Court of Justice against South Africa. The International Court of Justice and South Africa dispute reflected the nature of the Namibian inhabitants' appeal for recognition at the United Nations. This paper explores the Namibian inhabitants' appeals for recognition at the United Nations. It adopts qualitative research design and utilises secondary and primary data, to describe the nature of those appeals. The paper will shed light on the patterns followed by Namibians in their attempts to end South Africa's administration of the Territory.

Keywords**—**International Court of Justice, Namibia, Petitions, United Nations.

I. Introduction

INHABITANTS of Namibia (formerly South West Africa) decided upon the establishment of the United Nations (UN) to craft a solution to end South Africa's administration of the territory, especially the apartheid policies. One workable solution to end South Africa's ruling was to petition the UN. This paper explores the nature of Namibian inhabitants' appeals for recognition at the UN from 1947-1962. It adopts qualitative research design and utilises secondary and primary data to describe the nature of those appeals. Divided into five parts, the first section introduces the subject. The second section concerns petition by Reverend Michael Scott on behalf of the Namibians at the UN. The third concerns petitions by indigenous Namibians at the UN. The fourth section relates to the petitions by Namibian national liberation movements at the UN— South West Africa National Union (SWANU); South West Africa People's Organisation (SWAPO); and South West African United National Independence Organisation (SWAUNIO). The last and the final section concludes the paper.

Seane Mabitsela is with University of Venda, South Africa (e-mail: seanemabitsela@yahoo.com).

II. Reverend Michael Scott's Petition

The British Anglican missionary, Reverend Michael Scott presented the first petition to the UN on behalf of inhabitants of South West Africa in 1947. Scott was deputized by the Herero and Nama tribes to address the General Assembly on their behalf [1]. He requested to be heard by the Fourth Committee of the General Assembly in New York on 4 October 1949. Scott submitted a series of communications, statements and a petition from representatives of various tribes in South West Africa, to the UN Secretary-General, Trygve Halvdan Lie [2].

During the Committee discussion concerning Scott's request, an issue arose as to whether native inhabitants from Namibia should be provided the privilege of presenting their grievances before the Fourth Committee. The Committee's response was affirmative, despite South African opposition [3].

Scott's request was supported by the UN Association of the United Kingdom, the World Federation of the UN Associations, the Anti-Slavery Society of England and the International League for the Rights of Man [4]. The General Assembly appointed a sub-committee comprised delegates from Colombia, the Dominican Republic, Egypt, India, Poland and the United States of America, appointed to verify his credentials. The delegates met on 25 November 1949 and agreed unanimously that Scott's credentials were in order and that he should be provided full faith and credit [5].

Scott took his place at the Fourth Committee on 26 November 1949. He appealed to the Committee to consider the following proposals from the Herero and *Berg* (mountain) Damara that: (a) an opportunity should be provided to these African people to state their case directly to the UN (or before a Commission appointed specially for that purpose); (b) no final decision regarding Namibians should be reached until the petitioners were provided an opportunity to express their views through nominated spokespersons; (c) their territories should be returned to them; and (d) their territory must be brought under the UN Trusteeship System [6].

Based on Scott's statement, the Committee adopted a resolution at its 140th meeting on 6 December 1949, proclaiming the desirability of obtaining an advisory opinion from the International Court of Justice (ICJ) on the international status of Namibia. The ICJ provided its advisory opinion on 11 July 1950, judging that whilst South Africa was not obliged to govern Namibia as a trust territory, it was legally required to submit annual reports and transmit petitions to the UN, observing the terms of the mandate. This resulted in the Fourth

Committee requesting more submissions from Scott [7].

In the closing months of 1950, the Fourth Committee received, through the Secretary-General, correspondences from Reverend Scott, Hosea Kutako and David Witbooi, the Unitarian Fellowship for Social Justice in Los Angeles, and from the African National Congress (ANC) of South Africa [8].

The circulation of those documents resulted in an extended debate within the Fourth Committee. For example, South Africa expressed its strong objections to their circulation, arguing that the documents originated from private individuals; and that the Committee presented the ICJ's opinion. Accordingly, it was difficult to see how Michael Scott, or any other private individual could assist the Committee in considering their opinion [9].

On 13 December 1950, the General Assembly adopted a resolution based on the requests contained in Scott's correspondence. It appointed an Ad Hoc Committee of Five UN member states to contemplate petitions concerning matters pertaining Namibia. The report of the Ad hoc Committee was considered by the Fourth Committee during December 1951 to January 1952. Subsequently, the Fourth Committee invited Scott to represent Hosea Kutako, Nikanor Hoveka, Theophilus Katjiuongua and David Witbooi (representing the Herero, Nama and *Berg* and Damara tribe respectively) in the Committee, again on 8 December 1951. His address concerned issues such as racism, governance and administration in Namibia; trusteeship and international accountability; the possibility of a visit by the UN Commission to Namibia; and the international status of the territory [10].

Scott, further, resumed his address to the Fourth Committee on 12 January 1952. He affirmed that the UN was uninformed regarding Namibia's concerns; and reiterated his request, that the Ad Hoc Committee on the territory be referred to re-examine the situation concerning the region. Based on his statements, the Fourth Committee adopted a resolution concerning Namibia, on 17 January 1952. This adoption resulted in a further convening for submissions of Scott's verbal requests for hearings [11].

On 16 December 1952, the Fourth Committee received three letters from Scott justifying his interest on the Namibian issue. He offered a verbal submission in his communications, after which, the Committee approved the request for discussing the item. The discussion was, however, postponed after a decision within the Committee which agreed to constitute an Ad Hoc Committee concerning Namibia whose purpose was to examine petitions in accordance with the League of Nations mandates' procedure [12].

The discussion on submission of verbal hearings was reopened in the Fourth Committee in November 1955. Scott appeared with a statement prior to the Committee meetings expressing concerns regarding the hopes amongst the Herero inhabitants. He indicated that the UN would rescue them from their vile living conditions; and requested that responses be directed to him by committee members at its meeting on 11 November 1955 [13]. The Fourth Committee, thereafter, transferred Scott's statement for investigation to the Committee concerning South West Africa. This would include providing appropriate attention to Scott's recommendation and matters raised regarding the situation in South West Africa [14].

III. Petitions by Indigenous South West African Inhabitants to the UN

Mburumba Kerina

During 1955, Mburumba Kerina, a South West African citizen studying at the Lincoln University in the United States of America, joined Michael Scott in petitioning the UN. Kerina was requested by Chief Hosea Kutako to act on behalf of Namibia at the General Assembly [15]. Kerina corresponded with the Chairperson of the Fourth Committee, Luciano Joublang-Rivas (of Mexico) twice in September 1955, requesting an opportunity for granting a verbal statement at the UN's meeting [16]. His request was supported by Jariretundu Kozonguizi, chairperson of Organising Committee of the Student Body of Namibian Cape Town [17].

On 3 December 1955, following Kerina's request for a verbal hearing, the General Assembly, acting on recommendation of the Fourth Committee, adopted Resolution 942 (X), requesting an opinion from the ICJ concerning whether a South West African native could petition the UN directly. The Court delivered a ruling on the matter on 1 June 1956, stating that granting of a verbal hearing would be legally permissible [18]. Consequently, Kerina appeared before the Fourth Committee on 7 December 1956. He communicated the circumstances of his departure from South West Africa; how he was compelled to falsely declare himself a 'Cape Mulatto' to obtain a passport; how he was warned that the US was a communist country (because it expounded the principle of racial equality); and that if he would preach any such doctrine upon his return (or talk about the mistreatment of Africans, whilst abroad), he would be shot [19].

Kerina appeared again before the Fourth Committee at its meeting on 26 September 1957, on behalf of Andimba Toivo Ja Toivo of the Ovamboland People's Congress (OPO), Selma Shoombe, and other Ovambos [20]. Acting based on Kerina's latest statement, the Committee adopted a resolution establishing a committee (Good Offices Committee) on 25 October 1957. Comprising United States of America, the United Kingdom and Ethiopia, the Committee was mandated to negotiate with the Union Government regarding acceptable ways of resolving South West African impasse [21].

Together with the Committee concerning South West Africa, the Good Offices Committee granted Kerina a hearing on 6 October 1958. Kerina stated before the two Committees that the Namibians had for the last seven years, earnestly hoped in vain that South Africa as a member of the UN would be persuaded to place their country under the UN Trusteeship System as required by the Charter [22]. Immediately, his mission garnered attention of world bodies for the OPO, upon which its leader, Andimba Toivo Ja Toivo was returned from Cape Town to Namibia [23].

Fanuel Jariretundu Kozonguizi

In 1959, Jariretundu Kozonguizi joined Kerina and Scott in

petitioning the UN. Kozonguizi was a member of the Herero Chiefs' Council. He was delegated by Chief Kutako to serve as a permanent petitioner at the UN. In 1957, Kozonguizi was denied a passport while he was a student at the Union of South Africa, for no reason. The refusal to grant him a passport had occurred after the Fourth Committee announced its twelfth session that it was willing to grant him a hearing [24].

On 10 December 1957, the Fourth Committee referred Konzonguizi's failed passport application to the Committee concerning South West Africa for consideration. Kozonguizi requested to be heard by the Committee in April 1959. He was supported by Hosea Kutako and Johannes Dausab [25].

The Committee for South West Africa granted his request and Kozonguizi addressed it, on 1 May 1959. He appealed to the UN to rescue inhabitants of Namibia from South African rule and emphasised that the Windhoek location would create an explosive situation in Namibia; and requested the UN to grant him a further hearing at a later session in the year where he would provide a detailed account on the conditions in Namibia; and expressed his desire to provide a full report on developments in South West Africa [26]. Thereafter, the Committee concerning South West Africa provided Kozonguizi with a further hearing during the examination of conditions in Namibia, for which the date was set for 5 July 1959. But he was unable to appear before the Committee. Kozonguizi's mission, however, steadily moved the centre of the struggle around the future of Namibia, from the UN to the territory because individuals commenced to organise their strength and to prepare for the quarrel that was initiated at Lake Successes, New York some years back [27].

Hans Beukes

Hans Beukes was the third non-White citizen from Namibia to address the General Assembly. Beukes arrived as a petitioner at the UN in summer 1959. He was a Coloured man from the Rehoboth Community, chosen amongst the non-White students in South African universities, to resume a three-year scholarship programme at the University of Oslo in Norway. Beukes received a passport and was about to embark for Norway when his passport was withdrawn. His passport was withdrawn because he wanted to come and give evidence at the UN [28].

Beukes requested to heard by the Committee concerning South West Africa on 15 July 1959, of which the Committee granted at its 103rd meeting. He could not, however, address the Committee as arranged because of a scheduling clash [50]. But Beukes still depicted a petition, further reflecting on social, economic and educational conditions in Namibia. In the petition, he also described the circumstances leading to the withdrawal of his passport. He then appealed to the UN to consider assisting him to use the opportunity to study in Oslo [29].

On 11 October 1959, the Committee for South West Africa approved a draft resolution based on Beukes. By this resolution, the Committee articulated that the withholding or withdrawal of a passport from a qualified South West African student was not only a direct interference in the educational and general advancement of an individual, but a hindrance to the educational development of the territory. It, therefore, requested the South African Government to withdraw the decision [30].

Beukes' mission (his petition) significantly captured the attention of activists concerning the conditions in Namibia globally and threatened South Africa's relations with the UN, Great Britain and the United States of America [31].

Sam Nujoma

Sam Nujoma joined other petitioners from Namibia at the UN in 1960. He was the President of the OPO. Nujoma escaped from Namibia into exile after being arrested three times at Windhoek after the December 1959 disturbances among residents of the Old Windhoek Location. He was instructed by the OPO to escape to the UN as a representative of the Ovambo tribe in Namibia [32].

Nujoma requested to be heard by the Committee on South West Africa while in Accra, on 6 May 1960. His request was supported by Louis Nelengani, the Vice-President of the OPO, and submitted to the Committee by Oliver Tambo of the ANC of South Africa [33]. The Committee granted his hearing at its 128th meeting of which the date for that was arranged for 5 July 1960. Nujoma appeared before the Committee at its meetings on 8 and 11 July 1960. He stated before the Committee that about 200 location residents (including himself) had been deported from Windhoek, following the 1959 disturbances in the area [34]. The Committee, thereafter, adopted a draft resolution, noting (with a deep concern) the action taken by the police and soldiers against residents of the location which had resulted in several residents being killed or injured. It, therefore, considered the police and soldiers' action as contrary to the mandate system of the League of Nations, the Charter of the UN, and the Universal Declaration of Human Rights [35].

Nujoma pressed for the submission of more verbal hearings to the South West Africa Committee, and informed it that the South Africa Government had intensified its repressive actions against inhabitants of Namibia since his last appearance before that Committee on 11 July 1960. He requested an urgent hearing which the Committee approved on 10 August [36]. Consequently, Nujoma appeared before the Committee for South West Africa on 11 August 1960 and responded to questions addressed to him by members of the Committee the following day. Nujoma argued that the territory's inhabitants wanted South Africa removed from Namibia, to be replaced by the UN trusteeship over the area, to ensure the territory's preparation for self-determination and self-rule; urged the UN to station a UN Commission, or a similar body in Namibia; and appealed to the body for further technical assistance for the territory [37].

Based on Nujoma's statement, the Committee for South West Africa approved the recommendation by the General Assembly, presenting a draft resolution on the status and conditions in Namibia. It covered the so-called 'Native' reserves; the imprisonment of political leaders, particularly Toivo Ja Toivo; the return of the Hereros from exile in Bechuanaland; and scholarships for students [38].

Nujoma's mission at the UN shifted the observation of the world body regarding the prevailing conditions in Namibia—thereby making the situation in the territory a threat to global peace and security [39].

Reverend Markus Kooper

In May 1961, the Reverend Markus Kooper, a pastor of the African Methodist Episcopal Church (AME) at the Hoachanas community in Namibia, became a petitioner to the UN. Kooper was one of those South West African inhabitants who were removed from the Hoachanas Native Reserve in January 1959. The reason for his removal was because he translated petitions submitted by residents of the reserve to the UN [40].

Kooper petitioned the UN on behalf of his tribe and congregation on 25 February 1959. His petition was supported by Chief Hosea Kutako. He requested to be heard by the Committee on South West Africa, on 16 May 1960, while he was in Bechuanaland (currently Botswana). Kooper's application for hearing was transmitted to the Committee by the Reverend Micahel Scott, and the date for his hearing was arranged for 5 July 1960. He could not, however, appear before the Committee because he did not have the necessary travel documents [41].

In his petition which concerned the situation in Hoachanas Reserve, Kooper stated that the situation in the area was critical and needed sympathetic attention and immediate action without hesitation, argument or delay. He reflected on the Government of South Africa's refusal to allow their representatives to appear before the appropriate UN forums to state the real conditions in the territory; detailed the circumstances leading up to his deportation and the effects it had on his family and church; and emphasised that removal constituted the first step towards the partition of South West Africa [42].

Based on Kooper's petition, the South West Africa Committee adopted Resolution 1357 (XIV) for the General Assembly's approval. By this resolution, the Assembly would, among other things, urge the South African Government to desist from performing the removal of other residents of the Hoachanas Native Reserve and to arrange for the return of Kooper and his family [43].

IV. South West African National Liberation Movements Petitions at the UN

SWANU and SWAPO petitioned the UN in 1961. Whilst SWANU was founded in May 1959 and most of its members originated from the Herero inhabitants, SWAPO was founded in April 1960 and obtained its support primarily from the Ovambo tribe. Harassed and imprisoned by the South African security forces, SWANU and SWAPO members fled their country into exile to seek assistance from other sympathetic African countries [44].

In 1961 the UN Committee concerning South West Africa considered alternative means of obtaining additional information. It considered the possibility of visiting African countries neighbouring Namibia, and interviewing refugees from the territory. On 10 May 1961 (as part of this consideration), the Committee granted hearings by petitioners from Namibia in New York The petitioners were: Mburumba Kerina, Reverend Markus Kooper, and Jacob Kuhangua, a founding member of SWAPO [45].

Feeling confident that the African States would assist the Committee for South West Africa, Kerina and Kooper urged the Committee to visit Namibia, before 31 May 1961. The petitioners held the opinion that even if the Committee was physically prevented from entering the territory, the effort would inspire hope amongst inhabitants of the territory and enhance the prestige of the UN in Africa [46].

Kerina informed the Committee that there was continual contact between them and those in Namibia concerning Hereros in Bechuanaland, indicating considerable movements across the border. Believing that the South African Government would intensify measures to prevent Africans from crossing the borders, into Bechuanaland, Kerina stated that the Committee's presences could ensure these measures. Kuhangua doubted whether the Committee could protect Namibians seeking to cross the border [47].

Based on the petitioners' views, the Committee on South West Africa decided to visit African states. On 19 May 1961, the Committee sent a telegram to all member states of the UN in Africa, inquiring about the presence of Namibian refugees in their countries, and willingness to be interviewed. Subsequently, the Committee received replies from Ghana, the United Arab Republic (currently Egypt) and Tanzania (through the United Kingdom)—confirming those refugees and welcoming its visit [48].

The Committee on South West Africa accepted invitations from these African states and visited the continent from 21 June to 25 July 1961. At the meeting between the Committee and the politically affiliated refugees belonging to SWAPO and SWANU, the movements urged the Committee to visit the territory to observe the conditions [49].

On 19 December 1961, the Committee South West Africa, based on the testimony of SWANU and SWAPO politically affiliated refugees and of other petitioners, adopted a recommendation which dissolved it. It established the UN Special Committee for South West Africa, specifically entrusted with certain urgent functions, preparatory to granting full independence to Namibia and a visit to Namibia before 1 May 1962 [50].

In April 1962, Victorio Carpio of the Philippines, the Chairperson of the Special Committee, approached Brand Fourie, South Africa's permanent representative to the UN in New York, to seek South Africa's cooperation regarding a visit to Namibia. Carpio reported to the Committee On 5 April 1962, that the South African representative was impressed with the approach [51].

On 12 April 1962, South Africa accepted the Special Committee's request. The Special Committee considered the invitation on 13 April 1962. Accordingly, Victorio Carpio and Hassan Nur Elmi, his Vice, arrived in South Africa on 5 May and proceeded to Namibia where they arrived on 9 May 1962 [52].

In Namibia, Carpio and Nur Elmi met with deputations from SWANU, SWANU and the SWAUNIO during their journey.

The latter was formed by David Gertze to oppose SA's homeland policy. These organisations expressed strong opposition to the South African administration and appealed to the UN to immediately take control of the government of the territory in preparation for early self-government and independence [53].

Upon the Chairperson and Vice-Chairperson's return to the Headquarters, on 23 July 1962, the Special Committee received information relating to South West Africa. The Committee considered the information at its meetings in New York from 30 July to 1 August 1962. The information came from petitioners: Jariretundu Kozonguizi of SWANU, Moses Garoeb (SWAPO) and Reverend Markus Kooper (SWAUNIO). It concerned the December 1959 killings at the Old Location in Namibia; rejection of south African presences in Namibia; as well as, the urgency of the UN to take all measures necessary to stop removals and arrests of people in Windhoek [54].

By the end of August 1962, the Special Committee had received 81 petitions and communications from SWAPO, SWANU, and the SWAUNIO, in addition to those presented verbally at its Headquarters in New York. The Special Committee reproduced those scripts on 24 August 1962. Concerning the visit by Chairperson and Vice-Chairperson to Namibia, another petition appealed to the UN to send a group to investigate conditions in the whole territory and for the return of the balance of their land [55].

V. Conclusion

From the discussion, it is concluded that petitioning the UN, particularly in Namibia, was initiated by individuals and later followed the national liberation movements. As observed, petitioning the UN commenced with the Reverend Michael Scott, on behalf of the inhabitants of Namibia. He was later joined at the UN by other indigenous Namibians, including Mburumba Kerina, Jariretundu Kozonguizi, Hans Beukes, Sam Nujoma; and, the Reverend Markus Kooper. This, as the paper has shown, ended with the most prominent national liberation movements in that territory which included, among others, SWAPO, SWANU and the SWAUNIO.

References

[1] *Historical Papers Research Archive*, Collection Number: AD1517, University of Witwatersrand Johannesburg.

[2] *Official Records of the General Assembly, Fourth Committee Trusteeship, Annex to the Summary Records of Meetings*, Lake Success, New York, 1949, p.13.

[3] SC Saxena, "Namibia and the United Nations", *The Indian Journal of Political Science*, Volume 36, No.3, Indian Political Science Association, July-September 1975, p.278.

[4] *Official Records of the General Assembly, Fourth Committee Trusteeship, Annex to the Summary Records of Meetings*, Lake Success, New York, 1949, p.13.

[5] *Yearbook of the United Nations*, New York, 1948/49, p.868.

[6] [48/49, p.870].

[7] J Duguard, "Namibia (South West Africa): The Court's Opinion, South Africa's Response, and the Prospects for the Future", *Columbia Journal of Transnational Law*, 1972, p.14.

[8] *Historical Papers Research Archive*, Collection Number: AD1715, University of Witwatersrand Johannesburg.

[9] [Collection Number: AD1715].

[10] Official Records of the General Assembly, Fourth Session, *Agenda Item 38*, Palais de Chaillot, Paris, 1951-1952, p.17.

[11] *Official Records of the General Assembly,* Seventh Session, 308th Meeting of the Fourth Committee, New York, 1952, p.119.

[12] WF Courtney, "Michael Scott Speaks", *Friends Journal,* Volume 1, No. 27, 31 December 1955, p.427.

[13] D Baily, "Africa and the United Nations, International Affairs Reports, Volume 11, No.29,

[14] Hilda and Rusty Bernstein Papers, 1931-2006, Collection No: A3299, *Historical Research Archive*, University of Witwatersrand Johannesburg.

[15] JM Morgan, "A Global Struggle: Namibian Nationalism and South African Imperialism at the United Nations, 1945-1960", *Dissertation presented to the Faculty of the Graduate School of the University of Texas at Austin partial fulfilment for the Degree of Doctor of Philosophy*, University of Texas, Austin, 2014, p.210.

[16] Official Records on the General Assembly, Eleventh Session, *Supplement No. 12 (A/3151)*, New York, 1956, p.34.

[17] *Yearbook of the United Nations*, New York, 1955, p.272.

[18] *Reports of Judgements, Advisory Opinions and Orders,* International Court of Justice (ICJ), The Hague, 1956, p. 27.

[19] M Kerina, "Hearings on South West Africa", *Africa-UN Bulletin*, No.2, 28 December 1956, p.2.

[20] Official Records of the General Assembly, Thirteenth Session, *Supplement No. 12 (A/3906)*, New York, 1958, p.61.

[21] SB Idowu, "Namibia from Colonisation to Statehood: The Paradoxical Relationship between Law and Power in International Society", *A Dissertation submitted to the Department of International Relations, Faculty of Economics, London School of Economics in the Candidacy for the Degree of Doctor of Philosophy*, London, 2000, p.118.

[22] Mburumba Kerina, Statement at the 653rd meeting of the Fourth Committee, New York, 26 September 1957, *National Archive of South Africa (NARSSA)*, BTS1/18/59, Vol. 37, Pretoria, South Africa.

[23] SM Nelson, "A People between Two Fires": The Church of Namibia Caught between South Africa and SWAPO', *A Thesis submitted to the Faculty of Wartburg Theological Seminary in partial fulfilment of the requirements for the Degree of Master of Divinity*, Dubuque, Iowa, May 2014, p.9.

[24] American Committee in Africa (ACOA), *South West Africa: the UN's Step Child*, New York, 1960, p.12.

[25] Official Records of the General Assembly, Fourteenth Session, *Supplement No. 12 (A/4191),* New York, 1959, p.37.

[26] J Kozonguizi, "Background to the Violence", *Africa South*, Volume 4, No.3. April-June 1960, Africa South Publications, p.75.

[27] Hilda and Rusty Beirnstein Papers, 1931-2006, *Historical Papers Research Archive*, Collection Number A3299, University of Witwatersrand Johannesburg.

[28] American Committee on Africa (ACOA)*South West Africa: The UN's Stepchild*, New York, 1960, p12.

[29] [60, p.66].

[30] Official Records of the General Assembly, Fourteenth Session, *Supplement No. 12, (A/4191)*, New York, 1959, p.36.

[31] [31] JM Morgan, "A Global Struggle: Namibian Nationalism and South African Imperialism at the United Nations, 1945-1960", *Dissertation presented to the Faculty of the Graduate School of the University of Texas at Austin partial fulfilment for the Degree of Doctor of Philosophy*, University of Texas, Austin, 2014, p.216

[32] American Committee on Africa (ACOA), *South West Africa: the UN's Step Child*, New York, 1960, p.13.

[33] [33] Official Records of the General Assembly, Fifteenth Session, *Supplement No.2 (A/4464)*, New York, 1960, p.5.

[34] [60, p.5].

[35] [60, p. 67].

[36] [60, p.5].

[37] [37] EI Udogu, *Liberating Namibia: The Long Diplomatic Struggle between the United Nations and South Africa*, North Carolina, 2012, p.102.

[38] Official Records of the General Assembly, Fifteenth Session, *Supplement No. 12 (A/4464),* New York, 1960, p.58.

[39] EI Udogu, *Liberating Namibia: The Long Diplomatic Struggle between the United Nations and South Africa*, North Carolina, 2012, p.102.

[40] Official Records of the General Assembly, Fourteenth Session, *Supplement No. 12 (A/4191)*, New York, 1959, p.49

[41] Official Records of the General Assembly, Fourteenth Session, *Supplement No. 12 (A/4464)*, New York, 1960, p.5.

[42] Official Records of the General Assembly, Fifteen Session, *Supplement No. 12, (A/4191*), New York, 1947, p.47.

[43] "South West Africa (Rev. Markus Kooper)", *Hansard*, volume 627, 29 July 1960, p.432.
[44] TJ Stapleton, *Warfare and Tracking in Africa, 1952-1990*, London & New York, 2015, p.102.

[45] Official Records of the General Assembly, Sixteenth Session, *Supplement 12 (A/4926)*, New York, 26 October 1961, p.18
[46] [61, pp.18-19].
[47] [47] Official Records of the General Assembly, Sixteenth Session, *Supplement 12 (A/4926)*, New York, 26 October 1961, p.19.
[48] [61, p.19].
[49] [61, p.3].
[50] [61, p.3].
[51] Official Records of the General Assembly, Seventeenth Session, *Supplement No. 12 (A/5212)*, New York, 1963, p.16.
[52] [63, p.1].
[53] [63, p.4].
[54] [63, p.4].
[55] [63, pp.8-9].
[56] [63, pp.10-11].

Navigating Otherness, Translation and Appropriation: A Study of Miya Poetry in Assam

Deepshikha Behera

***Abstract*—** In the wake of growing affinity towards world literature, it is important to ask questions that threaten the presumed coherence in the process of translation, on which world literature thrives. The struggle of indigenous communities to resist the homogenization and cultural appropriation can be attributed to the epistemological violence that is baked by social and political factors. Untranslatability then is the resistance to such appropriation, thus marking the inevitable differences recorded in encounters across language-cultures. I aim to discuss the plight of the Miya community in the North-Eastern state of Assam, India, who migrated from then undivided Bengal for various socio-economic and political reasons decades ago and have been subject to racial and political subjugation. Miya Poetry, a recently emerging phenomenon, saw the rise of assertion of one's mother tongue over the dominant Assamese language when poets began to write in their native Miya dialect. This created an uproar among the Assamese people who felt that the Miya poets were portraying the picture of Assam as a xenophobic state and thus an FIR was lodged against ten of the poets. Through their poetry the Miya Poets seek to embrace the very slur that is used to vilify them. Miya, an Urdu word, meaning gentleman is used here as a racial slur usually connotative of those who have migrated to Assam from Bangladesh, (then a part of undivided Bengal) and roughly translates to "a refugee deprived of self-esteem". In this paper I shall discuss the importance of referentiality in semiotics that shall be crucial in understanding the formation of untranslatables(literally) and otherness(metaphorically) in cross-cultural encounters. I also aim to discuss my findings during the field visit in Assam where I studied Miya language and culture from an ethno-semiotic point of view. Language politics has played a crucial role in shaping the identities of Miya people, whose language and culture is under threat of assimilation and appropriation by the dominant Assamese culture. Adding to their distress, the state sponsored violence in the name of National Register of Citizens has led to detention, questionable citizenship status and homelessness among them. I shall discuss the implications of unhomeliness, marginalization and refusing to be assimilated in the dominant discourse that seeks to erase differences that are latent within alternate ways of expression and claiming the signifiers of a language that aims to vilify.

***Keywords*—** translation, untranslatability, world literature, otherness, semiotics, language politics, cultural appropriation.

Deepshikha Behera is with the English and Foreign Languages University, Hyderabad, India (e-mail: beheradeepshikha@gmail.com).

Real-Time Inequalities and Policies during the Pandemic in the US

Luisa Corrado[1], Daniela Fantozzi[1,2], and Simona Giglioli[1,3]

[1]Department of Economics and Finance, University of Rome Tor Vergata
[2]National Statistical Institute (Istat)
[3]Bank of Italy

September 2021

Abstract

In this paper we investigate the effects of different policies implemented during the Covid-19 pandemic on real-time inequalities in the United States. We use a novel database built using anonymized data from the private sector, which enables us to compute daily measures of consumption inequality at the county level. Using a narrative approach combined with high frequency data for the identification of shocks, we evaluate the impact of monetary and fiscal policy in a VAR framework by constructing impulse response functions of our daily inequality measures. Our approach allows us to augment standard Cholesky identification with additional information coming from key policy announcements by the Fed in the last year and evaluate their effectiveness. The main findings show that consumption inequality rose during the pandemic, but the effect of monetary policies has been to mitigate such an increase. In particular, we distinguish two kind of interventions: those regarding federal funds rate, Repo agreements and QE programs, that we call "purely monetary", and those concerning emergency plans for firms to avoid mass layoffs and a sharp decrease in employment, to which we refer to as "quasi-fiscal" policies. Our evidence suggests a greater contribution by the former type of intervention in mitigating the rise in inequality.

Keywords: monetary policy, inequality, quasi-fiscal policy, high-frequency data, Covid-19

1 Introduction

The Covid-19 pandemic has drastically changed our daily life. Aside from the terrible health consequences, it has resulted in an unparalleled economic crisis, which countries all over the world have been attempting to address since March 2020. In the United States, the pandemic led to a large and immediate decline in aggregate spending and a sharp increase in unemployment. The response of the Federal Reserve, through a series of monetary stimulus and emergency lending initiatives has, according to many economists (Fleming et al. 2020, Bullard 2020, Crouzet 2020 among others) prevented the pandemic from causing a financial crisis and a much deeper and more prolonged recession. In this paper we investigate whether the measures that the Fed has taken in response to the pandemic had an effect on inequality. Indeed, although inequalities in the United States have been under attention for the past few decades, during Covid-19 the situation has drammatically worsened: inequality in the US has reached record levels since mid-March 2020, when tens of millions of Americans across the country started losing their jobs as a result of the economic fallout.

Two main streams of the literature are at the basis of this work. The first one is related to the effects of Covid-19 on consumption inequality. Several studies have analysed this aspect using high-frequency data for different countries, finding an increase in consumption inequality during the pandemic. Among others, Aspachs et al. (2021) with Spanish data from bank records, Gathergood et al. (2021) and Chronopoulos et al. (2020) with UK data, Andersen et al. (2021) for Denmark, Bachas et al. (2020) and Cotton et al. (2021) with US credit card data. The second stream concerns the empirical analysis of the effects of monetary policy on inequality. The debate on the topic is still open, and the empirical literature is sometimes ambiguous. Some studies exploit survey data on household income at the quarterly level: the paper of Coibion et al. (2017), for example, uses quarterly data from the US Consumer Expenditure Survey (CEX) in a VAR framework with narrative shocks to estimate the effects of conventional monetary policy on the Gini coefficient for consumption and income. Also for the US, Montecino and Epstein (2015) found that unconventional monetary policy led to rising inequality via raising asset returns. Some other studies perform similar analysis for different countries: Saiki and Frost (2014) look at how unconventional monetary policy affected inequality in Japan after 2008, using micro level data of Japanese households in a VAR framework. Mumtaz and Theophilopoulou (2016) provide similar evidence for the UK using the Family Expenditure Survey (FES), finding that contractionary monetary policy shocks lead to an increase in earnings, income and consumption inequality. For the Euro area, Guerello (2017) constructs measures of income dispersion using data from the European Commission Consumer Survey and evaluates the effects of both types of

monetary policy on income distribution, while Lenza and Slacalek (2018) use the Household Finance and Consumption Survey (HFCS) by the European Central Bank to evaluate the impact of quantitative easing on income and wealth of individual euro area households.

In our analysis we consider disparities across the level of consumption spending, using anonymized bank transaction data recently released by Chetty et al. (2020) to evaluate the microeconomic dynamics underlying aggregate data. We first build the dataset by creating daily indices to measure inequality across counties in the US and descrbe the evolution of these indices during the pandemic. Then, we estimate a VAR model augmenting standard Cholesky identication with additional information coming from key policy announcements by the Fed in the last year in order to measure the impact of Fed's measures in mitigating or reinforcing real-time inequalities.

Our main contribution is the use of high-frequency data on consumption spending to study the effect of Fed's policies during Covid-19. In particular, we distinguish between two kinds of intervention in a narrative framework: those regarding the federal funds rate, the Repo agreements and the QE programs, that we call "purely monetary", and those concerning emergency plans for firms to avoid mass layoffs and a sharp decrease in employment, to which we refer to as "quasi-fiscal" policies. As discussed above, many authors have analyzed the development of consumption spending in the US with similar data, but to the best of our knowledge, the empirical literature linking these trends with Fed's monetary and quasi-fiscal policy interventions is very scarce. Our main findings show that consumption inequality rose during the pandemic, and the effect of Fed's policies has been to mitigate, especially in the medium run, such an increase. In particular, when distinguishing between monetary and quasi-fiscal policies, our evidence suggests a greater contribution by the former type of intervention in mitigating inequality.

The paper is articulated as follows: Section 2 presents the data used, explains how daily inequality indices are created and describes our identification strategy for the shocks. Section 3 shows the evolution of consumption inequality during the pandemic, the empirical analysis through the estimation of a VAR model, and presents the results. Section 4 concludes.

2 Data and methodology

Our aim is to assess whether and how inequality in the United States has evolved during the Covid-19 pandemic, and what has been the role of Fed's policies in this sense. For our analysis we use different types of data. The kind of inequality we consider is the one across consumption levels. Many authors have analyzed consumption patterns to study inequalities: according to Blundell and Preston (1998) and Krueger and Perri (2006), the distribution

of consumption expenditures gives greater insight into the distribution of household well-being, compared to income distribution. We combine the two measures: after an analysis of inequality in consumption spending across all counties, we divide them in quartiles based on per capita income, and look at the response of consumption at different quartiles. Differently from the above mentioned papers, we use high-frequency spending data to provide a real-time dynamic analysis of inequality of consumption spending.

2.1 Real economy data

The database recently released and constantly updated by Chetty et al. (2020) provides daily information on percent changes in consumption expenditure, employment and Covid-19 cases by county in the US. The changes refer to January, 14 2020 and our sample period is from 20th January 2020 to 31st March 2021, with daily data. This database is built using anonymized data from several private companies. In particular, they measure consumer spending changes using data on credit and debit card spending collected by Affinity Solutions Inc, which capture nearly 10% of debit and credit card spending in the US. Since we are working with card spending data, we miss cash transactions in our analysis, as well as other transactions that are made, for example, through other agents such as insurance companies. This dataset, nonetheless, provides satisfactory information about spending on retail, some service expenditures, and some durable goods. In the Affinity data provided by Chetty et al. (2020), daily changes in card spending are available at the county level, and each county is associated to a zip code. In order to get a measure of the ex-ante inequality across counties, we use data on 2019 per capita income by county from the US Bureau of Economic Analysis (BEA).

For employment, Chetty et al. (2020) provide a representative picture of private non-farm employment in the United States by combining different data sources to obtain information on employment and earnings: payroll data from Paychex and Intuit, worker-level data from Earnin, and time sheet data from Kronos. As for consumption data, also data on employment are provided as percent changes with respect to January 14, 2020.

Since we are interested in working with economic data in levels and not in percent changes, we apply those changes to annual 2019 data on employment and per capita consumption from the BEA, so as to have a measure in levels of daily consumption and employment thoughout 2020. Our assumption is that annual 2019 data are a good proxy for the situation on 14th January 2020, to which data in percent changes refer to. Finally, we remove weekend days from the sample to be able to merge all data. We end up with a dataset of 310 observations for each variable, for 3,142 counties. To the best of our knowledge, we are the first who perfom

an analysis of consumption inequality using this dataset with the described arrangements, to study diparities across US counties and to assess the role of the Fed in the evolution of inequality.

Figure 1: Consumption and employment trends (7-day moving averages)

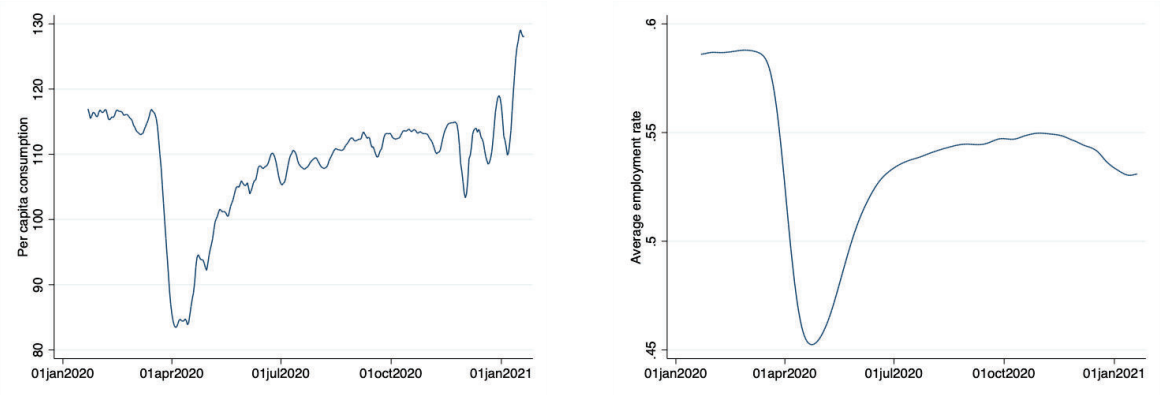

(a) Average per capita consumption spending

(b) Average employment rate

Figure 1 reports the daily average (intended as average across counties) per capita consumption spending and the daily average employment rate in the US during the sample period considered. One can easily notice the similar trend of the two variables, with the minimum level reached in April 2020 (among others, EarnestResearch 2020 and Alexander and Karger 2020 provide the same evidence). Moreover, while the consumption spending returns to pre-pandemic levels (and also above those) towards the end of 2020, the employment rate remains significanlty lower.

2.2 Monetary policy shock identification and data

As many researchers claim (Labonte 2021, Clarida et al. 2021, Ferrero and Giglioli 2020, among others), the Fed promoted economic and financial stability throughout the Covid-19 emergency by exploiting its monetary policy and lender of last resort functions. Some of these actions aimed to encourage economic activity by lowering interest rates (traditional monetary policy measures), while others aimed to provide liquidity so that businesses could access required funding. In particular, in 2020, differently from the past, the Fed has also acted as a lender for nonbank firms and markets by creating a series of emergency lending facilities.

For the scope of our analysis, we divide Fed's measure announcements in two broad categories. The first, that we call "purely monetary policies", includes those announcements of conventional and unconventional monetary policy actions that the Fed took during the

Covid-19 emergency (and that are classified as "Monetary Policy" by the Fed website). These include federal funds rate, Repo agreements and QE programs. The second group, instead, consists of announcements of liquidity and funding operations, subsidized lending, other tools to provide more direct support to credit, such as under-remunerated reserve requirements and other banking initiatives. This second category includes emergency plans for firms to avoid mass layoffs and a sharp decrease in employment: they can be easily seen as complement to fiscal measures and therefore we refer to them as "quasi-fiscal policies". As described by Montanjees (1995), these are operations undertaken for public policy reasons by units outside the government definition, like the Fed. Most of these activities might be carried out by fiscal authorities, rather than being inherent to central banks (Gil Park 2012).

In order to recognize the shocks, we use an innovative setup combining high frequency (HF) data with a narrative approach for the identification of monetary policy shocks, but with some differences from other authors who used similar strategies such as Kuttner (2001), Gurkayanak et al. (2005), Hamilton (2008), Campbell et al. (2021). First, since we have daily data, we don't isolate a 30-minute window around the announcements to guarantee the orthogonality of the shock, but we assume that no other shock occurs in the same day to change the response of the variables [1]. Second, we look at the spread between the long-term and the short-term interest rates on Treasury bills (that is, the change in the slope of the yield curve) in the days of Covid-19 related Fed press conferences as a measure for the shock. Indeed, the great majority of actions in 2020 were not based on interest rate increases, but rather on forward guidance and asset purchases. When a central bank gives forward guidance on future monetary policy, it shapes investors' expectations for future policy interest rates, which influence the yield curve. Forward guidance refers to central banks' commitment to keep policy interest rates low for a period of time or until they accomplish a measurable goal (such as an increase in inflation and/or a decrease in unemployment). Hence, the yield curve is predicted to flatten between the short end and the term of the yield curve that corresponds to the guidance's term, and to flatten farther out. Similarly, asset purchases involve the outright purchase of assets by the central bank in the secondary market, including government bonds. By purchasing assets, the central bank adds to demand for them, so their price increases and their yield falls. As a result, asset purchases can change the slope of the yield curve, usually by lowering the additional yield investors require to compensate for the uncertainty that interest rates or inflation could rise in the future (term risk). As a result, we consider a narrowing of the spread between long and short-term rates as an indicator of an unconventional expansionary monetary policy intervention.

[1] The hypothesis will be tested with orthogonality data, following Forni and Gambetti (2014) and Ricco and Miranda-Agrippino (2021)

As a robustness check, we repeat the analysis using a Cholesky identification strategy without the narrative-HF component, using different variables to detect the two shocks: following Peersman (2011) and Mumtaz & Theophiopoulou (2016), all policy measures that affect the real economy beyond the policy rate, such as operations that change the composition of the central bank's balance sheet, actions that try to guide longer-term interest rate expectations, or measures that expand or reduce the size of the balance sheet or monetary base, are classified as non-standard policy actions. Specifically, such monetary measures have been identified as innovations to the Fed balance sheet and so, as in Guerello (2018), to the Fed total asset growth rate[2].

All the data we use to analyse the effects of monetary policy are taken from the FRED database and have a daily frequency. In particular, we use data on short term (3 month) and log term (10 year) Treasury bill rates. For the robustness check using the Cholesky identification without the narrative-HF component, we use the LIBOR overnight rate as a policy indicator for the conventional monetary policy and the Fed's total asset volume for the unconventional monetary policy. We also include stock market variables in our econometric model, using the NASDAQ 100 Index, which represents the daily index value at market closing. It includes 100 of the largest domestic and international non-financial securities listed on The NASDAQ Stock Market based on market capitalization. Finally, we construct a timeline of the Fed press conferences with Covid-19 related policy announcements, taking data from the Fed's public website. Figures 2 and 3 show the 2020 trend of the Treasury bill rates and the Fed's assets.

[2]In our robustness check, the lag length is chosen to be the average of the optimal lag according to AIC and BIC criteria, and it is equal to 18. The ordering of the vector of variables is: consumption, employment, short term interest rate, Fed's assets, stock market variable and Gini index. The implicit restrictions behind this ordering imply that consumption and the employment rate do not contemporaneously respond to innovations in both the short run interest rate and the Fed's balance sheet, while the latter measure responds contemporaneously to innovations in consumption and employment. This scheme allows us to disentangle monetary shocks from demand shocks but not vice-versa. Additionally, the restrictions imposed disentangle the purely monetary shocks from the quasi-fiscal policy measures, by assuming that these latter actions affect directly the Fed's balance sheet and the financial market but their effect is lagged on the short run interest rate. Finally, the inequality index is assumed to be weakly exogenous to the model and, hence, to not affect contemporaneously all the other variables as in Saiki and Frost (2014). Our results are similar to what we find using the narrative-HF approach. Figures are available on request.

Figure 2: Treasury bill rates

Figure 3: Fed's asset

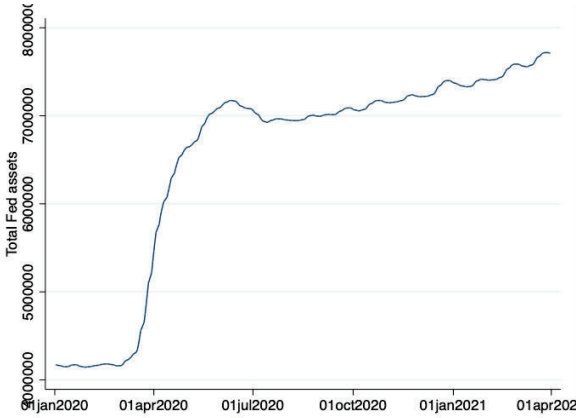

3 Consumption inequality and Fed's policies during the pandemic

As a first step, we want to describe how inequality has evolved in the US during 2020 and at the beginning of 2021. To do so, we construct several consumption indices of inequality across counties at a daily frequency and compare them. Figure 4 reports four of these indices: the difference between the 90th and the 10th percentile in consumption spending (4a), the variance of the logarithm of consumption (4b), the Gini index (6) and the Atkinson index (4d). For all these indicators, a higher value means a higher level of inequality across counties. It appears that the Covid-19 pandemic had a large and heterogeneous economic impact leading to consumption inequality US counties in 2020. Indeed, we can notice a common trend in the four plots, indicating an increase in consumption inequality. In particular, a peak is evident around mid-April, which corresponds to the outbreak of the pandemic, and at the beginning of 2021. Similar results were found by Cotton et al. (2021) with an analogous dataset and by Cox et al. (2020), Baker et al. (2020), Karger and Rajan (2020) using different sources of spending data.

Figure 4: Consumption inequality indices

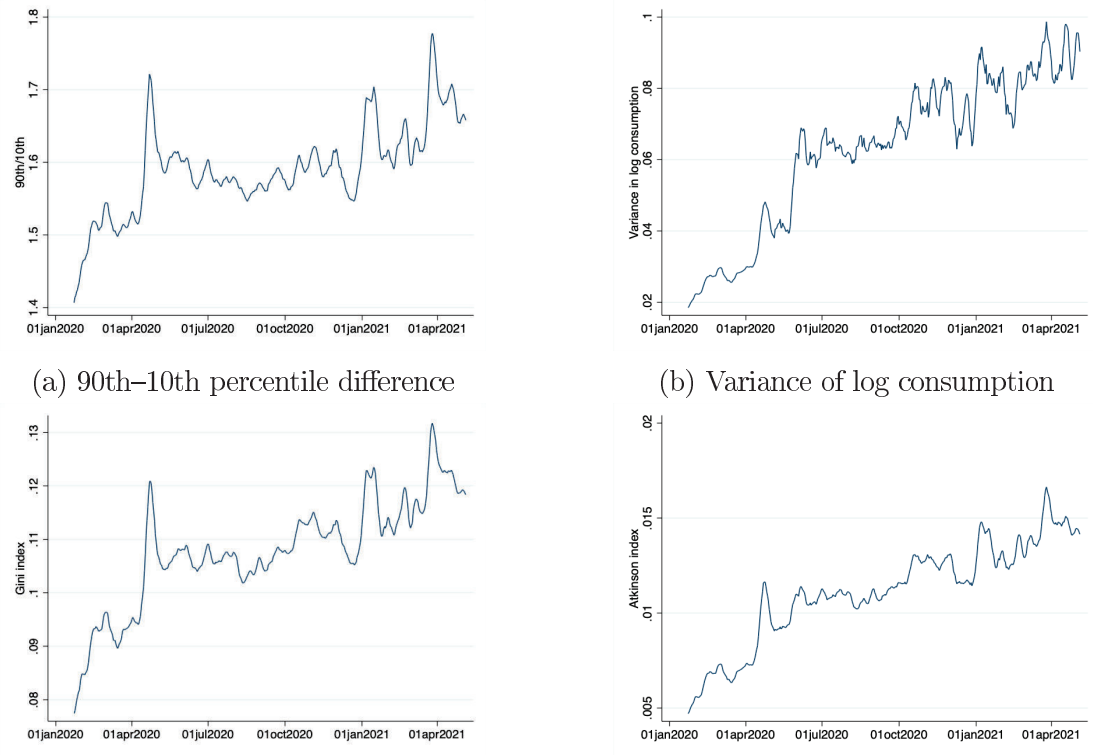

(a) 90th–10th percentile difference

(b) Variance of log consumption

(c) Gini index

(d) Atkinson index

Now, we want to see what has been the effect of Fed's policies on consumption inequality in the US from 20th January 2020 to 31st March 2021, and in particular whether there is any difference in the effect of pure monetary policies and quasi-fiscal policies. We do so by constructing a VAR framework that we estimate for the top quarter and the bottom quarter of the income distribution separately, as well as for the two kinds of shock, pure monetary and quasi-fiscal. We then look at the differences in the responses. Moreover, to further assess the effects of the policies on the level of inequality, we build another VAR model in which we include the average level of consumption and the Gini coefficient. Our first VAR is described by the model:

$$Y_t = B_0 + B_1 Y_{t-1} + B_2 Y_{t-2} + \cdots + B_p Y_{t-p} + e_t \qquad e_t \sim \mathcal{N}(0, \Sigma) \tag{1}$$

where Y_t is a vector of variables containing consumption, employment rate, our narrative-HF shock and a stock market variable represented by the NASDAQ 100 index. Consumption (in dollars per day) employment rate and the stock market variable (as index) are expressed as deviations from the 20-day centered moving average and are stationary according to the Augmented Dickey–Fuller (ADF) test and the Kwiatkowski-Phillips-Schmidt-Shin (KPSS)

test. p is the number of lags computed by averaging the optimal lag lengths according to BIC and AIC criteria and it is equal to 27, Bs are matrices of coefficients and e is a vector of normally distributed errors. Figure 5 reports the cumulative impulse response functions of consumption and employment to a pure monetary policy shock and a quasi-fiscal shock for the top and bottom quartiles of the income distribution of counties, together with the 95% confidence intervals. We look at the cumulative response because we are considering deviations from the centered 20-days moving average: the cumulative IRFs mitigate the variability in the response. Both types of policy intervention had a greater impact on consumption and employment for the bottom quartile than for the top one. However, this difference is greater for the pure monetary policy interventions than for the quasi-fiscal policy, suggesting that the first had a more important role in limiting the increase in inequality than the second.

Figure 5: Consumption and employment responses to shocks

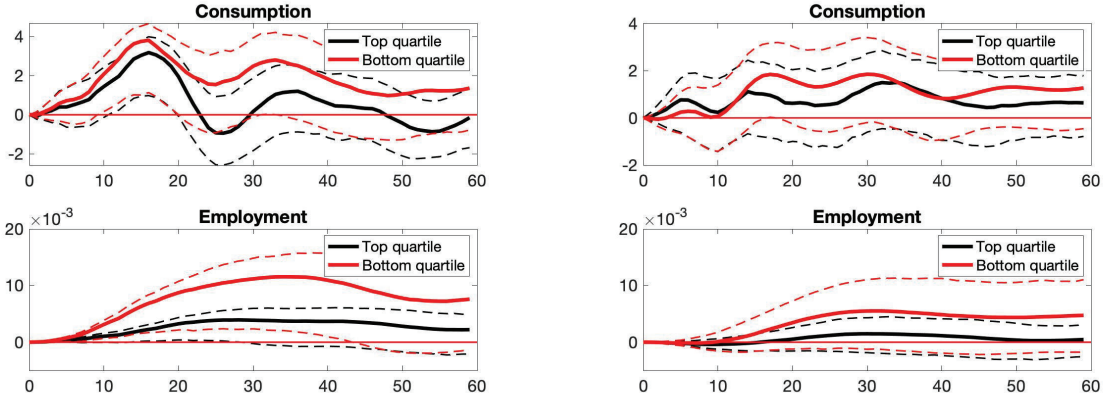

(a) Pure monetary shock

(b) Quasi-fiscal shock

We find similar results if we look at the effect of pure monetary and quasi-fiscal policies on the Gini index [3]. We recall that a higher level of Gini indicates a greater level of inequality, whereas a lower one expresses lower inequality. The specification of the VAR is the same as above, with the vector of variables containing the average consumption spending and the average employment level across countries, the narrative-HF shocks constructed as explained in Section 2.2, the stock market variable and the Gini coefficient. The lag length is again chosen to be the average between the optimal lag according to the AIC and BIC criterion,

[3] As a robustness check, we perform the analysis shown in Figure 6 using different measures of inequality: the variance of the logarithm of consumption, and the difference between the 90th and the 10th percentile of the distribution of consumption. The results, available on request, are similar to our main findings: the inequality index initially grows, and then decreases by more following a pure monetary shock than after a quasi-fiscal shock.

and it is equal to 10 in this case. Figure 6 shows that in response to the shocks, inequality grows at first, and then decreases, reaching the initial level after 20 days when the shock is of pure monetary policy, and after 30 days when it is a quasi-fiscal shock. Importantly, after a pure monetary shock, the level of inequality decreases below the initial level in the medium run, before converging again to the equilibrium, whereas this does not happen with a quasi-fiscal stimulus.

Figure 6: Gini coefficient's response to shocks

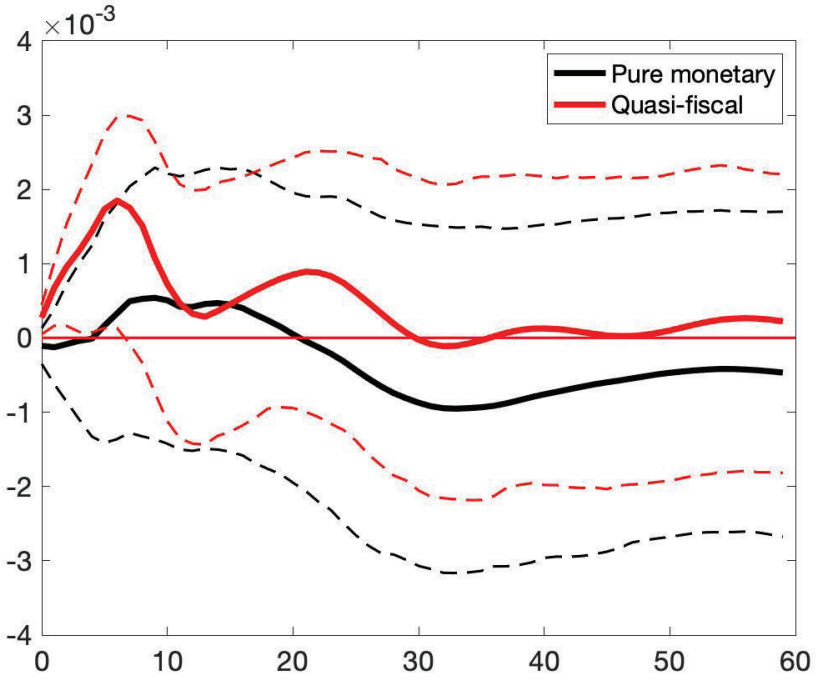

4 Conclusions

In this paper, we investigate the development of consumption inequality in the US during Covid-19 pandemic, and the effect of Fed's policies on such inequality. Our main contribution, relative to previous work on monetary policy and inequality, is the use of recently released high-frequency (daily) data from credit card transactions, that allow us to compute inequality measures at a daily frequency up to a very recent point in time, combined with a narrative approach, to evaluate the impact of monetary and quasi-fiscal policies. We find that inequality in consumption spending has increased during the crisis, but the Fed gave a greater stimulus to consumption and employment to the bottom quartile of the distribution than to the top quartile, suggesting a mitigating impact of its policies. Moreover, interventions of monetary

policy in the form of asset purchases and changes of interest rates seem to have attenuated more the rise in inequality than the quasi-fiscal policies represented by subsidized lending programs and Fed's policies aimed at avoiding mass layoffs.

References

[1] Alexander, D. and Karger, E. *Do Stay-at-Home Orders Cause People to Stay at Home? Effects of Stay-at-Home Orders on Consumer Behavior*. FRB of Chicago Working Paper No. 2020-12, 2020

[2] Andersen, A., Hansen, E. and Sheridan, A., *Consumer Responses to the COVID-19 Crisis: Evidence from Bank Account Transaction Data*. Covid Economics, 7: 88–114., 2020

[3] Aspachs,O. , Durante, R., Graziano, A., Mestres, J,. Reynal-Querol, M,. and Montalvo, J.G., *Tracking the impact of COVID-19 on economic inequality at high frequency*. PLoS ONE, 2021

[4] Bachas, N., Ganong, P., Noel, P.J., Vavra,, J.S. , Wong, A., Farrell, D. and Greig, F.E., *Initial Impacts of the Pandemic on Consumer Behavior: Evidence from Linked Income, Spending, and Savings Data*. NBER Working Paper Series 27617, 2020

[5] Baker, S. R., Farrokhnia, R. A., Meyer, S., Pagel, M., and Yannelis, C., *How Does Household Spending Respond to an Epidemic? Consumption During the 2020 COVID-19 Pandemic*. Working Paper 26949, National Bureau of Economic Research, 2020

[6] Blundell, R. and Preston, I., *Consumption Inequality and Income Uncertainty*. Quarterly Journal of Economics, 113(2), 1998

[7] Bullard, J., *Monetary Policy and Fiscal Policy Responses to the COVID-19 Crisis*. Federal Reserve Bank of St. Louis' Regional Economist, Fourth Quarter 2020, 2020

[8] Campbell, J. R., Evans, C. L., Fisher, J. D. M., Justiniano, A., *Macroeconomic effects of federal reserve forward guidance*. Brookings Papers on Economic Activity 42 (1), 2012

[9] Chetty, R., Friedman, J., Hendren, N. , Stepner, M. and the Opportunity Insights Team, *The Economic Impacts of COVID-19: Evidence from a New Public Database Built Using Private Sector Data*. Harvard University Working Paper, 2020

[10] Chronopoulos, D. K.,Lukas, M., and Wilson,J.O., *TConsumer Spending Responses to the COVID-19 Pandemic: An Assessment of Great Britain*. Covid Economics (34), 2020

[11] Clarida, R., Duygan-Bump, B. and Schotti, C. *The COVID-19 Crisis and the Federal Reserve's Policy Response*. Finance and Economics Discussion Series 2021-035. Washington: Board of Governors of the Federal Reserve System, 2021

[12] Coibion, O. , Gorodnichenko, Y. , Kueng, L. and Silvia., J. , *TInnocent bystanders? Monetary policy and inequality*. Journal of Monetary Economics, 88(C), 2017

[13] Cotton, C.D., Garga, V., Rohan, J. , *Consumption spending and inequality during the Covid-19 pandemic*. Covid Economics, CEPR Press, Issue 83, 2021

[14] Cox, N., Ganong, P., Noel, P., Vavra, J., Wong, A., Farrell, D., Greig, F., and Deadman, E., *Initial Impacts of the Pandemic on Consumer Behavior: Evidence from Linked Income, Spending, and Savings Data*. Brookings Papers on Economic Activity, 2020

[15] Crouzet, N., *Unpacking the Federal Reserve's Aggressive Response to COVID-19*, KelloggInsight, 2020

[16] EarnestResearch, *Where States Stand: Measuring the Reopenings One Step at a Time*. https://www.earnestresearch.com/insights/where-states-stand-measuring-the-reopening-one-step-at-a-time, 2020

[17] Ferrero, A. and Giglioli, S. , *How did central banks respond to the coronavirus crisis?*. Economic Observatory, 2020

[18] Fleming, M., Sarkar, A. and Van Tassel, P. , *The COVID-19 Pandemic and the Fed's Response*. Federal Reserve Bank of New York Liberty Street Economics, 2020

[19] Gathergood, J., Gunzinger, F., Guttman-Kenney, B., Quispe-Torreblanca, E., and Stewart, N., *Levelling Down and the COVID-19 Lockdowns: Uneven Regional Recovery in UK Consumer Spending*. Covid Economics 67, 2021

[20] Gertler, M. and Karadi, P., *Monetary Policy Surprises, Credit Costs, and Economic Activity*. American Economic Journal: Macroeconomics, 7 (1), 2015

[21] Gil Park, S., *Central Banks Quasi-Fiscal Policies and Inflation* . IMF Working Papers No 12/14, 2012

[22] Guerello, C., *Conventional and unconventional monetary policy vs. households income distribution: An empirical analysis for the Euro Area*. Journal of International Money and Finance, Elsevier, vol. 85(C), 2018

[23] Gurkaynak, R. S., Brian Sack, B., and Swanson, E. T., *Do Actions Speak Louder than Words? The Response of Asset Prices to Monetary Policy Actions and Statements*. International Journal of Central Banking 1 (1), 2005

[24] Hamilton, J. D., *Daily monetary policy shocks and new home sales.* Journal of Monetary Economics 55 (7), 2008

[25] Karger, E. and Rajan, A., *Heterogeneity in the Marginal Propensity to Consume: Evidence from Covid-19 Stimulus Payments.* Tech. Rep. WP 2020-15, Federal Reserve Bank of Chicago, 2020

[26] Krueger, D. and Perri, F., *Does Income Inequality Lead to Consumption Inequality? Evidence and Theory.* Review of Economic Studies, 73, 2006

[27] Labonte, M, *The Federal Reserve's Response to COVID-19: Policy Issues*. Congressional Research Service Report, 2021

[28] Lenza, M. and Slacalek, J., *How does monetary policy affect income and wealth inequality? Evidence from quantitative easing in the euro area.* Working Paper Series 2190, European Central Bank, 2018

[29] Montanjees, M. , *Government Finance Statistics in the Countries of the Former Soviet Union: Compilation and Methodological Issues*. IMF Working Papers No 1995/002, 1995

[30] Montecino, J. and Epstein, G., *Did quantitative easing increase income inequality?*. SSRN Electronic Journal, 2015

[31] Mumtaz, H. and Theophiopoulou, A., *The Impact of Monetary Policy on Inequality in the UK. An Empirical Analysis.* Queen Mary University of London School of Economics and Finance Working Paper, 2016 (783), 2016

[32] Peersman, G., *Macroeconomic effects of unconventional monetary policy in the Euro Area.* ECB Working Paper, Issue 1397, 2011

Text Data Preprocessing Library: Bilingual approach

Kabil BOUKHARI

Abstract—In the context of information retrieval, the selection of the most relevant words is a very important step. In fact, the text cleaning allows keeping only the most representative words for a better use. In this paper, we propose a library for the purpose text preprocessing within an implemented application to facilitate this task. This study has two purposes. The first, is to present the related work of the various steps involved in text preprocessing, presenting the segmentation, stemming and lemmatization algorithms that could be efficient in the rest of study. The second, is to implement a developed tool for text preprocessing in French and English. This library accepts unstructured text as input and provides the preprocessed text as output, based on a set of rules and on a base of stop words for both languages. The proposed library has been made on different corpora and gave an interesting result.

Keywords—Text preprocessing, Segmentation, Knowledge extraction, Normalization, Text generation, Information retrieval.

I. Introduction

Textual information still rising on the Internet, and the documents' volume is increasing very rapidly. With the accumulation of text information, satisfying the user's needs becomes more and more challenging. Faced with the large amount of data and the voluminous documents' database, access to information via algorithms remains easier than manual research. Automatic text processing is one of the most active areas of research in Data Science today. It is a field at the intersection of machine learning and linguistics. Natural Language Processing (NLP) is a discipline that focuses on the understanding, manipulation and generation of natural language by machines. Hence, the NLP is really the interface between computer science and linguistics. There is why, it is based on the machine capacity to interact directly with humans. Its purpose is to extract information and meaning from textual content. Faced with the diversity of languages available to represent textual data, it is necessary to develop various language processing tools that could effectively manage large textual data. In many Automatic Language Processing and Information Retrieval (IR) applications, building a base of words and language models remains an important task. But, the large number of morphological variations in words - especially languages that are morphologically rich (i.e: English and French) - pose a great challenge. Indeed, the automatic analysis of the text [1] requires an extremely primordial phase which allows to select, both, the relevant words and terms and refine the analysis process. NLP is a fairly generic term that covers a very wide field of application (e.g, Automatic translation, sentiment analysis [2], marketing, chatbot, text classification, document indexing [3] [4], information retrieval [5] [6]...). In this study, we present a text preprocessing library for English and French. An approach that can select only the most representative words and remove all 'noise' and useless words.

This paper, discusses all the preprocessing phases and presents the related work of each part. It also presents the proposed approach, its steps, and explains the application's operating mode. In the final section, we summarize the work and we present some future works.

K. BOUKHARI is with ENIB / Lab-STICC (UMR 6285) CNRS, Brest, France. e-mail: (kabil.boukhari@gmail.com).

II. Text data preprocessing

A text may have some valueless and uninformative data that hinders analysis operations, hence pre-processing is often required.

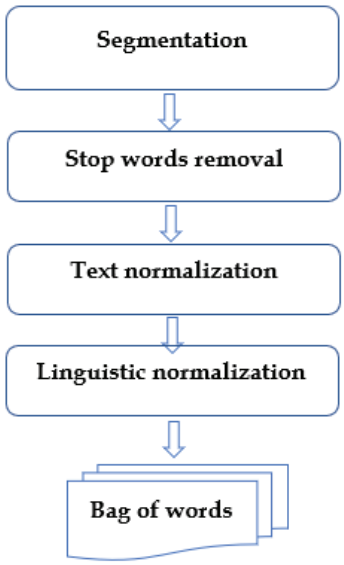

Fig. 1. Stages of text data preprocessing

The pre-processing phase, also called the text preparation phase, consists in analyzing the text by removing the non-informative data and eliminating useless words. The objective of pre-processing is to obtain a uniform representation compatible with subsequent analysis tools. It involves the segmentation of the text into sentences then into words followed by the removal of punctuation and stop words, and the elimination of symbols and numbers. Leading up to the word normalization phase. The preprocessing process is summarized in the figure (fig.1).

A. Segmentation

Text segmentation [7] [8] [9] remains a preliminary phase for automatic language processing. This latter is not taken very

seriously by the most laboratories that process the language automatically. Tokenization is a the process which splits longer strings of text into smaller parts, or tokens. Larger parts of text can be tokenized into sentences, sentences can be segmented into words, etc. Additional processing is usually done after a piece of text has been tokenized appropriately. Tokenization is also referred to as text segmentation or lexical analysis. Sometimes segmentation is used to refer to the decomposition of a large extract into chunks larger than words (e.g. paragraphs or sentences), while tokenization is reserved for the breakdown process which results exclusively in words. To create an automatic segmenter, it is necessary to take into account the treatment of punctuation which constitutes a mark to identify the sentences. Each punctuation mark carries information that can replace sentences or statements. The segmentation phase is based primarily on punctuation marks " . ", " , ", " ; " , " : ", " ! " , " ? ", " $\backslash r$ ". Once the text is segmented into sentences, these will then be segmented into words using spaces. Several approaches have been proposed in this context, we can cite: Khmer Word Segmentation [10] and C-HTS algorithm [11].

B. Stop words removal

This step is the second manipulation performed in text processing: it is the deletion of useless words or empty words, also called "stopwords". The last ones are a set of commonly used words in a language that does not provide informative value for understanding the "meaning" of a text, document or corpus. Stopword removal is very efficient for data manipulation and knowledge extraction. These are the very common words in the language studied.

Examples of stopwords:

- French: le, la, ce, à, de, en, et ...
- English: the, are, is, a, an, to, in, at ...

They are very frequent and slow down the algorithms performance. Removing the 'noise' from the text allows to focus only on the important words. However, it helps to reduce the number of features taken into account and the number of operations to be performed, which keeps the models lighter with a decent size.

C. Normalization

Normalization is the process of transforming text into a standard form, it is very useful for denoising texts such as social media comments, text messages and comments on articles and weather texts... . Studies have shown the importance of the normalization phase, in terms of accuracy and robustness, for text processing (e.g., normalization for Tweets, they were able to improve the accuracy of sentiment classification by about 4%).

There are two types of text normalization:

- Text normalization
- Linguistic normalization

1) Text normalization:

a) : Text normalization consists in cleaning up and then laying out the text according to the usual standards. It renders a standardized text based on the formatting process and vocabulary rules.

Examples of Text normalization:

- Remove dots from acronyms (e.g. U.S.A. $\rightarrow$ USA)
- Remove accents (e.g. météo $\rightarrow$ meteo)
- Remove some capitals (e.g. And $\rightarrow$ and)
- Normalizing particular values, e.g.:
  Dates, e.g. July 14, 1789 $\rightarrow$ 14/07/1789
  Monetary values, e.g. \$400 $\rightarrow$ 400 dollars
  Organizations, e.g. United Nations $\rightarrow$ UN

2) Linguistic normalization:

a) : Linguistic normalization allows to put all words on equal footing, and permits processing to proceed uniformly. Stemming and lemmatization are the most popular and well-known ways to normalize text and the major parts of a text preprocessing endeavor.

1) *Stemming*
   Stemming is the name given to the process that aims to transform the inflections into their roots. It seeks to bring together the different inflectional and derivational variants of a word around a radical.
   The root of a word corresponds to the remaining part of the word, namely its radical, after the deletion of its prefix and/or its suffix. It is also sometimes known as the stem of a word. Contrary to the lemma which corresponds to a real word of the language, the root does not generally correspond to a real word. e.g., the word "changing" has the radical "chang" which does not correspond to a real word. On the other hand, in the example of "connected", the root is "connect".
   The stemming operation consists in removing inflectional and derivational suffixes to reduce the different forms of a word to their appropriate root. This root must be understood in a morphological sense: two words can have the same morphological root, but with different meanings.
   The stemming algorithm (Stemmer) proceeds in various steps by which the words to be processed pass successively, according to the rules, when the parser recognizes a suffix from the list, it either removes it or transforms it. Also, the longest suffix determines the rule to apply. Each algorithm has its own steps and its own rules.

   Example:
   Several algorithms have been proposed for the search of lexical roots for several languages. The main algorithms developed in this sense are the Carry algorithm [12], [13], Raid [14], XSTEM [15], Yass [16] New Porter [17] and Musa algorithm [18]. In the following part, we present the two most well-known algorithms, namely

French		English	
Oroginal word	Stemmed word	Oroginal word	Stemmed word
malade	malad	connect	connect
malades	malad	connected	connect
maladie	malad	connection	connect
maladies	malad	connections	connect
maladive	malad	connecting	connect

TABLE I
STEMMING EXAMPLES IN FRENCH AND ENGLISH

French		English	
Oroginal word	Lemma	Oroginal word	Lemma
cherche	chercher	change	change
cherchait	chercher	changing	change
cherchons	chercher	changed	change
cherché	chercher	changes	change
cherchent	chercher	changer	change

TABLE II
LEMMATIZATION EXAMPLES IN FRENCH AND ENGLISH

Lovins [19] and Porter [20], for the English language on which all other algorithms are based.

Porter
The Porter algorithm [20] is one of the most famous stemming algorithms. It was created in 1979 by PORTER at a computer laboratory in Cambridge (England). It is part of a large project in the field of information retrieval. The Porter algorithm is composed of more than fifty stemming rules divided into five successive steps. These phases include a complete study of English morphology, namely verb processing, plural processing and conjugation times. The word to be processed necessarily passes through all the phases, in the case where more than one rule can be applied, then the longest suffix is chosen. Transformation rules are applied during this operation if needed.

Lovins
This is the first stemmer [19] that was written by Julie Beth Lovins in 1968. The design of the algorithm was greatly influenced by the technical vocabulary that Lovins found in her work (Subject Term Keywords attached to documents in the materials science and engineering field). The Lovins stemmer has 294 endings, 29 conditions, and 35 transformation rules. Each termination is associated with one of the conditions. In the first step, if the longest termination found satisfies its associated condition, that termination will be discarded. In the second stage, the 35 rules are applied to transform the termination. The second step is performed whether or not a termination is removed in the first step.

Example of text processing after applying stemming:

"Reductions in breath ethanol readings in normal male volunteers following mouth rinsing with water at differing temperatures"

After the preprocessing phase, we obtain the following text:

"reduct breath ethanol read norm mal volunte follow mouth rins wat differ temper"

2) *Lemmatization*
Lemmatization is a lexical analysis which makes it possible to group the words of the same family together: it is a grouping by lemma. It is the operation of transforming a word into its canonical form, which takes into consideration the context in which the word is written. The lemma corresponds to the infinitive form of verbs and to the singular masculine form of nouns and adjectives.
Several algorithms have been proposed in this context. The main algorithms developed are the leolemmatizer algorithm [1] [21], Fernández [22] and Sychev algorithm [23].
Examples:
Here is a list of some developed lemmatization algorithms: Wordnet Lemmatizer [2],Pattern Lemmatizer[3] and Stanford CoreNLP Lemmatization [4]

In conclusion, stemming can be considered as a rough and fast form while lemmatization tries to preserve the meaning of sentences as much as possible.

III. PROPOSED APPRAOCH: DEVELOPED TOOL FOR TEXT PREPROCESSING

In this part, we will present the proposed approach for the text preprocessing as well as the application developed to do this task. The library has 3 steps: Segmentation, stop words removal and text normalization.
The following algorithm shows the flow of the proposed approach.

Text segmentation is based on linguistic study on the one hand, on computer modeling on the other. These two studies complement each other. Segmentation has - like other types

[1]Detailed descriptions at homepage: https://github.com/leileibama/leolemmatizer
[2]https://wordnet.princeton.edu/
[3]https://www.clips.uantwerpen.be/pages/pattern
[4]https://stanfordnlp.github.io/CoreNLP/index.html

Algorithm 1: Algorithm of the proposed approach

```
Input: td: text document
Output: ptd: preprocessed text document
Begin Algorithm 1
Select a language
Select source file (td)
while (! end_of_document (td)) do
    Line = ""
    Words_List ⟵ []
    Line ⟵ Read_Line(td)
    Words_List ⟵ Line_Cleanning(Line)
    Words_List1 ⟵ []
    for i ⟵ 1 to Length(Words_List) do
        if ( Words_List[i] ∈ StopWords_ListFile) then
            Words_List1 ⟵ Words_List1 +
              Words_List[i]
        end
    end
    Add_Word_List(Words_List1, Words_Final_List)
end
Create_File(Words_Final_List, ptd)
End Algorithm 1
```

of automatic language processing - its particularities, whether at the linguistic level or at the computer level. Our approach is to define a text preprocessing library from a systematic study of punctuation marks. In addition, the segmentation is based on punctuation marks which are considered pivot marks for triggering the segmentation rules, and also on a study of the left and right contexts of these markers. The first phase consists in selecting each line of the text and processing it in order to add it, afterwards, to the final list of words. Each line is segmented into sentences and each line goes through a tokenization step. This is the process that divides the sentence into tokens; that is to say atomic elements of the sentence. A token is not necessarily a word, it can be for example a punctuation mark. In this phase, various problems have been pointed out by other approaches. For this, several problems of ambiguity have been taken into consideration, e.g., absence of the space after the point, succession of punctuation marks, acronyms and errors related to capitalization.

Based on a list of stop words both in - French and English -, the ”stop words removal” step has the task of removing all the useless words that belong to the list and only keeping the most significant words. Each text line corresponds to a bag of relevant words which will then be added to the final list.

The implementation was carried out with Python to develop an application (Fig.2) that facilitates the task of preprocessing. The proposed approach has been tested with several corpora and has given good results. In the following section, we present two examples (two text extracts), one in French and the other in English.

Example 1:

- **Original text:** *”Paris est la capitale de la France. L’agglomération de Paris compte plus de 10 millions d’habitants. Un fleuve traverse la capitale française, c’est la Seine. Dans Paris, il y a deux îles : l’île de la Cité et l’île Saint-Louis.”*
  preprocessed text *”paris capitale france agglomération paris compte millions habitants fleuve traverse capitale française seine Paris îles île cité saint louis”*

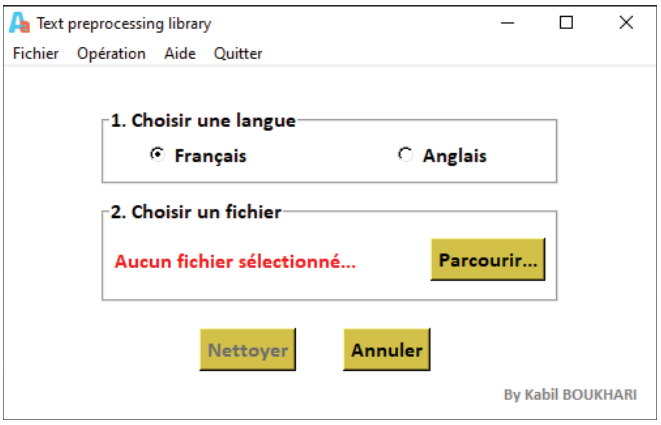

Fig. 2. Application interface for text preprocessing

Example 2:

- **Original text:** *”London is the capital and largest city of England and the United Kingdom with a total population of 9 million. It stands on the River Thames in south-east England at the head of a 50-mile (80 km) estuary down to the North Sea, and has been a major settlement for two millennia.”*
  preprocessed text *”london capital largest city england united kingdom total population million stands River thames south east england head mile estuary north sea major settlement millennia”*

IV. Conclusion

In this paper, we have proposed a library for text preprocessing in both; English and French. The proposed approach, allows to pretreat a textual file and extract only the most significant word. Data processing is done in 3 steps: the first consists in selecting the file lines and segmenting them into sentences. The second is the tokinization step in which the text is divided into words based on a list of punctuation marks. The third and the last step is the selection of the final list of words after removing all ’noise’ from the text. The implementation of this library has been translated into a desktop application, in Python, allowing users to best use this library.

In a future work, we plan to to focus more on the ambiguity problems, aim to enrich the list of stop words - to cover the majority of special cases -, and add other languages to this libraby.

References

[1] F. S. Hasan, HM Mahedi and D. Chaki, “A novel approach to extract important keywords from documents applying latent semantic analysis,” *10th International Conference on Knowledge and Smart Technology (KST). IEEE*, pp. 1–6, 2018.

[2] ——, "A novel approach to extract important keywords from documents applying latent semantic analysis," *10th International Conference on Knowledge and Smart Technology (KST). IEEE*, pp. 1–6, 2018.
[3] K. Boukhari and M. N. Omri, "Approximate matching-based unsupervised document indexing approach: application to biomedical domain," *Scientometrics*, pp. 903–924, 2020.
[4] R. Aravazhi and M. Chidambaram, "An efficient indexing mesh term description logic using in medical subject headings," *Journal of Computer and Mathematical Sciences*, vol. 9, no. 10, pp. 1556–1567, 2018.
[5] K. boukhari and M. N. Omri, "Information retrieval based on description logic: Application to biomedical documents," *Conference: International Conference on High Performance Computing and Simulation (HPCS 2017)*, vol. 15, pp. 1–8, 2017.
[6] L. Yuan, "Supporting relevance feedback with concept learning for semantic information retrieval in large owl knowledge base," *Pacific Rim Knowledge Acquisition Workshop*, pp. 61–75, 2018.
[7] V. Ramesh and A. Kolonin, "Interpretable natural language segmentation based on link grammar," *Science and Artificial Intelligence conference*, pp. 1–8, 2020.
[8] D. Aumiller, S. Almasian, S. Lackner, and M. Gertz, "Structural text segmentation of legal documents," *International Conference on Artificial Intelligence and Law*, pp. 1–10, 2021.
[9] P. Badjatiya, L. J. Kurisinkel, M. Gupta, and V. Varma, "Attention-based neural text segmentation," *European Conference on Information Retrieval*, pp. 180–193, 2018.
[10] V. Chea, Y. K. Thu, C. Ding, M. Utiyama, A. Finch, and E. Sumita, "Khmer word segmentation using conditional random fields," *Khmer Natural Language Processing*, pp. 1–8, 2015.
[11] S. L. Mostafa Bayomi, "C-hts: A concept-based hierarchical text segmentation approach," *International Conference on Language Resources and Evaluation*, pp. 1519–1528, 2018.
[12] M. Paternostre, P. Francq, J. Lamoral, and D. W. M. Saerens, "Carry, un algorithme de désuffixation pour le français," *Generic Analyser and Listener for Indexed and Linguistics Entities of Information*, pp. 1–15, 2002.
[13] K. Boukhari and M. N. Omri, "SAID: A new stemmer algorithm to indexing unstructured document," *The International Conference on Intelligent Systems Design and Applications*, pp. 59–63, 2015.
[14] ——, "Raid: Robust algorithm for stemming text document," *International Journal of Computer Information Systems and Industrial Management Applications*, vol. 8, pp. 235–246, 2016.
[15] K. Baker, "Xstem: An exemplar-based stemming algorithm," *Computation and Language*, pp. 1–11, 2022.
[16] P. Majumder, M. Mitra, S. K. Parui, G. Kole, P. Mitra, and K. Datta, "Yass: Yet another suffix stripper," *ACM Trans. Inf. Syst.*, vol. 25, pp. 1–14, 2007.
[17] W. B. A. Karaa, "A new stemmer to improve information retrieval," *International Journal of Network Security & Its Applications (IJNSA)*, vol. 5, no. 4, pp. 143–154, 2013.
[18] S. Musa, G. N. Obunadike, and M. M. Yakubu, "An improved hausa word stemming algorithm," *FUDMA Journal of Sciencess*, pp. 291–295, 2022.
[19] J. B. Lovins, "Development of a stemming algorithm," *Mechanical Trans lation and Computational Linguistics*, pp. 22–31, 1968.
[20] M. F. Porter, "An algorithm for suffix stripping," *Program: electronic library and information systems*, pp. 130–137, 1980.
[21] L. Lei, "leolemmatizer: A package that postags and lemmatizes english texts in a folder," *Language from a quantitative linguistic perspective*, 2019.
[22] L. G. Fernández, "Sources and steps of corpus lemmatization: Old english anomalous verbs," *Revista Espanola de Linguistica Aplicada*, pp. 416 – 442, 2020.
[23] O. Sychev and N. A. Penskoy, "Method of lemmatizer selections in multiplexing lemmatization," *Conference Series Materials Science and Engineering*, pp. 1–7, 2019.

Dr. Kabil BOUKHARI PhD, degree from Sousse University, Tunisia. He is Assistant Professor at Brest National School of Engineers, France and member of LabSTICC laboratory. His field of interest includes information retrieval, artificial intelligence, document indexing, stemming and knowledge extraction.

The Branching Patterns of Human Evolution, and the Acceleration of Human Evolution

Christopher Portosa Stevens

***Abstract*—** Given that natural selection is commonly treated as a constant or near constant across species (such as across primate species and the human species), and given that comparing clones to a natural population of the human species identifies assortative mating as a variable (i.e., natural populations have more assortative mating across categories of dissimilar characteristics and similar characteristics than populations of genetic identicals or clones), I propose that increasing assortative mating may explain greater brain encephalization, greater brain complexity, and greater diversity of behavioral characteristics in the evolution of species, including humans compared to primate species, sea mammals compared to fish, and bird species (including flight, song, and greater parental investment) compared to reptiles. Moreover, since this strategy of predictive science may be used to visualize branching patterns, I discuss how this strategy of predictive science may complement conventional reductionism in science.

***Keywords*—** branching patterns, brain encephalization, functional specialization, alternation of functions.

Christopher Portosa Stevens is with the Phoenix College, United States (e-mail: acceleration207@gmail.com).

Readout Development of a LGAD-based Hybrid Detector for Microdosimetry (HDM)

E. Pierobon, M. Missiaggia, M. Castelluzzo, F. Tommasino, L. Ricci, E. Scifoni, V. Monaco, M. Boscardin, C. La Tessa

***Abstract*—**Clinical outcomes collected over the past three decades have suggested that ion therapy has the potential to be a treatment modality superior to conventional radiation for several types of cancer, including recurrences, as well as for other diseases. Although the results have been encouraging, numerous treatment uncertainties remain a major obstacle to the full exploitation of particle radiotherapy.

To overcome therapy uncertainties optimizing treatment outcome, the best possible radiation quality description is of paramount importance linking radiation physical dose to biological effects.

Microdosimetry was developed as a tool to improve the description of radiation quality. By recording the energy deposition at the micrometric scale (the typical size of a cell nucleus), this approach takes into account the non-deterministic nature of atomic and nuclear processes, and creates a direct link between the dose deposited by radiation and the biological effect induced. Microdosimeters measure the spectrum of lineal energy *y*, defined as the energy deposition in the detector divided by most probable track length travelled by radiation. The latter is provided by the so-called "Mean Chord Length" (MCL) approximation, and it is related to the detector geometry.

To improve the characterization of the radiation field quality, we define a new quantity replacing the MCL with the actual particle track length inside the microdosimeter. In order to measure this new quantity, we propose a two-stage detector consisting of a commercial Tissue Equivalent Proportional Counter (TEPC) and 4 layers of Low Gain Avalanche Detectors (LGADs) strips. The TEPC detector records the energy deposition in a region equivalent to 2 um of tissue, while the LGADs are very suitable for particle tracking, because of the thickness thinnable down to tens of micrometers and fast response to ionizing radiation.

The concept of HDM has been investigated and validated with Monte Carlo simulations. Currently, a dedicated readout is under development. This two stages detector will require two different systems to join complementary information for each event: energy deposition in the TEPC and respective track length recorded by LGADs tracker. This challenge is being addressed by implementing SoC (System on Chip) technology, relying on Field Programmable Gated Arrays (FPGAs) based on the Zynq architecture. TEPC readout consists of three different signal amplification legs and is carried out thanks to 3 ADCs mounted on a FPGA board. LGADs activated strip signal is processed thanks to dedicated chips, and finally, the activated strip is stored relying again on FPGA-based solutions.

In this work, we will provide a detailed description of HDM geometry and the SoC solutions that we are implementing for the readout.

***Keywords*—**Particle traking, ion therapy, microdosimetry, FPGA.

E. Pierobon, M. Missiaggia, M. Castelluzzo, F. Tommasino, L. Ricci, C. La Tessa are with the department of Physics, University of Trento, Trento Italy (e-mail: chiara.latessa@ unitn.it).

M. Boscarding, is with FBK, Trento Italy

V. Monaco is with department of Physics, University of Torino, Torino Italy

E. Scifoni, is with TIFPA, INFN, Trento Italy

Strategies by National Health Systems in the Northern Hemisphere Against COVID-19

Aysha Zahidie, Meesha Iqbal

***Abstract*—** This paper aims to assess the effectiveness of strategies adopted by national health systems across the globe in different 'geographical regions' in the Northern Hemisphere to combat COVID-19 pandemic. Data is included from the first case reported in November 2019 till mid-April 2020. Sources of information are COVID-19 case repositories, official country websites, university research teams' perspectives, official briefings, and available published research articles to date. We triangulated all data to formulate a comprehensive illustration of COVID-19 situation in each country included. It has been found that the 2002-2004 SARS outbreak experienced in China, Taiwan, and South Korea saw better strategies adopted by leadership to combat COVID-19 pandemic containment as compared to Iran, Italy, and the United States of America. Saudi Arabia has so far been successful in the implementation of containment strategies as there have been no large outbreaks in major cities or confined areas such as prisons. The situation has yet to unfold in India and Pakistan, which exhibit their own weaknesses in policy formulation or implementation in response to health crises.

***Keywords*—** national health systems, COVID-19, prevention, response.

Aysha Zahidie is with the Fazaia Ruth Pfau Medical College, Pakistan (e-mail: ayshazahidie@outlook.com).

Standing in the Frontline: How Could We Improve Nurses' Cultural Competence During Emergency?

Ortal Slobodin, Odeya Cohen

***Abstract*—** We developed a novel online intervention designed to increase nurses' cultural competence in emergency. The first study used a randomized controlled trial to test the intervention effectiveness in increasing nursing students' cultural competence (n=72). The intervention was effective in increasing the participants' culturally competent knowledge.

In the second study, we adapted the intervention to the specific needs of the COVID-19 pandemic. Healthcare professionals (n=154) found the online program useful in improving their cultural competence attitudes. Using online interventions offers a promising strategy for increasing cultural competence in nursing education but also as a short, real time, and available training during an ongoing emergency.

***Keywords*—** cultural competence, COVID-19, disaster nursing, nursing education.

Ortal Slobodin is with the Ben-Gurion University, Israel (e-mail: ortal.slobodin@gmail.com).

Older Adults Coping during a Pandemic

Aditya Jayadas

***Abstract*—**During a pandemic like the one we are in with CoViD-19, older adults, especially those who live in a senior retirement facility, experience even bigger challenges as they are often dependent on other individuals for care. Many older adults are dependent on caregivers to assist with their instrumented activities of daily living (IADL). With travel restrictions imposed during a pandemic, there is a critical need to ensure that older adults who are homebound continue to be able to participate in physical exercise, cognitive exercise, and social interaction programs. The objective of this study was to better understand challenges that older adults faced during the pandemic and what they were doing specifically to cope with the pandemic physically, mentally and through social interaction. A focus group was conducted with 10 older adults (age: 82.70 ± 7.81 years; nine female and one male) who resided in a senior retirement facility. During the course of one hour, seven open-ended questions were posed to the participants: a) What has changed in your life since the start of the pandemic; b) What has been most challenging for you; c) What are you doing to take care of yourself; d) Are you doing anything specifically as it relates to your physical health; e) Are you doing anything specifically as it relates to your mental health; f) What did you do for social interaction during the pandemic; g) Is there anything else you would like to share as it relates to your experience during the pandemic. The focus group session was audio-taped and verbatim transcripts were created to evaluate the responses of the participants. The transcript consisted of 4,698 words and 293 lines of text. The data was analyzed using content analysis. The unit of analysis was the text from the audio recordings that were transcribed. From the review of the transcribed text, themes and sub-themes were identified along with salient quotes under each sub-theme. The major themes that emerged from the data were: having a routine, engaging in activities, attending exercise classes, use of technology, family, community, and prayer. The quotes under the sub-themes provided compelling evidence of how older adults coped during the pandemic while addressing challenges they faced and developing strategies to address their physical and mental health while interacting with others. Lessons learned from this focus group can be used to develop specific physical exercise, cognitive exercise and social interaction programs that benefit the health and wellbeing of older adults.

***Keywords*—**Cognitive exercise, pandemic, physical exercise, social interaction.

A. Jayadas is with the Department of Design, Housing & Merchandising at Oklahoma State University (e-mail: aditya.jayadas@okstate.edu).